

HYDROLOGICAL
CHARACTERIZATION OF
A SULPHIDE WASTE ROCK DUMP

GREGORY THOMAS CARNEY

1998

**HYDROLOGICAL CHARACTERIZATION
OF A
SULPHIDE WASTE ROCK DUMP**

A Thesis Submitted to the College of
Graduate Studies and Research
in Partial Fulfillment of the Requirements
for the Degree of Master of Science
in the Department of Civil Engineering
University of Saskatchewan
Saskatoon, CANADA

By
Gregory Thomas Saretzky
Fall 1998

© Copyright Greg T. Saretzky, 1998. All rights reserved.

The University of Saskatchewan claims copyright in conjunction with the author. Use shall not be made of the material contained herein without proper acknowledgment.

Permission to use

In presenting this thesis in partial fulfillment of the requirements for a Postgraduate degree from the University of Saskatchewan, I agree that the Libraries of this University may make it freely available for inspection. I further agree that permission for copying of this thesis in any manner, in whole or in part, for scholarly purposes may be granted by the professor or professors who supervised my thesis work or, in their absence, by the Head of the Department or the Dean of the College in which my thesis work was done. It is understood that any copying or publication or use of this thesis or parts thereof for financial gain shall not be allowed without my written permission. It is also understood that due recognition shall be given to me and to the University of Saskatchewan in any scholarly use which may be made of any material in my thesis.

Requests for permission to copy or to make other use of material in this thesis in whole or part should be addressed to:

Head of the Department of Civil Engineering
University of Saskatchewan
Saskatoon, Saskatchewan
S7N 0W0
CANADA

Dedication

This thesis is dedicated to my parents;
who have taught me that anything may be accomplished
by use of a good attitude and diligent ambition

Abstract

Acid rock drainage (ARD) from sulphide bearing waste rock dumps poses a serious threat to the environment and has become problematic to the mining industry. Water that is discharged from sulphide waste rock dumps has the potential to be low in pH, thus having the ability to transport heavy metals. The acid water and the heavy metals in solution became toxic to the environment. Acid rock drainage from sulphide bearing waste rock dumps is the most serious environmental liability in the mining industry; believed to be \$3.2 billion for 750 million tonnes of waste rock in Canada alone (Feasby *et al.*, 1997). The understanding of the characteristics and quantity of water flow through waste rock has become fundamental.

A complete hydrologic characterization was performed for the sulphide waste rock dump at Equity Silver Mine Ltd. near Houston, BC (575 km north northwest of Vancouver, Canada). The characterization of the hydrologic system entailed the investigation of five elements: geologic structure, topography, surface hydrology, groundwater and water chemistry.

The hydrologic budget was determined for the waste rock dump. The components are as follows: precipitation, runoff, sublimation, mass transfer, evapotranspiration, changes in storage, infiltration and groundwater. Precipitation was measured with an on site weather station. The runoff was measured for the 1998 freshet with a series of weirs and culverts that were instrumented to measure runoff water. The remaining surface components were determined by the SoilCover (1997) model, a one dimensional finite difference heat and mass transfer program.

The groundwater component was investigated using a numerical model, FEMWATER (ECGL, 1998), which can solve three dimensional saturated or unsaturated groundwater flow regime systems.

All of the surface hydrological components are required in order to equalize the surface water balance for the waste rock dump. The components of the surface hydrological budget during the one year study period over the area of the waste rock dump are as follows: precipitation of 642 mm, 94 mm (15 %) runoff, 327 mm (51 %) evapotranspiration, 27 mm (4 %) infiltration, 97 mm (15 %) sublimation and 97 mm (15 %) mass transfer. The cover system lost 9 mm of water during the one year study period; thus the net surface infiltration was 36 mm (6 %).

The water balance relationship for the acid rock drainage collection ditch that surrounds the waste rock dump was evaluated. The contributions to the ditch are: runoff, infiltration, groundwater discharge and changes in storage. The water balance for the drainage ditch showed that the acid rock drainage flow reporting to the ditch is equivalent to 318 mm of water per year over the area of the waste rock dump. The components of this total flow are estimated to be 36 mm (11 %) infiltration, 27 mm (9 %) runoff, 252 mm (79 %) groundwater discharge and 3 mm (1 %) due to changes in storage within the waste rock.

Acknowledgments

This thesis was prepared under the supervision and direction of Dr. G. Ward Wilson. His knowledge, experience, enthusiasm and positive attitude were a source of inspiration for me. I appreciate his leadership and the time and energy Dr. Wilson devoted to this study.

I would like to thank Keith Ferguson from Placer Dome, Canada for the financial support provided for this thesis and gratefully acknowledge Mike Aziz at Equity Silver Mine Ltd. for his help and keen interest in this study. The assistance of Morris, Jerry and Keith during site visits was also greatly appreciated.

I owe a special thanks to Dr. Malcolm Reeves from Geological Sciences for his assistance during the modelling program. I also extend thanks to the faculty of Civil Engineering at the University of Saskatchewan; including Dr. S. Lee Barbour, Dr. Gordon Putz, Dr. Bill Stolte, Dr. Jim Kells, Dr. Moir Haug and Dr. Dennis Pufahl. It was a privilege to receive advice from such a wide array of technical expertise that these professors exhibit. I would also like to thank Lori Newman for her help with SoilCover and her efforts with some of the data collection and reduction from the mine site.

Many new friendships were made during my years as a graduate student. I am grateful to Dwayne Rowlette, Man Feng, Thu Minh Trinh and Ravi Khanzode for their friendship and assistance in my graduate classes and during my research work.

I wish to acknowledge my parents for their involvement prior to and during this study. I thank my father for his diligence in the editing process of this thesis and his visits to the mine site. I also thank my mother for her endless support and encouragement.

I reserve special recognition for Jennifer who has stood by me since the beginning of this study, offering me boundless love and support. Words cannot express the sincere gratitude I feel for her patience and encouragement.

Table of Contents

| | |
|--|-----------|
| Abstract..... | i |
| Acknowledgments | iii |
| Table of Contents | iv |
| List of Tables..... | viii |
| List of Figures..... | x |
| | |
| Chapter 1 Introduction | 1 |
| 1.1 General Background and Site Description | 1 |
| 1.2 Purpose and Scope | 8 |
| 1.3 Thesis Outline..... | 10 |
| Chapter 2 Literature Review | 11 |
| 2.1 Introduction..... | 11 |
| 2.2 Previous Studies at Equity Silver Mine Ltd..... | 12 |
| 2.3 Hydrogeologic Characterization of Waste Rock Dumps | 15 |
| 2.4 Hydrological Characterization of Waste Rock Dumps | 22 |
| 2.5 Modelling Using FEMWATER..... | 28 |
| 2.6 Summary | 31 |
| Chapter 3 Theoretical Background | 32 |
| 3.1 Introduction..... | 32 |
| 3.2 Hydrologic Budget Equation | 33 |
| 3.2.1 Soil-atmosphere Interface Hydrologic Budget Equation | 33 |
| 3.2.2 Waste Rock Dump Hydrologic Budget Equation | 34 |
| 3.3 Formulation of Groundwater Flow..... | 38 |
| 3.3.1 Derivation of the Three Dimensional Groundwater Flow Equations | 38 |
| 3.3.2 Auxiliary Equations | 43 |
| 3.4 Formulation of FEMWATER..... | 45 |

| | | |
|------------------|---|------------|
| 3.5 | Solving Groundwater Flow Problems..... | 47 |
| 3.5.1 | Introduction to Solving Groundwater Flow Problems..... | 47 |
| 3.5.2 | The Finite Element Method Used in FEMWATER..... | 49 |
| 3.6 | Summary | 53 |
| Chapter 4 | Field Program | 55 |
| 4.1 | Introduction..... | 55 |
| 4.2 | Waste Rock Dump Piezometer Installation - Phase I..... | 55 |
| 4.2.1 | Becker Hammer Drill Rig..... | 55 |
| 4.2.2 | Testhole Completion and Piezometer Installation | 59 |
| 4.2.3 | Materials..... | 61 |
| 4.2.4 | Drill Hole Logs..... | 61 |
| 4.3 | Spring Runoff Response - Phase II..... | 69 |
| 4.3.1 | Surface Runoff..... | 69 |
| 4.3.2 | Waste Rock Dump Piezometer Levels..... | 76 |
| 4.3.3 | Seepage Flow Rates..... | 77 |
| Chapter 5 | Hydrologic Characterization | 79 |
| 5.1 | Introduction..... | 79 |
| 5.2 | Geologic Structure..... | 79 |
| 5.2.1 | Skeena Group..... | 86 |
| 5.2.2 | Tip Top Hill Formation..... | 88 |
| 5.2.3 | Goosly Lake Formation | 88 |
| 5.2.4 | Nanika Intrusion | 89 |
| 5.2.5 | Goosly Intrusion | 90 |
| 5.2.6 | Glacial Till..... | 90 |
| 5.2.7 | Waste Rock | 92 |
| 5.2.8 | Till Cover Material | 96 |
| 5.3 | Topography | 98 |
| 5.4 | Surface Hydrology..... | 104 |
| 5.4.1 | Hydrology | 105 |
| 5.4.1.1 | Precipitation..... | 105 |

| | | |
|------------------|--|------------|
| 5.4.1.2 | Sublimation and Mass Transfer of Snow..... | 106 |
| 5.4.1.3 | Water Fluxes..... | 107 |
| 5.4.1.4 | Measured Infiltration..... | 110 |
| 5.4.1.5 | Changes in Storage | 111 |
| 5.4.2 | Surface Water Measurements..... | 112 |
| 5.4.3 | Creeks and Diversion Channels | 114 |
| 5.4.4 | Seepage Faces | 114 |
| 5.4.5 | ARD Collection System..... | 118 |
| 5.4.6 | ARD Sumps | 120 |
| 5.4.7 | ARD Weirs..... | 122 |
| 5.5 | Groundwater | 124 |
| 5.5.1 | Regional Piezometers..... | 125 |
| 5.5.2 | Waste Rock Dump Piezometers..... | 129 |
| 5.6 | Water Chemistry | 132 |
| 5.6.1 | Surface Water..... | 133 |
| 5.6.2 | Creeks and Diversion Channels | 136 |
| 5.6.3 | Seepage Water..... | 136 |
| 5.6.4 | ARD Collection Water..... | 138 |
| 5.6.5 | ARD Sump Water..... | 139 |
| 5.6.6 | Piezometer Water | 140 |
| 5.6.6.1 | Regional Piezometers..... | 140 |
| 5.6.6.2 | Waste Rock Dump Piezometers | 143 |
| 5.6.7 | Runoff Water..... | 143 |
| Chapter 6 | Modelling Program | 144 |
| 6.1 | Introduction..... | 144 |
| 6.2 | Three Dimensional Mesh Generation | 144 |
| 6.2.1 | Conceptual Model | 145 |
| 6.2.2 | Two Dimensional Mesh | 146 |
| 6.2.3 | Triangulated Irregular Network (TIN) | 147 |
| 6.2.4 | Three Dimensional Mesh..... | 148 |

| | | |
|-------------------|--|------------|
| 6.3 | Boundary Conditions | 150 |
| 6.4 | FEMWATER Run Options | 151 |
| Chapter 7 | Data Analysis and Discussion | 153 |
| 7.1 | Introduction..... | 153 |
| 7.2 | Spring Freshet | 153 |
| 7.2.1 | Runoff..... | 153 |
| 7.2.2 | Waste Rock Dump Piezometers..... | 157 |
| 7.2.3 | Seepage Faces | 158 |
| 7.3 | FEMWATER Results..... | 159 |
| 7.4 | Water Chemistry | 164 |
| 7.5 | Water Budget | 167 |
| 7.6 | Summary | 170 |
| Chapter 8 | Summary and Conclusions | 171 |
| 8.1 | Summary of Thesis Objectives..... | 171 |
| 8.2 | Conclusions..... | 173 |
| 8.3 | Recommendations | 175 |
| 8.4 | Future Research | 175 |
| References | | 177 |
| Appendix A | Detailed Water Quality Analysis | A-1 |
| A.1 | Introduction..... | A-1 |
| Appendix B | Detailed Climatological and Hydrological Data | B-1 |
| B.1 | Introduction..... | B-1 |

List of Tables

| | | |
|------------|--|-----|
| Table 2.1 | Factors affecting waste rock dump hydrology (Whiting, 1985)..... | 23 |
| Table 4.1 | Waste rock dump piezometer configuration. | 61 |
| Table 4.2 | Drill hole log for P 97-01. | 63 |
| Table 4.3 | Drill hole log for P 97-02. | 64 |
| Table 4.4 | Drill hole log for P 97-03. | 64 |
| Table 4.5 | Drill hole log for P 97-04. | 65 |
| Table 4.6 | Drill hole log for P 97-05. | 66 |
| Table 4.7 | Description of runoff catchment areas. | 70 |
| Table 4.8 | Spring freshet response in the waste rock dump piezometers. | 77 |
| Table 5.1 | The stratigraphical column (after Blyth and Freitas, 1984)..... | 82 |
| Table 5.2 | Summary of hydraulic conductivities (after Klohn Leonoff, 1991b)..... | 85 |
| Table 5.3 | The till cover material properties (O’Kane, 1995)..... | 96 |
| Table 5.4 | Monthly precipitation (after Equity Silver Mine Ltd., 1997). | 105 |
| Table 5.5 | Summary of water fluxes. | 108 |
| Table 5.6 | Surface water elevations. | 113 |
| Table 5.7 | Creek hydraulic data. | 114 |
| Table 5.8 | Waste rock dump Seep coordinates..... | 116 |
| Table 5.9 | Waste rock dump seep flow data..... | 116 |
| Table 5.10 | Sump data. | 121 |
| Table 5.11 | Sump flow data..... | 121 |
| Table 5.12 | Weir coordinates..... | 123 |
| Table 5.13 | Weir flow data. | 123 |
| Table 5.14 | Regional piezometers coordinates. | 127 |
| Table 5.15 | Regional piezometer water level elevations. | 128 |
| Table 5.16 | Waste rock dump piezometer coordinates. | 130 |
| Table 5.17 | Waste rock dump piezometer water level elevations..... | 131 |
| Table 5.18 | Surface water chemistry..... | 134 |

| | | |
|------------|---|-----|
| Table 5.18 | Surface water chemistry, <i>continued</i> | 135 |
| Table 5.19 | Creek and diversion channel water chemistry. | 136 |
| Table 5.20 | Water quality for seepage discharge. | 137 |
| Table 5.21 | Water quality analysis for the ARD collection channels. | 138 |
| Table 5.22 | Sump water quality. | 139 |
| Table 5.23 | Regional piezometer water chemistry data..... | 141 |
| Table 5.23 | Regional piezometer water chemistry data, <i>continued</i> | 142 |
| Table 5.24 | Waste rock dump piezometer water chemistry. | 143 |
| Table 5.25 | Runoff water chemistry..... | 143 |
| Table 6.1 | Description of the three dimensional elements. | 149 |
| Table 7.1 | Summary of the runoff flow measurements..... | 154 |
| Table A.1 | Detailed chemical data for the surface water areas..... | A-2 |
| Table A.2 | Detailed chemical data for the waste rock dump seeps (Seep 97-01 to Seep 97-04)..... | A-3 |
| Table A.3 | Detailed chemical data for the waste rock dump seeps (Seep 97-05 to Seep 97-08)..... | A-4 |
| Table A.4 | Detailed chemical data for the waste rock dump seeps (Seep 97-09 to Seep 97-11)..... | A-5 |
| Table A.5 | Detailed chemical data for the waste rock dump seeps (S - 1, S - 2 and S - 3)..... | A-6 |
| Table A.6 | Detailed chemical data for the ARD collection system. | A-7 |
| Table A.7 | Detailed chemical data for the waste rock dump piezometers. | A-8 |
| Table A.8 | Detailed chemical data for runoff water..... | A-9 |
| Table B.1 | Climatological data. | B-2 |
| Table B.1 | Climatological data, <i>continued</i> | B-3 |
| Table B.1 | Climatological data, <i>continued</i> | B-4 |
| Table B.2 | Hydrological data for the waste rock dump area..... | B-5 |
| Table B.2 | Hydrological data for the waste rock dump area, <i>continued</i> | B-6 |
| Table B.2 | Hydrological data for the waste rock dump area, <i>continued</i> | B-7 |

List of Figures

| | | |
|-------------|---|----|
| Figure 1.1 | Location of Equity Silver Mine. | 2 |
| Figure 1.2 | Equity Silver Mine site plan. | 3 |
| Figure 1.3 | Diversion and Sludge Ponds and the Water Treatment Plant..... | 4 |
| Figure 1.4 | Main Zone Pit and Waterline Zone Pit in the background. | 5 |
| Figure 1.5 | Waste rock dump prior to till cover placement. | 7 |
| Figure 1.6 | Main Dump after till cover placement..... | 7 |
| Figure 1.7 | Acid rock drainage collection ditch. | 8 |
| Figure 2.1 | Structure of a waste rock dump (after Herasymuik, 1996)..... | 18 |
| Figure 2.2 | Laboratory column experiment (after Newman <i>et al.</i> , 1997)..... | 20 |
| Figure 2.3 | Hydraulic conductivity functions (after Newman <i>et al.</i> , 1997) | 21 |
| Figure 2.4 | Components of the hydrologic budget for La Mine Doyon (after Isabel <i>et al.</i> , 1997). | 26 |
| Figure 3.1 | Terms used in the surface hydrologic budget equation..... | 34 |
| Figure 3.2 | Terms used in the regional hydrologic budget equation. | 35 |
| Figure 3.3 | Representative elementary volume for groundwater flow. | 39 |
| Figure 3.4 | Problem solving methods for groundwater simulations. | 48 |
| Figure 4.1 | Becker Hammer drill rig..... | 56 |
| Figure 4.2 | Doubled walled casing construction. | 57 |
| Figure 4.3 | Cuttings from a Becker Hammer drill rig..... | 58 |
| Figure 4.4 | Plan of the piezometers installed in the waste rock dump..... | 60 |
| Figure 4.5 | Waste rock dump piezometer configuration diagram. | 62 |
| Figure 4.6 | Waste rock dump piezometer locations. | 62 |
| Figure 4.7 | Water content profile for the waste rock dump testholes. | 67 |
| Figure 4.8 | Paste pH profile for the waste rock dump testholes. | 68 |
| Figure 4.9 | Runoff stations and corresponding contributing areas..... | 70 |
| Figure 4.10 | Culvert flow instrumentation (R 98-01 station). | 71 |
| Figure 4.11 | Weir flow instrumentation (R 98-02 station). | 71 |
| Figure 4.12 | Weir flow instrumentation (R 98-03 station). | 72 |

| | | |
|-------------|--|-----|
| Figure 4.13 | Flow measurement for R 98-01..... | 73 |
| Figure 4.14 | Flow measurement for R 98-02..... | 74 |
| Figure 4.15 | Flow measurement for R 98-03..... | 75 |
| Figure 4.16 | Water level in the waste rock dump piezometers..... | 76 |
| Figure 4.17 | Waste rock dump seepage flow rate hydrograph..... | 78 |
| Figure 5.1 | General geology of the Buck Creek area (after Church and Barakso, 1990)..... | 80 |
| Figure 5.2 | Cross section (points A, B, and C in Figure 5.1) of the geology of the Buck Creek area (after Church and Barakso, 1990)..... | 81 |
| Figure 5.3 | Detailed geology of the Equity Silver Mine area (after Church and Barakso, 1990 and Klohn Leonoff, 1991b)..... | 84 |
| Figure 5.4 | Time scale of the geologic units at Equity Silver Mine..... | 85 |
| Figure 5.5 | Till isopachs..... | 91 |
| Figure 5.6 | Waste rock dump isopachs..... | 93 |
| Figure 5.7 | Grain size curves for three waste rock samples (Newman, 1994)..... | 94 |
| Figure 5.8 | Soil-water characteristic curves and the hydraulic conductivity relationships for three waste rock samples (Herasymuik, 1996)..... | 95 |
| Figure 5.9 | Grain size curve for the till cover material (O’Kane, 1995)..... | 96 |
| Figure 5.10 | Soil-water characteristic curves and the hydraulic conductivity relationship for the till cover material (Swanson, 1995)..... | 97 |
| Figure 5.11 | Natural topographical contours of Equity Silver Mine..... | 99 |
| Figure 5.12 | Natural three-dimensional topography of Equity Silver Mine..... | 100 |
| Figure 5.13 | Current topographical contours of Equity Silver Mine..... | 102 |
| Figure 5.14 | Current three-dimensional topography of Equity Silver Mine..... | 103 |
| Figure 5.15 | Monthly precipitation for the study period (Aziz, 1998)..... | 106 |
| Figure 5.16 | Water fluxes for the study period..... | 109 |
| Figure 5.17 | Components of the surface water budget..... | 110 |
| Figure 5.18 | Lysimeter data..... | 111 |
| Figure 5.19 | Drainage of the waste rock with cover construction..... | 112 |
| Figure 5.20 | Seep locations..... | 115 |

| | | |
|-------------|---|-----|
| Figure 5.21 | Waste rock dump seep flow rates..... | 117 |
| Figure 5.22 | ARD collection system..... | 119 |
| Figure 5.23 | ARD collection flow chart. | 120 |
| Figure 5.24 | Sump flow rates for the study period..... | 122 |
| Figure 5.25 | Weir flow rates for the study period. | 124 |
| Figure 5.26 | Regional piezometer locations..... | 126 |
| Figure 5.27 | Water levels versus time for the regional piezometers..... | 129 |
| Figure 5.28 | Waste rock dump piezometer locations. | 130 |
| Figure 5.29 | Water levels versus time for the waste rock dump piezometers..... | 132 |
| Figure 6.1 | Conceptual model. | 145 |
| Figure 6.2 | Two dimensional mesh..... | 146 |
| Figure 6.3 | Three dimensional mesh. | 149 |
| Figure 6.4 | Boundary conditions. | 150 |
| Figure 7.1 | Available runoff from total precipitation during the freezing period..... | 155 |
| Figure 7.2 | Comparison between daily air temperature, incoming radiation and R 98-02 flow rate..... | 156 |
| Figure 7.3 | Computed pressure heads in the waste rock dump area for non- continuous till and 30 % of precipitation recharge rate. | 161 |
| Figure 7.4 | Total head in the fractured rock for non-continuous till and 30 % of precipitation recharge rate. | 161 |
| Figure 7.5 | Total head in the glacial till for non-continuous till and 30 % of precipitation recharge rate..... | 162 |
| Figure 7.6 | Total head in the waste rock for non-continuous till and 30 % of precipitation recharge rate..... | 163 |
| Figure 7.7 | Conductivity of seepage discharge. | 166 |
| Figure 7.8 | Acid rock drainage flow rates out of the waste rock dump. | 169 |
| Figure 7.9 | Water balance components of the acid rock drainage..... | 170 |

Chapter 1 Introduction

1.1 General Background and Site Description

Equity Silver Mine is located 575 km north northwest of Vancouver (see Figure 1.1). The mine is located in the central interior of British Columbia in the Omineca Mining Division (O’Kane, 1995). It is situated in the Buck Creek area at an approximate elevation of 1,300 m above mean sea level on the drainage divide between Foxy and Buck Creek (Church and Barakso, 1990). The orebody was discovered in 1967, followed by construction of the mining facilities in 1979 and the beginning of mining operations in 1980 (Church and Barakso, 1990). The mine ceased operations in 1994 due to lack of economic minerals. A collection and treatment facility has been operating since 1981 to abate the acid rock drainage (ARD) problems discovered in 1981. The ARD flows in the recent past have been extremely higher than expected and virtually unchanged since placement of a soil cover. The high flow rates form the main objective of this thesis. A detailed drawing of the site plan is shown in Figure 1.2.

The coordinate units shown in Figure 1.2 are specific for the Equity Silver Mine. They are the UTM (Universal Transverse Murcator) coordinate units minus 6,000,000 for the northings and the UTM coordinate units minus 670,000 for the eastings.

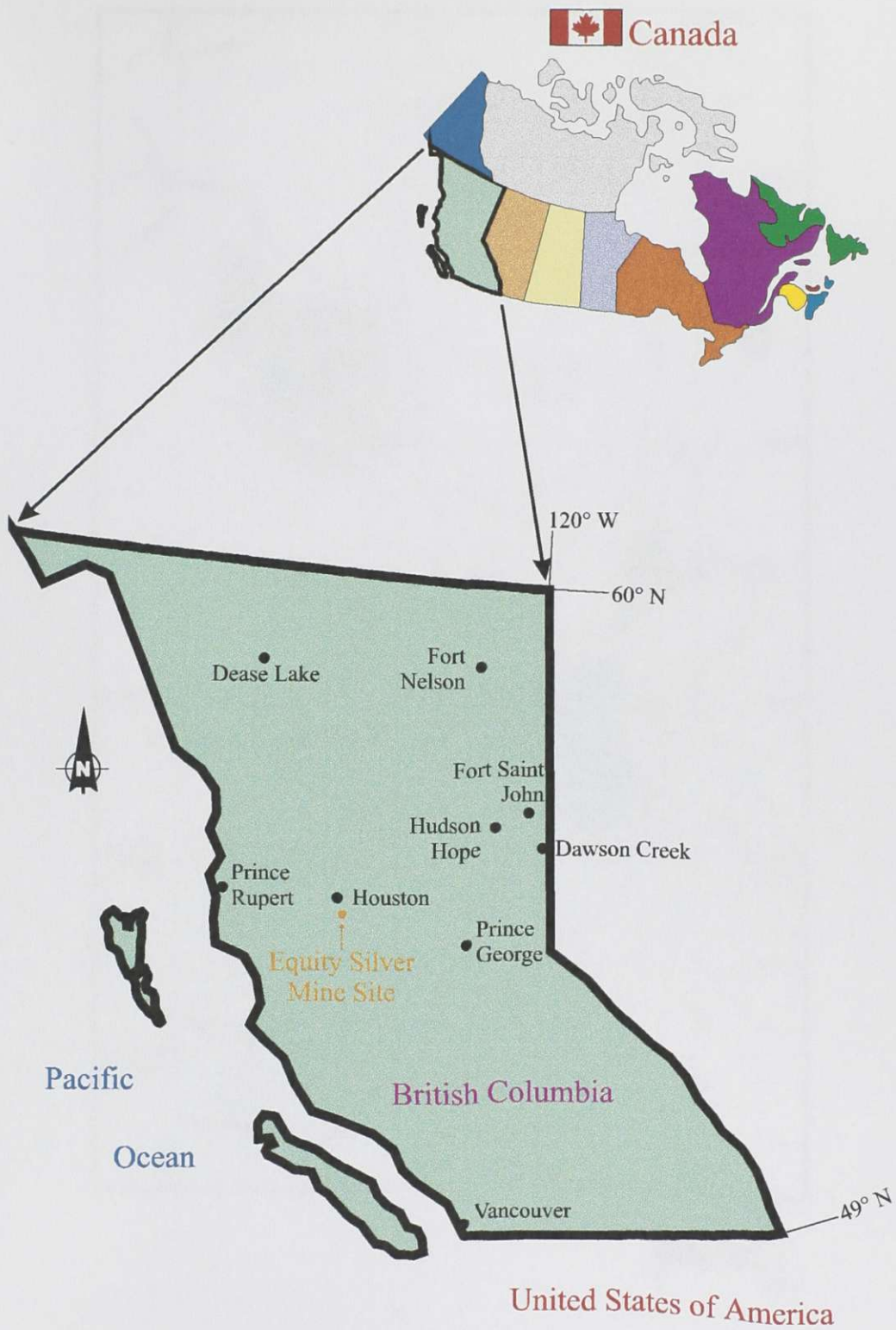


Figure 1.1 Location of Equity Silver Mine.

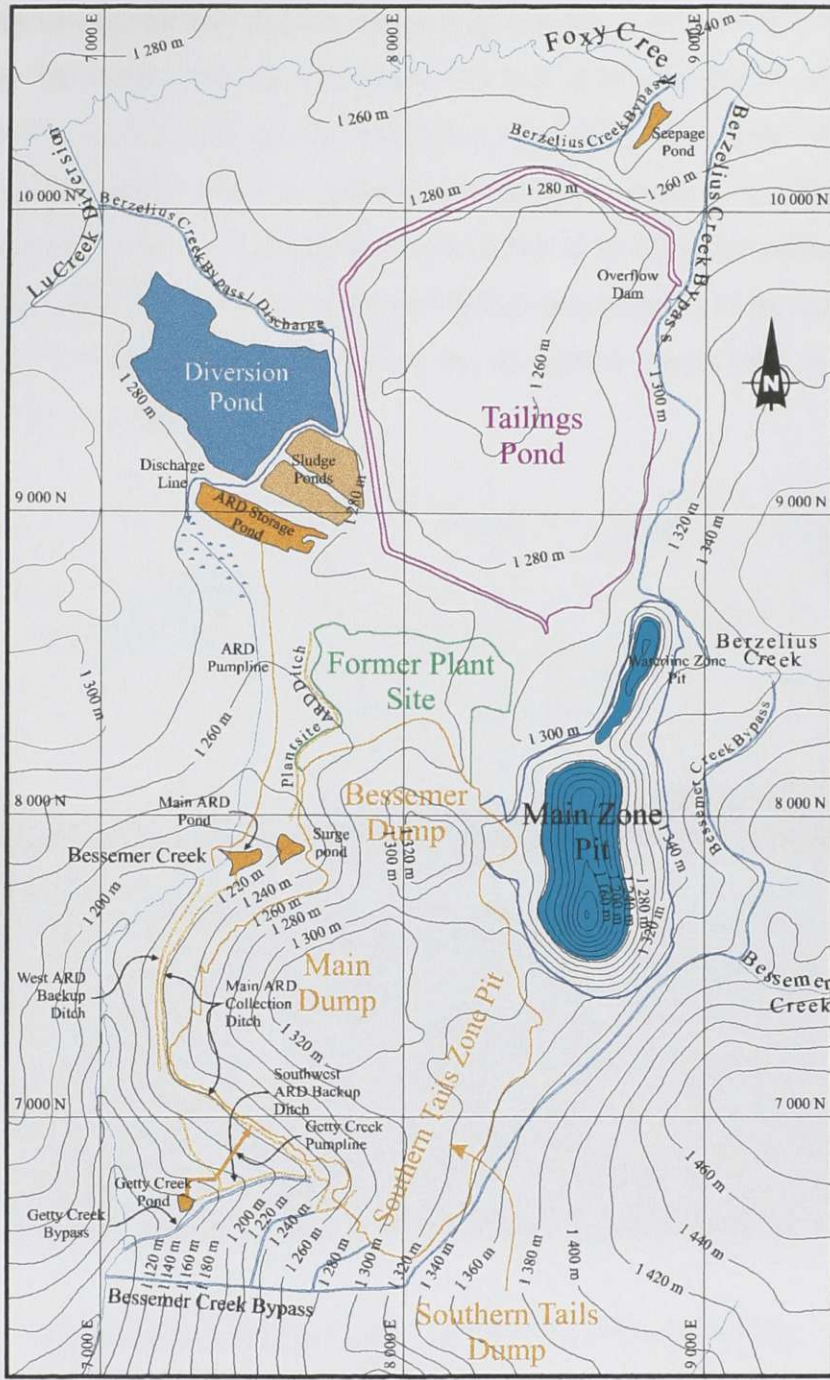


Figure 1.2 Equity Silver Mine site plan.

The mine was an open pit and underground mining operation with a 9,000 tonne per day mill capacity. The mining operation consisted of a haul truck and shovel method for the open pits and a scoop tram for the underground portion. Economic minerals were extracted from the ore by crushing, grinding and floatation circuits. A 120 hectare (ha) tailings pond north of the mining area was constructed to facilitate the milling operation. Four economic mineral zones were developed during the operation of the mine and three waste rock piles were constructed to house the 80 million tonnes (Mt) of waste rock covering 117 ha of surface area.



Figure 1.3 Diversion and Sludge Ponds and the Water Treatment Plant.

Four mining zones were developed: Southern Tails Zone, Main Zone, Waterline Zone and the North Zone (north of the Waterline Zone). The Southern Tails orebody contained 7.2 Mt and milling began in April, 1980 with a 4,000 tonne per day mill. The Southern Tails orebody production ceased in May, 1984. The Southern Tails Zone Pit is currently filled with waste rock from the Main Zone Pit and the general area is referred

to as the Southern Tails Dump in this thesis. The mill capacity increased with a scavenger circuit installed to recover a greater percentage of the precious metal (Church and Barakso, 1990). Open pit mining of the 29 Mt Main Zone area began in March, 1983 and was completed at the end of 1991. The Waterline Zone, northeast of the Main Zone, was developed for open pit mining in 1988 until closure in early 1994. Underground mining in the North Zone, north of the Waterline Zone, began in August, 1992 and was completed in early 1994.



Figure 1.4 Main Zone Pit and Waterline Zone Pit in the background.

The most abundant metallic mineral in the waste rock and the mineralized zones was pyrite, FeS_2 (Wright Engineers Limited, 1976) at 3.8 % (Church and Barakso, 1990). The high pyrite content of the waste rock leads to pyrite oxidation, resulting in acid rock drainage. Acid rock drainage is defined as the water that is drained through an oxidizing zone of sulphide minerals. The oxygen in the air and water oxidizes the sulphide minerals. The water is characteristically low in pH and has the ability to carry heavy metals in

solution. These heavy metals in solution, coupled with the low pH, migrate through the groundwater system and have detrimental effects on the receiving environment. Acid rock drainage is extremely toxic to aquatic life.

The waste rock dump contains 80 Mt of material and has a projected area of 117 ha and a surface area of 125 ha. The waste rock dump is subdivided into three individual waste rock dumps: the Main Dump, Southern Tails Dump and the Bessemer Dump. The waste rock dumps were constructed directly on the cleared ground surface (Klohn Leonoff, 1984). The Main Dump was constructed first with the development of the Southern Tails Zone in 1980. The Main Dump contains 52 Mt of material and covers 47 ha. Backfilling of the Southern Tails Dump started in 1985 when the open pit mining operations ceased in 1984. This dump contains 18 Mt of waste rock with a surface area of 36 ha. The Bessemer Waste Dump contains 10 Mt of material covering an area of 34 ha. The former plant site occupies an area of 25 ha.

The waste rock is shown in Figure 1.5, photographed in the fall of 1993. The location is the north side of the Main Dump, viewed from the Low Grade 2 section. The individual layers are easily defined in this figure. The inclined layers represent successive end dumping from trucks during construction of the waste rock dump. The horizontal layers suggest leveling of the waste rock between end dumping.

A till cover was placed over the dump in partial portions from 1991 to 1997. The cover consists of 0.3 m of non-compacted till over 0.5 m of compacted till. The purpose of the cover is to reduce acid rock drainage by limiting oxygen and water flux into the underlying waste rock.



Figure 1.5 Waste rock dump prior to till cover placement.



Figure 1.6 Main Dump after till cover placement.

A water collection system was constructed to transport the acid rock drainage to the water treatment plant where it is treated with lime to neutralize the acidic water. This increase in pH causes most of the toxic heavy metals to precipitate, resulting in water suitable for discharge into the environment.



Figure 1.7 Acid rock drainage collection ditch.

1.2 Purpose and Scope

Equity Silver Mine has been reporting an inequality in the water balance for the waste rock dump during the past three years. SoilCover (1997) modelling predicts that 3 % of total precipitation infiltrates through the cover into the dump (Swanson, 1995). Measurements from lysimeters installed beneath the cover support these values. However, the seepage discharge collected in the ditches indicates that infiltration rates through the dump are approximately an order of magnitude greater than the lysimeters

measurements and SoilCover Modelling. Several explanations may account for this phenomenon:

1. The cover is leaking in certain areas,
2. The waste rock dump has not yet reached a state of equilibrium and is still draining water,
3. Groundwater is infiltrating into the waste rock dump in response to a regional groundwater flow regime system or
4. Infiltration through the cover is higher than expected.

The primary object of this thesis project is to characterize the complete hydrologic system for the waste rock dump. This characterization includes five major topics:

1. Geologic structure,
2. Topography,
3. Surface hydrology,
4. Groundwater and
5. Water chemistry.

A surface hydrologic (water) budget analysis for the waste rock dump was performed in order to account for precipitation, runoff, evapotranspiration, sublimation, mass transfer (snow) and infiltration. The groundwater component that enters into the waste rock dump is a part of the regional hydrologic system. The groundwater flow regime for the waste rock dump area was modelled in order to assess this component. The determination of the hydrologic components will lead to a clearer understanding of the surface and regional hydrologic systems and will allow future predictions for acid rock drainage with respect to variations in climate.

1.3 Thesis Outline

This thesis examines the hydrological characterization of a sulphide waste rock dump. Chapter 2 reviews the current literature available that pertains to this thesis project. The theoretical principles and processes are included in Chapter 3. A two phase field program was initiated and is described in Chapter 4. The hydrologic system is characterized in Chapter 5 while Chapter 6 describes the groundwater modelling program. Discussions and analysis is provided in Chapter 7 followed by the summary and conclusions in Chapter 8.

Chapter 2 Literature Review

2.1 Introduction

Limited knowledge exists on the quantity and characteristics of water flow through waste rock dumps but it is crucial in terms of predicting water quantities and quality of the toe discharge. Determining individual components of the hydrologic budget is difficult and requires extensive instrumentation; including piezometers, a meteorological station, flow rates on toe discharge and runoff and the following information: hydrological, hydrogeological, and topographical data as well as soil properties and water quality. Most mine sites do not have all of the required instrumentation or data, however, partial data usually exists and predictions of water movement may be made based on other extensive studies.

The following sections review the literature pertaining to hydrologic studies on waste rock dumps or in particular the waste rock dump at Equity Silver Mine. Previous studies at the mine site are reviewed and hydrogeologic and hydrologic studies on waste rock dumps are discussed. Literature pertaining to modelling of groundwater flow regimes is also reviewed.

2.2 Previous Studies at Equity Silver Mine Ltd.

Equity Silver mine is a large acid producing site and several research reports and theses are available regarding the acid rock drainage problem. A hydrogeological investigation was conducted by Golder Associates (1983) which preceded Kohn Leonoff (1991b). The purpose of the Golder Associates (1983) study was to evaluate the quantity and quality of groundwater in the vicinity of the mine site, to evaluate the impact of mining activities on the groundwater quality and to estimate the dewatering requirements for the Main Zone Pit. The report identified several recharge areas including the Tailings Pond and exposed fractured rock at high elevations. The groundwater flow regime was depicted as a typical regional flow system and the weathered bedrock was identified as the primary flow path. The Tailings Pond was indicated as a low risk source of contamination in the surrounding creeks while the weathered altered Nanika Intrusion was identified as a high risk in terms of contaminant migration due to its high hydraulic conductivity and proximity to Bessemer Creek.

Kohn Leonoff (1991b) conducted a hydrogeological study on the mine site. The purpose of the study was to develop a groundwater flow model for the existing hydrogeology and subsequently predict post closure groundwater conditions. One of the conditions was that the Main Zone Pit be full of water. The fractured bedrock was found to be the primary flow path for the area. Kohn Leonoff (1991b) described the hydrogeology as groundwater that originates in the uplands to the east and west of the site and flows to either Bessemer or Getty Creek or local sinks such as the open pits. The local flow paths are altered by the structure of the fractured bedrock.

Kohn Leonoff (1991b) calculated that approximately 50 % of the average total precipitation reports to the ARD collection system. Precipitation, watershed areas and ARD pumping records were used to determine these results. Possible flow paths from the waste dump to Bessemer Creek vary in length from 250 m to 1,000 m. The travel time for groundwater to pass through the till and into the weathered bedrock was estimated by

the computer model to vary between 0.5 and 5 years. Groundwater flow rates in the weathered bedrock were estimated to be between 1 m/year and 500 m/year. The report included a water balance over the contributing ARD collection area in order to calibrate the computer model. The MODFLOW model suggested that a total of 372,000 m³/year of water (25 % of total precipitation) passed through the waste rock dump and into the ARD collection system and 0.3 % may be discharged into the creeks. The groundwater simulation was run with the Main Zone Pit at a water elevation of 1,300 m. This would produce an increase of 10 % of the water from the waste rock dump into the ARD collection system. This increase, however, would be counteracted by decreases in flow from the Tailings Pond and the Former Plant Site to an overall value slightly lower than the current conditions.

KPA Engineering Ltd. (1993) performed a surface water hydrological study for the mine area. The main purpose of the study was to determine maximum flow rates for the design of drainage ditches. Flood unit discharge curves and hydrographs were determined. The mean monthly hydrograph yielded an annual average of 10.9 L/s/km² (not including seepage) for undisturbed catchments and approximately 9.8 L/s/km² (not including seepage) for the waste rock dump. The 24 hour flood hydrograph yielded a 24 hour average of 700 L/s/km² for a 200 year return flood event. It is interesting to note that the report explains that an estimated 95 % of the snow was shed or lost due to evaporation; however, the ARD flow was in the same magnitude as the runoff. The explanation given was that groundwater east of the Southern Tails Dump may be entering the waste rock dump by way of the Southern Tails Zone Pit. The report further suggested that ARD flows may not be substantially decreased with the soil cover since groundwater will still enter the dump and emerge as acid rock drainage.

Swanson (1995) studied the moisture movement in waste rock dump covers for wet and dry conditions. Equity Silver Mine represented the wet site and a mine in Montana represented the dry site. The soil cover systems were modelled with SoilCover (1997) which is a one dimensional finite difference model for water movement in soils.

SoilCover incorporates both heat and mass (liquid water and water vapor) transfer in soil cover systems in response to atmospheric forcing. The hydraulic and thermal soil properties were determined for input into the model.

Swanson (1995) determined that the SoilCover model was a valid tool in describing field conditions. The model calibration required daily readings of climate data to ensure accurate results. The most important climate parameter was net radiation while the most critical soil parameter was the saturated hydraulic conductivity and the air entry value. The modelling suggested an infiltration rate of 3 % of precipitation through the cover suggesting a low hydraulic conductivity of the cover material. Oxygen diffusion was calculated as a 98 % reduction from uncovered conditions.

O'Kane (1995) studied the instrumentation and the monitoring of the waste rock cover. The ability of the cover to reduce the flux of oxygen and water into the waste rock material was examined. Laboratory and field instrumentation of the cover material was performed in order to analyze the performance of the cover. The laboratory program consisted of the analysis of the following parameters: grain size distribution, Proctor curve, soil-water characteristics and consolidation. A weather station was installed at the mine site to assess the climate data, including precipitation, air temperature, relative humidity, wind speed and direction and net radiation. Instrumentation of the soil cover included: matric suction, gaseous oxygen, soil temperature and water content.

O'Kane (1995) showed that the cover maintained a high degree of saturation throughout the yearly cycle, thus restricting the ingress of oxygen into the underlying waste rock. The oxygen concentrations in the waste rock decreased with time supporting the positive performance of the cover. Lysimeters showed that as low as 4 % of the total precipitation infiltrated through the soil cover which is close to the 3 % value determined by Swanson (1995). Infiltration into uncovered waste rock may be as high as 70 % of the total precipitation (O'Kane, 1995). Soil suction profiles indicated that there was an upward hydraulic gradient in the soil cover for all periods other than the spring freshet

and heavy rainfall events in the fall. The study also confirmed that the erosion layer provided freeze / thaw protection of the lower compacted cover layer.

2.3 Hydrogeologic Characterization of Waste Rock Dumps

Whiting (1985) discusses the pollution potential of waste rock dumps in terms of hydrogeology and hydrology. There is inherently some overlap between these sciences, hence this paper is also reviewed in Section 2.4. Whiting (1985) also discusses some of the geochemical reactions that take place within waste rock dumps and the subsequent characteristics of the quality of discharge water.

The mobility of metallic compounds from the dump is dependant on several factors, including: composition of the waste rock, hydraulic conductivity characteristics of underlying soils and bedrock as well as the frequency of bedrock fractures (Whiting, 1985). The major physical factors relating to waste rock dump hydrology is presented in Table 2.1.

The hydraulic conductivity of waste rock is initially high as the rock is usually dumped and has not undergone any compression or physical and chemical alteration. The hydraulic conductivity will, however, decrease with time once subjected to these processes. The alteration process will lead to channeling in the waste rock dump as the groundwater will flow in the path of least resistance. The method of dump construction will lead to stratification or segregation as fine material will typically be separated from the course material during end dumping. This will result in gross heterogeneity and anisotropy and hydraulic conductivities may vary over two orders of magnitude throughout the waste rock (Whiting, 1985). The contrast in material properties within the waste rock dump may lead to preferential flow paths in the dump (Herasymuik, 1996 and Newman *et al.*, 1997).

Smith *et al.* (1995) conducted a comprehensive study of waste rock dumps including the hydrostratigraphy, hydrogeology, monitoring and work plans of waste rock dumps on a micro and macro scale. The report identifies the importance of understanding water flow through waste rock due to its effect on the contamination of the environment. Smith *et al.*, (1995) state the most important parameters for hydrological characterization are: water content and temperature in the unsaturated zone, water table elevation, discharge rates at the toe of the dump, rainfall and air temperature.

Smith *et al.* (1995) examines the hydrostratigraphy by distinguishing the waste rock as either a rock-like or soil-like material at approximately the 20 % sand content point (by mass). The method of dump placement can affect the hydrostratigraphy; for example, the degree of segregation caused by end dumping as opposed to free dumping. This report recognizes that an infinite number of hydrostratigraphic systems can result, depending on the texture and placement procedure of waste rock. These systems often include highly heterogeneous and anisotropic material.

Water tables may develop in waste rock dumps due to the following conditions (Smith *et al.*, 1995):

- Seepage into the dump as a result of groundwater discharge;
- Clogged channels in rock-like waste rock;
- Perched water table due to the topographic lows of the previous ground surface;
- Perched water tables as a result of layers of compacted waste rock on travel roads or
- Perched water tables as a result of a layer of fine material.

Smith *et al.* (1995) states that the hydrostratigraphy is best characterized by temperature profiles within the waste rock. The temperature is proportional to the water movement since the chemical reactions that take place in oxidizing sulphide minerals are exothermic.

The fluctuation of the water table in response to infiltration is based on the spatial distribution of hydraulic conductivity (Smith *et al.*, 1995).

Piezometer water level hydrographs are useful instruments in determining the hydraulic conductivity of the waste rock (Smith *et al.*, 1995). The hydraulic conductivity of a waste rock dump can also be characterized by using the kinematic wave theory, given an outflow hydrograph and a rainfall hydrograph. This technique is explained later (Germann and Beven, 1985).

Herasymuik (1996) examined the physical and hydrogeologic characteristics of a sulphide waste rock dump. The characteristics of water flow from the exterior of the waste rock dump to the toe discharge are important in terms of predicting water quality. Hydrogeologic characterization of waste rock dumps are often difficult, as they are usually unsaturated, structured and heterogeneous.

Herasymuik (1996) determined the internal structure, hydrogeologic properties and moisture distribution upon relocation of a waste rock dump. Hence, the characteristics of the unsaturated heterogeneous flow were determined.

The waste rock dump construction consisted of an end dumped, terraced configuration. This procedure led to successive tilting layers (40°) of fine and coarse layers. The fine and coarse layers were predominant as other intermediate layers were insignificant in terms of varying grain sizes. Thin horizontal layers of compacted waste rock resulting from haul trucks and leveling practices of bulldozers separated the tilting layers. Segregation of the waste rock, due to gravity, produced a coarse rubble zone at the bottom of the pile because of end dumping practices. The waste rock weathered dramatically with time (Herasymuik 1996). The structure of the waste rock dump can be seen in Figure 2.1.

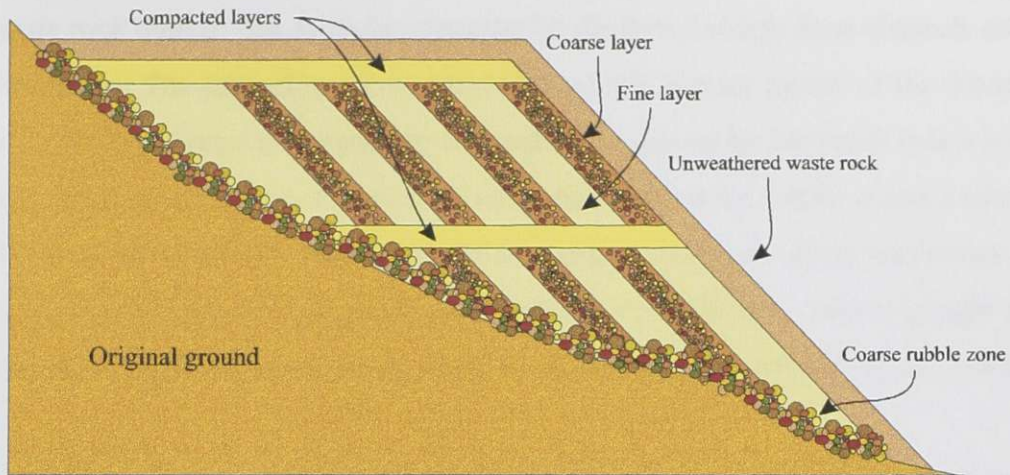


Figure 2.1 Structure of a waste rock dump (after Herasymuik, 1996).

A wetting front was identified at the top of the dump, supported by higher volumetric water contents of 9 % while volumetric water contents at the base were approximately 2 %. The fine layers had greater ability to retain water during unsaturated conditions and were thus found to be the main avenue of flow. The hydraulic conductivity was four orders of magnitude higher for the fine material at the water contents experienced (approximately 4 kPa matric suction). Water vapor flow was also shown to be a significant process responsible for water removal from the waste rock dump. The vapor originates from evaporation of liquid water in the fine layers which is then transported through the coarse layers (Herasymuik, 1996).

López *et al.* (1997) uses the kinematic wave theory (Germann and Beven, 1985) to characterize infiltrating water through a waste rock dump. The flow paths are assumed to be through vertical channels or macropores and the unsaturated porous matrix. Factors like toe discharge and rainfall hydrographs are used to determine the internal structure and hydraulic conductivity of the waste rock dump.

The kinematic wave theory is based on a water balance approach in the channels and the porous matrix. The channels are assumed to act independently, that is to say, they are not interconnected. However interconnected channels are the rule rather than the exception

for waste rock dumps. The formulae characterize the flow through these channels and the porous matrix. The time of travel of water through the porous matrix of the dump and exiting as toe discharge is assumed to be small as compared to the travel time of water through the channel system. Sorption of water into the porous matrix is also accounted for and is based on mineral composition and the porous structure of the waste rock. The toe discharge hydrograph represents outflow from the collective channel groups while the rain hydrograph represents water input to the system (Germann and Beven, 1985).

The application of the model entails three main steps: 1) Toe seepage hydrographs are used to determine the range of the base flow recession coefficient. 2) The physical parameters including number of channels, channel conductance, areal portion of channels and matrix sorbance coefficient must also be determined. Some of these parameters may be determined using rain and toe seepage hydrographs. 3) A new toe seepage hydrograph produced by a rainfall event is constructed and then compared to the observed toe discharge hydrograph (López *et al.*, 1997).

The kinematic wave theory approach for uncovered dumps was taken using data from an actual mine site. The results suggest that the kinematic wave theory is applicable in describing large scale water flow through waste rock piles. There is, however, further research necessary in describing the water flow recession portion of the hydrograph, modelling actual rain events as opposed to square pulses and characterizing discontinuous flow channels (López *et al.*, 1997).

López *et al.* (1997) stresses the need for the simultaneous collection of internal hydrogeologic responses in the waste rock, toe seepage hydrograph and rainfall hydrographs to completely characterize the hydrogeology of a waste rock dump using the kinematic wave theory.

Newman *et al.* (1997) examined unsaturated preferential flow in heterogeneous waste rock dumps. The theory is based on the characteristics of the hydraulic conductivity

function and the soil-water characteristic curve. Water flow through a vertical column of coarse and fine material is measured and modelled as seen in Figure 2.2. The experiment simulates the water flow through the structure of a waste rock pile that is constructed from end dumping which results in tilting layers of fine and coarse material. The waste rock that was modelled was described by Herasymuik (1996) and seen in Figure 2.1.

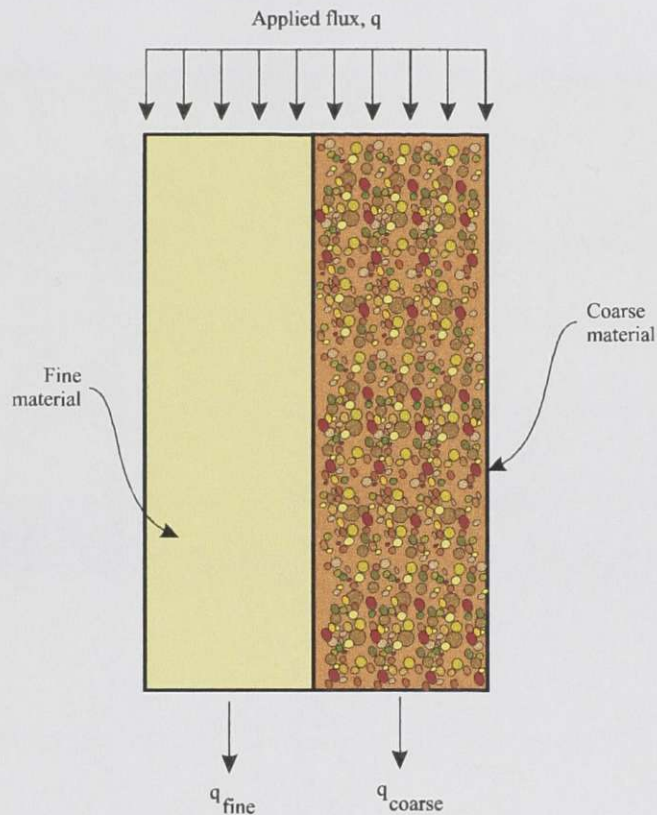


Figure 2.2 Laboratory column experiment (after Newman *et al.*, 1997)

Water flow in saturated soils follows Darcy's Law, in that the flux is equal to the hydraulic conductivity multiplied by the hydraulic gradient. The same is true in the unsaturated zone; however, the hydraulic conductivity is a function of the matric suction. If the hydraulic gradient is assumed to be one (i.e. the change in hydraulic head is equal to the change in elevation head), the flux is then equal to the hydraulic conductivity. The hydraulic conductivity is almost constant in the saturated zone and may decrease several orders of magnitude in the unsaturated zone, as described by the hydraulic conductivity

function. Coarse materials usually have a high saturated hydraulic conductivity, low air entry value and a rapidly decreasing hydraulic conductivity with increasing matric suction while fine materials are usually the opposite as seen in Figure 2.3. This leads to a reversal in the magnitudes of hydraulic conductivity values for the two materials at the crossover value. The fine material will have a greater hydraulic conductivity than the coarse material at matric suctions greater than the crossover value.

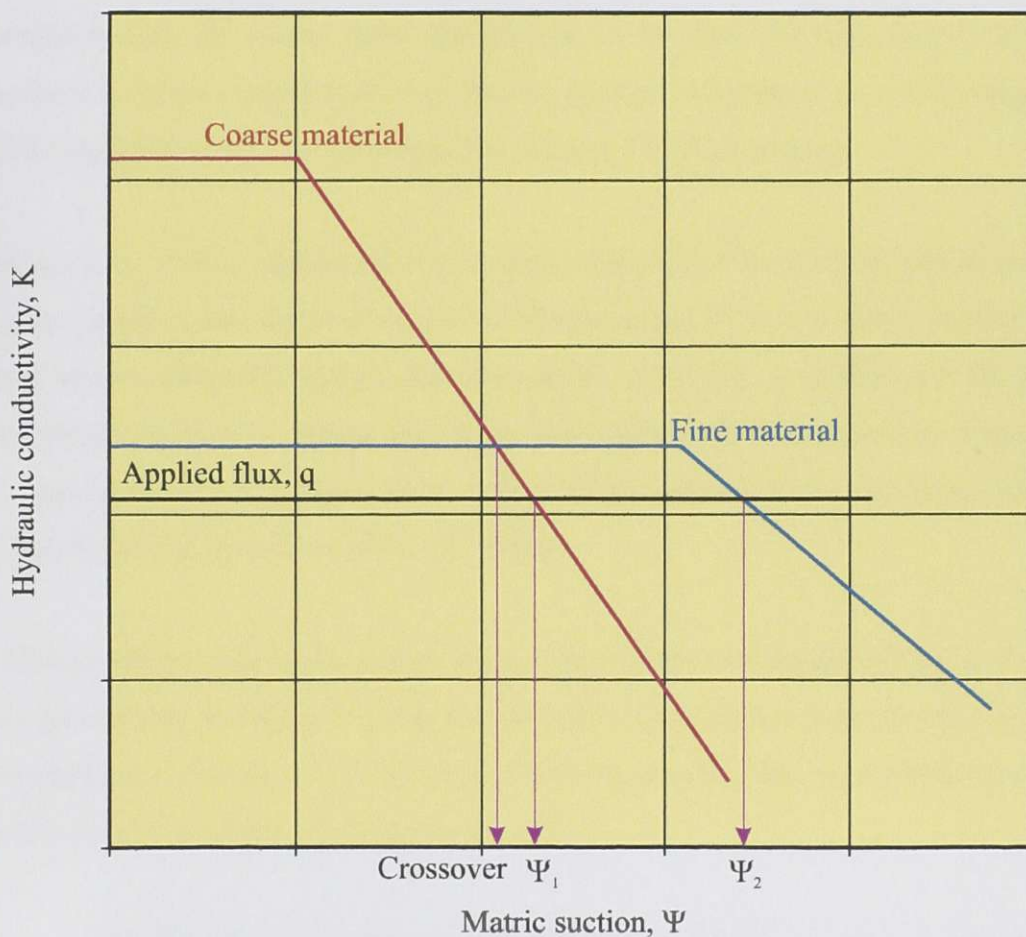


Figure 2.3 Hydraulic conductivity functions (after Newman *et al.*, 1997)

Water initially flows through the fine and coarse layers when a flux is applied to the surface of both materials. Water flow in the coarse material will transfer to the fine material once the crossover value of matric suction is reached. This phenomenon is known as preferential flow. This process will only take place when the applied flux is less

than the saturated hydraulic conductivity of the fine material as illustrated in Figure 2.3. Preferential flow will not take place at flux values greater than the saturated hydraulic conductivity of the fine material. This concept is in contradiction to previous speculations of flow occurring through the coarse macro-pore channels (Newman *et al.*, 1997).

The suctions of the material will be the same and will fall between the values shown in Figure 2.3 (Ψ_1 and Ψ_2). It is clear that the fine material will have a greater hydraulic conductivity than the coarse, hence the majority of the flow will take place in the fine material at a value of matric suction in the stated range. Newman *et al.* (1997) states the partitioning of flow as 97 % in the fine material and 3 % in the coarse.

Newman *et al.* (1997) also stated that another crossover of flow would take place near the water table; in fact the re-crossover will occur at the crossover matric suction. This occurs because the matric suction decreases as the water table is reached and the values of hydraulic conductivity change once again (see Figure 2.3). Once saturation is reached, the coarse material has a higher value of hydraulic conductivity and will thus transport the majority of the flow (Newman *et al.*, 1997).

An adverse effect on the water quality drained from waste rock dumps will occur if water flows through fine materials. The fine material has a large surface area per unit mass and will experience a high degree of oxidation. Oxidizing layers of fine material may also lead to slope stability problems (Newman *et al.*, 1997).

2.4 Hydrological Characterization of Waste Rock Dumps

Whiting (1985) reviewed waste rock dump hydrology and the related potential of polluting the environment. A list of the main factors affecting the waste rock dump hydrology is listed in Table 2.1 and is grouped into three main areas: physical, chemical and others (Whiting, 1985).

Table 2.1 Factors affecting waste rock dump hydrology (Whiting, 1985).

| Physical | Chemical | Others |
|------------------------|----------------------------|---------------------------|
| Stratification | pH control | Pollution control methods |
| Channeling | Precipitation / hydrolysis | Precipitation rates |
| Segregation | Temperature | Evaporation |
| Sorption | Alteration | Transpiration |
| Foundation | Oxidation | |
| Hydraulic conductivity | Solution type | |
| Construction method | | |

Infiltration into waste rock dumps can originate from rainfall, snowmelt, runoff from surrounding regional areas and groundwater discharge into the dump (Whiting, 1985). Precipitation onto the dump cannot be avoided, however, diversion ditches can be constructed to divert runoff water from the dump itself and surrounding regional areas. Groundwater discharge into waste rock dumps can be partially controlled with drainage ditches, pumps, varying pond heights with pumping, etc. (Whiting, 1985).

Runoff from waste rock dumps is dependant on the following factors: transpiration and evaporation characteristics, infiltration into the dump and underlying materials plus topographic features of the dump and the surrounding regional area that is within the catchment area (Whiting, 1985).

A comprehensive hydrologic budget analysis was performed by Isabel *et al.* (1997) on a large acid producing waste rock dump in eastern Canada (La Mine Doyon, Quebec). The purpose of the study was to determine the amount of infiltration into the waste rock, which is discharged as acid rock drainage. The objectives of the report were as follows: build a hydrologic database, present methodologies for monitoring hydrological processes and to present a comprehensive hydrologic budget for the waste rock dump. The hydrologic budget equation used in this analysis is shown in Equation [2.1].

$$P - R - \Delta S - ET - G - B = 0 \quad [2.1]$$

Where: P = Total precipitation (mm)
R = Runoff (mm)
 ΔS = Change in storage (mm)
ET = Evapotranspiration (mm)
G = Groundwater seepage (mm)
B = Base flow (mm)

The methodology used by Isabel *et al.* (1997) to assess the components of the hydrologic budget were derived from measurements of the following instruments: weather stations, weir stations, piezometers and lysimeters.

Isabel *et al.* (1997) determined precipitation using meteorological data from a weighted average of three surrounding regional weather stations. The total precipitation in 1991 and 1992 was 832 mm and 875 mm respectively, with a mean precipitation of 855 mm.

Runoff was calculated using base flow separation from hydrographs measured at weir stations based on the rainfall hydrograph. The average total runoff coefficient was about 0.06 (or 6 % of total precipitation), which represents the waste rock dump and a portion of the surrounding area (47 % of the total area) that was included in the weirs catchment area. The runoff was the surface runoff only, which excluded surficial flow and base flow or groundwater recharge. The runoff coefficient was analyzed in terms of surface type and topography. Portions of the waste rock dump were steep while others were level and the surface types are composed of vegetation, earth fill, bedrock outcrop and waste rock (Isabel *et al.*, 1997).

Isabel *et al.* (1997) states that the change in storage should not exceed 5 % of total precipitation and the waste rock is assumed to be at this value. The water contents within

the dump have not yet increased to a state of equilibrium; thus, the maximum amount was assumed.

Evaporation from the uncovered waste rock surface was calculated at 57 % of the total precipitation by using the hydrologic budget equation seen in Equation [2.1]. Transpiration was assumed to be negligible since no vegetation exists (Isabel *et al.*, 1997).

In order to calculate the groundwater flow component, the groundwater flow regime was modelled using MODFLOW (a three dimensional finite difference groundwater model) which runs within the GMS interface. The geology consisted of 130 m of deep bedrock overlain by 5 m of fractured bedrock with hydraulic conductivities of 3.45×10^{-9} m/s and 1.04×10^{-6} m/s respectively. A 5 m silty clay layer covers the fractured bedrock with a hydraulic conductivity of 6.98×10^{-7} m/s. The 30 m thick waste rock has a hydraulic conductivity of 1.00×10^{-3} m/s. Upon model calibration, 8 % of the total precipitation flowed out of the waste rock dump and into the regional groundwater flow regime system, suggesting that the dump was located in a groundwater recharge area (Isabel *et al.*, 1997).

The base flow into the waste rock was calculated at 23 % of the total precipitation from the results of MODFLOW. The base flow yielded 25 % of total precipitation using the base flow separation technique; however, the 23 % value was used in determination of the hydrologic budget (Isabel *et al.*, 1997).

The runoff and base flow at the waste rock dump are the source of acid rock drainage. The total acid rock drainage flow rates are approximately 200,000 m³ of water per year. This translates into 29 % of the annual precipitation (855 mm) that falls on 81.8 ha of area (Isabel *et al.*, 1997).

The infiltration is the sum of the base flow, change in storage and water lost due to groundwater seepage. Hence, the total infiltration was calculated to be 36 % of the total precipitation which agrees with field lysimeter readings (Isabel *et al.*, 1997).

Isabel *et al.* (1997) states that the hydrologic budget does not explain the dynamic nature of water flow in waste rock which is needed to calculate physical and geochemical processes. The need for calculation of evapotranspiration based on the energy budget is also stressed by Isabel *et al.* (1997). The individual components of the hydrologic budget are illustrated in Figure 2.4.

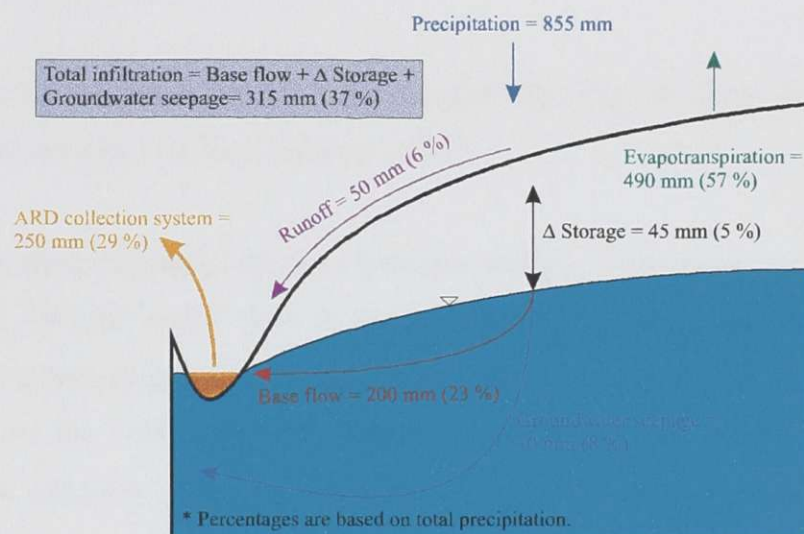


Figure 2.4 Components of the hydrologic budget for La Mine Doyon (after Isabel *et al.*, 1997).

Ghomshei *et al.* (1997) performed a water balance on a 9.6 Mt waste rock dump with an area of 13.9 ha. The waste rock is blended with carbonate-bearing ultra-mafic rock and covered and reclaimed with glacial till. The purpose of the hydrologic budget was to provide some background to the geochemical examination.

Precipitation was calculated by correcting data from nearby weather stations (Ghomshei *et al.*, 1997).

The snow pack on the dump was found to melt and subsequently evaporate due to the exothermic process of oxidizing sulphides during previous freshets; thus, runoff is minimal and assumed negligible. The runoff from the surrounding area is diverted from the waste rock dump; thus, it is not included in the hydrologic budget (Ghomshei *et al.*, 1997).

Changes in storage exist on a monthly basis as infiltrating water during snowmelt may take many months to report to the toe discharge. However, all of the stored water throughout the year will be drained; thus changes in storage is nil in terms of a yearly hydrologic budget (Ghomshei *et al.*, 1997).

Evaporation from the dump surface was calculated using the hydrologic budget equation as seen in Equation [2.1] (Ghomshei *et al.*, 1997).

Areas surrounding the dump did not experience melting of the snow pack prior to the freshet. The diverted runoff flow is instrumented with a weir as is toe discharge. Correlations between the weir hydrographs and waste rock dump piezometers suggested that 80 % of the water that infiltrates the surrounding area enters the dump as groundwater discharge. This flow migrates directly to the base of the dump and subsequently to the toe discharge resulting in a zero storage factor. Losses due to groundwater are assumed negligible (Ghomshei *et al.*, 1997).

Base flow during the freshet accounts for a change in water content of approximately 0.5 to 1 % in the waste rock. The water percolates slowly through the dump to the toe discharge over a period of many months. This water is responsible for 30 to 50 % of the toe discharge over the three month freshet period and may be as high as 100 % of the toe discharge during the winter months (Ghomshei *et al.*, 1997).

The total water infiltrating through the dump becomes primarily base flow as changes in storage within the waste rock and losses due to groundwater are nil. Thus, the total flow

through the dump is derived from base flow and infiltrating groundwater from areas surrounding the waste rock dump. Peak flow from the toe discharge was 14 L/s during 1996 (Ghomshei *et al.*, 1997).

Ayres (1998) studied the net water flux through a uranium mill tailings pile and natural ground surfaces in order to assess the degree of saturation of the tailings, which relates to environmental concerns like radon gas emissions. A field and laboratory instrumentation program was initiated in order to measure or calculate the individual components of the water budget. These values were used to calibrate the soil-atmosphere model used in the analysis (Ayres, 1998).

The tailings area was situated in a groundwater discharge area and the net infiltrating water flux was found to be 9 % of precipitation. The natural ground surface was situated in a groundwater recharge area and had an infiltration rate of 36 % of precipitation (Ayres, 1998).

2.5 Modelling Using FEMWATER

The Groundwater Modelling System (GMS) is a graphical interface that supports a wide variety of groundwater analysis codes. These codes include finite difference flow models, finite difference contaminant transport models, two dimensional finite element flow models, etc (ECGL, 1998). FEMWATER is one of these analysis codes and is a three dimensional finite element saturated and unsaturated flow and transport numerical model (Lin *et al.*, 1997). Jones *et al.* (1995) critiqued the FEMWATER models ability to perform groundwater simulations and its role in practical applications.

Many finite difference, three dimensional flow and transport models have been developed in the past with little success in terms of an accurate grid design. Finite difference models are preferred due to ease of construction and solving method. These models do, however, lack the flexibility in grid design to accommodate elements in problem areas;

for example, highly unsaturated or large gradient areas. Another problem with finite difference grids is their inability to correctly represent the hydrostratigraphy. FEMWATER has attempted to eliminate these problems with the development of a three dimensional flow and transport finite element model (Jones *et al.*, 1995).

Jones *et al.* (1995) explains the three dimensional finite element mesh construction within GMS. The mesh may be constructed with borehole data or a series of three dimensional iso-surfaces. A series of borehole logs can be imported into GMS and a mesh may be generated based on the borehole data. The iso-surfaces are a three dimensional plane that represent the interface between stratigraphic zones. These iso-surfaces may be projected onto a two dimensional mesh in order to create a three dimensional mesh. The nodes are created by using the horizontal dimensions from the two dimensional mesh and the elevation dimension from the iso-surface. The interconnection of these nodes forms the three dimensional mesh. Two dimensional meshes may be constructed with similar tools. The resulting three dimensional mesh may be edited with a number of editing tools. Non-continuous geology may be simulated with renaming or deleting certain layers of elements (Jones *et al.*, 1995).

Visualization of post-processed results is extremely versatile in GMS. Color contoured data may be displayed in any view including cross sections. A number of animation tools are also available to view most transient processes including particle tracking, iso-surface data, flow traces and data along cross sections (Jones *et al.*, 1995).

Jones *et al.* (1995) presents a sample application of a groundwater simulation for a drainage basin with over 500 m of relief. The geology consists of bedrock, weathered bedrock and fractured bedrock. The relief and geology suggest a need for a three dimensional saturated unsaturated numerical model. Attempts to model this groundwater system proved to be unsuccessful with a three dimensional finite difference model. Steep gradients over small step-like elements were the cause of the problem. The same problem was simulated using FEMWATER where modifications to the mesh were made with the

ease of mesh editing provided by GMS. The resulting FEMWATER model was assumed to be valid.

Lin and Deliman (1995) performed two separate groundwater simulations using FEMWATER. The purposes of the simulations were to examine alternative techniques to lower a groundwater table on agricultural land and to assess the implications on groundwater quality due to herbicide application on agricultural land. The analysis was based on a three dimensional finite element model and utilized a coupled density dependant flow and transport simulation. In addition, portions of the porous media were unsaturated.

The first case study pertained to a high water table that developed during the wet season which had adverse effects on agriculture and residential housing. A number of control structures were constructed in order to correct these problems, with little success. The surficial geology consists of a highly permeable aquifer and groundwater flows into the aquifer with ease during the wet season causing the high groundwater table period. The implementation of a cut-off wall was successfully modelled using FEMWATER. The model showed that a 18 m deep cut-off wall lowered the groundwater table by 0.3 m from the normal level during the wet season (Lin and Deliman 1995).

The second case study examined the consequences of applying the chemical Atrazine to agricultural land. Groundwater flow and chemical transport were modelled followed by a sensitivity analysis. The simulation was run over a typical growing season for a corn field. Chemical diffusion and mechanical dispersion were assumed to be negligible as advection is the dominant transport process; accordingly the associated parameters were set to zero. The model showed that the Atrazine was confined only to the surficial soils and did not enter into the deep soil layers. Atrazine could not be detected at the end of the simulation due to its adsorption to clay and organic colloids, which is typical of this herbicide (Lin and Deliman 1995).

Sensitivity analysis of the model indicated that the Atrazine concentrations increased and decreased congruently with the application rate. The model was not affected by any significant amount with variations in the decay term (Lin and Deliman 1995).

Uwiera (1998) performed a FEMWATER flow and transport groundwater simulation at a potash tailings site where the characteristics of brine migration from the tailings pile was studied. The flow processes include advective flow, diffusive flow and density-dependant flow, all of which may be modelled in FEMWATER. The studied showed that brine migration will escape the containment area and be released into an adjacent aquifer at a concentration of 100 g/L.

2.6 Summary

Literature pertaining to hydrological and hydrogeological processes in waste rock dumps is limited. This is due, in part, to the extensive instrumentation required to completely characterize the hydrological system. Individual components of the water budget must be known in order to correlate rainfall to toe discharge from a waste rock dump.

A water balance problem exists at Equity Silver Mine, as the individual components of the water budget are not known. Hydrological characterization of the mine site will help explain the water balance problem and will shed light on future predictions of acid rock drainage and remedial techniques.

Chapter 3 Theoretical Background

3.1 Introduction

The theoretical background to the processes involved in this study are presented here. The hydrologic budget equation is examined at the soil-atmosphere layer and on a regional scale. The purpose of the regional hydrologic budget is to account for all components of water flux in a specific system, for example, a waste rock dump. Future predictions of water movement may be made once the water balance components of a system are determined.

The formulation of transient, three dimensional, anisotropic, unsaturated, heterogeneous groundwater flow is developed. The modified groundwater flow equation that FEMWATER uses to solve groundwater simulations is examined.

There are numerous procedures to solve groundwater flow problems, including analytical and numerical methods - FEMWATER uses the finite element method to numerically solve problems. An iterative method of solving the groundwater flow equations utilizing the finite element method is used in order to reach a solution within specified error limits. Other methods of solutions are also briefly covered.

3.2 Hydrologic Budget Equation

The hydrologic budget equation is a water balance relationship used to account for specific components of water. The water balance relationship can be applied at the soil-atmosphere interface and for a regional system such as a waste rock dump.

3.2.1 Soil-atmosphere Interface Hydrologic Budget Equation

The hydrologic budget equation may be applied at the ground surface to individual watersheds. The one dimensional surface hydrologic budget equation is shown in Equation [3.1].

$$P - R - ET - I - M - S = 0 \quad [3.1]$$

Where: P = Total precipitation (mm)
R = Runoff (mm)
ET = Evapotranspiration (mm)
I = Infiltration (mm)
M = Mass transfer of snow (mm)
S = Sublimation of snow (mm)

Total precipitation originates from rain and snowmelt and acts as the input to the system. Runoff is the overland flow which contributes, in part, to the river systems. Evaporation is simply the transformation of liquid water to water vapor which then enters the atmosphere. The uptake of liquid water by plants and subsequent loss of water vapor through the plants pores or stomata is termed transpiration. The combined effort of evaporation and transpiration is termed evapotranspiration. Portions of snow may be lost to sublimation which is the evaporation of water vapor from the solid snow surface. Some snow may also be lost due to wind and is termed mass transfer. Accumulation of snow may also result and hence this term will become negative. The remaining portion of

water that passes the soil-atmosphere interface is termed the infiltration. The terms used in Equation [3.1] are illustrated in Figure 3.1.

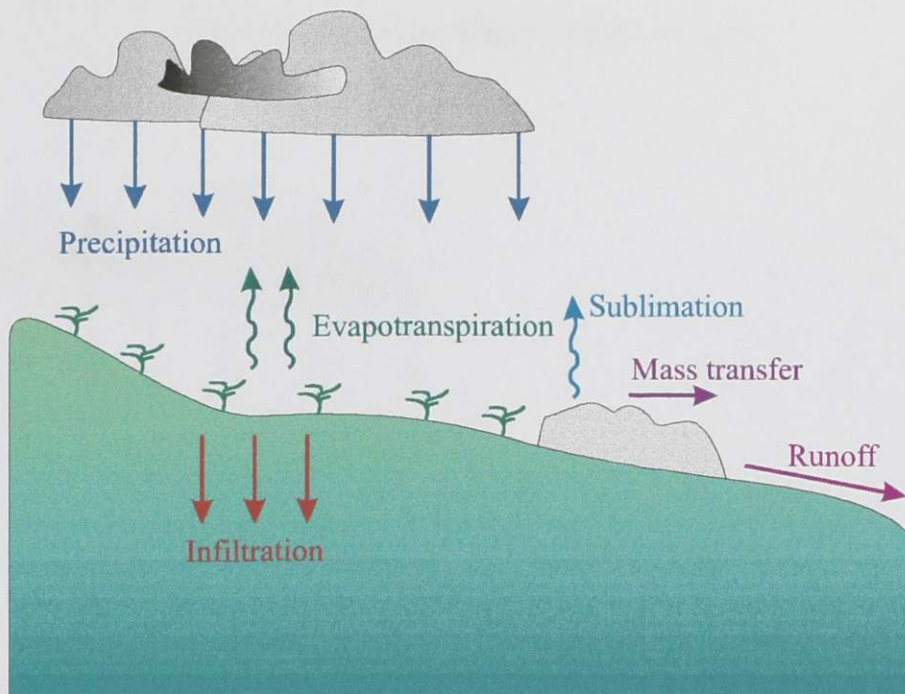


Figure 3.1 Terms used in the surface hydrologic budget equation.

3.2.2 Waste Rock Dump Hydrologic Budget Equation

The principles of the soil-atmosphere hydrologic equation may be applied to some regional systems. Storage factors and recharge or discharge of groundwater must be taken into account in a waste rock dump hydrological system. Hence, the hydrologic budget equation must be modified in order to include these terms to form a water balance relationship, shown in Equation [3.2] (Isabel *et al.*, 1997). The components of flow for the waste rock dump hydrologic system are illustrated in Figure 3.2.

$$P - R - \Delta S - ET - GS - B - M - S = 0 \quad [3.2]$$

Where: ΔS = Change in storage (mm)

GS = Groundwater seepage component (mm)

B = Base flow (mm)

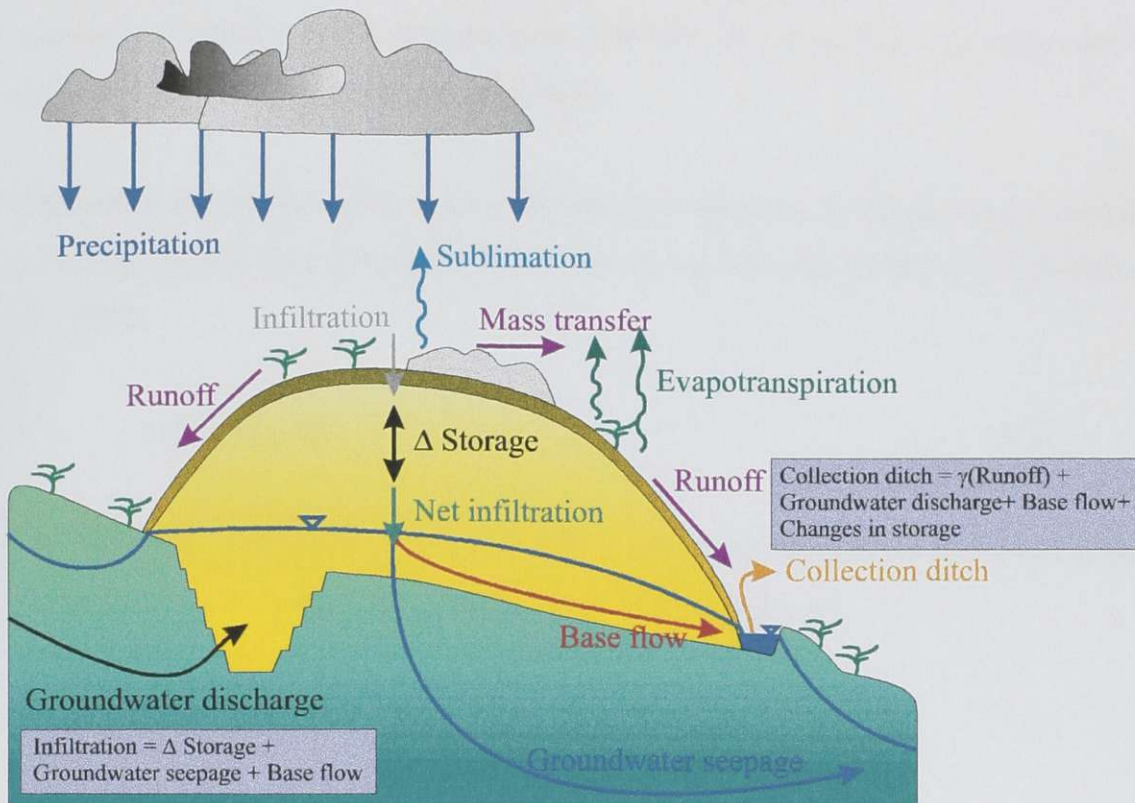


Figure 3.2 Terms used in the regional hydrologic budget equation.

Changes in storage in the unsaturated zone can occur, but this term usually approaches zero over a long period of time. If, however, the waste rock dump has recently been constructed and a state of equilibrium has not been reached, the change in storage may not be zero. The value is positive if the water content in the unsaturated zone is increasing or if this zone is wetting up. The value is negative when the unsaturated zone is draining water.

The groundwater seepage term takes into account the contribution or recharge to the regional groundwater flow regime system. This term is also referred to as deep percolation.

The base flow term in Equation [3.2] is the amount of water that is contributed to the local groundwater system which drains into a nearby stream. This flow component reports to a stream through seepage areas. The base flow is derived from water that is released from storage in the unsaturated zone.

The infiltration into the media at the soil-atmosphere interface will be the sum of changes in storage, groundwater seepage and base flow and is shown in Equation [3.3] (Isabel *et al.*, 1997).

$$I = \Delta S + GS + B \quad [3.3]$$

The water that contributes to the water table is termed the net infiltration and will be the infiltration less the changes in storage as shown in Equation [3.4].

$$NI = I - \Delta S \quad [3.4]$$

Where: NI = Net infiltration (mm)

The net infiltration will be divided into the base flow and groundwater seepage as shown in Equation [3.5].

$$NI = B + GS \quad [3.5]$$

If the waste rock dump is located on a groundwater recharge area, the groundwater seepage flow must be included. However, if the waste rock dump is situated on a groundwater discharge area, the groundwater term is neglected in Equation [3.2],

Equation [3.3] and Equation [3.5]; or all net infiltration is equal to base flow. In a situation where the waste rock dump is situated on both a groundwater recharge and discharge area, the groundwater seepage term must be used in both equations. The groundwater discharge term must be used in the waste rock dump water balance relationship explained later.

If Equation [3.3] is substituted into Equation [3.2], the result is identical to the soil-atmosphere hydrologic budget equation [3.1].

Another water balance relationship may also be developed at the collection ditch at the toe of the waste rock dump as shown in Equation [3.6].

$$\frac{Q_d t_d}{A_{wr}} = \gamma R + GD + B + \Delta S \quad [3.6]$$

Where: Q_d = Flow in the collection ditch (L/s)
 t_d = Time that the flow in the collection ditch occurs (s)
 A_{wr} = Area of the waste rock dump (m²)
 γ = Runoff collection coefficient
GD = Groundwater discharge component (mm)

The units of flow in the ditch must be corrected to accommodate the remaining terms. They are multiplied by the time and divided by the area of the waste rock dump. Some portion of runoff may be diverted off the waste rock dump by surface drainage ditches. This portion entrained in the collection ditch must be accounted for and is represented by a runoff collection coefficient multiplied by the runoff component.

Groundwater discharge that enters the dump will report to the collection ditch if the waste rock dump is situated in a groundwater discharge area. Groundwater seepage does

not enter into the toe discharge collection ditch and is therefore not included in Equation [3.6].

The waste rock dump may not be in equilibrium with respect to water content, if for example, a covered waste rock dump was uncovered for some period of time. The waste rock would come to a state of equilibrium during uncovered conditions. Water will continue to drain out of the waste rock when the cover is constructed and the infiltration decreased. Thus, the change in storage term must be included in the waste rock dump hydrological budget equation.

3.3 Formulation of Groundwater Flow

This section describes in detail the derivation of the three dimensional groundwater flow equations and associated auxiliary equations, which include the boundary conditions and initial conditions.

3.3.1 Derivation of the Three Dimensional Groundwater Flow Equations

The equations that describe groundwater flow are based on the law of conservation of mass which is applied to a representative elementary volume. The representative elementary volume is a small cubic unit of porous media that accurately represents a total volume of porous media and has equal dimensions on all sides. The representative elementary volume includes the soil particles, water and air and is shown in Figure 3.3. The units in the equations will be in SI units, however, any consistent unit of measurement may be used.

The law of conservation of mass states that the mass flow rate into one side of the cube minus the mass flow rate out of the opposite cubic face must be equal to the change in

mass stored per unit time. The law of conservation of mass is simplified in Equation [3.7].

$$Qm_{in} - Qm_{out} = \frac{\partial M}{\partial t} \quad [3.7]$$

Where: Qm_{in} = Mass flux of water into an elemental face (kg/s)

Qm_{out} = Mass flux of water out an elemental face (kg/s)

M = Mass of water stored within the element (kg)

t = Time (s)

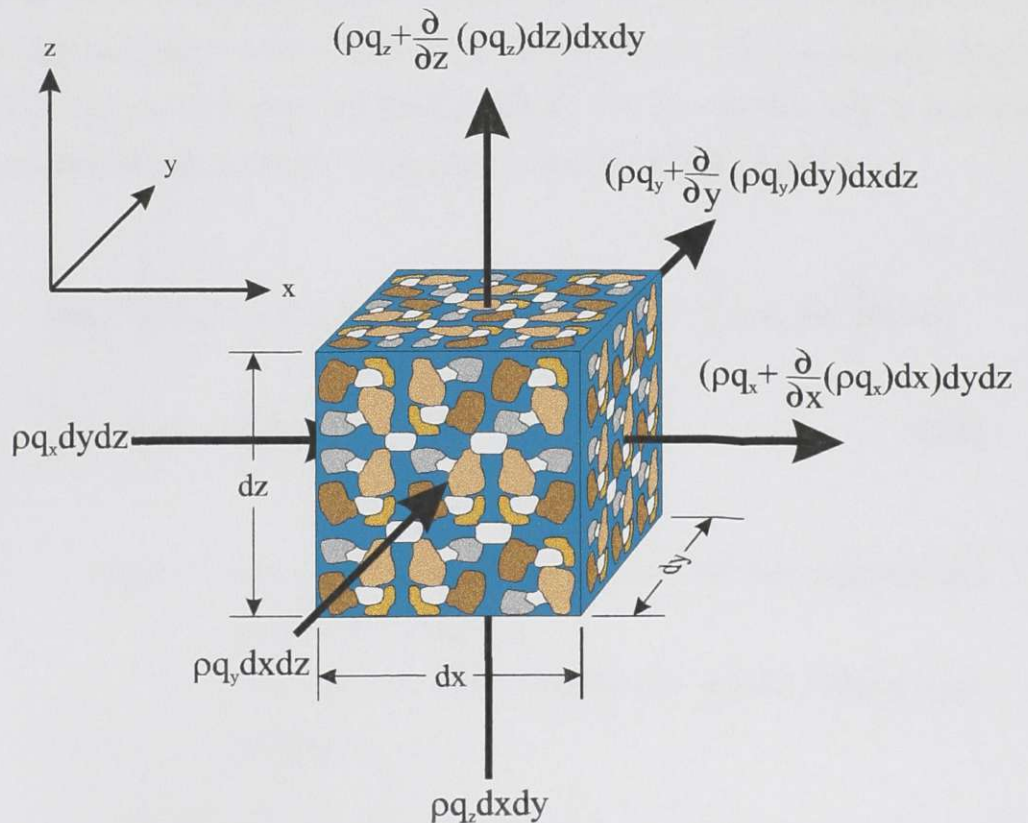


Figure 3.3 Representative elementary volume for groundwater flow.

Mass flux per unit area may be defined as the density of water (ρ) multiplied by the flux rate (q), as seen in Figure 3.3. Hence, the mass flux will be the mass flux per unit area

multiplied by the respective area, which in this case is the dimensions of the corresponding elemental face.

$$Q_m = \rho q A \quad [3.8]$$

Where: ρ = Density of water (kg/m^3)
 q = Water flux (m/s)
 A = Area of the elemental face (m^2)

Equation [3.8] must be applied to all of the input sides of the cube. The output sides of the cube are determined by using a Taylor Series approximation of Equation [3.8] and neglecting the higher order terms (Istok, 1989). The six three dimensional mass flux terms in the representative elementary volume may be implemented in the law of conservation of mass (Equation [3.7]) and is presented in Equation [3.9].

$$\left\{ \rho q_x - \left[\rho q_x + \frac{\partial}{\partial x} (\rho q_x) dx \right] \right\} dy dz + \left\{ \rho q_y - \left[\rho q_y + \frac{\partial}{\partial y} (\rho q_y) dy \right] \right\} dx dz + \left\{ \rho q_z - \left[\rho q_z + \frac{\partial}{\partial z} (\rho q_z) dz \right] \right\} dx dy = \frac{\partial M}{\partial t} \quad [3.9]$$

Where: dx, dy and dz = Dimensions of the representative elementary volume (m)
 x, y and z = Three dimensional normal Cartesian axis directions

Equation [3.9] may be simplified into Equation [3.10].

$$-\left[\frac{\partial}{\partial x} (\rho q_x) dx \right] dy dz - \left[\frac{\partial}{\partial y} (\rho q_y) dy \right] dx dz - \left[\frac{\partial}{\partial z} (\rho q_z) dz \right] dx dy = \frac{\partial M}{\partial t} \quad [3.10]$$

The total volume of the representative elementary volume ($dx dy dz$) appears in each term of the left hand side of Equation [3.9]. The total volume may be collected and placed on the right hand side of Equation [3.9] as shown in Equation [3.10].

$$-\frac{\partial}{\partial x}(\rho q_x) - \frac{\partial}{\partial y}(\rho q_y) - \frac{\partial}{\partial z}(\rho q_z) = \frac{1}{V_t} \frac{\partial M}{\partial t} \quad [3.11]$$

Where: V_t = Total volume of the representative elementary volume (m^3)

The total volume may be taken into the mass partial differential. The mass of water stored in the element may be expressed as the density of water multiplied by the volume of water.

$$-\frac{\partial}{\partial x}(\rho q_x) - \frac{\partial}{\partial y}(\rho q_y) - \frac{\partial}{\partial z}(\rho q_z) = \frac{\partial}{\partial t} \left(\rho \frac{V_w}{V_t} \right) \quad [3.12]$$

Where: V_w = Volume of water stored within the representative elementary volume (m^3)

The volume of water stored within the element divided by the total volume of the representative elementary volume is the volumetric water content.

$$-\frac{\partial}{\partial x}(\rho q_x) - \frac{\partial}{\partial y}(\rho q_y) - \frac{\partial}{\partial z}(\rho q_z) = \frac{\partial}{\partial t}(\rho \theta_w) \quad [3.13]$$

Where: θ_w = Volumetric water content of the representative elementary volume

Darcy's Law empirically describes flow through porous media and is presented in Equation [3.14].

$$q = -K \frac{\partial h}{\partial l} \quad [3.14]$$

Where: K = Hydraulic conductivity (m/s)
 h = Hydraulic head (m)
 l = Length between head measurements (m)

Substituting Equation [3.14] into Equation [3.13] results in Equation [3.15].

$$\frac{\partial}{\partial x} \left(\rho K_x \frac{\partial h}{\partial x} \right) + \frac{\partial}{\partial y} \left(\rho K_y \frac{\partial h}{\partial y} \right) + \frac{\partial}{\partial z} \left(\rho K_z \frac{\partial h}{\partial z} \right) = \frac{\partial}{\partial t} (\rho \theta_w) \quad [3.15]$$

The hydraulic conductivity is nearly constant in the saturated zone and may vary over several orders of magnitude in the unsaturated zone. The hydraulic conductivity is a function of the negative pressure head (matric suction).

The total hydraulic head is equal to the pressure head (elastic energy) plus the elevation head (potential energy). Using this relationship and the chain rule, Equation [3.16] may be derived and is referred to as the Richards Equation.

$$\frac{\partial}{\partial x} \left(\rho K_x \frac{\partial \psi}{\partial x} \right) + \frac{\partial}{\partial y} \left(\rho K_y \frac{\partial \psi}{\partial y} \right) + \frac{\partial}{\partial z} \left(\rho K_z \left(\frac{\partial \psi}{\partial z} + 1 \right) \right) = \frac{\partial}{\partial t} (\rho \theta_w) \quad [3.16]$$

Where: ψ = Pressure head (m)

Equation [3.15] or Equation [3.16] is the transient three dimensional unsaturated, heterogeneous anisotropic groundwater flow equation expressed in terms of hydraulic

head or pressure head respectively. Alternatively, the volumetric water content may be expressed as the porosity multiplied by the degree of saturation on the right hand side of Equation [3.15] and Equation [3.16].

Directional derivatives are commonly expressed in del (∇) notation or as gradients (grad) (Stewart, 1991). Del notation is common in expressing three dimensional groundwater flow formulae. An example of del notation is given in Equation [3.17].

$$\nabla f = \frac{\partial f}{\partial x} \mathbf{i} + \frac{\partial f}{\partial y} \mathbf{j} + \frac{\partial f}{\partial z} \mathbf{k} \quad [3.17]$$

Where: f = Some function

\mathbf{i} , \mathbf{j} and \mathbf{k} = Unit vectors in the positive x , y and z directions

Del notation may be applied to Equation [3.15] and shown in Equation [3.18].

$$\nabla[\rho K \nabla(h)] = \frac{\partial}{\partial t}(\rho \theta_w) \quad [3.18]$$

The hydraulic conductivity, K and hydraulic head, h become tensors when Equation [3.18] is used.

3.3.2 Auxiliary Equations

Initial conditions must be specified for all transient problems. The initial conditions for a groundwater flow problem are the initial values of hydraulic head at each node in the mesh or grid and is expressed in Equation [3.19].

$$h = h_i(x, y, z) \quad [3.19]$$

Where: h_i = Initial hydraulic head (m)

The Dirichlet boundary condition is a prescribed value of hydraulic head at a the soil-water interface. Examples of Dirichlet head are found at ponds, rivers and coastal lines and is presented in Equation [3.20].

$$h = h_d(x, y, z, t) \quad [3.20]$$

Where: h_d = Dirichlet hydraulic head (m)

The flux boundary condition describes the flux across a boundary face due to a gradient. This form of boundary condition applies to the known infiltration rates into specific layers (Lin *et al.*, 1997) and is shown in Equation [3.21].

$$-K(\nabla h) = q(x, y, z, t) \quad [3.21]$$

The variable flux boundary condition applies to the soil-atmosphere interface and simulates evaporation and seepage due to precipitation processes. The condition is variable since it corresponds to a flux boundary condition or a Dirichlet boundary condition depending on the potential evaporation, the hydraulic conductivity of the media, the availability of water and the level of groundwater (Lin *et al.*, 1997). The variable flux boundary condition is presented in Equation [3.22].

$$-K(\nabla h + \nabla z) = q(x, y, z, t) \quad [3.22]$$

The flux in Equation [3.22] refers to infiltrating water or evaporating water based on the conditions stated above. If the capacity of the soil or rock is exceeded due to high

precipitation, the subsequent ponded water will be represented by the Dirichlet boundary condition. The reverse holds true when water is removed from the soil-atmosphere interface and a lower limit of pressure head results. The boundary condition switches to a Dirichlet boundary condition when this limit is reached (Lin *et al.*, 1997).

3.4 Formulation of FEMWATER

This section will develop the governing equations for Darcian groundwater flow used in FEMWATER. The formulation begins with Equation [3.23] (Lin *et al.*, 1997).

$$\nabla \left[\frac{\rho k}{\mu} (\nabla \psi + \rho g \nabla z) \right] - \nabla (\rho n S V_s) + \rho q_s = \frac{\partial}{\partial t} (\rho n S) \quad [3.23]$$

- Where:
- k = Intrinsic permeability (m^2)
 - μ = Dynamic viscosity ($kg/m/s$)
 - S = Degree of saturation
 - g = Acceleration due to gravity (m/s^2)
 - V_s = Velocity of the deformable material due to consolidation (m/s)
 - q_s = Internal source or sink flux rate ($m^3/s/m^3$)
 - z = Elevation head (m)

Equation [3.23] may be compared to Equation [3.18] that was developed in the previous section. The first term on the left hand side of Equation [3.23] describes the ability of the fluid to have various densities. The term therefore relates back to the basics of the energy of fluids (Frind, 1982). Density dependant flow or mass transport mechanisms will not be discussed as they are out of the scope of this project. With this assumption, the first term on the left hand side of Equation [3.23] will match the left hand side of Equation [3.18]. The second term on the left hand side of Equation [3.21] accounts for the consolidation of the material while the third term adjusts for pumped or injected fluid into the system.

Fluid may be pumped out through wells or sumps while injection wells may introduce water into the media and must be included in the FEMWATER formulation to ensure water balance. The right hand side of Equation [3.23] has substituted the volumetric water content for the porosity multiplied by the degree of saturation, thus it also matches Equation [3.18].

Equation [3.23] simplifies to Equation [3.24] by a series of substitutions, general assumptions and rules of calculus (Lin *et al.*, 1997).

$$\nabla[K\nabla(h)] + q_s = F \frac{\partial h}{\partial t} \quad [3.24]$$

Where: F = Storage coefficient (1/m)

The storage coefficient is expressed in Equation [3.25] (Lin *et al.*, 1997).

$$F = \frac{\alpha \rho g \theta_w}{n} + \beta \rho g \theta_w + n \frac{\partial S}{\partial \psi} \quad [3.25]$$

Where: α = Compressibility of the media (1/Pa)

β = Compressibility of the water (1/Pa)

Substituting Equation [3.24] into Equation [3.25] is shown in equation [3.26] and is the equation used by FEMWATER to solve groundwater flow problems.

$$\nabla[K\nabla(h)] + q_s = \left(\frac{\alpha \rho g \theta_w}{n} + \beta \rho g \theta_w + n \frac{\partial S}{\partial \psi} \right) \frac{\partial h}{\partial t} \quad [3.26]$$

Equation [3.26] does not include the density dependant flow or mass transport mechanisms as described previously (Lin *et al.*, 1997). The procedure used to solve Equation [3.26] is discussed in later sections.

3.5 Solving Groundwater Flow Problems

The solution to the partial differential equations and auxiliary equations that were developed in Section 3.3 tends to be difficult due to the complexity of these equations. Many alternative methods of solutions are available and some are presented in this section.

3.5.1 Introduction to Solving Groundwater Flow Problems

A conceptual model is usually the first step in the development of a groundwater model. The conceptual model describes the major physical processes that are present in the desired system which must then be explained in terms of a mathematical problem. The mathematical problem consists of a set of partial differential equations that describe groundwater flow, and auxiliary equations which explain initial and boundary conditions. A flow chart explaining problem solving techniques for groundwater simulations is shown in Figure 3.4 followed by an explanation.

Analytical methods attempt to solve a partial differential equation using calculus based on boundary and initial conditions (Fetter, 1993). The separation of variable technique is often used to obtain solutions or equations for analytical problems (Freeze and Cherry, 1979). Gross restrictions are usually put on the analytical solutions; for example, the porous media must be homogenous and of simple geometry (Fetter, 1993). The analytical method does, however, provide a solution that is simple to compute.

Two types of problems are considered under the analytical method: boundary value problems and initial value problems. Boundary value problems are a steady state model.

Boundary conditions such as constant head (pressure or total), constant recharge rates, constant pump rates, etc. may be applied to the groundwater model.

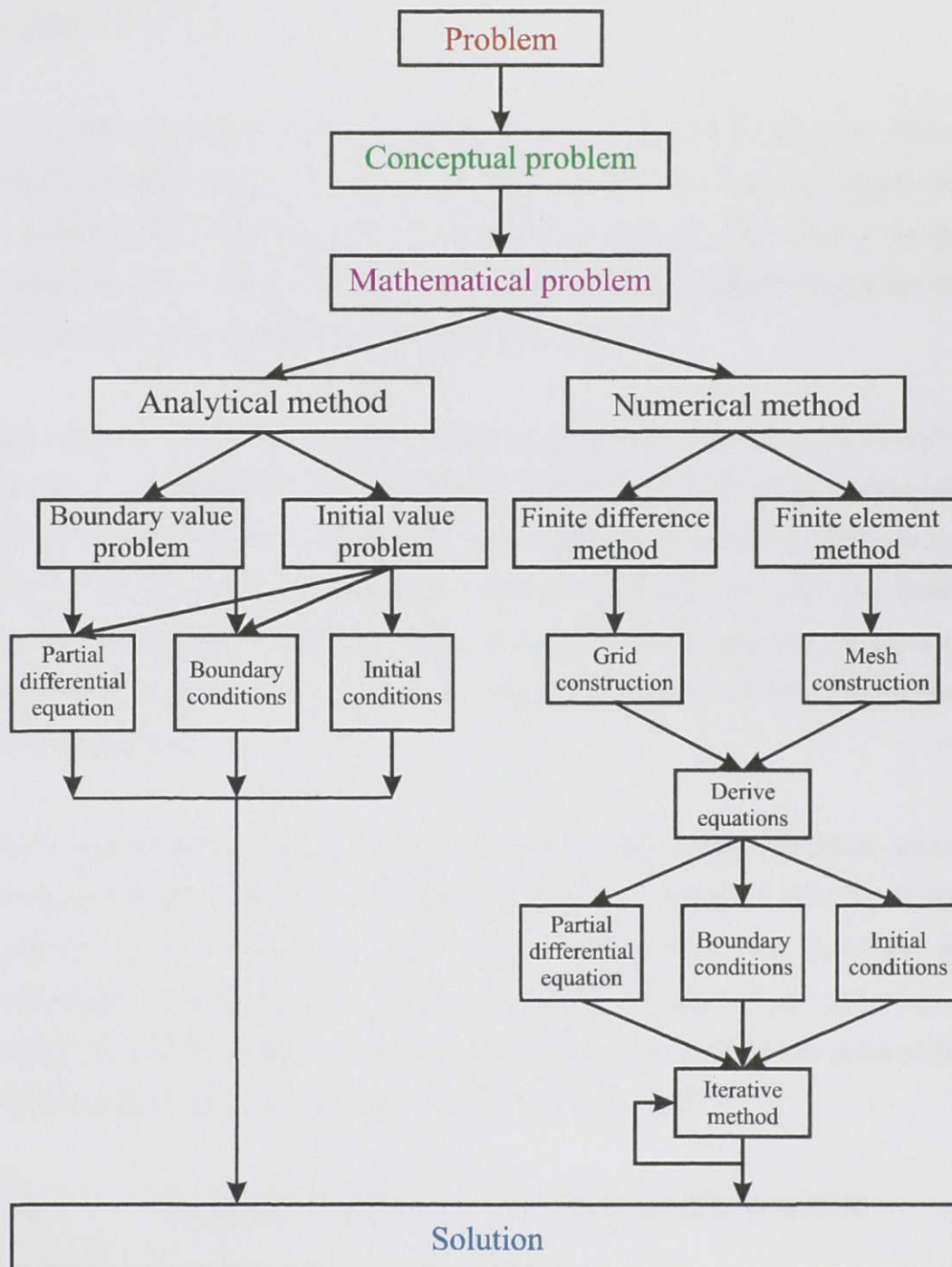


Figure 3.4 Problem solving methods for groundwater simulations.

The initial value problem is similar to the boundary value problem. This model is transient and simulations with transient boundary conditions may be performed. Initial conditions must also be applied to all points in the model. These problems tend to be more complex in nature.

The numerical method solves the partial differential equations using the numerical method of analysis (Fetter, 1993). The numerical method offers a discrete approximation to problems with complex physical properties and geometry, but requires numerous calculations (Istok, 1989). This task is lessened by the use of digital computers which have the ability to perform numerous calculations quickly.

Finite difference refers to a simple calculation applied to nodes on a discretized grid consisting of quadrilaterals. The finite difference method is based on approximating the derivatives of the function, resulting in a solution only at the discrete points (Lin *et al.*, 1997). Darcy's Law may be applied to nodes in a quadrilateral grid. The heads at individual nodes may be calculated based on a water balance approach applied at each node. For n number of nodes there will be n linear equations, hence the problem may be solved (Freeze and Cherry, 1979).

The finite difference method has many advantages, including: simple problems are easily solved, abundance of literature, successful algorithms are available to solve the system of equations and the accuracy is good (Istok, 1989). There are, however, some disadvantages: problems are restricted to portions of quadrilateral geometry, the directions of anisotropy must be congruent with the coordinate directions and inaccurate solutions with respect to mass transport problems (Istok, 1989).

3.5.2 The Finite Element Method Used in FEMWATER

The finite element method used in FEMWATER is a numerical method of solution (see Figure 3.4) similar to that of the finite difference method. The finite element method is

based on approximating the head function, resulting in a spatially continuous solution (Lin *et al.*, 1997). The model consists of an irregular network of triangular or quadrilateral elements. The finite element method calculates an error associated with the heads at each node and then attempts to reduce this error to a prescribed limit.

The first step in solving a finite element problem is the construction of a nodal grid. The nodes should be placed at problem boundaries, layer boundaries, point source or sink, or any other point where a solution is desired. Node spacing should decrease in regions where high gradients are expected. The nodes should also be numbered systematically to minimize the semi-bandwidth (Istok, 1989).

The elements within the problem domain must be constructed based on the nodal arrangement described above. The simplest type of element should be used in construction of the mesh without leaving any gaps or overlaps. Exceedingly distorted elements should be avoided as accuracy will diminish for transient and mass transport problems. Element size variations should not occur abruptly as a smooth transition of elemental size should take place (Istok, 1989). The rule of thumb is based on the one-half rule; that is elements should not vary by less than one half of the size of an adjacent element (Lin *et al.*, 1997).

The next step in the finite element method is to derive the finite element equations for solving the groundwater flow Equation [3.26]. The integral formulation used in FEMWATER is the Galerkin's Method as it is the most common method for flow and transport problems. Many other methods are available, including: method of residual errors, subdomain method and collocation method (Istok, 1989). The Galerkin Method is shown in Equation [3.27].

$$h \cong \hat{h} = \sum_{j=1}^N h_j(t)N_j(x, y, z) \quad [3.27]$$

- Where: h = Actual hydraulic head (m)
 \hat{h} = Approximate hydraulic head (m)
 j = A nodal point
 N = Total number of nodes
 h_j = Amplitude of h at nodal point j
 N_j = Base function at nodal point j

After some manipulation of the complex calculus, the flow equation is approximated in Equation [3.28] (Lin *et al.*, 1997).

$$[M] \left\{ \frac{\partial h}{\partial t} \right\} + [S] \{h\} = \{Q\} + \{G\} + \{B\} \quad [3.28]$$

- Where: $[M]$ = Mass matrix resulting from the storage term (m)
 $\left\{ \frac{\partial h}{\partial t} \right\}$ = Column vectors containing the values of the partial differential of hydraulic head with respect to time (m/s)
 $[S]$ = Stiff matrix resulting from the action of hydraulic conductivity (m/s)
 $\{h\}$ = Column vectors containing the values of hydraulic head at each node (m)
 $\{Q\}$ = Column Load vectors from the internal source / sink (m^2/s)
 $\{G\}$ = Column Load vectors from the gravity force (m^2/s)
 $\{B\}$ = Column Load vectors from the boundary conditions (m^2/s)

The explanation and simplification of Equation [3.28] is complex and beyond the scope of this study, hence, the detailed derivation is not covered. The reader is referred to (Lin *et al.*, 1997) and (Istok, 1989) for further information.

After the application of Darcy's Law, base and weighting function, numerical integration, mass lumping, finite difference approximation in time and numerical implementation of boundary conditions to Equation [3.28], the following matrix equation is developed (Lin *et al.*, 1997):

$$[C]\{h\} = \{R\} \quad [3.29]$$

Where: $[C]$ = Coefficient matrix
 $\{h\}$ = Pressure head (m)
 $\{R\}$ = The known vector (m)

Equation [3.29] may be highly non-linear as the hydraulic conductivity function and water capacity function may vary several orders of magnitude with changes in pressure head. The solution for the Galerkin Method can be obtained by an iterative process of Equation [3.29]. An arbitrary initial value of hydraulic head is set and then successively improved with subsequent calculations.

The iterative method used by FEMWATER is the Picard Method, sometimes referred to as the substitution method. The first step is an initial guess of the unknown hydraulic heads $\{h\}$. The coefficient matrix $[C]$ may be solved using linear algebra as the known vector $\{R\}$ is already determined. The new estimate of hydraulic head is obtained by a weighted average of the previous estimate as described by Equation [3.30].

$$\{h_{k+1}\} = \omega\{h\} + (1 - \omega)\{h_k\} \quad [3.30]$$

Where: $\{h_{k+1}\}$ = New estimate of hydraulic head (m)

ω = Iteration parameter

$\{h\}$ = New solution of hydraulic head (m)

$\{h_k\}$ = Previous estimate of hydraulic head (m)

The iterative process will continue until the prescribed error criterion is met; thus a solution is determined.

If the iteration parameter is less than one and greater than zero, it is termed underrelaxation. If it is less than two and greater than one, it is termed overrelaxation.

Some of the advantages of the finite element method are: irregular geometry may be used, accuracy for flow and transport is good and computer programming is simple (Istok, 1989). Some of the disadvantages are: small problems still require a large amount of computer programming and lack of literature (Istok, 1989).

3.6 Summary

The hydrologic budget equation has been used to solve engineering problems for decades and is thus reliable in terms of accuracy and practical applications. This water balance approach is helpful in solving acid rock drainage problems, ditch design and groundwater flow problems.

Three dimensional flow is well understood and has also been used extensively in the past. The methods of equation development are based on the rules of calculus and some assumptions.

The finite element method of solving groundwater flow problems has been used extensively in the past. FEMWATER was developed in the early 1990's from the integration of two older groundwater flow and transport problems (Lin *et al.*, 1997). The program has been used to solve a wide variety of groundwater flow and transport problems and is valid (Lin and Deliman, 1995, Jones *et al.*, 1995 and Uwiera, 1998)

Chapter 4 Field Program

4.1 Introduction

Two field programs were initiated at Equity Silver Mine: Phase I - waste rock dump piezometer installation in the fall of 1997 and Phase II - spring runoff response in the spring of 1998. The individual components of Equity Silver Mine are described in Chapter 5.

4.2 Waste Rock Dump Piezometer Installation - Phase I

Five piezometers were installed in the waste rock dump at Equity Silver Mine in September, 1997. The holes were drilled with a Becker Hammer (SDS Drilling, 1997) and standpipe piezometers were installed for measurements of groundwater levels and the collection of water samples.

4.2.1 Becker Hammer Drill Rig

A truck mounted Becker Hammer drill rig, shown in Figure 4.1, was used for the field drilling program. This drill uses a diesel hammer to advance through geological material

and air circulation to retrieve the cuttings. The drill rig is most effective in cohesionless granular material, i.e. sand and gravel deposits; however, the drill rig performed exceptionally well in the waste rock dump.

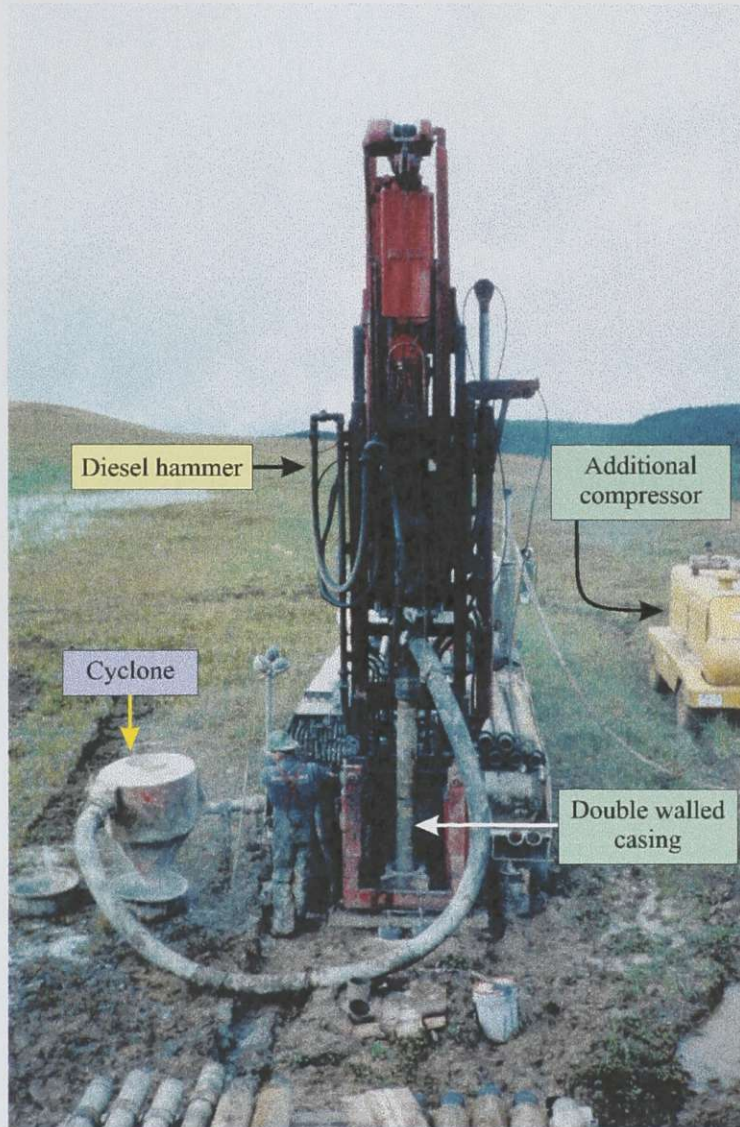


Figure 4.1 Becker Hammer drill rig.

A double walled casing is driven through the formation by a diesel pile driving hammer. Compressed air is continuously forced down the annulus and returns through the center portion of the casing as shown in Figure 4.2. The pile driving hammer shatters the rock

formation into small fragments as shown in Figure 4.3 and the airflow entrained in the double walled casing forces the cuttings to the surface.



Figure 4.2 Doubled walled casing construction.

The Becker Hammer was mounted on a 21,750 kg truck which is 9.8 m long, 2.5 m wide and 3.8 m in height. The diesel hammer was a 180 Linkbelt with 10.8 kJ of energy. The drill rig is equipped with a 280 L/s air compressor and an additional 280 L/s mobile air compressor (see Figure 4.1). It is rated for an approximate depth limit of 35 m with the single compressor. The additional compressor was used since difficult drilling conditions were expected. The maximum depth obtained in the waste rock was 39 m when testhole P 97-04 was terminated; however, refusal criteria was not met. Refusal criteria is defined as no movement of the casing after a prolonged period of drilling. Refusal criteria was encountered only at P 97-05, at a depth of 29 m due to an anticipated large boulder. The drilling rate was approximately 10 metres per hour. Setup time was usually greater than drilling time due to difficult conditions for site access.

The bit had an outside diameter of 168 mm with an inside diameter of 103 mm in the center pipe resulting in a hole approximately 168 mm in diameter with all cuttings less than 103 mm in diameter.



Figure 4.3 Cuttings from a Becker Hammer drill rig.

The drill rig was also capable of retrieving Shelby tube samples, density of sand and gravel formations, coring of bedrock and Standard Penetration (SPT) tests. None of these tests were performed at Equity Silver Mine.

Drilling a cased hole with air circulation is superior to using water or drilling mud. Accurate information regarding hydraulic conductivity and groundwater samples is obtained since no contamination of the formation takes place.

4.2.2 Testhole Completion and Piezometer Installation

The Becker Hammer drill rig provides continuous samples of the penetrated formation. The crushed waste rock is entrained in the airflow and samples are blown to the drill head, passed through a cyclone and into the sample bin (see Figure 4.1). Samples were taken approximately every 1.2 to 1.5 m for the entire depth. Water contents and paste pH were determined for each sample and additional samples were retrieved for future analysis, which may be required.

The configuration of the piezometers installed in the waste rock dump is shown in Figure 4.4.

Drilling was terminated and the drill head was removed when the natural glacial till layer was encountered. Bentonite pellets were set down the center of the double walled casing and the natural till layer was sealed to prevent hydraulic influences between the waste rock and the till layer. The sealed piezometer tip and riser pipes were placed down the hole and located above the lower bentonite seal. The riser pipes were connected by threaded joints and the piezometer tips were backfilled with approximately 4 m of sand. A 150 mm bentonite seal was placed over the filter sand to eliminate any hydraulic influences from above the piezometer tip. The casing was then removed (tripped out) and the open hole was backfilled with gravel or inert rock material. The upper 0.8 m of the hole was sealed with bentonite chips to prevent any water or oxygen from entering the dump. A removable cap was installed at the top of the piezometer to allow for groundwater level elevation readings and the retrieval of groundwater samples.

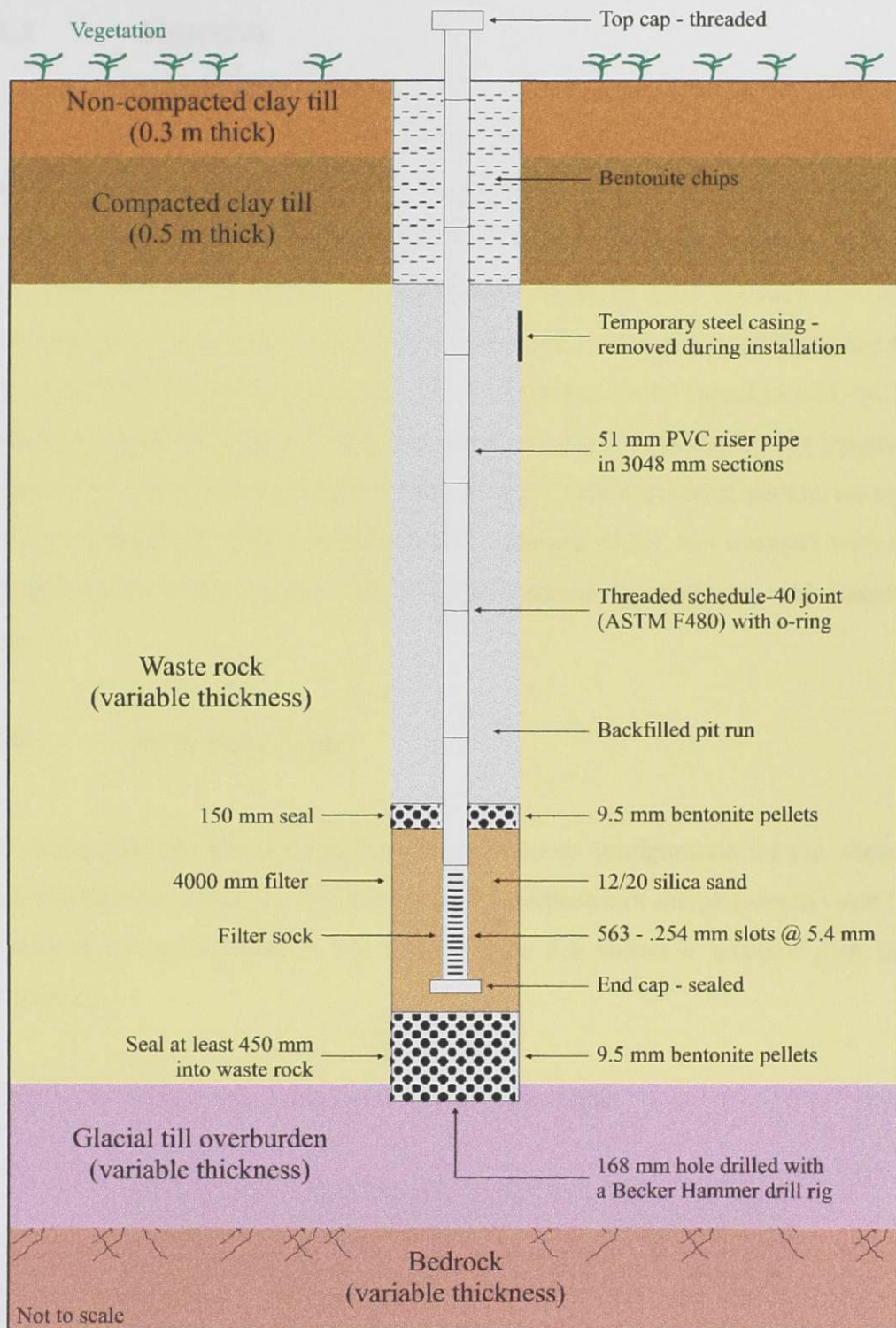


Figure 4.4 Plan of the piezometers installed in the waste rock dump.

4.2.3 Materials

The lower seal consisted of 9.5 mm diameter bentonite pellets manufactured by Economy Mud Products Co. The filter material was typical 12/20 silica sand manufactured by Unimen Corporation and the brand name was Unimen silica sand-industrial quartz. The upper seal consisted of bentonite chips, manufactured by Mud Products Co. and the brand name was Econo Plug-medium sodium bentonite chips. The standpipe piezometers were made of typical PVC material. The piezometers were manufactured by Timco Manufacturing Inc. and were 51 mm in diameter and 3.048 m in length. The lengths were connected by a threaded schedule-40 joint (ASTM F480) and sealed with an o-ring. The PVC tip consisted of 563-0.254 mm slots at a spacing of 5.4 mm wrapped with a filter sock and sealed at the bottom. All of the piezometer material was acid washed and rinsed.

4.2.4 Drill Hole Logs

This section presents the testhole logs and piezometer configuration for the waste rock dump piezometers. Table 4.1 lists the physical coordinates of the piezometers and Figure 4.5 defines the terms used in the table. Figure 4.6 shows a location plan for the piezometers.

Table 4.1 Waste rock dump piezometer configuration.

| Piezometer | Coordinates | | Casing elevation (m) | Tip elevation (m) | Length (m) |
|------------|-------------|--------------|----------------------|-------------------|------------|
| | Easting (m) | Northing (m) | | | |
| P 97-01 | 8047.501 | 7696.383 | 1292.018 | 1271.673 | 20.345 |
| P 97-02 | 7811.257 | 6995.958 | 1281.486 | 1266.002 | 15.484 |
| P 97-03 | 7654.608 | 7019.440 | 1259.485 | 1244.728 | 14.757 |
| P 97-04 | 7917.660 | 7404.033 | 1327.369 | 1288.507 | 38.862 |
| P 97-05 | 8020.126 | 7528.878 | 1326.307 | 1297.326 | 28.981 |

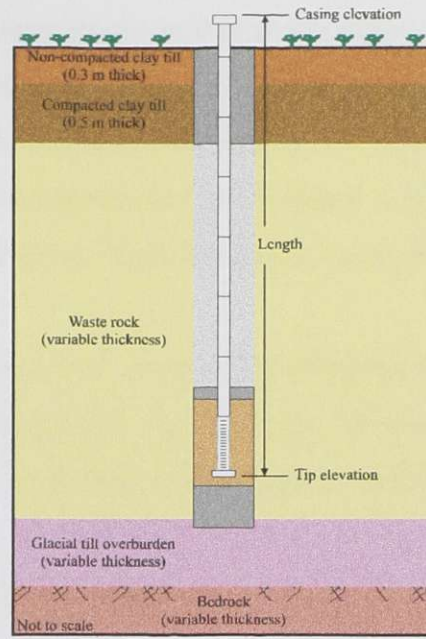


Figure 4.5 Waste rock dump piezometer configuration diagram.

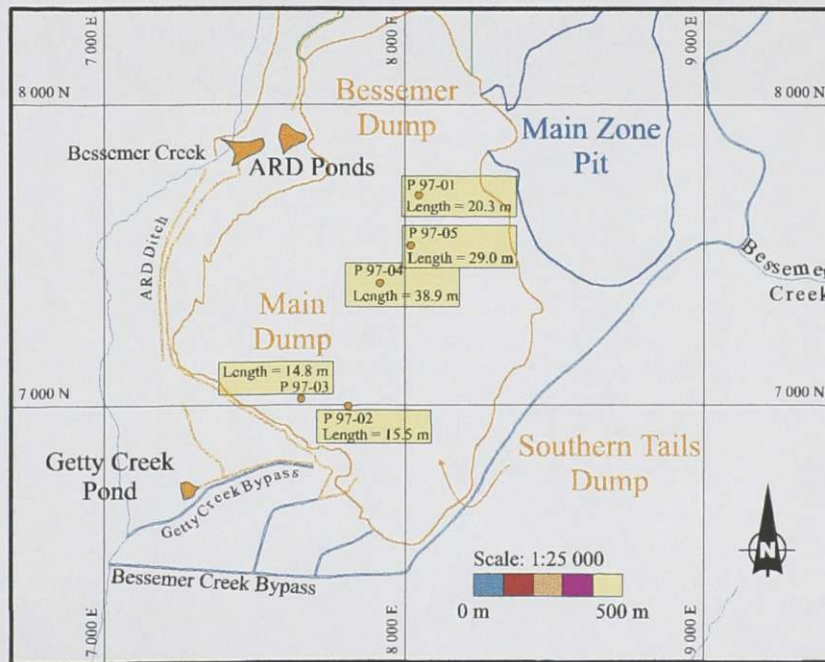


Figure 4.6 Waste rock dump piezometer locations.

Tables 4.2 through 4.6 summarize the results of the drilling for piezometers P 97-01, P 97-02, P 97-03, P 97-04 and P 97-05. A tree stump was encountered while drilling for piezometer P 97-02, which lodged into the casing. The hole was abandoned and termed TH 97-01. The water content profile for each testhole is plotted on Figure 4.7 and the paste pH profile, as determined by Placer Dome Inc., is plotted in Figure 4.8.

The water contents were measured for the highly disturbed representative 100 g samples. The oxidation state of the material was identified by examination of the physical or chemical break down of the rock with evidence of iron staining.

Table 4.2 Drill hole log for P 97-01.

| Date: September 14, 1997 | | | | | |
|---|-----------|---------------|-----------------|-------------------------|----------|
| Start drilling: 9:00 am | | | | | |
| Finish drilling: 12:00 pm | | | | | |
| Sample number | Depth (m) | Water content | Sample recovery | State of oxidation | Paste pH |
| #23301 | 4.88 | 1.3% | fair | unoxidized | 7.05 |
| #23302 | 6.10 | 1.5% | good | unoxidized | 5.41 |
| #23303 | 7.32 | 1.6% | very good | unoxidized | 3.87 |
| #23304 | 8.53 | 2.9% | very good | oxidized | 3.88 |
| #23305 | 9.75 | 3.9% | good | oxidized and unoxidixed | 3.54 |
| #23306 | 10.97 | 2.7% | very good | oxidized | 4.71 |
| #23307 | 12.19 | 0.7% | very good | unoxidized | 3.63 |
| #23308 | 13.41 | 1.5% | very good | oxidized and unoxidixed | 4.44 |
| #23309 | 14.63 | 2.3% | very good | oxidized and unoxidixed | 3.63 |
| #23310 | 15.85 | 3.3% | very good | oxidized and unoxidixed | 3.54 |
| #23311 | 17.07 | 1.8% | good | oxidized and unoxidixed | 4.48 |
| #23312 | 18.29 | 1.1% | good | unoxidized | 3.98 |
| #23313 | 19.51 | 1.6% | poor | unoxidized | 4.60 |
| #23314 | 20.42 | 14.9% | very good | oxidized and unoxidixed | 6.18 |
| Comments: | | | | | |
| Natural glacial till sample at 20.42 m. | | | | | |

Table 4.3 Drill hole log for P 97-02.

| Date: September 14, 1997 Start drilling: 9:00 am Finish drilling: 12:00 pm | | | | | |
|---|-----------|---------------|-----------------|-------------------------|----------|
| Sample number | Depth (m) | Water content | Sample recovery | State of oxidation | Paste pH |
| #23326 | 2.44 | 4.7% | fair | oxidized and unoxidized | 3.59 |
| #23327 | 3.66 | 2.2% | very good | oxidized and unoxidized | 3.74 |
| #23328 | 4.88 | 1.6% | good | oxidized | 3.52 |
| #23329 | 6.10 | 2.6% | fair | oxidized and unoxidized | 4.16 |
| #23330 | 7.32 | 1.9% | good | oxidized | 5.60 |
| #23331 | 8.53 | 8.6% | very good | oxidized and unoxidized | 3.82 |
| #23332 | 9.75 | 2.8% | poor | oxidized | 3.93 |
| #23333 | 10.97 | 1.0% | fair | unoxidized | 6.93 |
| #23334 | 12.19 | 2.0% | poor | oxidized | 6.94 |
| #23335 | 13.41 | 1.1% | fair | unoxidized | 4.94 |
| #23336 | 14.63 | 2.0% | fair | unoxidized | 3.28 |
| #23325 | 15.54 | 14.9% | very good | unoxidized | N/A |
| Comments: Latite dike material at 14.63 m. Natural glacial till sample at 15.54 m. | | | | | |

Table 4.4 Drill hole log for P 97-03.

| Date: September 14, 1997 Start drilling: 1:00 pm Finish drilling: 2:00 pm | | | | | |
|---|-----------|---------------|-----------------|-------------------------|----------|
| Sample number | Depth (m) | Water content | Sample recovery | State of oxidation | Paste pH |
| #23337 | 2.44 | 2.5% | fair | oxidized and unoxidized | 4.29 |
| #23338 | 3.66 | 3.8% | very good | oxidized and unoxidized | 6.10 |
| #23339 | 4.88 | 4.3% | poor | oxidized | 4.10 |
| #23340 | 6.10 | 1.5% | fair | unoxidized | 3.82 |
| #23341 | 7.32 | 2.4% | poor | oxidized and unoxidized | 3.51 |
| #23342 | 8.53 | 1.3% | very good | oxidized and unoxidized | 3.86 |
| #23343 | 9.75 | 2.9% | fair | oxidized | 3.66 |
| #23344 | 10.97 | 2.5% | poor | unoxidized | 5.47 |
| #23345 | 12.19 | 2.0% | poor | unoxidized | 6.67 |
| #23346 | 13.41 | 2.2% | fair | oxidized and unoxidized | 6.07 |
| #23347 | 14.63 | 1.7% | very good | oxidized and unoxidized | 6.14 |
| #23348 | 15.24 | 15.7% | very good | oxidized | 3.47 |
| Comments: Natural glacial till sample at 15.24 m. | | | | | |

Table 4.5 Drill hole log for P 97-04.

| Date: September 15, 1997 Start drilling: 10:30 am Finish drilling: 3:30 pm | | | | | |
|--|-----------|---------------|-----------------|-------------------------|----------|
| Sample number | Depth (m) | Water content | Sample recovery | State of oxidation | Paste pH |
| #23349 | 2.44 | 3.9% | poor | unoxidized | 6.73 |
| #23350 | 3.66 | 5.6% | very good | oxidized and unoxidized | 7.12 |
| #23351 | 4.88 | 2.1% | very good | oxidized and unoxidized | 4.90 |
| #23352 | 6.10 | 0.6% | very good | oxidized and unoxidized | 5.64 |
| #23353 | 7.32 | 1.0% | fair | oxidized and unoxidized | 6.07 |
| #23354 | 7.92 | 1.2% | fair | oxidized and unoxidized | 5.35 |
| #23355 | 8.53 | 1.6% | poor | unoxidized | 5.94 |
| #23356 | 9.75 | 1.0% | very good | unoxidized | 6.83 |
| #23357 | 10.97 | 1.0% | poor | unoxidized | 6.10 |
| #23358 | 12.19 | 1.4% | poor | unoxidized | 6.71 |
| #23359 | 13.41 | 2.2% | poor | oxidized and unoxidized | 6.83 |
| #23360 | 14.63 | 2.0% | fair | unoxidized | 6.79 |
| #23361 | 15.85 | 2.1% | poor | unoxidized | 5.95 |
| #23362 | 17.07 | 6.4% | fair | oxidized | 6.16 |
| #23363 | 18.29 | 4.0% | fair | oxidized | 6.05 |
| #23364 | 19.51 | 3.7% | poor | oxidized | 4.78 |
| #23365 | 20.73 | 2.3% | poor | unoxidized | 6.41 |
| #23366 | 21.95 | 3.0% | fair | unoxidized | 7.81 |
| #23367 | 23.16 | 1.8% | fair | unoxidized | 7.41 |
| #23368 | 24.38 | 2.9% | fair | oxidized and unoxidized | 7.14 |
| #23369 | 25.91 | 3.0% | poor | unoxidized | 7.58 |
| #23370 | 27.43 | 2.3% | very good | unoxidized | 8.09 |
| #23371 | 28.96 | 1.8% | very good | unoxidized | 4.31 |
| #23372 | 30.48 | 1.9% | very good | oxidized and unoxidized | 5.23 |
| #23373 | 32.00 | 1.8% | very good | oxidized and unoxidized | 6.78 |
| #23374 | 33.53 | 2.0% | very good | oxidized and unoxidized | 6.37 |
| #23375 | 35.05 | 1.4% | very good | oxidized and unoxidized | 7.77 |
| #23376 | 36.58 | 1.8% | fair | unoxidized | 7.62 |
| #23377 | 38.10 | 1.2% | poor | unoxidized | 7.87 |
| #23378 | 38.71 | 1.8% | very good | oxidized and unoxidized | 6.29 |
| #23379 | 39.01 | 1.2% | fair | unoxidized | 6.70 |

Comments:
Hit intertill layer at 17.07 m.
Latite dike material at 25.91 m.
Trace of till at 38.71 m.
Hit bedrock at 39.01 m with a trace of till.

Table 4.6 Drill hole log for P 97-05.

| Date: September 16, 1997 | | | | | |
|--------------------------|-----------|---------------|-----------------|-------------------------|----------|
| Start drilling: 10:30 am | | | | | |
| Finish drilling: 2:30 pm | | | | | |
| Sample number | Depth (m) | Water content | Sample recovery | State of oxidation | Paste pH |
| #23380 | 2.44 | 1.4% | fair | unoxidized | 7.68 |
| #23381 | 3.66 | 1.5% | fair | unoxidized | 8.06 |
| #23382 | 4.88 | 1.8% | fair | unoxidized | 7.76 |
| #23383 | 6.10 | 2.7% | fair | unoxidized | 8.05 |
| #23384 | 7.32 | 2.0% | very good | oxidized and unoxidized | 6.42 |
| #23385 | 8.53 | 4.7% | very good | oxidized and unoxidized | 5.07 |
| #23386 | 9.75 | 6.4% | good | oxidized and unoxidized | 3.47 |
| #23387 | 10.97 | 2.8% | fair | unoxidized | 5.78 |
| #23388 | 12.19 | 4.0% | good | oxidized and unoxidized | 4.17 |
| #23389 | 13.41 | 3.5% | very good | oxidized and unoxidized | 6.48 |
| #23390 | 14.63 | 2.2% | poor | unoxidized | 6.93 |
| #23391 | 15.85 | 3.1% | very good | oxidized and unoxidized | 7.06 |
| #23392 | 17.07 | 1.8% | very good | oxidized and unoxidized | 5.29 |
| #23393 | 18.29 | 2.8% | fair | oxidized and unoxidized | 5.48 |
| #23394 | 19.51 | 2.2% | fair | oxidized and unoxidized | 4.18 |
| #23395 | 20.73 | 3.1% | very good | unoxidized | 3.70 |
| #23396 | 21.95 | 5.0% | very good | unoxidized | 3.16 |
| #23397 | 23.16 | 0.9% | very good | oxidized and unoxidized | 5.17 |
| #23398 | 24.38 | 1.4% | very good | oxidized and unoxidized | 4.43 |
| #23399 | 25.91 | 0.9% | very good | unoxidized | 4.36 |
| #23400 | 27.43 | 0.7% | very good | unoxidized | 4.34 |
| #23401 | 28.96 | 0.4% | very good | unoxidized | 3.84 |

| |
|---|
| Comments: Hit bedrock at 28.96 m with no till. Samples at depths of greater than 23 m were very warm. Warm moist air blowing out of the hole at completion. |
|---|

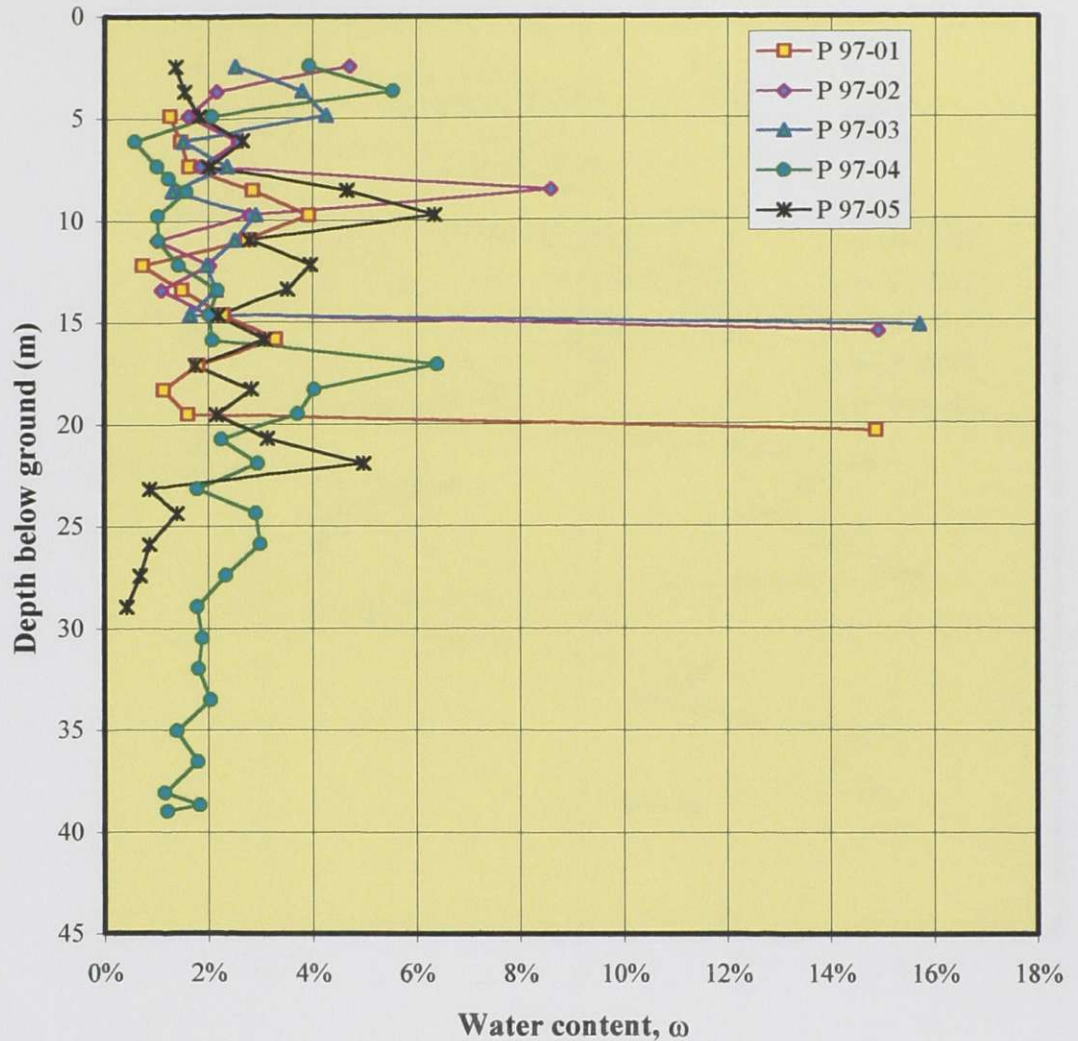


Figure 4.7 Water content profile for the waste rock dump testholes.

It can be seen that the water content for the waste rock is typically near 2 % with high values up to 6 % near the surface. The underlying natural glacial till layer has a water content of approximately 15 %. Since the samples are retrieved by air circulation, a quantity of water may have evaporated during transport to the surface; however, the plot does offer qualitative comparison.

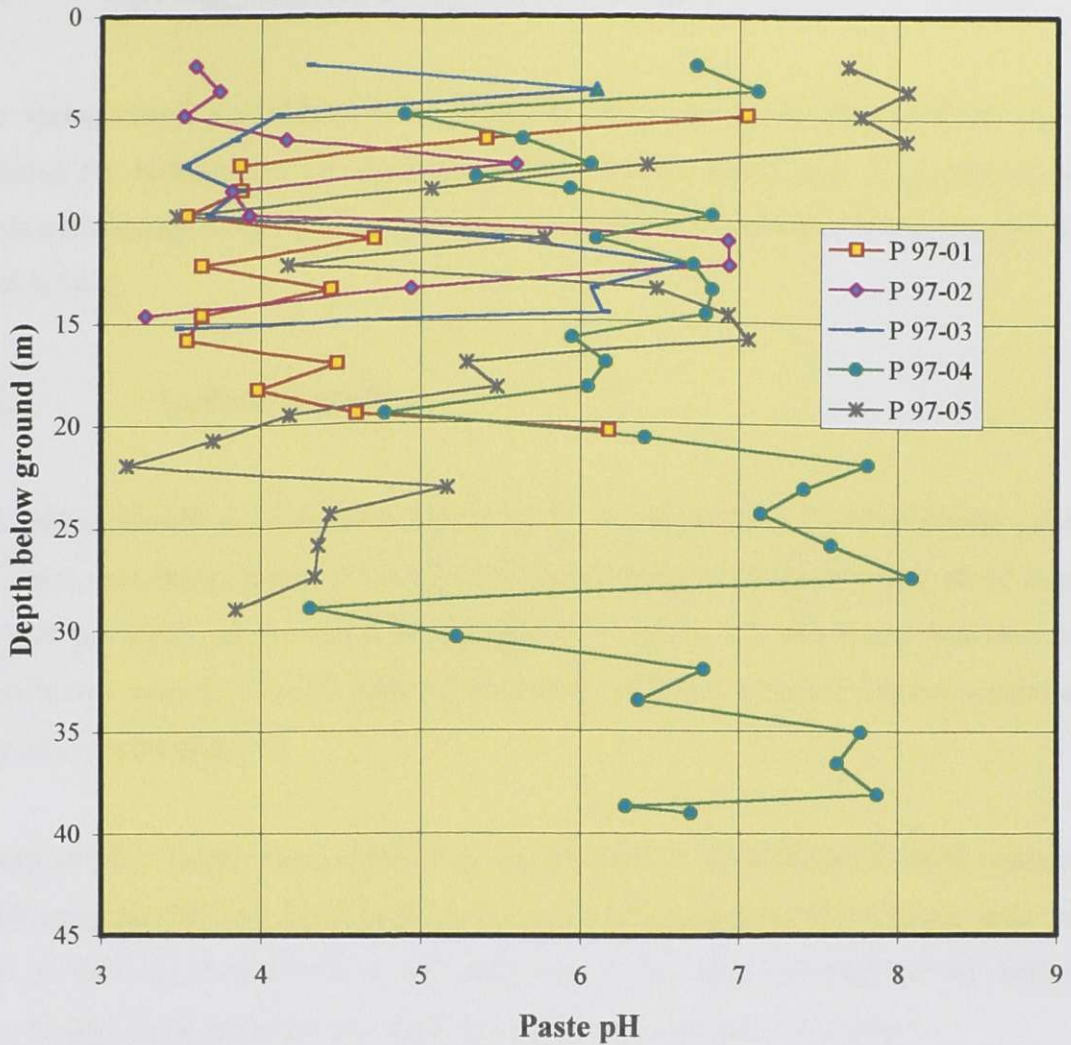


Figure 4.8 Paste pH profile for the waste rock dump testholes.

Figure 4.8 shows that there is no correlation between the field determined state of oxidation (see Table 4.2 through 4.6) and the paste pH. Most values fall between 3 and 7 pH units in no particular ordered sequence.

4.3 Spring Runoff Response - Phase II

The spring runoff was characterized in the second phase of the field program which included the hydrographs for surface runoff flow rates, waste rock dump piezometer levels and seepage flow rates out of the waste rock dump and surrounding area for the 1998 freshet.

4.3.1 Surface Runoff

The surface runoff was measured at three of the five stations for the 1998 freshet off of the waste rock dump, termed R 98-01, R 98-02 and R 98-03 (R 98-04 and R 98-05 were not instrumented). All five locations are shown in Figure 4.9 which also indicates the contributing areas for runoff. Table 4.7 lists each catchment area and relative portion of the total contributing area.

A total of 111.5 ha are characterized through the R 98-01, R 98-02 and R 98-03 stations, which accounts for 50.2 % of the total area or 70.1 % of the runoff catchment area. An area of 63.1 ha, or 28.4 % of the total area is not able to runoff to the natural environment and is entrained into the ARD system, as explained in Chapter 5.

The flows were measured at five minute intervals using a pressure transducer and a data logger installed in a weir or culvert station. There are two 900 mm diameter culverts at the R 98-01 station as shown in Figure 4.10. A pressure transducer was installed in the culvert to measure hydraulic head, which was used to calculate a flow rate with the brink depth method for a free outlet of a level circular pipe. The slope of the culvert is, however, 7.85 % over a total length of 12 m. A close correlation was found using this formula during the calibration process.

A combination V-notch and broad crested weir was used at R 98-02 as shown in Figure 4.11. The heads were measured using a pressure transducer and a data logger located

upstream of the weir. The 90° angle V-notch was 85 mm in depth and was the base of a 927 mm wide broad crested weir. Calibration determined the V-notch weir coefficient to be 1.345 and the broad crested weir coefficient to be 1.678.

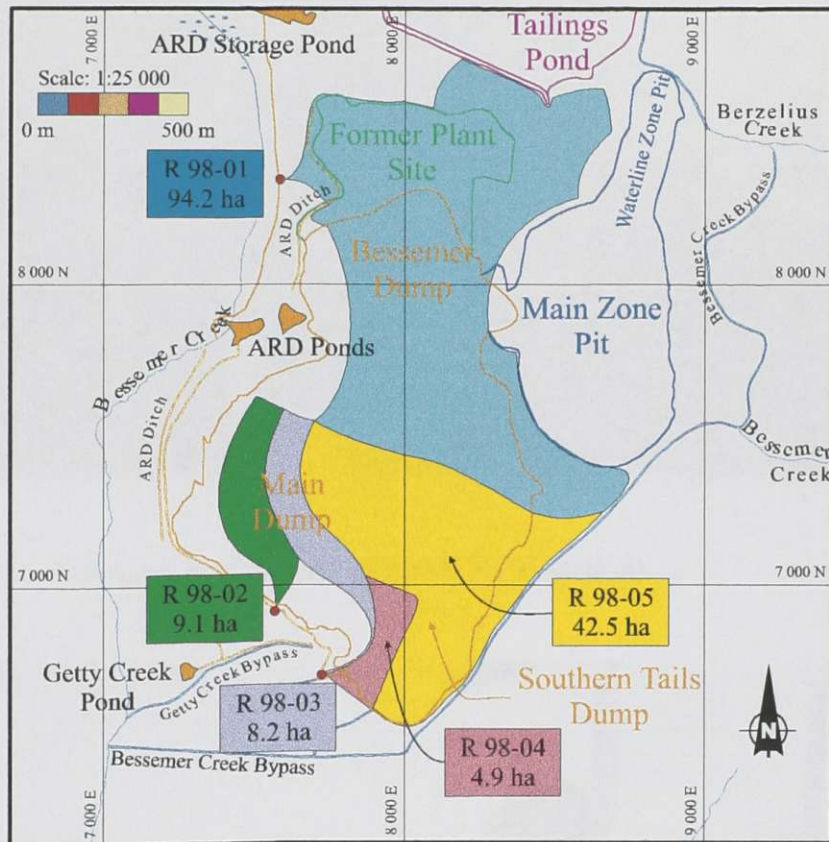


Figure 4.9 Runoff stations and corresponding contributing areas.

Table 4.7 Description of runoff catchment areas.

| Contributing area | Area (ha) | Portion of total area |
|-------------------|--------------|-----------------------|
| R 98-01 | 94.2 | 42.4% |
| R 98-02 | 9.1 | 4.1% |
| R 98-03 | 8.2 | 3.7% |
| R 98-04 | 4.9 | 2.2% |
| R 98-05 | 42.5 | 19.1% |
| Outside catchment | 63.1 | 28.4% |
| Total | 222.0 | 100.0% |



Figure 4.10 Culvert flow instrumentation (R 98-01 station).



Figure 4.11 Weir flow instrumentation (R 98-02 station).

A dual broad crested weir was used at the R 98-03 station as shown in Figure 4.12. The hydraulic head was measured using a pressure transducer and a data logger which was located upstream of the weir. The first broad crested weir was 205 mm in depth and was 245 mm wide and was in the base of the second broad crested weir. The second weir was 1,495 mm wide. Calibration determined a broad crested weir coefficient to be 1.678.



Figure 4.12 Weir flow instrumentation (R 98-03 station).

The flows were measured at five minute intervals and indicated that the freshet exhibited a definite diurnal process in which the flow rates peaked around 6:00 PM daily. The maximum flow rates occurred on April 28. The following three figures display the flow measurements for the three runoff stations: R 98-01, R 98-02 and R 98-03.

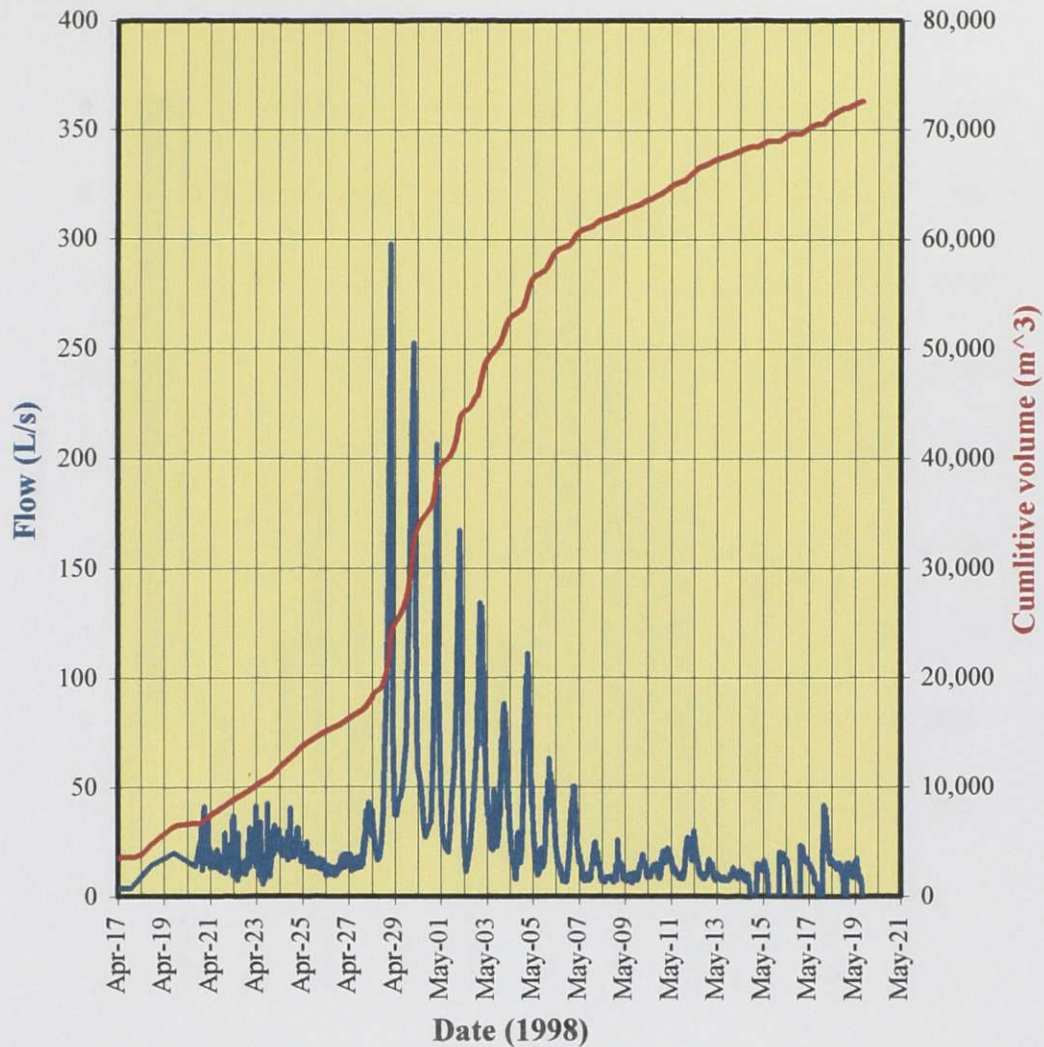


Figure 4.13 Flow measurement for R 98-01.

The freshet started on March 18 and the flows were estimated until April 20, 1998. The scatter in the data at low flow rates is the result of turbulent flow in the culverts as a consequence of low hydraulic head. There was a drastic increase in flow for a short period on April 24 and April 28 to May 2 and was suspected to be the result of an ice jam. The interim values were estimated based on previous characteristic flow rates.

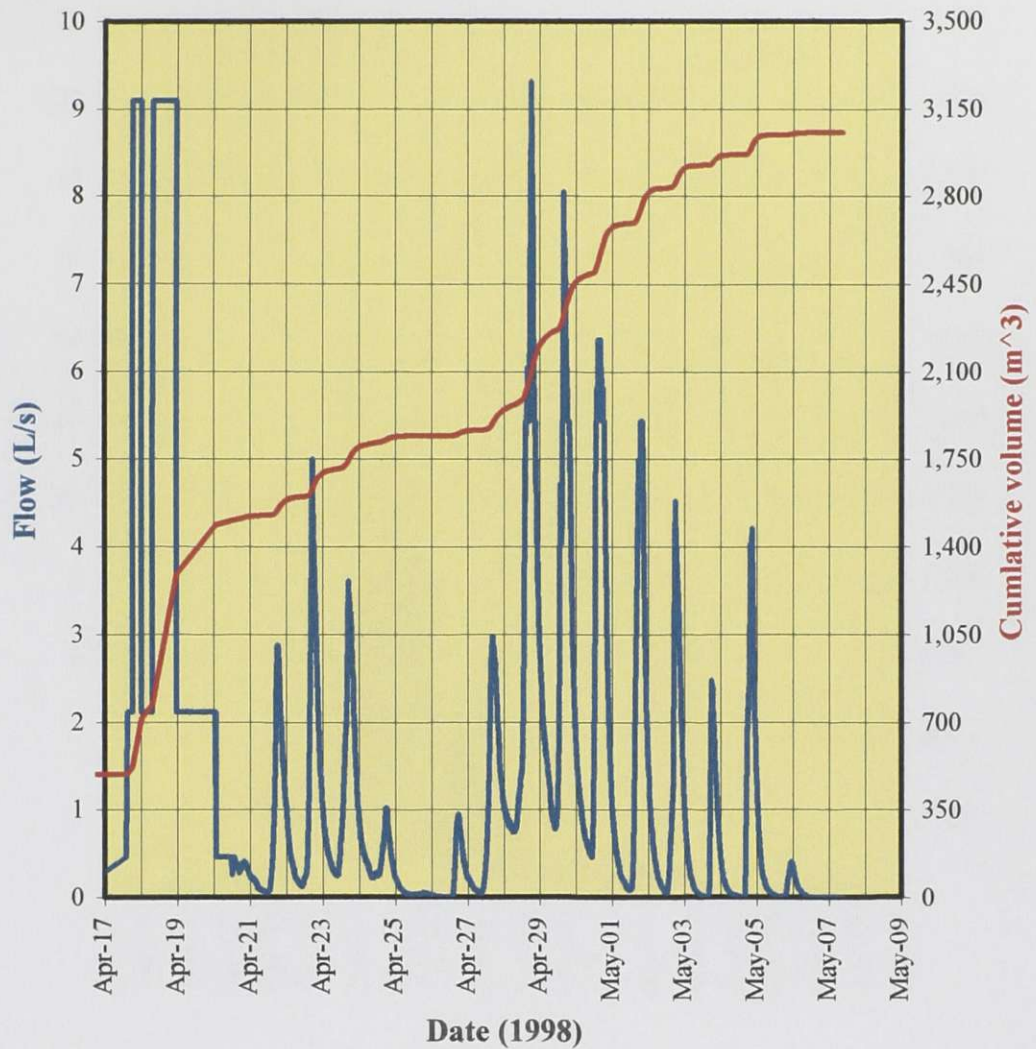


Figure 4.14 Flow measurement for R 98-02.

The runoff water did not reach the R 98-02 station until March 20 and the flows were estimated until April 20, 1998 based on field observations.

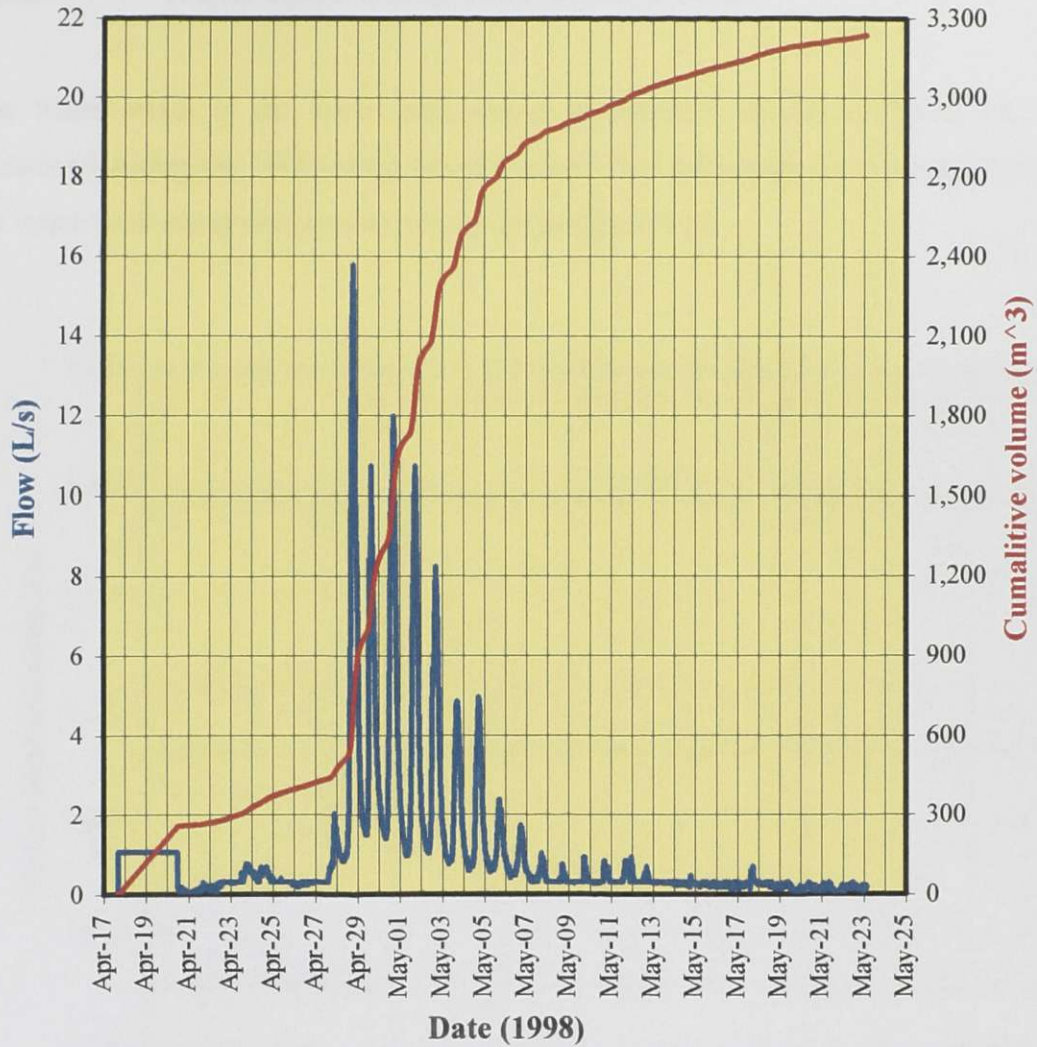


Figure 4.15 Flow measurement for R 98-03.

The freshet did not start at the R 98-03 station until April 17, 1998 and the flows were set to zero beforehand but were however estimated until April 20.

4.3.2 Waste Rock Dump Piezometer Levels

The water levels in the waste rock dump piezometers shown in Figure 4.6 were monitored during the 1998 spring runoff period. The hydrograph for the water levels in the waste rock dump piezometers are shown in Figure 4.16.

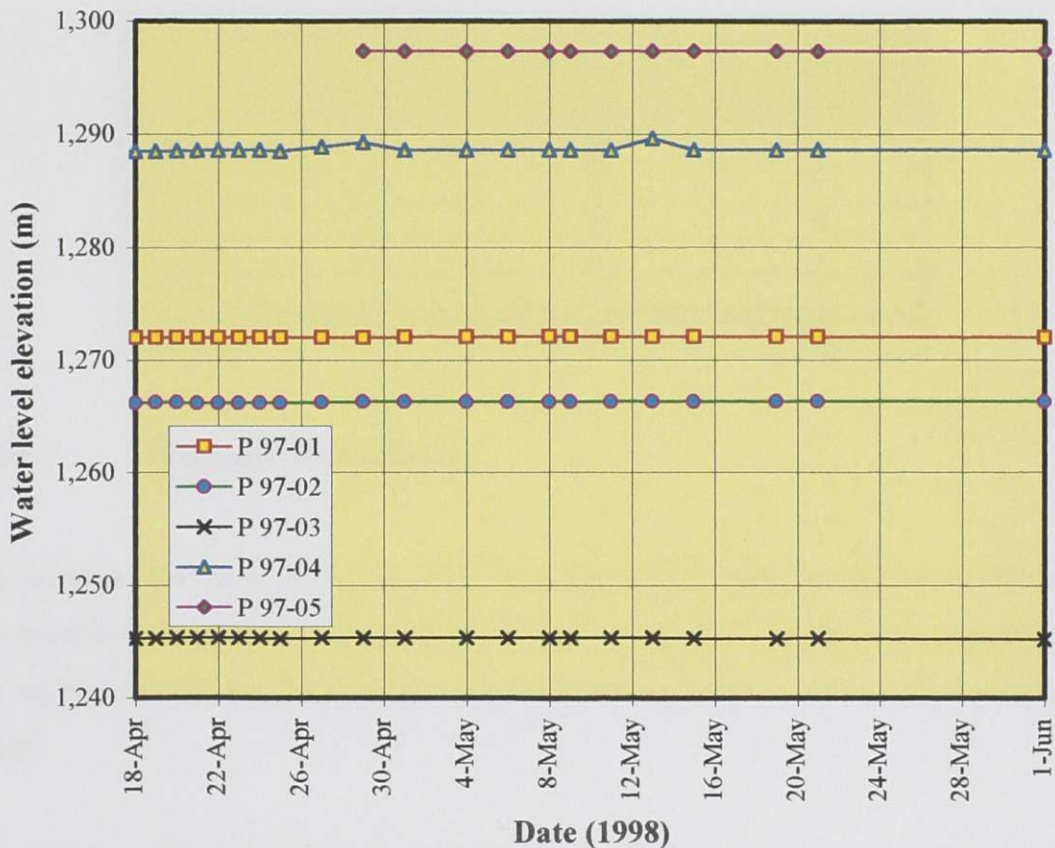


Figure 4.16 Water level in the waste rock dump piezometers.

Figure 4.16 shows that there is no significant response in water level elevations for the waste rock dump piezometers. The unusually high value for P 97-04 on May 13 seems unlikely as measurements from a 40 m piezometer are not reliable and may be disregarded.

Table 4.8 lists the maximum rise in water elevation in the waste rock dump piezometers and the number of days from the piezometer peak to the freshet peak (April 28). The average rise in piezometer water level elevation was 35 mm and occurred two days after the freshet peak.

Table 4.8 Spring freshet response in the waste rock dump piezometers.

| Piezometer | Rise in water level (mm) | Peak after freshet peak (days) |
|----------------|--------------------------|--------------------------------|
| P 97-01 | 40 | 3 |
| P 97-02 | 11 | 1 |
| P 97-03 | 70 | 6 |
| P 97-04 | 12 | 1 |
| P 97-05 | 40 | 1 |
| Average | 35 | 2 |

4.3.3 Seepage Flow Rates

The seepage flow rates out of the waste rock dump (described in Section 5.4.4) were also measured during the 1998 spring runoff with a graduated cylinder and a stop watch. The hydrograph for the seepage flow rates is shown in Figure 4.17 and do not include runoff.

The majority of the seeps peaked at the freshet peak with the others peaking only one or two days after. This immediate response is in contrast to the delayed three day response in the waste rock dump piezometers.

The average increase in seepage flow at the maximum peak is in the order of 8 times the nominal flow values.

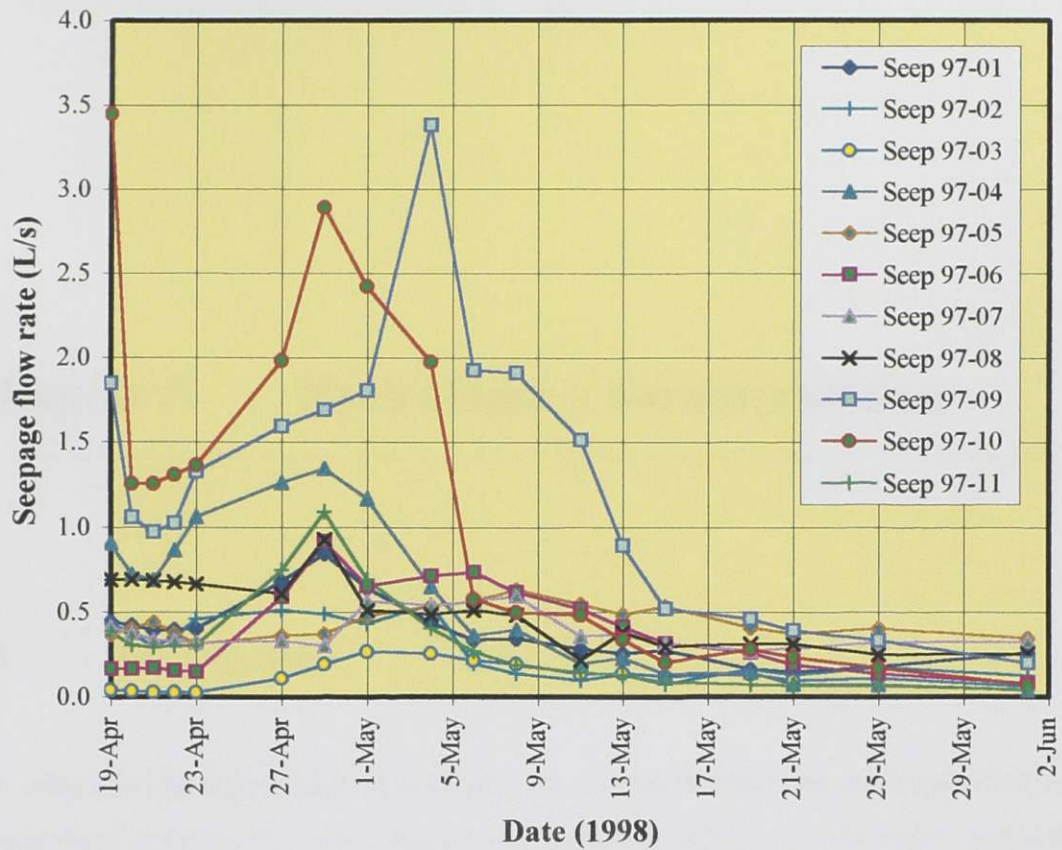


Figure 4.17 Waste rock dump seepage flow rate hydrograph.

Chapter 5 Hydrologic Characterization

5.1 Introduction

The complete characterization of a hydrologic system requires the examination of five components: geologic structure, topography, surface hydrology, groundwater and water chemistry. The following sections will describe these five elements in detail for the Equity Silver Mine hydrologic system.

5.2 Geologic Structure

Equity Silver Mine is located in a region termed the Buck Creek area. The regional geology in the Buck Creek area, as shown in Figure 5.1, consists mainly of sedimentary and volcanic rocks in addition to a number of igneous intrusions of the Mesozoic Era and the Tertiary Period (Church and Barakso, 1990). The rock formations are chiefly covered with glacial deposits of the Pleistocene Epoch which vary in thickness' up to 25 m. The outline of Equity Silver Mine has been superimposed on Figure 5.1 and the components of the mine will be discussed later in the chapter.

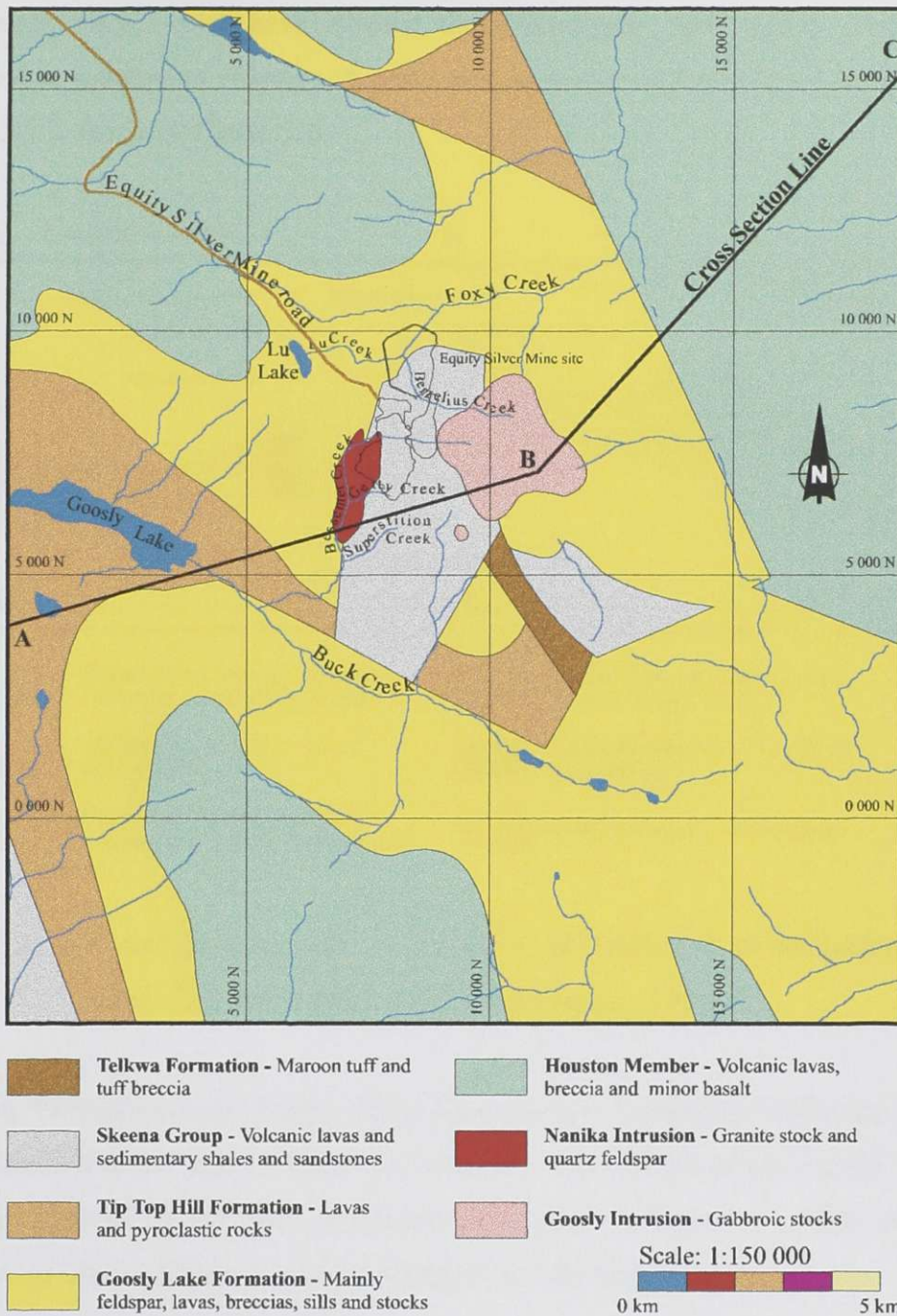


Figure 5.1 General geology of the Buck Creek area (after Church and Barakso, 1990).

Figure 5.1 depicts the natural setting of the Buck Creek area. Since mining activities have been initiated, many of the creeks have been rerouted and excavation and filling activities

have taken place, which have affected the groundwater flow regime. This will be discussed in subsequent chapters. A cross section (points A,B and C) of the geology in Figure 5.1 is shown in Figure 5.2.

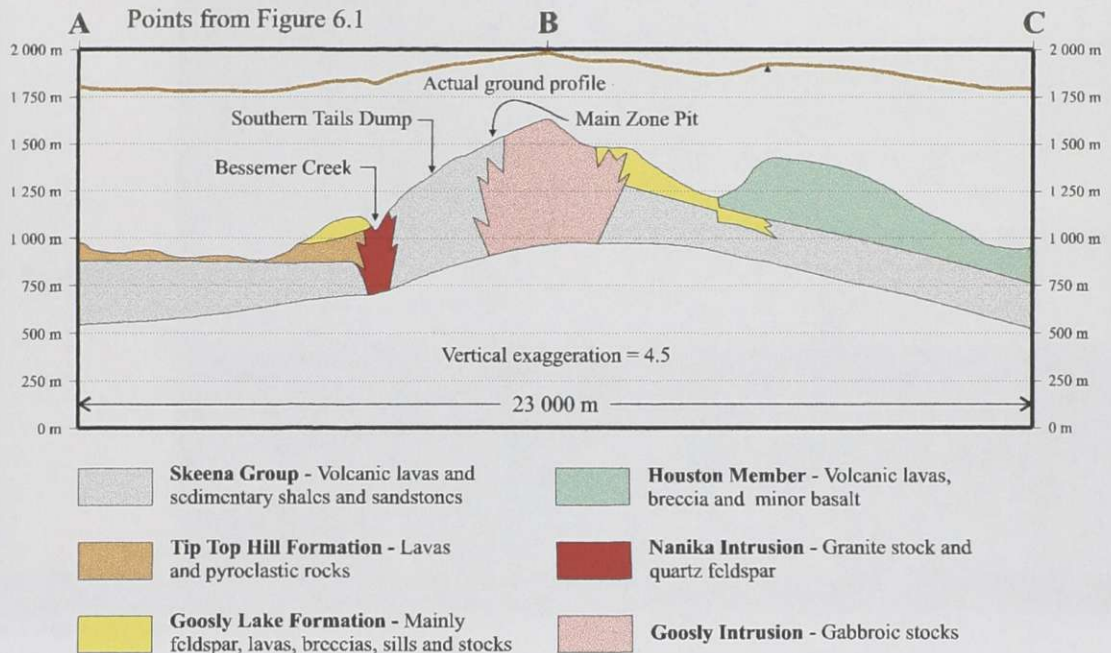


Figure 5.2 Cross section (points A, B, and C in Figure 5.1) of the geology of the Buck Creek area (after Church and Barakso, 1990).

The rock formations in the Equity Silver Mine area are discussed in following sections. The Houston Member and the Telkwa Formation will not be discussed in detail, however brief descriptions of the rock formations are given in Figure 5.1. The geological terminology used in Figure 5.1 is also explained in following sections.

A stratigraphical column that displays the name, duration and age of the geological units is depicted in Table 5.1.

Table 5.1 The stratigraphical column (after Blyth and Freitas, 1984).

| Eon | Era | Period | Epoch | Duration (x 10 ⁶ years) | Age (x 10 ⁶ years) |
|-------------|-----------|---------------|-------------|---------------------------------------|----------------------------------|
| Phanerozoic | Cenozoic | Quaternary | Holocene | 0.01 | 0.01 |
| | | | Pleistocene | 1.99 | 2 |
| | | Tertiary | Pliocene | 10 | 12 |
| | | | Miocene | 13 | 25 |
| | | | Oligocene | 15 | 40 |
| | | | Eocene | 14 | 54 |
| | Paleocene | | 11 | 65 | |
| | Mesozoic | Cretaceous | N/A | 79 | 144 |
| | | Jurassic | N/A | 69 | 213 |
| | | Triassic | N/A | 35 | 248 |
| | Paleozoic | Permian | N/A | 38 | 286 |
| | | Carboniferous | N/A | 74 | 360 |
| | | Devonian | N/A | 48 | 408 |
| | | Silurian | N/A | 30 | 438 |
| | | Ordovician | N/A | 67 | 505 |
| | | Cambrian | N/A | 85 | 590 |
| Precambrian | | | | | |

N/A implies that there are too many types of Epochs to list.

The general geology of the Equity Silver Mine area consists of late Cretaceous volcanic features that outcrop throughout the center portion of the mining area. Eocene (Tertiary Period) volcanic deposits cover the western and northern region while a Paleocene (Tertiary Period) igneous intrusion outcrops in the southwestern region of the mine vicinity. Another igneous intrusion of the Eocene Epoch (Tertiary Period) outcrops on the eastern border as shown in Figure 5.3. The Equity Silver Mine gold, copper and silver deposits are found within the late Cretaceous volcanic and sedimentary beds which are exposed through a window in the overlying early Cretaceous and Tertiary units. The host rock was previously believed to belong to the Hazleton Group of Jurassic age; however, it is believed to be of the Skeena Group of the late Cretaceous age (Wright Engineers Limited, 1976). The upper 10 m of all bedrock formations in this region are believed to be fractured, which appear to be the source for Bessemer and Getty Creeks (Klohn Leonoff, 1991b). The geology of the Equity Silver Mine with the generic rock names is shown in Figure 5.3. The generic names are discussed in following subsections.

The hydraulic conductivities of the rock formations and an outline of Equity Silver Mine is superimposed on Figure 5.3 with rivers from the natural setting displayed. The rivers were relocated during development of the mine.

Table 5.2 lists the hydraulic conductivities taken from the Klohn Leonoff (1991b) hydrogeological report.

The range of hydraulic conductivity columns were determined by numerous past hydrogeology studies that were performed at the mine. The representative bulk hydraulic conductivity was used as the initial conditions in the MODFLOW groundwater modelling simulation in the Klohn Leonoff (1991b) hydrogeological report. The value was determined on the range and amount of data available. The hydraulic conductivities were modified upon model calibration in the analysis.

Figure 5.4 illustrates to scale the ages and duration of the geological formations described in the previous subsections.

The following subsections give a detailed description of the geological units in the study area from oldest to youngest.

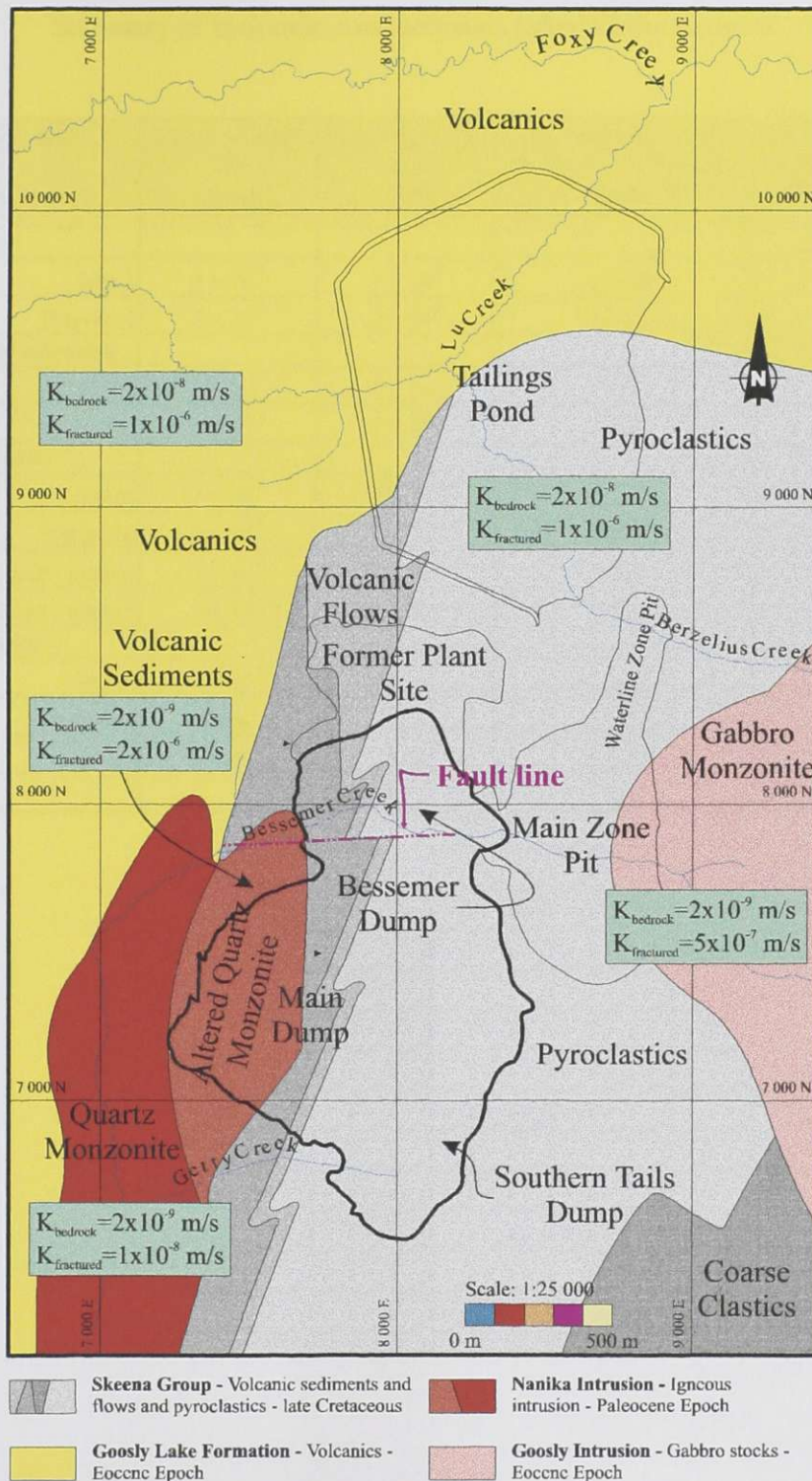


Figure 5.3 Detailed geology of the Equity Silver Mine area (after Church and Barakso, 1990 and Klohn Leonoff, 1991b).

Table 5.2 Summary of hydraulic conductivities (after Klohn Leonoff, 1991b).

| Geologic unit | Range of hydraulic conductivity | | Representative bulk hydraulic conductivity (m/s) | After MODFLOW model calibration (m/s) |
|------------------------------|---------------------------------|--------------------|--|---------------------------------------|
| | Low (m/s) | High (m/s) | | |
| Skeena Group | | | | |
| Intact | 1×10^{-9} | 3×10^{-7} | 2×10^{-7} | 2×10^{-8} |
| Fractured | 3×10^{-7} | 3×10^{-6} | 2×10^{-6} | 1×10^{-6} |
| Goosly Lake Formation | | | | |
| Intact | 1×10^{-9} | 1×10^{-6} | N/A | 2×10^{-8} |
| Fractured | 1×10^{-8} | 1×10^{-5} | N/A | 1×10^{-6} |
| Nanika Intrusion | | | | |
| Intact | 1×10^{-9} | 5×10^{-7} | 7×10^{-9} | 2×10^{-9} |
| Fractured | 5×10^{-9} | 5×10^{-8} | N/A | 1×10^{-8} |
| Intact - altered | 1×10^{-9} | 1×10^{-7} | N/A | 2×10^{-9} |
| Fractured - altered | 5×10^{-7} | 5×10^{-6} | N/A | 2×10^{-6} |
| Goosly Intrusion | | | | |
| Intact | 1×10^{-9} | 5×10^{-7} | 2×10^{-8} | 2×10^{-9} |
| Fractured | N/A | N/A | 5×10^{-7} | N/A |
| Glacial Till | | | | |
| | 1×10^{-9} | 1×10^{-7} | 5×10^{-7} | 2×10^{-8} |
| Waste Rock | | | | |
| | $> 1 \times 10^{-2}$ | | N/A | 1×10^{-1} |

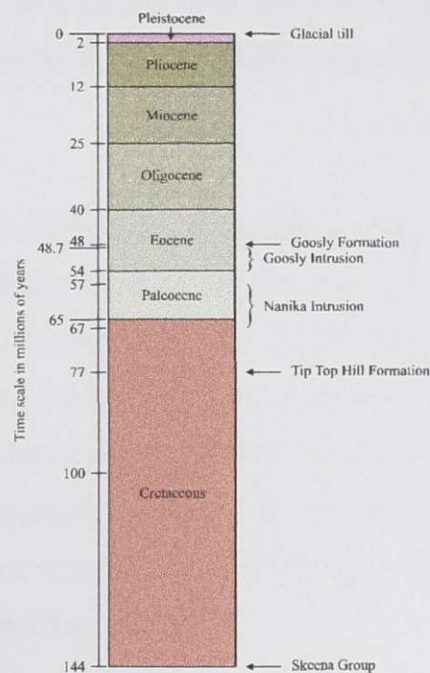


Figure 5.4 Time scale of the geologic units at Equity Silver Mine.

5.2.1 Skeena Group

The Skeena rocks are of late Cretaceous age and are defined by Tipper and Richards (1976) as a mixture of marine and nonmarine sedimentary and volcanic strata. The sedimentary rocks consist of greywackes, shale and conglomerates (Church and Barakso, 1990). Greywackes contain grains from quartz (SiO_2) and feldspar, which are cemented together with a fine matrix material with little sorting, and is usually caused by landmasses that are rapidly uplifted (Blyth and Freitas, 1984). Feldspar is defined as rock-forming minerals occurring principally in igneous rocks and consisting of a mixture of potassium, sodium or calcium aluminum-silicates. Shale is a sedimentary rock that is formed by the consolidation of a unit of colloidal sized clay particles. Conglomerates are cemented grains of sediments varying from gravel to pebble size.

The volcanic features include breccias, tuffs and lava flows. Breccia is rock composed of sharp-angled fragments embedded in a fine-grained matrix. Tuffs are rock that is formed from volcanic ash that vary in grain size from fine sand to gravel. Lava flows are simply rocks that are formed due to the flowing of molten lava, which originates from a volcano or fissure.

The Skeena rocks outcrop throughout the center portion of the mine site and other infrequent locations throughout the Buck Creek area (see Figure 5.1). They have been forced to the surface at Equity Silver Mine due to an uplifting process caused by adjacent igneous activity named the Goosly Intrusion (covered in Section 5.2.5). A similar but smaller igneous intrusion has cut through the Skeena rocks near the southwestern boundary of the mine site termed the Nanika Intrusion (covered in Section 5.2.4). The combined effort of these two intrusions are believed to be the source of mineralization in the Skeena rocks (Church and Barakso, 1990).

The Skeena rocks are approximately 750 m thick (60 m of orebody) and are strewn with a variety of almost vertical Tertiary age dikes (Church and Barakso, 1990). Church and

Barakso (1990) further state that the top of the Skeena rocks, which contain about 3.8 % pyrite (FeS_2), are comprised of soft tuffs and small fragments of lava while the mid-section region is composed mainly of tuff-breccia and coarse volcanic debris. The base of the geological unit consists of mainly tuff breccia and some conglomerates. Felsic and andesitic dikes cut through the ore zone from 48.3 to 49.9 million years ago (Cyr *et al.*, 1984). The dikes represent approximately 15 to 20 % of the total rock mass in the Main Zone area and only 3 % in the Southern Tails Zone area (Wright Engineers Limited, 1976).

The Skeena rocks generally strike north-south and dip west at 45° to 80° resulting in the oldest rocks being exposed on the eastern side of the group's overall outcrop. The Skeena Group is further divided into inter-subdivisions of three main groups (see Figure 5.3) which from oldest to youngest are Coarse Clastic Division, Pyroclastic Division and the Volcanic-Sedimentary Division (Wright Engineers Limited, 1976). The Coarse Clastic Division is mainly composed of conglomerate rocks and outcrops in the southeast corner of the mine site. The Pyroclastic Division (where the orebody occurs) stretches throughout the center portion of the Skeena Group which includes tuffs and volcanic tuff. Pyroclastic rocks are defined as rock fragments of explosive volcanic origin. The Volcanic-Sedimentary Division is largely composed of tuffs and pebble conglomerates (Wright Engineers Limited, 1976) and covers the extreme western region of the Skeena Group. A volcanic lava flow separates the Volcanic-Sedimentary Division and the Pyroclastic Division.

Klohn Leonoff (1991b) hydrogeological report indicates a hydraulic conductivity of 2×10^{-8} m/s for intact bedrock and 1×10^{-6} m/s for weathered bedrock.

A single fault exists along the divide between the Bessemer Dump and the Main Dump, which runs east and west and seems to be the origin of Bessemer Creek (Klohn Leonoff, 1984) This fault is believed to be a major groundwater discharge source. The fault line lies directly beneath Bessemer Dump and acts as a hydraulic connection between the

fractured bedrock and the waste rock. This connection could contribute significant amounts of groundwater to the acid water within the waste rock dump. The configuration of the fault is unknown as limited information exists.

5.2.2 Tip Top Hill Formation

The Tip Top Hill Formation of the early Cretaceous Period is a unit within the informally named Francois Lake Group described by Church (1971), consisting of andesitic lava and pyroclastic rocks. Andesite is a gray, fine-grained volcanic rock composed of mostly feldspar. The formation is void of sulphide mineralization (Wright Engineers Limited, 1976). Church and Barakso (1990) date the formation at 77.1 ± 2.7 million years old.

The formation is approximately 500 m in thickness and occurs in the western, northern and central regions of the Buck Creek region (see Figure 5.1). The rocks are mainly brown volcanic breccias (Church and Barakso, 1990).

Golder Associates (1983) hydrogeological report indicates a hydraulic conductivity of 9.2×10^{-10} m/s for the Tip Top Hill Formation.

The Tip Top Hill Formation was not used in this thesis, as it is out of the defined site area. However it was used in the Klohn Leonoff (1991b) hydrogeological report.

5.2.3 Goosly Lake Formation

The Goosly Lake formation of the Tertiary Period (Eocene Epoch) is a unit within the Francois Lake Group also named by Church (1971). It is mainly trachyandesite lava which is fine-grained volcanic rock consisting of mostly alkali feldspar. The formation is void of sulphide mineralization (Wright Engineers Limited, 1976). Church and Barakso (1990) date the formation at 48.8 ± 1.8 million years old.

The formation is approximately 500 m in thickness and covers most of the central and southeastern areas (see Figure 5.1) of the Buck Creek region (Church and Barakso, 1990). The probable cause of this formation is the Goosly Intrusion which is discussed in Section 5.2.5 (Church and Barakso, 1990).

Klohn Leonoff (1991b) hydrogeological report indicates a hydraulic conductivity of 2×10^{-8} m/s for intact bedrock and 1×10^{-6} m/s for weathered bedrock.

5.2.4 Nanika Intrusion

The Nanika Intrusion is of the Paleocene age (Tertiary Period) and consists of microporphyritic granite (Church and Barakso, 1990). Porphyritic rocks contain large feldspar crystals in a fine-grained igneous matrix. Granite is simply defined as a coarse-grained rock composed chiefly of quartz and feldspars. Wright Engineers Limited (1976), describe this unit as a quartz monzonite stock, composed largely of plagioclase and orthoclase. Plagioclase is triclinic feldspars consisting of a mixture of calcium and sodium aluminum-silicates while orthoclase are monoclinic feldspars, more particularly potassium aluminum-silicates. Stock refers to a body of intrusive rock that has less than 100 km² of exposed surface. This intrusion began 67.2 ± 2.0 million years ago and was completed 10.2 ± 2.4 million years later (Church and Barakso, 1990).

The Nanika Intrusion is located in the southwest region of the Equity Silver Mine area with the upper northeast portion containing altered quartz monzonite (see Figure 5.3).

Klohn Leonoff (1991b) hydrogeological report indicates a hydraulic conductivity of 2×10^{-9} m/s for intact bedrock, 1×10^{-8} m/s for weathered bedrock, 2×10^{-9} m/s for intact-altered bedrock and 2×10^{-6} m/s for weathered-altered bedrock

5.2.5 Goosly Intrusion

The Goosly Intrusions of Eocene Epoch are generally syenomonzonite-gabbro stock masses produced by an intrusive process. Syenomonzonite are alkali rocks composed chiefly of plagioclase and orthoclase. Gabbro simply refers to coarse-grained igneous rock.

The intrusion at the Equity Silver Mine site started approximately 54.3 million years ago and completed the intrusive process approximately 48.7 million years ago (Church and Barakso, 1990). Felsic and andesitic dikes cut through the gabbro stock from 48.3 to 49.9 million years ago (Cyr *et al.*, 1984).

The Goosly Intrusion occurs on the eastern border of the Equity Silver Mine area (see Figure 5.3) and other areas in the Buck Creek area (see Figure 5.1).

Klohn Leonoff (1991b) hydrogeological report indicates a hydraulic conductivity of 2×10^{-9} m/s for intact bedrock and 5×10^{-7} m/s for weathered bedrock.

5.2.6 Glacial Till

The till was deposited by regional and valley glaciation in the Pleistocene Epoch (Church and Barakso, 1990). The Wisconsin (Fraser) Cordilleran regional ice sheet generally came from the east and carried sediments with a wide variety of sizes (Church and Barakso, 1990). A glacial till formation consisting of sediments from boulder size to colloidal size was deposited over the bedrock upon retreat of the glacier.

The deposit is generally continuous with formation depth dependent on the bedrock topography. The till unit tends to be thick where valleys existed in the underlying bedrock and thin where bedrock highs were present (Golder Associates, 1983). The glacial till may be non-existent in the southwest portion of the Main Dump (Aziz, 1998).

The till cover on the side slope east of the Main Zone Pit is thin with a thickness of less than 5 m. The geological unit increases to a thickness of greater than 20 m in Bessemer and Getty Creek valleys and then thins out to the west up the opposite side slope. A till isopach for the waste rock dump area is shown in Figure 5.5 and is believed to have an accuracy of ± 1 m. There is no data available outside of this region.

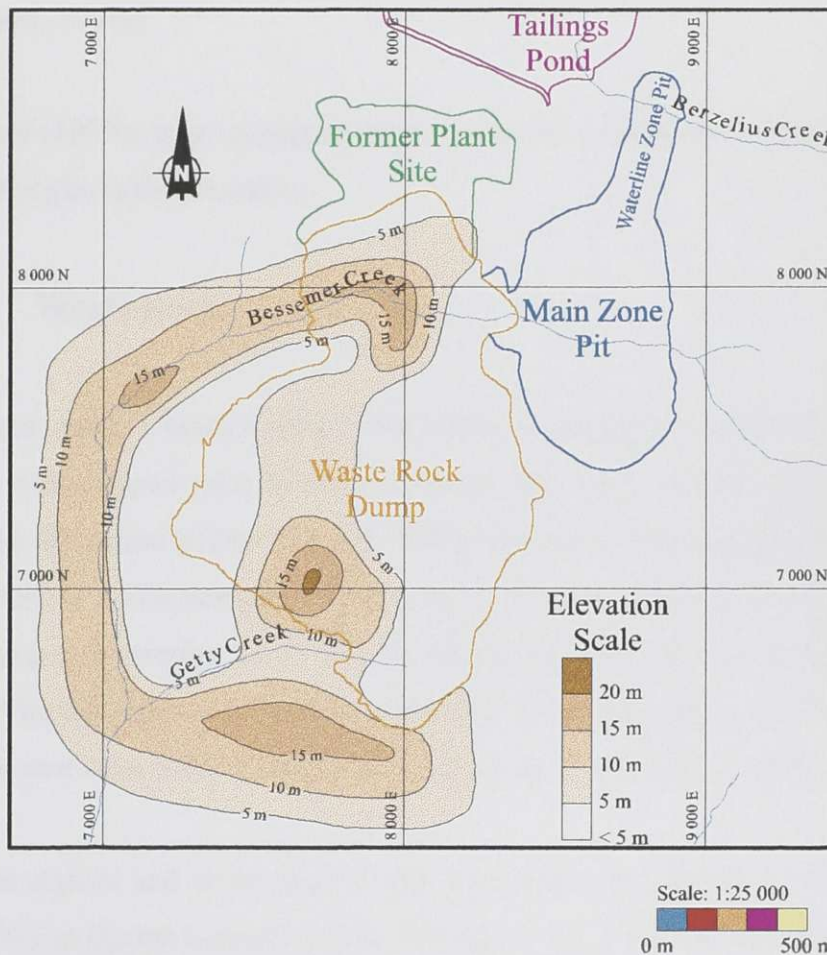


Figure 5.5 Till isopachs.

The till has a high percentage of clay and silt (30 to 50 %) coupled with cobble and boulder size rocks (Klohn Leonoff, 1991a). The till is firm to stiff and generally oxidized at the surface and near surface region and underlain by unoxidized till (Klohn Leonoff, 1984).

Klohn Leonoff (1984) reported an effective friction angle (ϕ') of 25° for the till from a consolidated undrained triaxial test. The average plastic limit was reported to be 18 %, with the water content at the plastic limit and a liquid limit of 41 % (Klohn Leonoff, 1984).

Luviosolic order soils have established on the glacial till cover under a coniferous forest (Klohn Leonoff, 1991a).

Klohn Leonoff (1991b) hydrogeological report indicates a hydraulic conductivity of 2×10^{-8} m/s for the glacial till formation.

5.2.7 Waste Rock

The waste rock dump consists mainly of the blasted and quarried overburden rock. The forest cover was stripped prior to construction of the waste dump which was placed directly on the till surface (Klohn Leonoff, 1984). The waste rock is mainly derived from the Skeena Group rocks (covered in Section 5.2.1) with a portion from the Goosly Intrusion (covered in Section 5.2.5) and the associated dikes that cut through the rock formations. Varying degrees of sulphide oxidation exists throughout the profile of the dump with no particular order or sequence based on the field drilling program.

The rock was angular and varies in grain size from sand size particles to boulders with diameters of 0.5 m (Klohn Leonoff, 1984). The waste rock dump was constructed by end dumping from trucks forming a side slope and tier arrangement in 10 m lifts and was regraded to a constant slope (maximum 21°) in 1991 (O'Kane, 1995). The Klohn Leonoff (1984) stability report states an overall friction angle (ϕ) of 37.5° . A photograph of the waste rock can be seen in Figure 1.5.

The dump varies in thickness from 0 to 61 m above natural ground, with the maximum thickness occurring in the Bessemer Dump. It reaches a maximum thickness of 113 m

above the excavated ground in the northern area of the Southern Tails Zone Pit. Waste rock from the Main Zone Pit was placed in the Southern Tails Zone Pit after this area was mined. The waste rock dump isopach is shown in Figure 5.6 with the modified creek and diversion channel configuration shown.

The accuracy is believed to be in the range of ± 2 m, as the data was taken from 10 m interval contour plots.

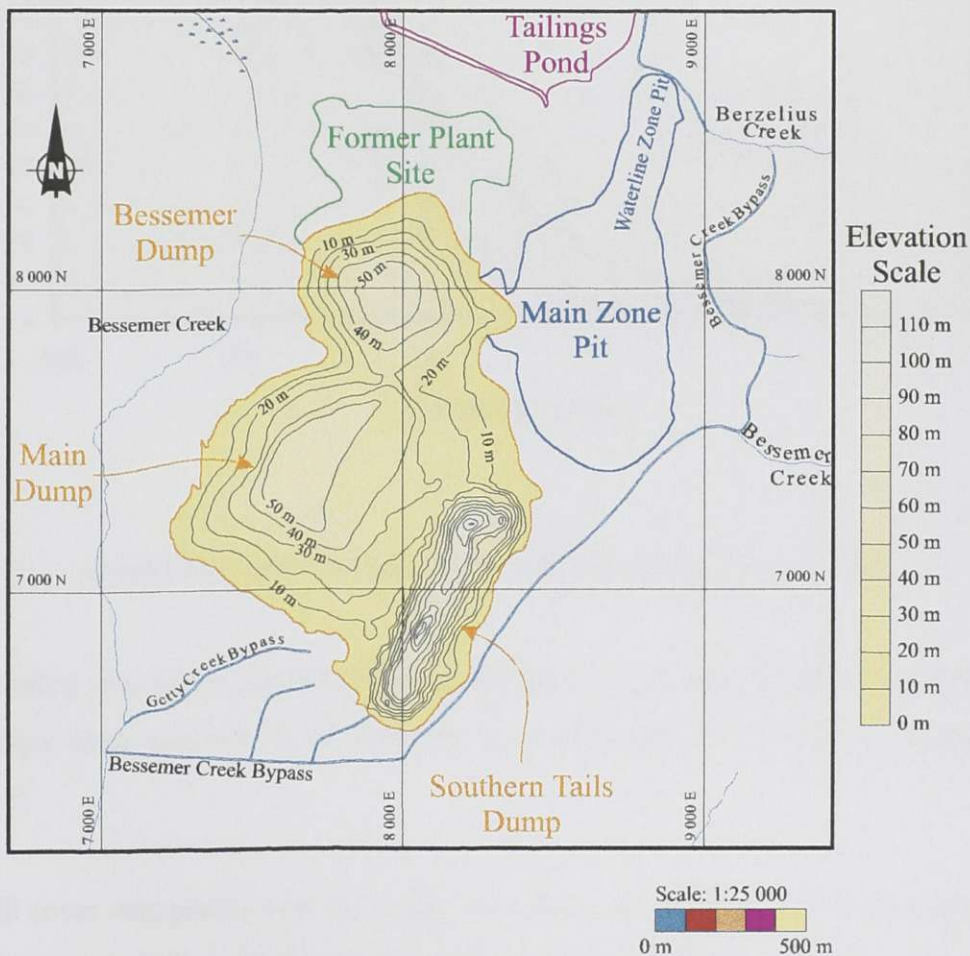


Figure 5.6 Waste rock dump isopachs.

Grain size curves were measured for three separate portions of the dump by the University of Saskatchewan during a regrading program in 1991 (Newman, 1994). The

waste rock has weathered since the regrading program and is assumed to be altered to a degree similar to the study conducted by Herasymuik (1996) and is therefore used in this analysis as no other information is available and it is the best available data. The study shows that the waste rock's grain size distribution falls within the range shown in Figure 5.7. The waste rock at the mine site is believed to be presently in the same order.

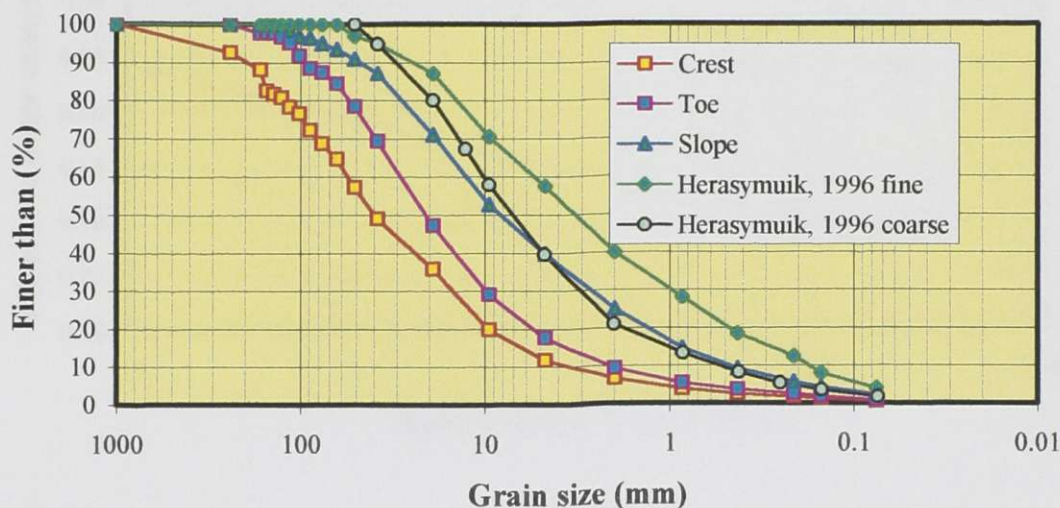


Figure 5.7 Grain size curves for three waste rock samples (Newman, 1994).

Corresponding soil-water characteristic curve (SWCC) and the hydraulic conductivity relationships were assumed to be the same as Herasymuik (1996) and are shown in Figure 5.8.

A clay till cover was placed over the waste rock dump from 1991 to 1997 consisting of 0.5 m of compacted till overlain by 0.3 m of non-compacted till. The till cover material is explained in Section 5.2.8.

Klohn Leonoff (1991b) hydrogeological report indicates a hydraulic conductivity of 2×10^{-1} m/s for the waste rock. The waste rock has since been exposed to chemical and biological oxidation and is believed to have a hydraulic conductivity in the range of 10^{-3}

m/s to 10^{-5} m/s at the present time based on other waste rock dumps (Smith, *et al.*, 1995). A saturated hydraulic conductivity of 3.4×10^{-5} m/s (fine material) is assumed for the waste rock which is based on the study conducted by Herasymuik (1996).

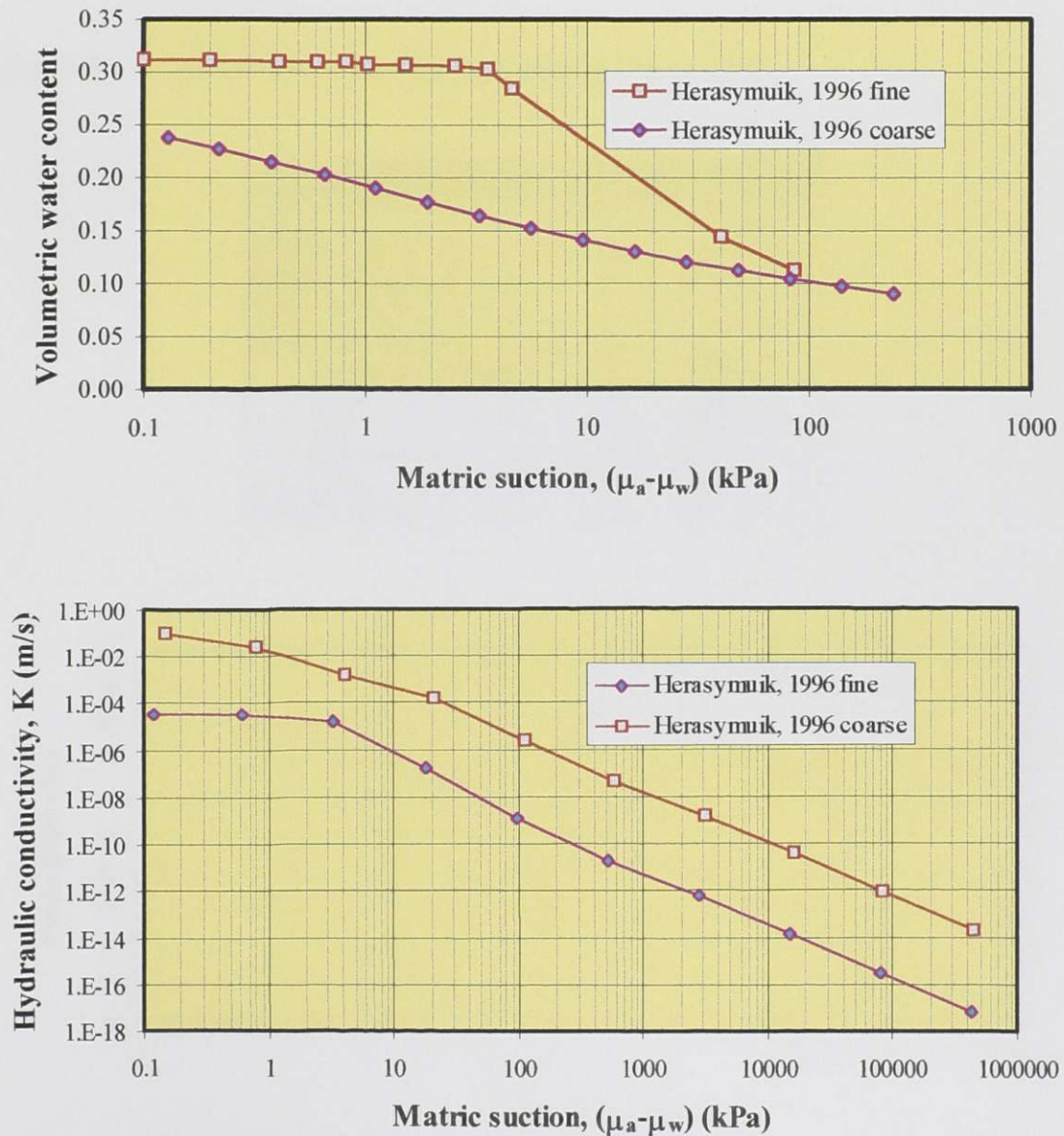


Figure 5.8 Soil-water characteristic curves and the hydraulic conductivity relationships for three waste rock samples (Herasymuik, 1996).

5.2.8 Till Cover Material

The till cover on the waste rock dump and the Former Plant Site consists of 0.3 m of non-compacted till overlaying 0.5 m of compacted till. Table 5.3 lists the material properties for the till by O’Kane (1995).

Table 5.3 The till cover material properties (O’Kane, 1995).

| Material property | Value |
|-----------------------------|------------------------|
| Density of solids, ρ_s | 2.77 kg/m ³ |
| Liquid limit, LL | 39.6% |
| Plastic limit, PL | 17.4% |
| Grain size analysis | |
| Cobbles and gravel | 23% |
| Sand | 28% |
| Silt | 40% |
| Clay | 9% |
| Classification | SC-CL |

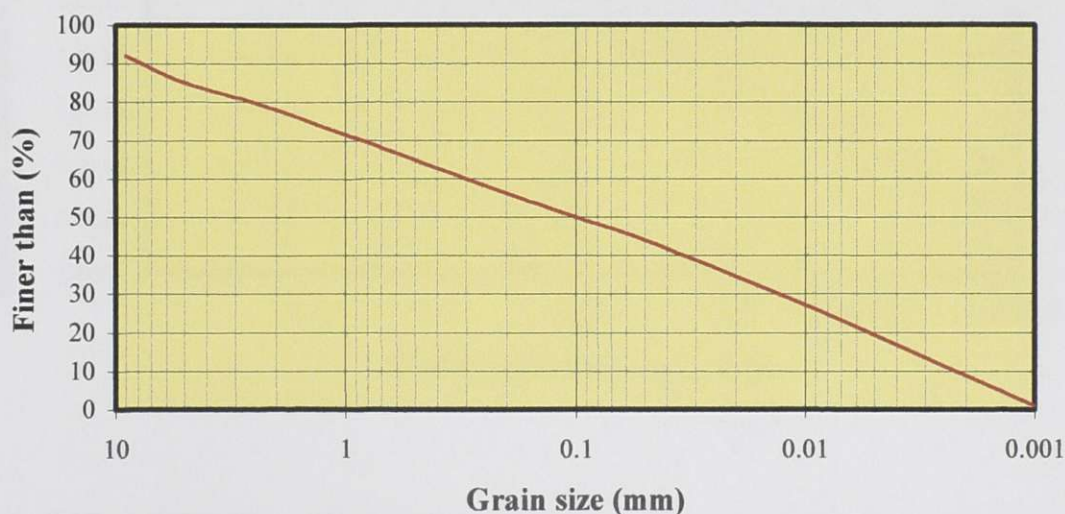


Figure 5.9 Grain size curve for the till cover material (O’Kane, 1995).

Figure 5.10 displays the soil-water characteristic curve and associated hydraulic conductivity relationship for the non-compacted and the compacted till cover material.

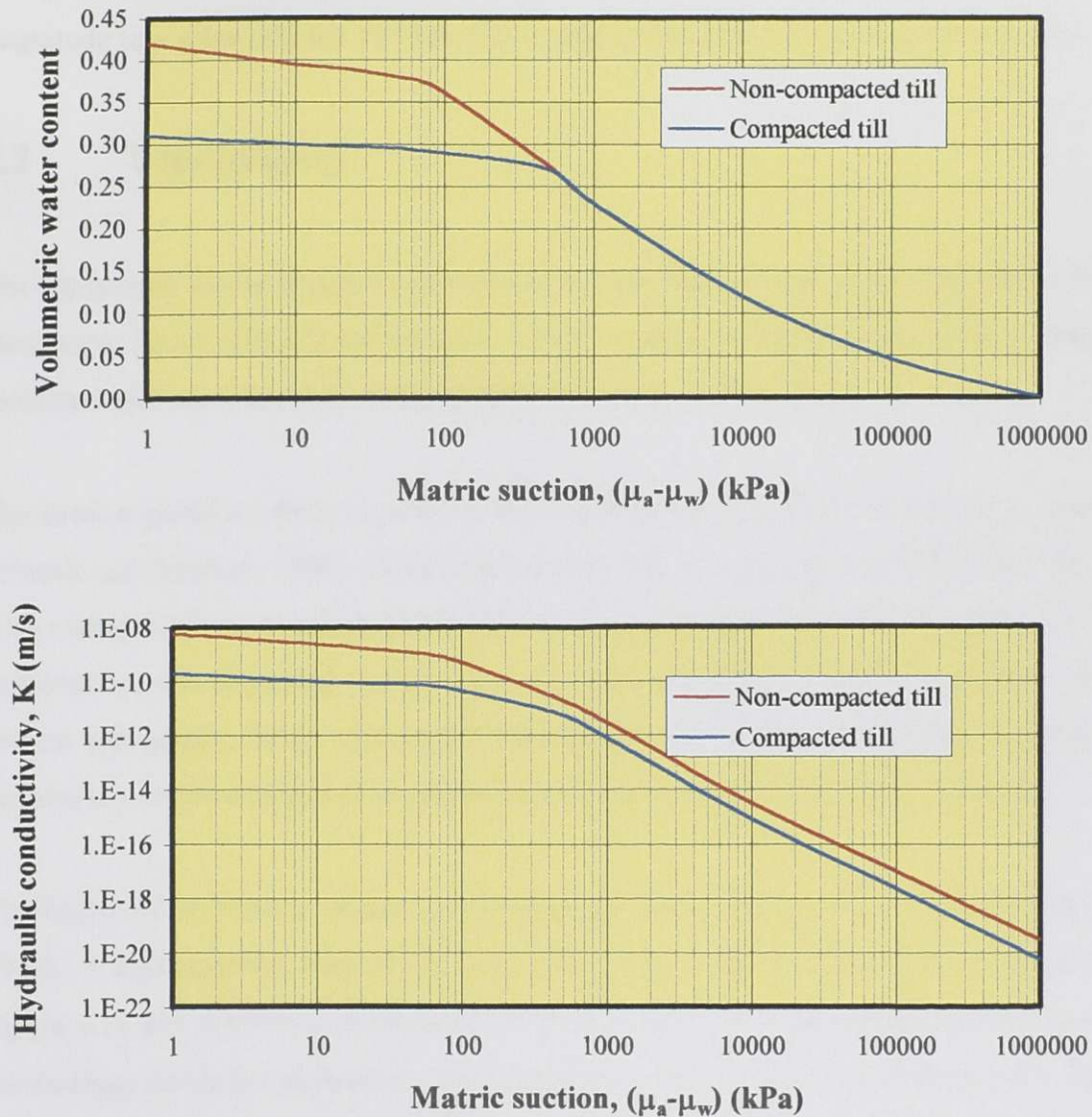


Figure 5.10 Soil-water characteristic curves and the hydraulic conductivity relationship for the till cover material (Swanson, 1995).

The saturated hydraulic conductivity was measured at 5.7×10^{-9} m/s for the non-compacted till using a falling head test (Swanson, 1995). This value is assumed to now

be at 5.7×10^{-6} m/s, the three order of magnitude increase is attributed to desiccation, weathering, freeze / thaw and the vegetation growth and decay cycles. The saturated hydraulic conductivity for the compacted till was measured at 2.0×10^{-10} m/s using a falling head test (Swanson, 1995). This value is assumed to increase only one order of magnitude to a value of 2.0×10^{-9} m/s due to desiccation and minor freeze / thaw cycles.

5.3 Topography

The topography has been significantly altered by past regional and valley glaciation in the Pleistocene Epoch (Church and Barakso, 1990) resulting in modification of the drainage patterns which are a function of topography and soil or rock texture.

The latest regional ice sheet to advance was the Wisconsin (Fraser) Cordilleran ice sheet (Church and Barakso, 1990) which traveled from the east and carried sediments with a wide variety of sizes. A glacial till formation consisting of sediments from boulder size to colloidal size was deposited over the bedrock upon retreat of the glacier resulting in the present topography. Many well sorted fluvio-glacial deposits were scattered throughout the area due to the drainage of lacustrine lakes which were formed by the melting ice.

The Equity Silver Mine is situated on the drainage divide between Foxy Creek and Buck Creek. A topographical map of the area prior to any mining disturbance is shown in Figure 5.11 and is believed to have an accuracy of ± 1 m. The topographical map shows the drainage divide (or watershed) plus the catchment areas for the individual creeks. The drainage divide runs approximately east to west within 8,000N and 9,000N (see Figure 5.11). The drainage basin to the north sheds runoff water to Berzelius Creek and Lu Creek which drain into the eastward flowing Foxy Creek. Runoff water south of the drainage divide flows to Bessemer Creek and Getty Creek which drain into the westward flowing Buck Creek. Both Buck Creek and Foxy Creek flow into the Bulkley River system.

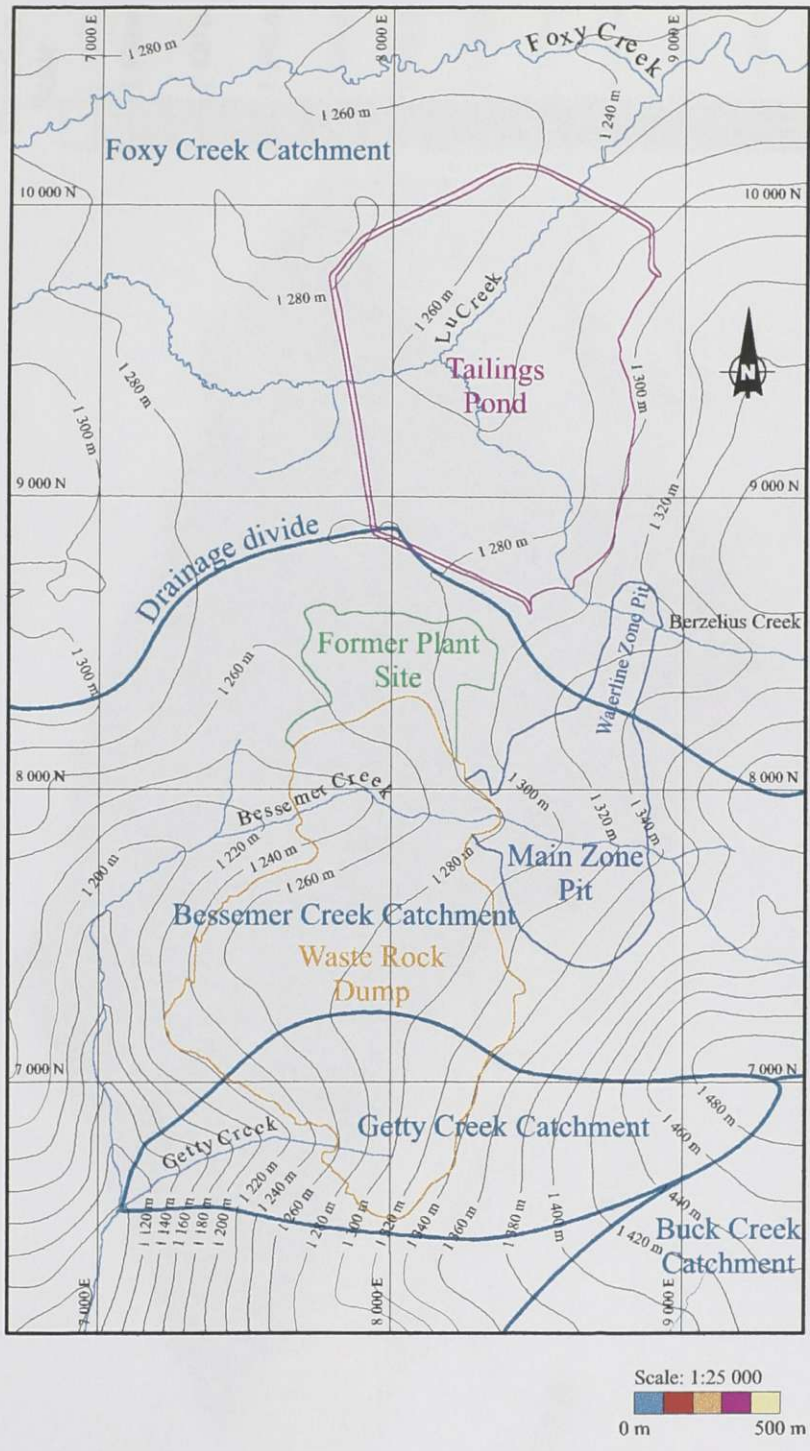


Figure 5.11 Natural topographical contours of Equity Silver Mine.

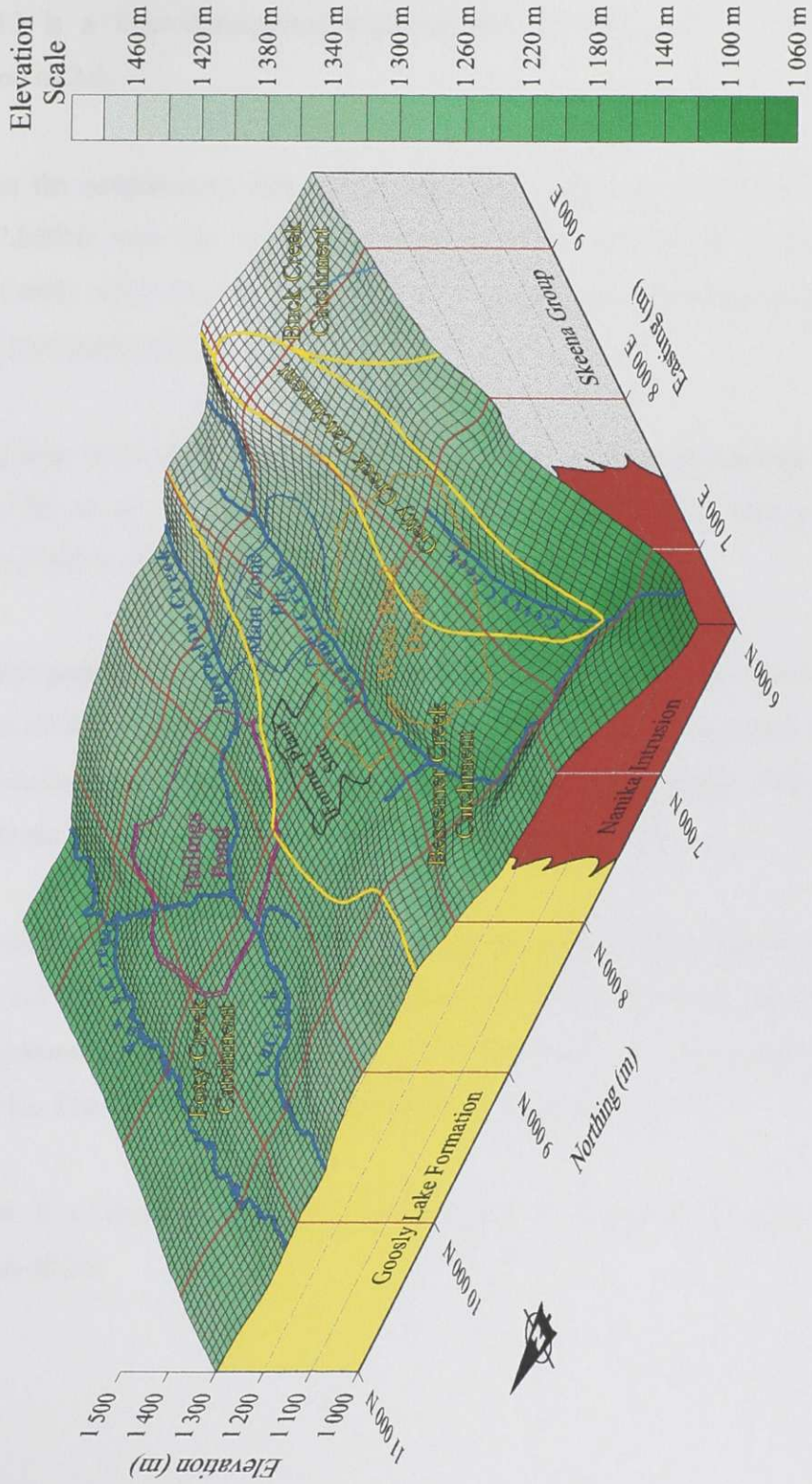


Figure 5.12 Natural three-dimensional topography of Equity Silver Mine.

Figure 5.12 is a three-dimensional representation of Figure 5.11 with a vertical exaggeration of 2.6.

The rise on the southeastern side of the map area reaches an elevation of 1,500 m (9,270E, 7,050N) with the lowest elevation at 1,070 m (6,900E, 6,140N) in the Bessemer Creek valley (southwest portion of the map area) resulting in a maximum differential topographical relief of 430 m.

The mining area is situated at an elevation of 1,370 m in the southeastern side of the Main Zone Pit to an elevation of 1,130 m at Getty Creek Pond with a maximum differential of 240 m of relief in the immediate mining area.

A current topographical map is shown in Figure 5.13 and is believed to have an accuracy of ± 1 m in all areas except the waste rock dump (which has an accuracy of ± 5 m). Surface disturbance caused by mining alters local drainage which will also alter catchment areas. Figure 5.13 includes the modified catchment areas.

The waste rock and surrounding areas that contribute to the ARD collection system are highlighted in Figure 5.13. The waste rock dump and Former Plant Site are encapsulated with an engineered cover system with areas of 117 ha and 25 ha respectively, for a total area of 142 ha. The surrounding regional area has a total area of 80 ha.

Figure 5.14 is a three-dimensional representation of Figure 5.13 with a vertical exaggeration of 2.6.

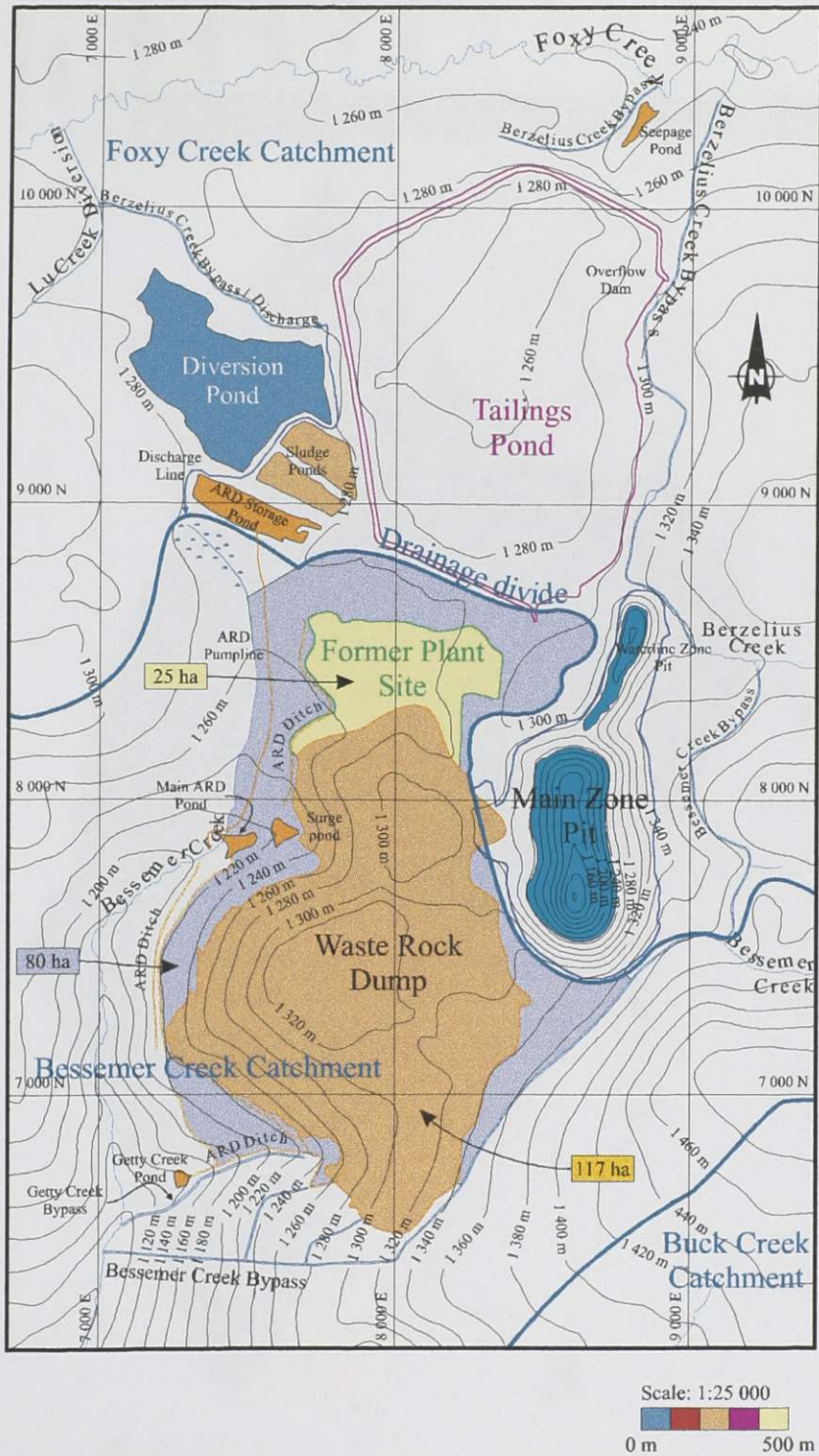


Figure 5.13 Current topographical contours of Equity Silver Mine.

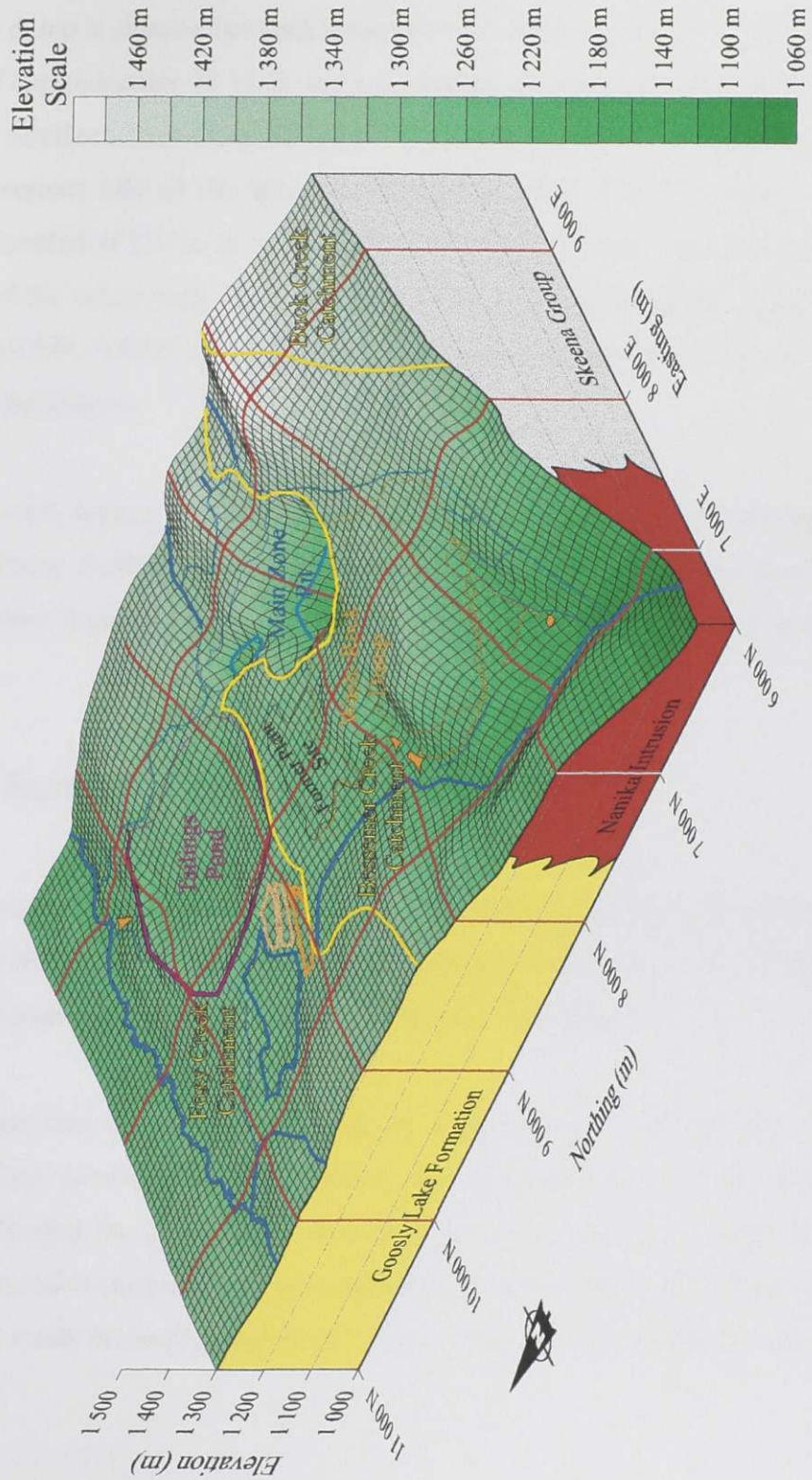


Figure 5.14 Current three-dimensional topography of Equity Silver Mine.

The waste dump is situated between Bessemer and Getty Creek valleys which both have a grade of approximately 30 %. It has a maximum elevation of 1,340 m on the eastern side of the Southern Tails Dump (8,350N, 7,080E) to a minimum elevation of 1,230 m at the southwestern side of the Bessemer Dump (7,700N, 7,880E), giving a maximum height differential of 110 m of waste rock over natural ground. However, the minimum elevation of the waste rock dump occurs at the base of the Southern Tails Zone Pit at 1,200 m (8,070N, 6,870E), giving a maximum height differential of 140 m of waste rock over modified ground.

The waste rock isopach reaches a maximum depth of 61 m in the central region of the Bessemer Dump (8,000N, 7,970E) over natural ground and a maximum depth of 113 m in the northern region of the Southern Tails Zone Pit (8,230N, 7,220E) over modified ground.

5.4 Surface Hydrology

An onsite weather station provides a complete database for the climatological data. More information regarding the weather station is contained in O'Kane (1995). A complete set of climatological and hydrological data is included in Appendix B.

Surface water that is in equilibrium with the surrounding terrain provides a hydraulic head boundary condition at that location. The hydraulic head for the surface water systems influences the groundwater flow regime system since groundwater flow occurs as fluid potential is applied across geological media. The surface water features may be a lake, pond, creek or seepage faces, etc. These features are described in the following sections.

5.4.1 Hydrology

This section includes the hydrological data at the mine site: namely precipitation, runoff, changes in storage, evapotranspiration and infiltration.

5.4.1.1 Precipitation

Table 5.4 lists the precipitation from rain and snow from 1992 to 1998. The water equivalent of snow is taken as 10 % of the total volume. Figure 5.15 presents the monthly precipitation from June 1, 1997 until June 1, 1998. This time span is to be the period that will be modelled in this study. The total rainfall for this period was 363 mm and 279 cm of snowfall which totals to 642 mm of equivalent water. Environment Canada has not currently verified the most recent data; however, the values are assumed to be identical.

Table 5.4 Monthly precipitation (after Equity Silver Mine Ltd., 1997).

| Period | 1992 | | 1993 | | 1994 | | 1995 | | 1996 | | 1997 | | 1998 | |
|---------------------------------|--------------|--------------|--------------|--------------|--------------|--------------|--------------|--------------|--------------|--------------|--------------|--------------|------------|------------|
| | Rain (mm) | Snow (cm) | Rain (mm) | Snow (cm) | Rain (mm) | Snow (cm) | Rain (mm) | Snow (cm) | Rain (mm) | Snow (cm) | Rain (mm) | Snow (cm) | Rain (mm) | Snow (cm) |
| January | 1.0 | 66.0 | | 27.0 | 3.0 | 130.0 | | 38.9 | 2.0 | 103.1 | | 81.0 | | 55.6 |
| February | | 62.0 | 2.0 | 2.0 | | 102.5 | | 33.0 | | 25.0 | | 34.0 | | 35.0 |
| March | 1.4 | 6.5 | 2.0 | 12.0 | | 33.5 | | 50.4 | | 57.0 | | 98.0 | 2.9 | 37.5 |
| April | 18.6 | 23.0 | 24.4 | 19.7 | 17.0 | 16.0 | | 27.3 | 27.0 | 23.4 | 17.7 | 24.5 | 8.9 | 13.5 |
| May | 27.7 | 1.9 | 74.0 | | 39.7 | 2.0 | 24.3 | | 21.3 | 7.8 | 24.0 | 10.6 | 25.4 | |
| June | 36.8 | | 136.8 | 3.5 | 79.0 | | 51.1 | | 52.5 | | 57.8 | | | |
| July | 35.6 | | 102.6 | | 68.9 | | 67.9 | | 97.3 | | 84.6 | | | |
| August | 21.2 | | 61.7 | | 60.6 | | 85.1 | | 50.8 | | 37.4 | | | |
| September | 58.9 | 3.0 | 10.6 | | 88.1 | 3.0 | 15.2 | | 77.9 | | 92.4 | 1.0 | | |
| October | 43.7 | 33.5 | 23.5 | 6.0 | 24.8 | 37.2 | 38.6 | 34.5 | 30.6 | 55.0 | 51.1 | 27.0 | | |
| November | 2.0 | 43.2 | 21.5 | 39.0 | | 102.8 | 0.4 | 89.7 | | 114.5 | 3.0 | 31.5 | | |
| December | 1.0 | 70.0 | | 52.5 | | 59.3 | | 105.0 | | 116.0 | | 77.5 | | |
| Sub total | 247.9 | 309.1 | 459.1 | 161.7 | 381.1 | 486.3 | 282.6 | 378.8 | 359.4 | 501.8 | 368.0 | 385.1 | N/A | N/A |
| Total Precipitation (mm) | 557.0 | | 620.8 | | 867.4 | | 661.4 | | 861.2 | | 753.1 | | N/A | |

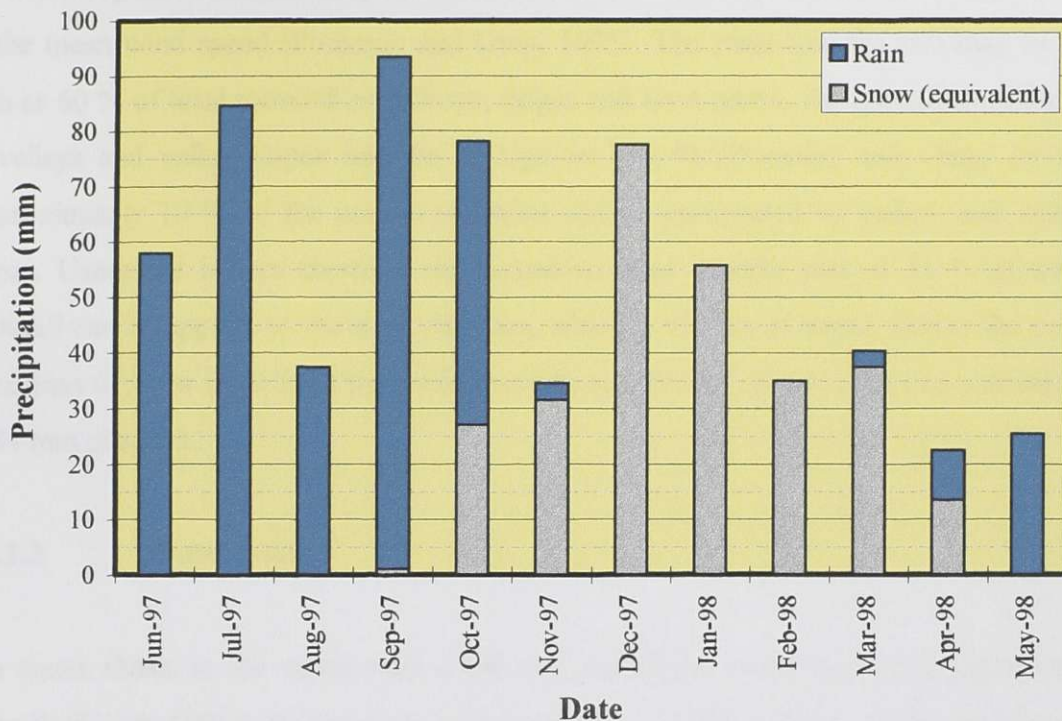


Figure 5.15 Monthly precipitation for the study period (Aziz, 1998).

5.4.1.2 Sublimation and Mass Transfer of Snow

Sublimation and mass transfer of snow is a difficult parameter to calculate or estimate. No data exists on these parameters; thus, they must be estimated on previous studies. Sublimation depends on: radius of snow particle, diffusion coefficient of water vapor in air, turbulence, water vapor density of air and at the particle surface, temperature, relative humidity, wind speed and incoming solar radiation (Pomeroy and Gray, 1995). The sublimation rate is estimated at 35 % of total snowfall, which is 97 mm of water. This value is based on numerous studies conducted by Pomeroy and Gray (1995) that match similar climatology to that of the mine site.

There are three general forms of mass transfer of snow. The propagation of snow waves, similar to sand dunes, is known as creep. Saltation is the skipping of snow particles at the

snow-atmosphere interface. Suspension is referred to as snow particles that are entrained in the mean wind speed (Pomeroy and Gray, 1995). The mass transfer rate may be as high as 60 % of total snowfall on hilltops, ridges and level plains. Accumulation of snow in valleys and valley slopes may be as high as 285 % (Pomeroy and Gray, 1995). Approximately 10 % of the area at the mine site is represented by valleys and valley slopes. Using the figures above, a representative mass transfer rate of 35 % of total snowfall can be applied to the mine site area, which is 97 mm of water. Hence the total relocation of snow is 70 % of the total snowfall, or 195 mm, which leaves an equivalent of 84 mm of water.

5.4.1.3 Water Fluxes

The water fluxes in the waste rock cover and underlying waste rock were calculated using SoilCover (1997) for the study period on June 1, 1997 to June 1, 1998. SoilCover does not calculate sublimation and mass transfer nor does it take into account rainfall during the freezing period. The freezing period started approximately on November 1, 1997 and lasted until April 15, 1998 which marked the beginning of the 1998 freshet. The freshet lasted 27 days or until May, 11, 1998. The input into the model consisted of the precipitation data in Table 5.4. The rainfall (14 mm) and corrected snow water equivalent (84 mm) during the freezing period is applied evenly at 3.6 mm of water per day throughout the runoff period for the SoilCover simulation. Thus the total precipitation for the study period is 447 mm. Evaporation and sublimation during the freezing period is not calculated in SoilCover which is why it must be estimated.

Material properties and initial and boundary conditions for the simulation are based on the results found in this study, field measurements plus work from O'Kane (1995) and Swanson (1995).

The results from SoilCover are plotted in Figure 5.16 and detailed data is included in Appendix B.

Table 5.5 lists a summary of the water fluxes on the waste rock dump for the study period. Figure 5.17 illustrates the components of the water budget.

Table 5.5 Summary of water fluxes.

| Water component | Water (mm) | Percent of total precipitation |
|------------------------|-------------------|---------------------------------------|
| Precipitation | 642 | 100% |
| Runoff | 94 | 15% |
| Evapotranspiration | 327 | 51% |
| Sublimation | 97 | 15% |
| Mass transfer | 97 | 15% |
| Infiltration | 27 | 4% |

The change in storage for the study period was calculated at -9 mm, or the cover system drained 9 mm. The net infiltration according to Equation [3.4] will be 36 mm or 6 % of total precipitation.

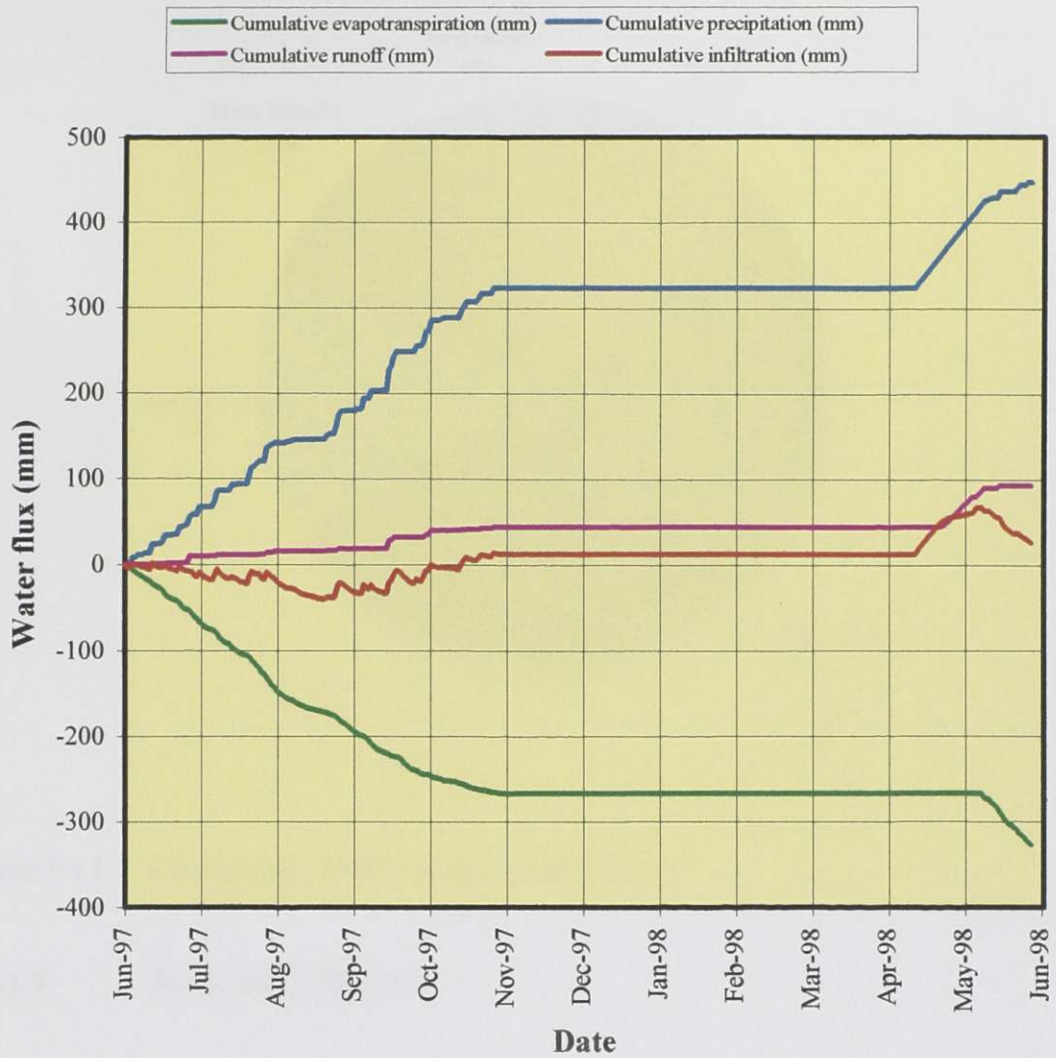


Figure 5.16 Water fluxes for the study period.

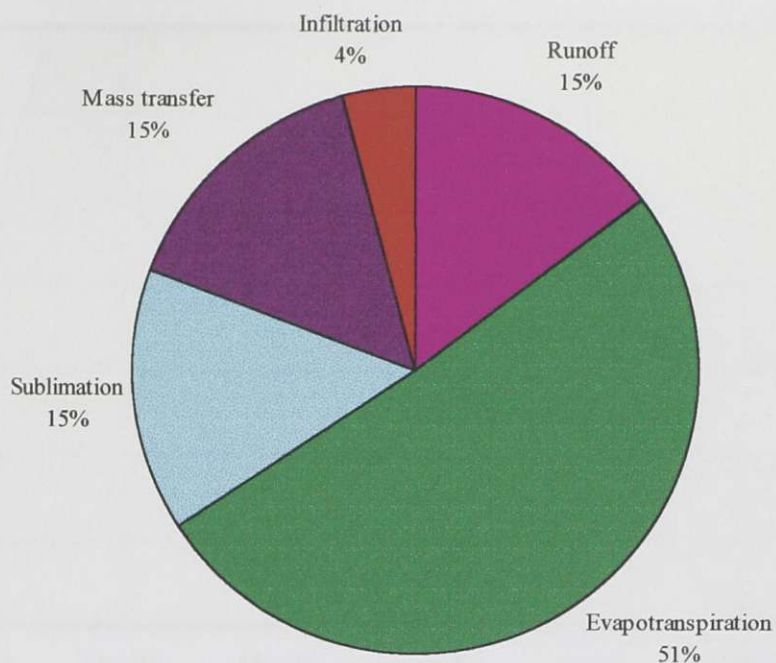


Figure 5.17 Components of the surface water budget.

5.4.1.4 Measured Infiltration

A total of twelve lysimeters have been installed in the waste rock dump in order to measure infiltration through the till cover (Klohn Leonoff, 1991c). Figure 5.18 displays the average infiltration of all lysimeters expressed as a percentage of the total precipitation. The average infiltration is 4.6 % over the six year period.



Figure 5.18 Lysimeter data.

5.4.1.5 Changes in Storage

The waste rock at the mine site was initially uncovered and experienced approximately 60 % infiltration (Aziz, 1998). The flux rate decreased to 5 % once the cover was constructed and would thus experience a time dependant drainage process. The characteristics under which the waste rock will drain is related to the soil-water characteristics of the material. A transient simulation of this process was modelled using SoilCover. A 20 m thick zone of fine waste rock was used and the initial conditions for water content were determined by a steady state analysis with the 60 % infiltration scenario. These initial conditions were used for a transient simulation with 5 % infiltration applied. The results are shown in Figure 5.19.

The majority of the cover was constructed in September, 1994 with completion in 1997. Hence the study period occurs at two to three years after cover placement and experiences 3 mm of extra drainage during that time period.

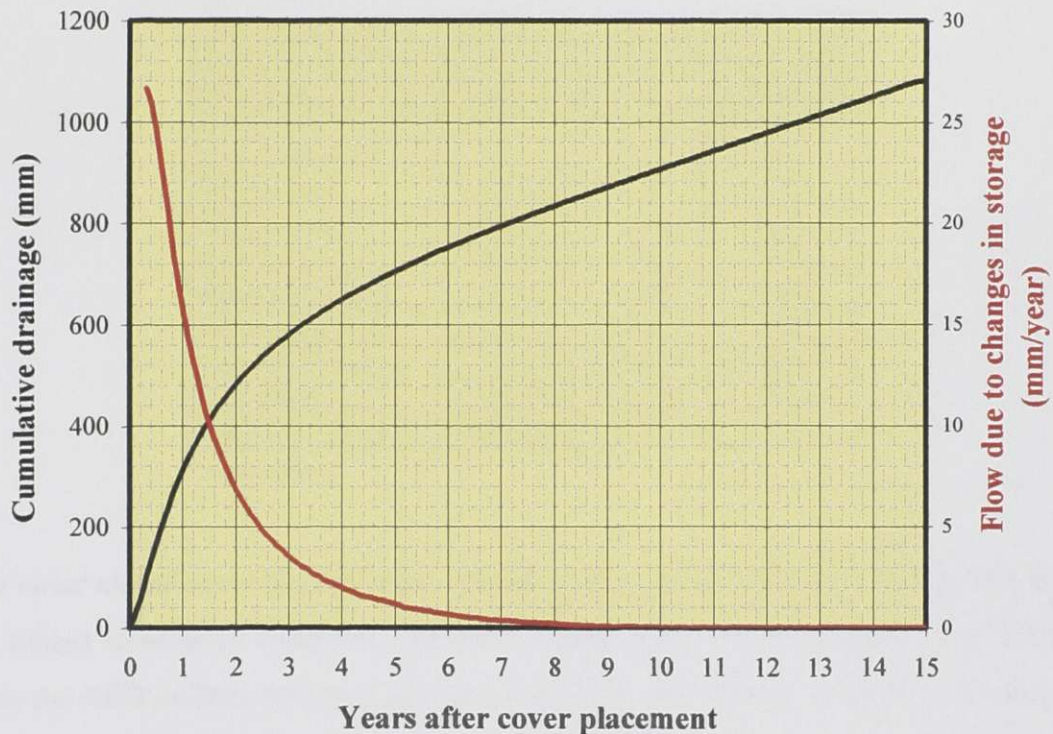


Figure 5.19 Drainage of the waste rock with cover construction.

This analysis shows that transient conditions are insignificant and a steady state analysis may be performed to accurately represent field conditions.

5.4.2 Surface Water Measurements

Numerous surface water ponds in the mine area are part of the ARD collection system (see Section 5.4.5).

Table 5.6 lists the current elevations for the surface water components on the Equity Silver Mine site (see Figure 5.13 for locations).

Table 5.6 Surface water elevations.

| Location | Elevation (m) | Approximate location | |
|--------------------|------------------|----------------------|-----------------|
| | | Easting (m) | Northing (m) |
| Diversion Pond * | 1273.0 | 7440 | 9450 |
| Tailings Pond | 1292.35 | 8350 | 9370 |
| Sludge Ponds * | 1280.0 | 7670 | 9120 |
| Main Zone Pit | 1239.25 | 8610 | 7820 |
| Waterline Zone Pit | 1264.0 | 8750 | 8450 |
| ARD Storage Pond * | 1275.0 | 7530 | 8980 |
| Main ARD Pond | 1205.0 | 7460 | 7840 |
| Surge Pond | 1216.0 | 7630 | 7880 |
| Getty Creek Pond | 1132.5 | 7280 | 6720 |

* Average value.

The water elevations of the Diversion, Sludge (north and south) and ARD Storage Pond are subject to seasonal variations. The ARD storage ponds store the acidic water derived from the ARD collection system (see Section 5.4.5). The storage is required because of substantially high spring runoff and periods of high precipitation. The Tailings Pond elevation is kept constant by an overflow weir that is located at the northeast corner of the pond (see Figure 5.13). The Main Zone Pit water elevation is currently rising due to groundwater, fall precipitation, runoff and sludge from the water treatment plant. The Waterline Zone Pit is spilling over into the Main Zone Pit. The Main Zone Pit and subsequently the Waterline Zone Pit is projected to fill to a water elevation of approximately 1,300 m. The Main ARD Pond elevation is controlled by the Main Pumphouse with little fluctuation (approximately ± 3 m). The Surge Pond elevation is held at a somewhat constant elevation (approximately ± 3 m) by means of a free flow pipe to the Main ARD Pond. Getty Creek Pond is also held at a somewhat constant elevation (approximately ± 1 m) as it is pumped into the Main ARD Collection Ditch.

5.4.3 Creeks and Diversion Channels

The creeks and diversion channels surrounding the waste rock dump collect seepage from the dump. The locations and elevations can be seen on the topographical map in Figure 5.13 (or Figure 5.11 for conditions prior to any mining activity). Table 5.7 lists the sample coordinates and the estimated flow rates for the surrounding creeks and diversion channels for September 15, 1997.

Table 5.7 Creek hydraulic data.

| River | Sample location | | Flow rate (L/s) |
|---------------------------------|-----------------|--------------|-----------------|
| | Easting (m) | Northing (m) | |
| Southeast Bessemer Creek | 9150 | 7500 | 0.345 |
| Northeast Bessemer Creek | 9200 | 7800 | 0.304 |
| Berzelius Creek | 9300 | 8500 | 0.001 |
| Lu Creek | 6450 | 9570 | 0.350 |
| Foxy Creek | 5020 | 11080 | 0.050 |
| Bessemer Creek | 5500 | 4400 | 25.2 |
| Buck Creek | 5390 | 4130 | 100.8 |
| Getty Creek | 7370 | 6620 | Trickle |
| Southeast Bessemer Creek Bypass | 7610 | 6660 | 5.6 |

5.4.4 Seepage Faces

Seepage faces can provide a measurement of hydraulic head in the same manner as free water since they are a known water elevation, i.e. a phreatic surface. There are a variety of seeps on the south and western portions of the waste rock dump which are shown in Figure 5.20. There are numerous seeps in the Main Zone Pit, rock cuts and other locations but they will not be studied herein as they fall outside of the scope of this project. The reader is referred to Klohn Leonoff (1990 and 1991b) for further information on this subject.

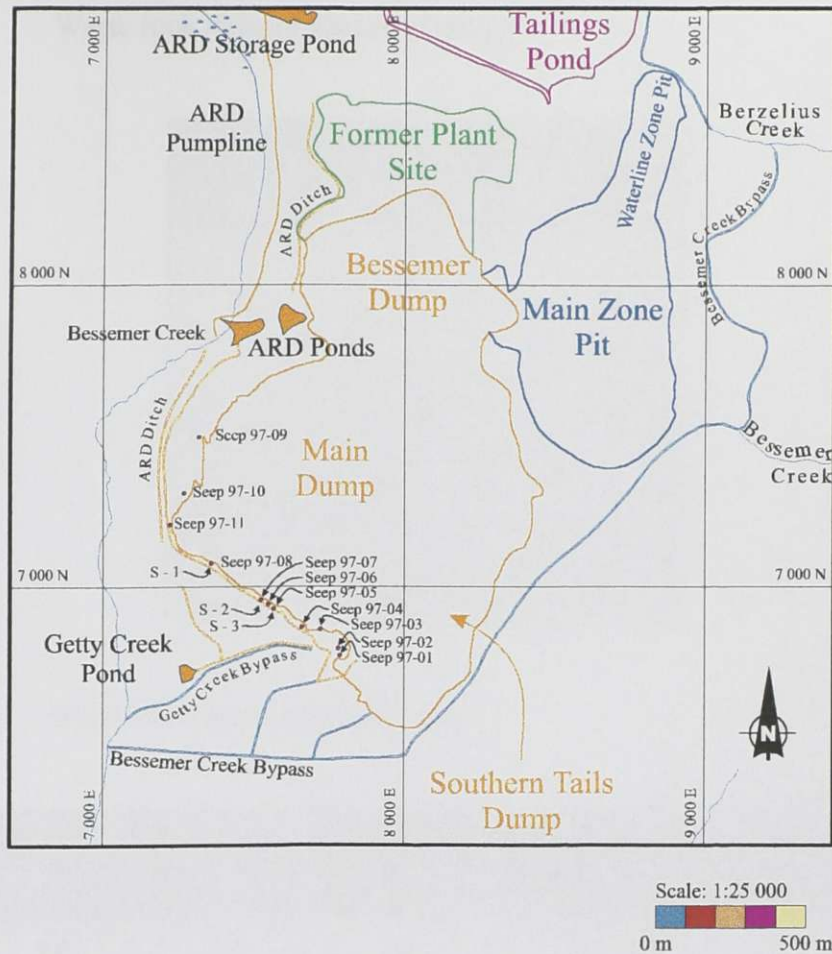


Figure 5.20 Seep locations.

The coordinates for the waste rock dump seeps are given in Table 5.8 while Table 5.9 lists the flow data.

S - 1, S - 2 and S - 3 are previous sample points on the waste rock dump and correlate to Seep 97-08, Seep 97-07 and Seep 97-05 respectively.

Table 5.8 Waste rock dump Seep coordinates.

| Seep | Coordinates | | |
|------------|----------------|-----------------|------------------|
| | Easting (m) | Northing (m) | Elevation (m) |
| Seep 97-01 | 7787.737 | 6771.432 | 1244.712 |
| Seep 97-02 | 7781.984 | 6795.151 | 1243.959 |
| Seep 97-03 | 7723.185 | 6858.540 | 1238.531 |
| Seep 97-04 | 7661.260 | 6865.322 | 1227.200 |
| Seep 97-05 | 7567.291 | 6926.605 | 1221.409 |
| Seep 97-06 | 7549.702 | 6942.031 | 1222.249 |
| Seep 97-07 | 7525.478 | 6956.471 | 1221.829 |
| Seep 97-08 | 7359.599 | 7078.472 | 1218.519 |
| Seep 97-09 | 7318.540 | 7497.347 | 1234.210 |
| Seep 97-10 | 7268.731 | 7310.637 | 1229.640 |
| Seep 97-11 | 7221.840 | 7205.383 | 1215.740 |

Table 5.9 Waste rock dump seep flow data.

| Date | Seep flow rates | | | | | | | | | | |
|-----------|-----------------|----------------|----------------|----------------|----------------|----------------|----------------|----------------|----------------|----------------|----------------|
| | 97-01 (L/s) | 97-02 (L/s) | 97-03 (L/s) | 97-04 (L/s) | 97-05 (L/s) | 97-06 (L/s) | 97-07 (L/s) | 97-08 (L/s) | 97-09 (L/s) | 97-10 (L/s) | 97-11 (L/s) |
| 25-Jun-97 | 0.06 | 0.13 | 0.01 | 0.02 | 0.26 | 0.01 | 0.10 | 0.30 | 0.28 | 0.04 | 0.01 |
| 16-Sep-97 | 0.16 | 0.36 | 0.08 | 0.01 | 0.83 | - | 0.01 | 0.16 | 0.16 | 0.04 | 0.08 |
| 19-Apr-98 | 0.44 | 0.43 | 0.04 | 0.91 | 0.37 | 0.17 | 0.41 | 0.69 | 1.84 | 3.45 | 0.39 |
| 20-Apr-98 | 0.42 | 0.38 | 0.03 | 0.72 | 0.40 | 0.17 | 0.38 | 0.69 | 1.06 | 1.25 | 0.31 |
| 21-Apr-98 | 0.39 | 0.29 | 0.02 | 0.69 | 0.44 | 0.17 | 0.33 | 0.69 | 0.97 | 1.25 | 0.29 |
| 22-Apr-98 | 0.40 | 0.35 | 0.03 | 0.87 | 0.38 | 0.16 | 0.33 | 0.68 | 1.03 | 1.31 | 0.30 |
| 23-Apr-98 | 0.40 | 0.46 | 0.03 | 1.06 | 0.31 | 0.15 | 0.32 | 0.67 | 1.33 | 1.36 | 0.30 |
| 27-Apr-98 | 0.68 | 0.51 | 0.11 | 1.26 | 0.36 | 0.59 | 0.33 | 0.61 | 1.59 | 1.98 | 0.75 |
| 29-Apr-98 | 0.85 | 0.49 | 0.19 | 1.34 | 0.37 | 0.92 | 0.30 | 0.93 | 1.69 | 2.89 | 1.09 |
| 01-May-98 | 0.64 | 0.43 | 0.27 | 1.17 | 0.48 | 0.66 | 0.56 | 0.51 | 1.80 | 2.42 | 0.69 |
| 04-May-98 | 0.44 | 0.55 | 0.26 | 0.65 | 0.54 | 0.72 | 0.54 | 0.49 | 3.38 | 1.97 | 0.41 |
| 06-May-98 | 0.33 | 0.20 | 0.22 | 0.36 | 0.57 | 0.74 | 0.57 | 0.51 | 1.92 | 0.58 | 0.27 |
| 08-May-98 | 0.34 | 0.13 | 0.19 | 0.40 | 0.63 | 0.62 | 0.59 | 0.48 | 1.91 | 0.50 | 0.19 |
| 11-May-98 | 0.28 | 0.10 | 0.13 | 0.19 | 0.55 | 0.52 | 0.36 | 0.22 | 1.51 | 0.48 | 0.14 |
| 13-May-98 | 0.25 | 0.13 | 0.14 | 0.23 | 0.48 | 0.42 | 0.37 | 0.38 | 0.89 | 0.34 | 0.13 |
| 15-May-98 | 0.28 | 0.08 | 0.12 | 0.13 | 0.54 | 0.32 | 0.31 | 0.30 | 0.52 | 0.20 | 0.09 |
| 19-May-98 | 0.16 | 0.16 | 0.13 | 0.14 | 0.41 | 0.26 | 0.27 | 0.31 | 0.46 | 0.28 | 0.07 |
| 21-May-98 | 0.15 | 0.13 | 0.09 | 0.07 | 0.37 | 0.19 | 0.29 | 0.31 | 0.39 | 0.24 | 0.06 |
| 25-May-98 | 0.18 | 0.17 | 0.11 | 0.07 | 0.40 | 0.13 | 0.32 | 0.25 | 0.33 | 0.17 | 0.07 |
| 01-Jun-98 | 0.26 | 0.13 | 0.06 | 0.04 | 0.35 | 0.08 | 0.33 | 0.26 | 0.20 | 0.07 | 0.04 |

- Indicates no flow.

There were no past records of flow rates for S - 1, S - 2 and S - 3.

Figure 5.21 shows a plot of the flow data presented in Table 5.9. There are numerous sample points for the spring of 1998 during Phase II of the field program (see Section 4.3).

The seeps account for approximately 50 % of the flow in the surrounding ditch (excluding Southern Tails flow) and approximately 5 % of the total ARD flow.

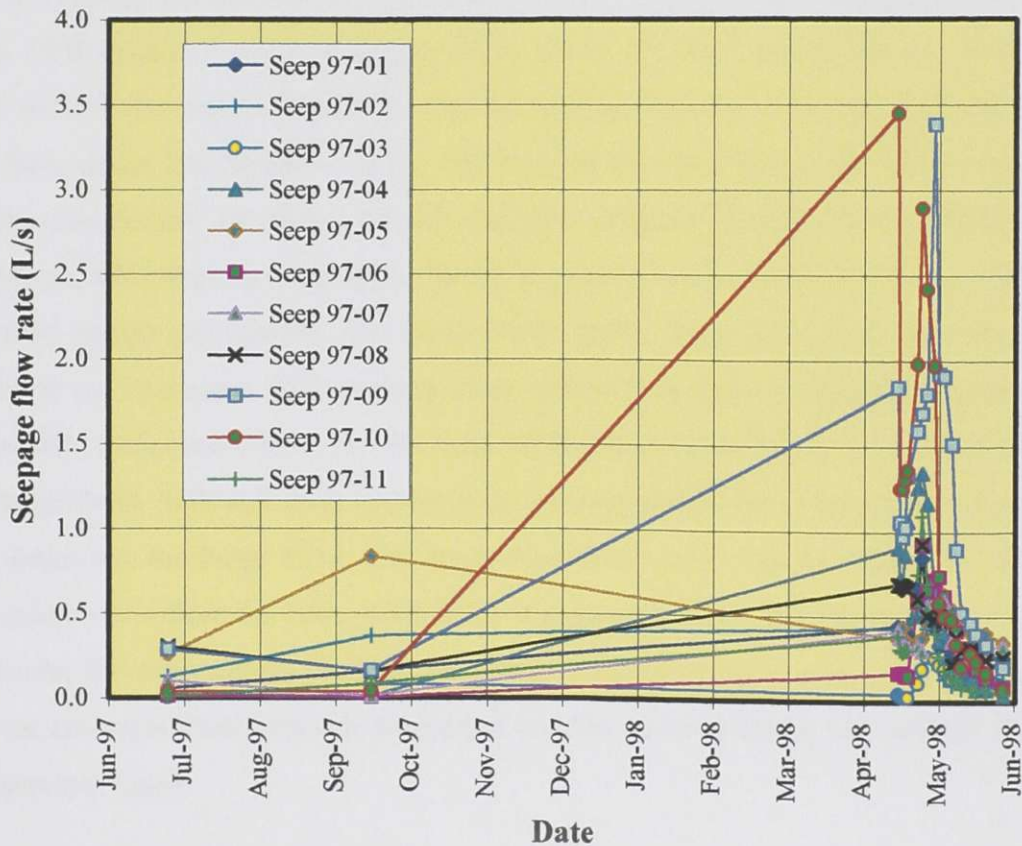


Figure 5.21 Waste rock dump seep flow rates.

5.4.5 ARD Collection System

A series of channels and sumps transport the acidic water as it seeps out of the waste rock dump. The water is pumped to a water treatment plant where lime (CaO) is added in order to raise the pH and precipitate the majority of the heavy metals, ensuring the water is suitable for discharge to the environment.

The Main ARD Collection Ditch drains the water that seeps out of the dump to the Main ARD Pond. Figure 5.22 displays the ARD trenches, sumps, weirs and ponds. There are also two backup ditches that are down gradient of the Main ARD Collection Ditch. The West ARD Backup Ditch (secondary ditch) drains any acidic water that bypasses the Main ARD Collection Ditch (runoff or groundwater). Sump #2 pumps groundwater into this ditch, drains into Sump #1 and is then pumped into the Main ARD Pond. Sump #4 pumps groundwater into Sump #3 and then into the Main ARD Collection Ditch. The Southwest ARD Backup Ditch serves the same purpose as the West ARD Backup Ditch. Sump #5 pumps groundwater into Getty Creek Pond. Getty Creek Pond also receives water via the Southwest ARD Backup Ditch. Getty Creek Pond is then pumped into the Main ARD Collection Ditch. The Plantsite ARD Ditch drains the Former Plantsite into the Surge Pond. A French drain is located on the west side of the Bessemer Dump which also drains into the Surge Pond. The Surge Pond flows freely into the Main ARD Pond. The acidic water from the Main ARD Pond is pumped to the ARD Storage Pond. After treatment, the water passes through two sludge ponds (north and south) and ultimately into the Diversion Pond which is discharged into the environment by way of Foxy Creek or Bessemer Creek.

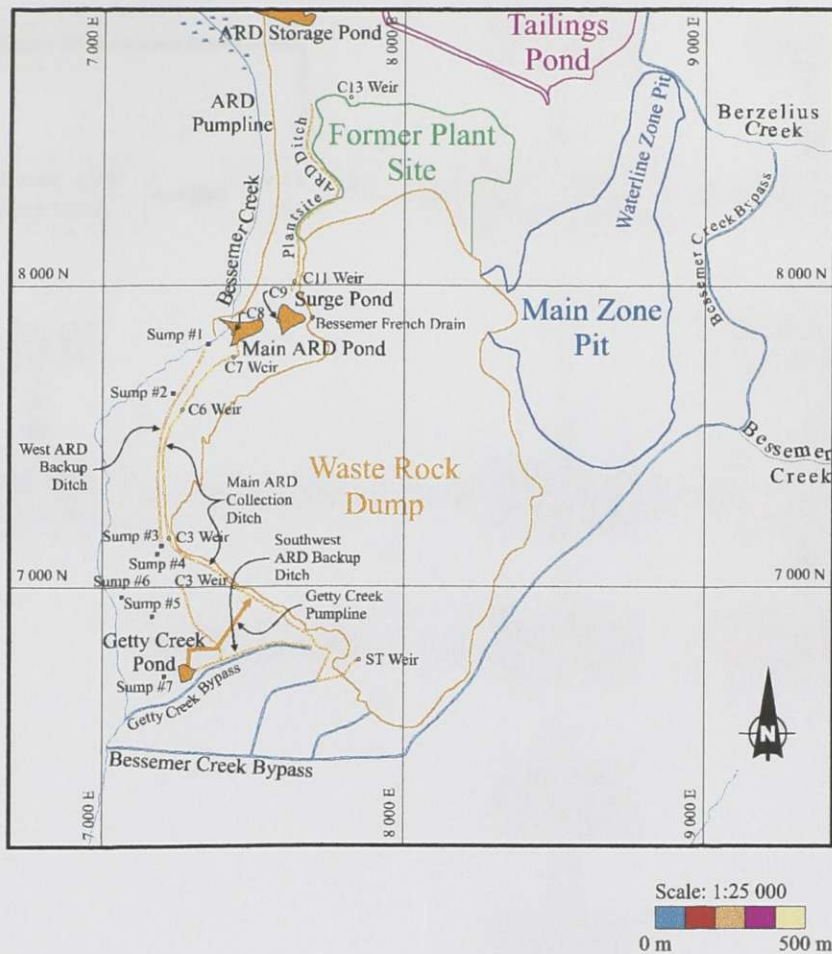


Figure 5.22 ARD collection system.

The ARD collection flow chart is shown in Figure 5.23. The measured flows at various locations along the collection system are summarized in the following sections.

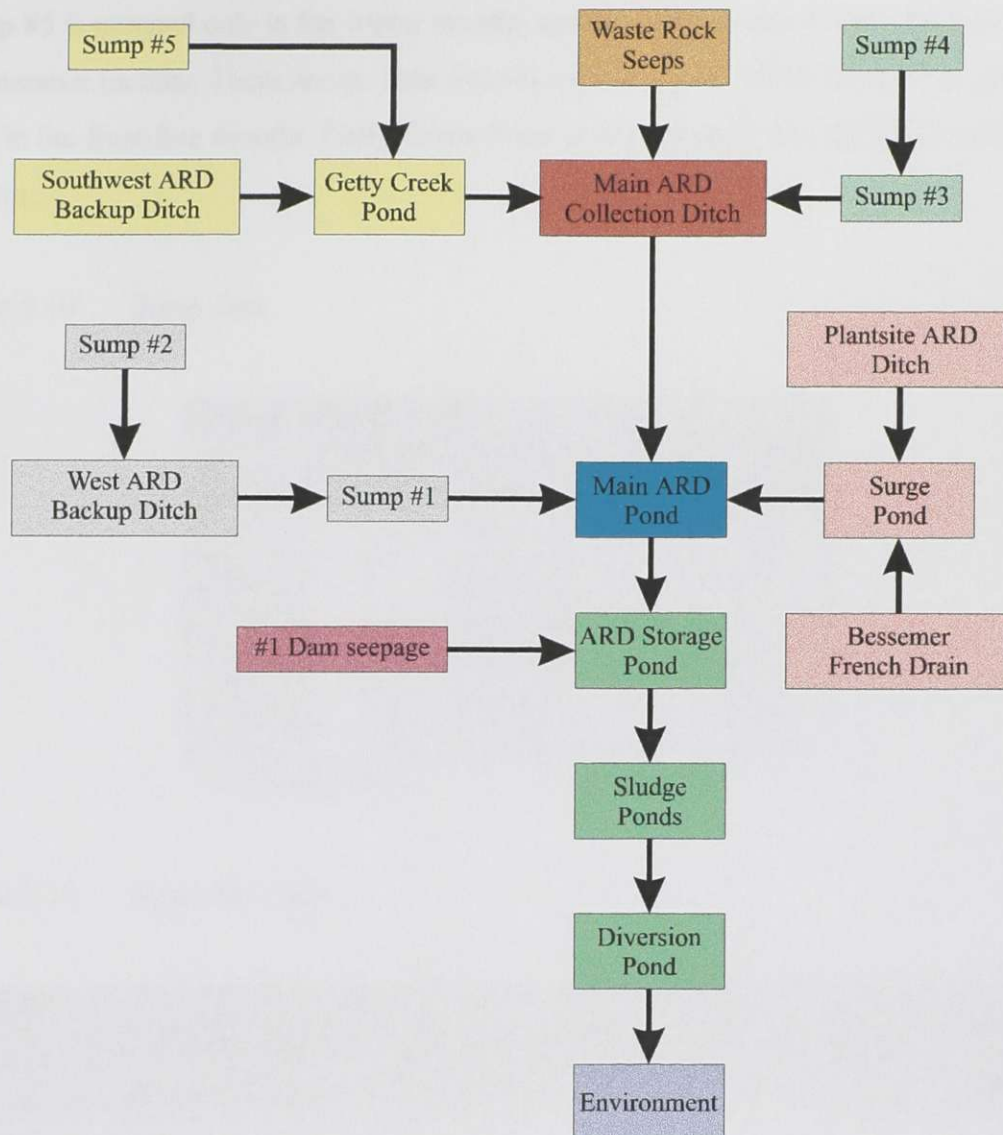


Figure 5.23 ARD collection flow chart.

5.4.6 ARD Sumps

A series of sumps have been installed to sample, collect and treat contaminated groundwater. Their locations can be seen in Figure 5.22. The total sump flow rate accounts for approximately 5 % of the total ARD flow rate. Table 5.10 summarizes the sump data including location and depth.

Sump #5 is pumped only in the winter months and flows freely into Getty Creek Pond in the summer months. There are no data recorded for Sump #6 while Sump #7 is pumped only in the frost-free months. Getty Creek Pond is also pumped into the ARD collection system.

Table 5.10 Sump data.

| Sump | Depth from ground (m) | Location | | |
|---------|-----------------------|-------------|--------------|--------------|
| | | Easting (m) | Northing (m) | Casing * (m) |
| Sump #1 | 2.9 | 7350.442 | 7803.493 | 1196.7 |
| Sump #2 | 2.5 | 7235.010 | 7642.080 | 1203.5 |
| Sump #3 | 5.7 | 7195.542 | 7138.533 | 1210.0 |
| Sump #4 | 2.6 | 7182.512 | 7110.358 | 1198.5 |
| Sump #5 | 3.7 | 7165.756 | 6902.749 | 1146.3 |
| Sump #6 | 1.8 | 7064 | 6968 | 1129.3 |
| Sump #7 | 2.4 | 7206 | 6705 | 1120.0 |

* Top of casing elevation.

Table 5.11 Sump flow data.

| Date | Sump flow rate | | | | | | | |
|--------|----------------|---------------|---------------|---------------|---------------|---------------|---------------|-------------|
| | Sump #1 (L/s) | Sump #2 (L/s) | Sump #3 (L/s) | Sump #4 (L/s) | Sump #5 (L/s) | Sump #6 (L/s) | Sump #7 (L/s) | Getty (L/s) |
| Jun-97 | 0.373 | 0.014 | 0.022 | 0.025 | 0.015 | N/A | 0.011 | 1.929 |
| Jul-97 | 0.160 | 0.003 | 0.009 | 0.012 | 0.026 | N/A | 0.019 | 0.785 |
| Aug-97 | 0.070 | 0.002 | 0.007 | 0.008 | 0.044 | N/A | 0.051 | 0.643 |
| Sep-97 | 0.349 | 0.009 | 0.030 | 0.039 | 0.044 | N/A | 0.009 | 1.490 |
| Oct-97 | 0.716 | 0.018 | 0.056 | 0.065 | 0.063 | N/A | 0.001 | 3.202 |
| Nov-97 | 0.096 | 0.004 | 0.027 | 0.033 | 0.033 | N/A | 0.023 | 1.243 |
| Dec-97 | 0.001 | 0.008 | 0.013 | 0.021 | 0.011 | N/A | 0.008 | 0.839 |
| Jan-98 | 0.092 | 0.009 | 0.008 | 0.018 | 0.008 | N/A | 0.006 | 0.596 |
| Feb-98 | 0.032 | 0.005 | 0.008 | 0.018 | 0.009 | N/A | 0.006 | 0.560 |
| Mar-98 | 0.032 | 0.004 | 0.020 | 0.018 | 0.028 | N/A | 0.020 | 1.006 |
| Apr-98 | 0.842 | 0.021 | 0.142 | 0.171 | 0.258 | N/A | 0.184 | 6.632 |
| May-98 | 1.004 | 0.056 | 0.055 | 0.063 | 0.099 | N/A | 0.071 | 4.098 |

Figure 5.24 displays flow rates versus time for the sumps and Getty Creek Pond for the modelling period.

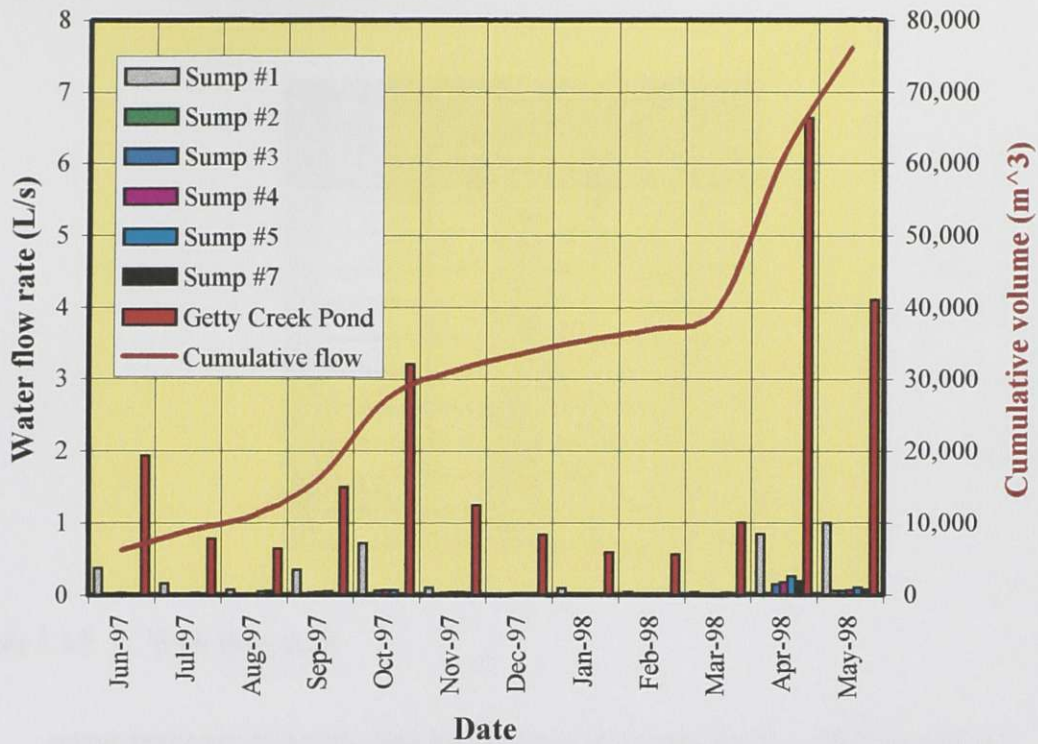


Figure 5.24 Sump flow rates for the study period.

There are two characteristic increases in the flow rates due to spring runoff and the fall rainy season.

5.4.7 ARD Weirs

A series of v-notch weirs have been installed in various locations in the ARD ditches for instrumentation purposes and can be seen in Figure 5.22. Table 5.12 summarizes the coordinates for the weirs and Table 5.13 includes flow rates for the study period.

Table 5.12 Weir coordinates.

| Weir | Approximate coordinates | |
|----------|-------------------------|-----------------|
| | Easting (m) | Northing (m) |
| C3 | 7480 | 7000 |
| C5 | 7221 | 7165 |
| C6 | 7265 | 7590 |
| C7 | 7435 | 7760 |
| C8 | 7430 | 7840 |
| C9 | 7585 | 7880 |
| C11 | 7635 | 8010 |
| C13 | 7820 | 8630 |
| Bessemer | 7700 | 7890 |
| ST | 7855 | 6755 |

Table 5.13 Weir flow data.

| Date | Weir flow rates | | | | |
|--------|-----------------|-------------|-------------|--------------|-------------|
| | C7 (L/s) | C8 (L/s) | C9 (L/s) | C11 (L/s) | ST (L/s) |
| Jun-97 | 8.95 | 47.90 | 37.00 | 2.75 | 5.80 |
| Jul-97 | 4.20 | 15.10 | 10.20 | 1.50 | 2.80 |
| Aug-97 | 2.65 | 10.00 | 6.80 | 1.15 | 0.90 |
| Sep-97 | 3.50 | 18.80 | 13.60 | 17.20 | 1.20 |
| Oct-97 | 1.03 | 29.90 | 17.60 | 2.60 | 4.90 |
| Nov-97 | 5.45 | 19.70 | 13.00 | 0.45 | 3.20 |
| Dec-97 | 5.75 | 10.10 | 3.10 | 0.55 | 1.00 |
| Jan-98 | 2.95 | 7.86 | 4.30 | 0.40 | 0.60 |
| Feb-98 | 3.00 | 15.22 | 11.60 | 0.70 | 0.60 |
| Mar-98 | 3.50 | 16.94 | 12.50 | 1.80 | 0.50 |
| Apr-98 | 8.85 | 34.25 | 18.80 | 9.08 | 0.50 |
| May-98 | 17.85 | 71.53 | 49.40 | 6.10 | 13.00 |

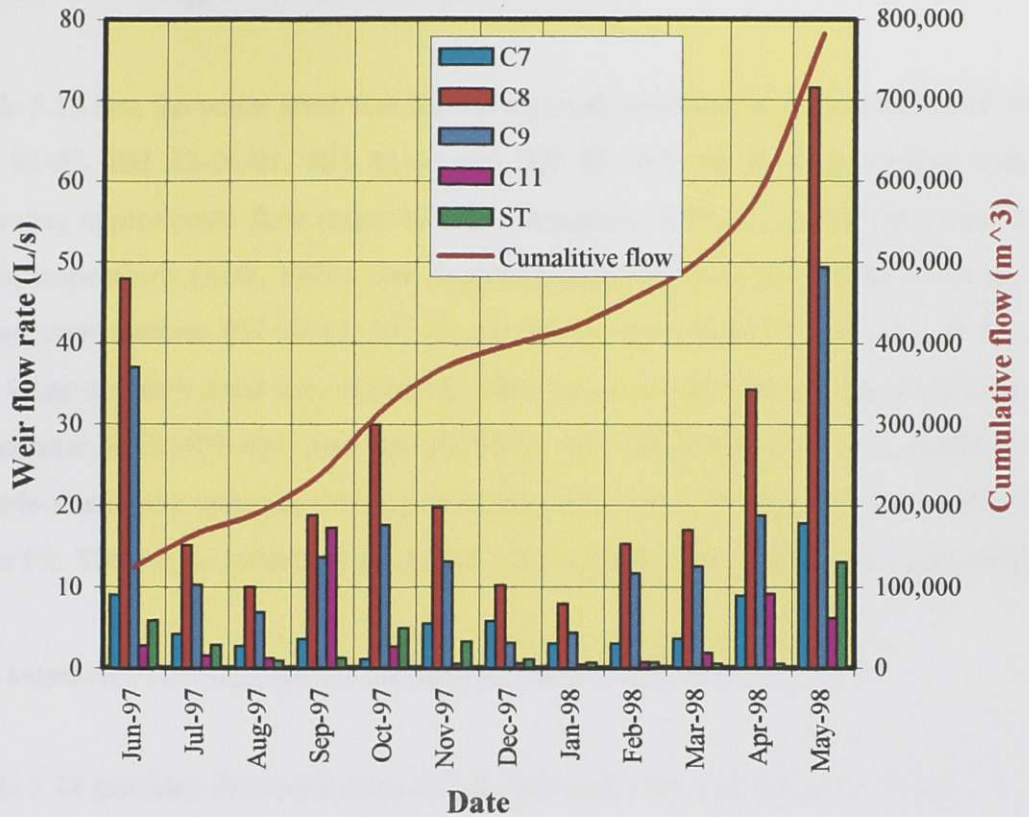


Figure 5.25 Weir flow rates for the study period.

5.5 Groundwater

A series of piezometers have been installed throughout the mine area in the past to monitor the groundwater levels. Five additional piezometers were installed in the waste rock dump to determine hydraulic heads within the waste rock.

This section deals with a series of regional piezometers surrounding the mine which were installed in the past as well as the piezometers that were installed in the waste rock dump (see Chapter 4).

5.5.1 Regional Piezometers

Table 5.15 lists the water level data for the regional piezometers. Piezometers RH 82-02, RH 82-03, RH 82-06-01, RH 82-06 and RH 82-06A are flowing artesian with the following approximate flow rates: 42 mL/s, (capped), 0.70 mL/s, 0.28 mL/s and 0.063 mL/s, respectively (Aziz, 1998). The remaining piezometers in the RH 82 series are dry. Piezometer numbers RH 90-13, 21, 22 and 23 are dry and RH 90-17, 18 and 19 were lost when a nearby road was relocated. There is recent data for the diamond drill hole piezometer 90CH403 and none for 90CH404 and 90CH405. Past data would not be reliable due to the hydraulic influences of the rising water elevation in the nearby Main Zone Pit. There is no record for the tip elevations for the diamond drill hole piezometers.

The locations of the regional piezometers are shown in Figure 5.26.

Table 5.14 provides the coordinates and elevations for the regional piezometers.

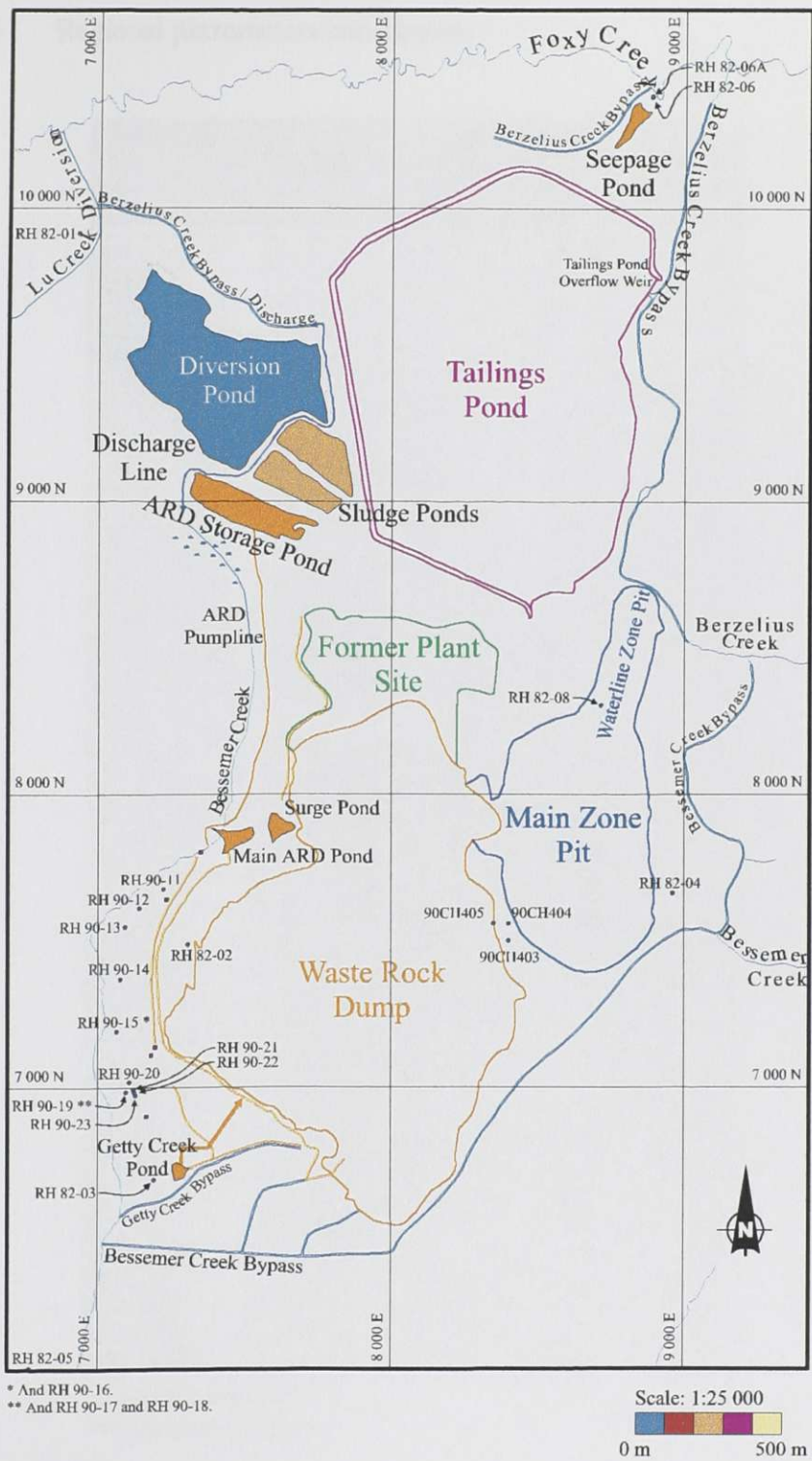


Figure 5.26 Regional piezometer locations.

Table 5.14 Regional piezometers coordinates.

| Piezometer | Coordinates | | | |
|--------------|----------------|-----------------|-----------------|---------------|
| | Easting (m) | Northing (m) | Casing * (m) | Tip ** (m) |
| RH 82-01-01 | 6927.328 | 9914.492 | 1280.280 | 1242.800 |
| RH 82-01-02 | 6927.328 | 9914.492 | 1280.280 | 1250.300 |
| RH 82-01-03 | 6927.328 | 9914.492 | 1280.280 | 1269.900 |
| RH 82-02-01 | 7307.021 | 7488.083 | 1237.660 | 1225.560 |
| RH 82-03-01 | 7192.513 | 6687.648 | 1123.110 | 1104.510 |
| RH 82-03-02 | 7192.513 | 6687.648 | 1123.110 | 1108.710 |
| RH 82-04-02 | 8961.647 | 7663.704 | 1359.520 | 1331.520 |
| RH 82-05-01 | 6765.500 | 6046.500 | 960.600 | 881.700 |
| RH 82-05-02 | 6765.500 | 6046.500 | 960.600 | 901.200 |
| RH 82-05-03 | 6765.500 | 6046.500 | 960.600 | 938.700 |
| RH 82-05-04 | 6765.500 | 6046.500 | 960.600 | 944.100 |
| RH 82-06-01 | 8885.688 | 10383.202 | 1227.150 | 1182.850 |
| RH 82-06-02 | 8885.688 | 10383.202 | 1227.150 | 1207.450 |
| RH 82-06A-01 | 8884.963 | 10387.282 | 1227.910 | 1216.410 |
| RH 82-07-01 | Abandoned | | | |
| RH 82-08-01 | 8716.102 | 8305.624 | 1331.750 | 1183.350 |
| RH 82-08-02 | 8716.102 | 8305.624 | 1331.750 | 1269.350 |
| RH 82-08-03 | 8716.102 | 8305.624 | 1331.750 | 1292.950 |
| RH 90-11 | 7222.990 | 7677.640 | 1191.260 | 1171.060 |
| RH 90-12 | 7141.470 | 7612.450 | 1180.960 | 1175.040 |
| RH 90-13 | 7092.760 | 7549.240 | 1182.820 | 1172.900 |
| RH 90-14 | 7076.730 | 7371.580 | 1176.410 | 1153.810 |
| RH 90-15 | 7064.220 | 7193.560 | 1155.320 | 1137.400 |
| RH 90-16 | 7064.220 | 7193.560 | 1155.370 | 1152.350 |
| RH 90-17 | 7096.290 | 6985.690 | 1130.630 | 1112.430 |
| RH 90-18 | 7096.290 | 6985.690 | 1130.300 | 1120.020 |
| RH 90-19 | 7096.290 | 6985.690 | 1130.270 | 1124.210 |
| RH 90-20 | 7107.980 | 7020.270 | 1158.440 | 1155.900 |
| RH 90-21 | 7121.540 | 6994.830 | 1156.050 | 1149.290 |
| RH 90-22 | 7124.920 | 6984.750 | 1155.470 | 1145.200 |
| RH 90-23 | 7129.100 | 6974.220 | 1153.950 | 1143.680 |
| 90CH403 | 8401.7 | 7500.3 | 1318.0 | N/A |
| 90CH404 | 8401.9 | 7558.9 | 1309.7 | N/A |
| 90CH405 | 8350.7 | 7559.8 | 1306.9 | N/A |

* Top of casing elevation.

** Piezometer tip elevation.

Table 5.15 Regional piezometer water level elevations.

| Date | Piezometer water level elevation | | | | | | |
|-----------|----------------------------------|-----------------|-----------------|-----------------|-----------------|-----------------|-----------------|
| | 90CH403 (m) | RH 90-11 (m) | RH 90-12 (m) | RH 90-14 (m) | RH 90-15 (m) | RH 90-16 (m) | RH 90-20 (m) |
| 24-Jan-91 | N/A | 1191.26 | 1179.76 | 1157.31 | 1141.72 | 1152.47 | 1157.34 |
| 23-Apr-91 | N/A | 1191.18 | 1180.88 | 1158.24 | 1141.95 | 1152.99 | 1157.36 |
| 05-Jun-91 | N/A | 1191.26 | 1179.93 | 1158.02 | | | 1157.69 |
| 30-Oct-91 | N/A | 1191.26 | 1179.74 | 1158.52 | | | 1157.34 |
| 24-Jun-92 | N/A | 1191.26 | 1180.41 | 1158.53 | 1142.57 | 1153.73 | 1157.44 |
| 02-Nov-92 | N/A | 1191.26 | 1179.80 | 1158.40 | 1142.67 | 1153.87 | 1157.41 |
| 26-May-93 | N/A | 1191.26 | 1179.93 | 1158.68 | 1142.44 | 1154.71 | 1157.60 |
| 19-Oct-93 | N/A | 1191.26 | 1180.13 | 1158.54 | 1142.63 | 1153.08 | 1157.69 |
| 22-Jun-94 | N/A | 1191.26 | 1180.45 | 1158.65 | 1142.49 | 1154.59 | 1157.71 |
| 19-Dec-94 | N/A | 1191.26 | 1180.44 | 1158.77 | | 1154.62 | 1157.74 |
| 03-Jul-95 | N/A | 1191.26 | 1180.52 | 1158.78 | 1142.34 | 1153.73 | 1157.74 |
| 21-Dec-95 | N/A | 1191.26 | 1179.89 | 1158.59 | 1142.21 | 1153.67 | 1157.70 |
| 28-Jun-96 | N/A | 1191.26 | 1180.62 | 1158.79 | 1142.19 | 1153.41 | 1157.66 |
| 04-Nov-96 | N/A | 1191.26 | 1180.60 | 1158.58 | 1142.33 | | 1157.71 |
| 30-Jun-97 | N/A | 1191.26 | 1180.96 | 1158.78 | 1143.10 | 1154.36 | 1157.68 |
| 29-Dec-97 | N/A | 1191.26 | 1180.66 | 1158.63 | 1142.73 | 1154.33 | 1157.64 |
| 30-Jun-98 | 1276.40 | 1191.26 | 1180.40 | 1158.72 | 1142.45 | 1154.14 | 1157.54 |

Blank value indicates a dry piezometer.

Figure 5.27 displays the water levels versus time for the regional piezometers.

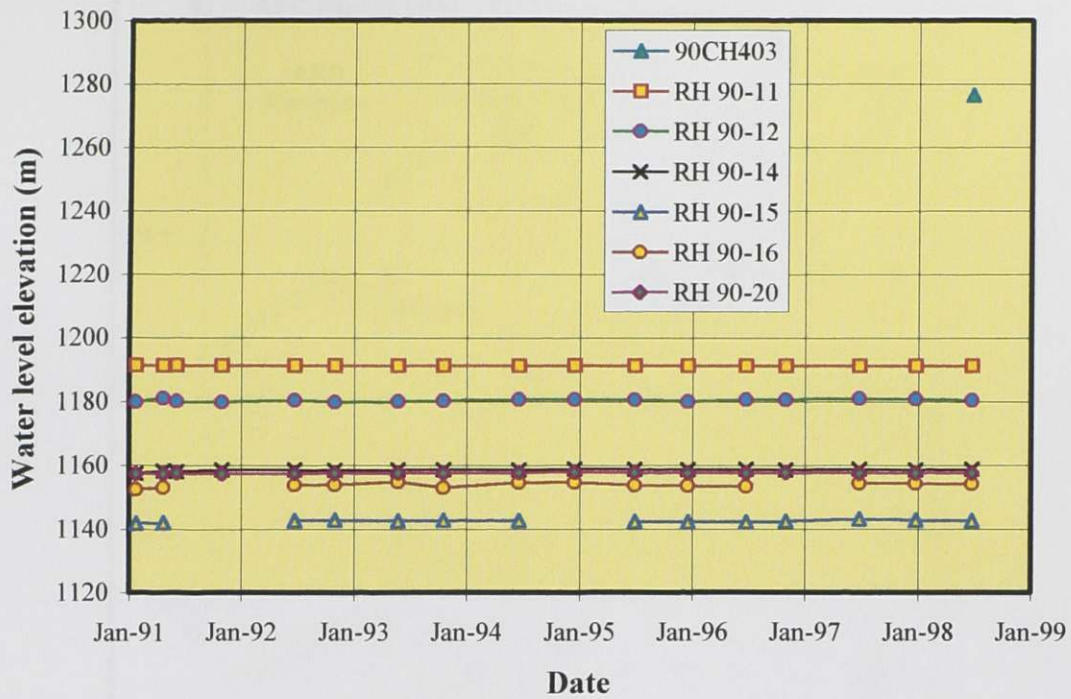


Figure 5.27 Water levels versus time for the regional piezometers.

5.5.2 Waste Rock Dump Piezometers

A total of five piezometers were installed in the waste rock dump (see Chapter 4) as shown in Figure 5.28.

Table 5.16 lists the coordinates for the waste rock dump piezometers and Table 5.17 lists the water level elevations.

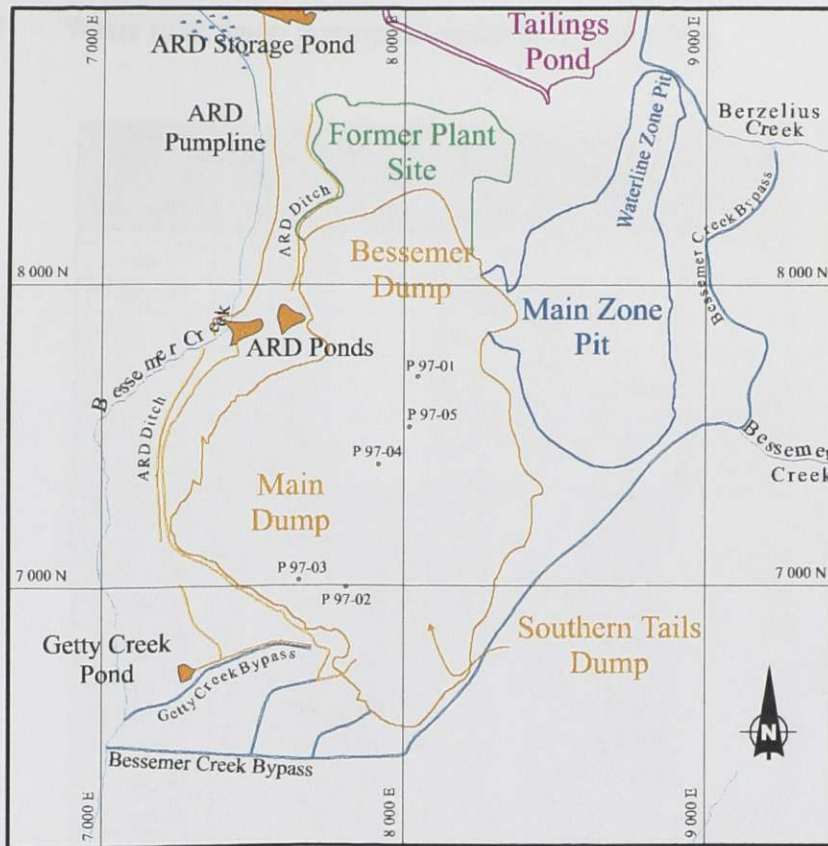


Figure 5.28 Waste rock dump piezometer locations.

Table 5.16 Waste rock dump piezometer coordinates.

| Piezometer | Coordinates | | | |
|------------|----------------|-----------------|-----------------|---------------|
| | Easting (m) | Northing (m) | Casing * (m) | Tip ** (m) |
| P 97-01 | 8047.501 | 7696.383 | 1292.018 | 1271.673 |
| P 97-02 | 7811.257 | 6995.958 | 1281.486 | 1266.002 |
| P 97-03 | 7654.608 | 7019.440 | 1259.485 | 1244.728 |
| P 97-04 | 7917.660 | 7404.033 | 1327.369 | 1288.507 |
| P 97-05 | 8020.126 | 7528.878 | 1326.307 | 1297.326 |

* Top of casing elevation.

** Piezometer tip elevation.

Table 5.17 Waste rock dump piezometer water level elevations.

| Date | Piezometer | | | | |
|-----------|----------------|----------------|----------------|----------------|----------------|
| | P 97-01 (m) | P 97-02 (m) | P 97-03 (m) | P 97-04 (m) | P 97-05 (m) |
| 17-Sep-97 | 1271.838 | | 1244.885 | | |
| 19-Sep-97 | 1272.478 | | 1244.865 | | |
| 14-Oct-97 | 1271.918 | | 1245.075 | | |
| 12-Nov-97 | 1271.948 | | 1245.205 | | |
| 30-Dec-97 | 1271.968 | | 1245.305 | 1288.449 | 1297.237 |
| 16-Feb-98 | 1271.948 | | 1245.265 | 1288.479 | 1297.197 |
| 31-Mar-98 | 1271.938 | | 1245.275 | 1288.449 | 1297.217 |
| 18-Apr-98 | 1271.968 | 1266.186 | 1245.285 | 1288.469 | |
| 19-Apr-98 | 1271.968 | 1266.226 | 1245.285 | 1288.469 | |
| 20-Apr-98 | 1271.968 | 1266.216 | 1245.295 | 1288.519 | |
| 21-Apr-98 | 1271.968 | 1266.206 | 1245.305 | 1288.569 | |
| 22-Apr-98 | 1271.968 | 1266.206 | 1245.305 | 1288.569 | |
| 23-Apr-98 | 1271.968 | 1266.206 | 1245.305 | 1288.569 | |
| 24-Apr-98 | 1271.968 | 1266.206 | 1245.305 | 1288.569 | |
| 25-Apr-98 | 1271.968 | 1266.186 | 1245.285 | 1288.469 | |
| 27-Apr-98 | 1271.978 | 1266.236 | 1245.295 | 1288.869 | |
| 29-Apr-98 | 1271.978 | 1266.316 | 1245.305 | 1289.229 | 1297.367 |
| 01-May-98 | 1272.008 | 1266.316 | 1245.315 | 1288.589 | 1297.367 |
| 04-May-98 | 1272.008 | 1266.306 | 1245.325 | 1288.589 | 1297.367 |
| 06-May-98 | 1272.008 | 1266.306 | 1245.325 | 1288.579 | 1297.367 |
| 08-May-98 | 1272.008 | 1266.316 | 1245.325 | 1288.589 | 1297.367 |
| 09-May-98 | 1272.008 | 1266.316 | 1245.315 | 1288.579 | 1297.367 |
| 11-May-98 | 1272.008 | 1266.316 | 1245.315 | 1288.579 | 1297.367 |
| 13-May-98 | 1272.003 | 1266.296 | 1245.315 | 1289.569 | 1297.357 |
| 15-May-98 | 1271.998 | 1266.306 | 1245.305 | 1288.579 | 1297.357 |
| 19-May-98 | 1271.988 | 1266.306 | 1245.275 | 1288.579 | 1297.357 |
| 21-May-98 | 1271.988 | 1266.306 | 1245.255 | 1288.579 | 1297.357 |
| 01-Jun-98 | 1271.968 | 1266.286 | 1245.195 | 1288.579 | 1297.327 |

Blank value indicates a dry piezometer.

Figure 5.29 shows the water levels versus time for the waste rock dump piezometers. There are numerous sample points for the spring of 1998 during Phase II of the field program (see Section 4.3).

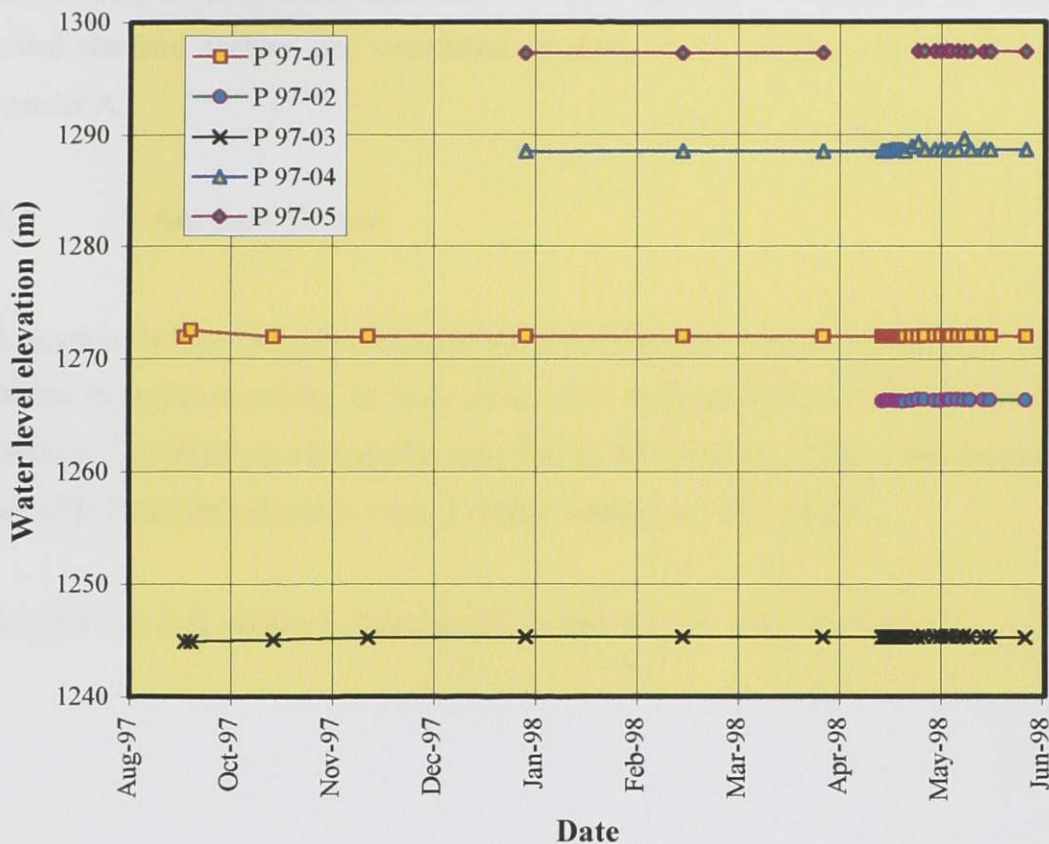


Figure 5.29 Water levels versus time for the waste rock dump piezometers.

5.6 Water Chemistry

The chemistry of the water offers an indication of the geochemical reactions that have taken place along the groundwater flow path. The reactions are dependent upon many variables such as the minerals present, chemical stability of the system, flow length and time. The evolution of groundwater may be mapped and areas of recharge and discharge may be identified. The water chemistry is explained for each of the components that pertain to Equity Silver Mine.

The following subsections tabulate only the most abundant constituents; however, a detailed chemical analysis was completed on some of the samples and is included in Appendix A.

5.6.1 Surface Water

The location for the collection of surface water samples can be seen in Figure 5.13. Table 5.18 lists the water chemistry for the surface water areas (see Table 5.7 for approximate locations). The chemical water quality data for the ARD Storage Pond is the same as the Main ARD Pond since the acid water is simply pumped to that location.

A detailed chemical analysis is also included in Appendix A, Table A.1.

Table 5.18 Surface water chemistry.

| Surface water location | pH | Acidity * (mg/L) | Dissolved constituents | | |
|---------------------------|------|---------------------|------------------------|--------------|--------------|
| | | | Cu (mg/L) | Fe (mg/L) | Zn (mg/L) |
| Getty Creek Pond | | | | | |
| 27-Jun-97 | 3.28 | 158 | 2.23 | 2.80 | 1.83 |
| 29-Aug-97 | 3.17 | 146 | 1.28 | 4.48 | 1.02 |
| 30-Oct-97 | 3.06 | 184 | 2.72 | 4.50 | 2.45 |
| 24-Dec-97 | 3.04 | 114 | 0.8 | 1.0 | 0.8 |
| 27-Feb-98 | 3.19 | 105 | 0.5 | 3.0 | 0.6 |
| 23-Apr-98 | 2.98 | 225 | 3.1 | 3.2 | 2.8 |
| 04-Jun-98 | 3.20 | 117 | 0.9 | 1.6 | 0.7 |
| Surge Pond (C9) | | | | | |
| 27-Jun-97 | 2.67 | 3330 | 37.2 | 350 | 147 |
| 29-Aug-97 | 2.64 | 5080 | 45.0 | 510 | 204 |
| 30-Oct-97 | 2.59 | 3683 | 34.6 | 410 | 153 |
| 24-Dec-97 | 2.47 | 6677 | 56.4 | 595 | 275 |
| 27-Feb-98 | 2.65 | 7194 | 51.2 | 670 | 300 |
| 23-Apr-98 | 2.56 | 7280 | 52.3 | 770 | 292 |
| 04-Jun-98 | 2.67 | 4148 | 39.8 | 365 | 172 |
| Main ARD Pond (C8) | | | | | |
| 27-Jun-97 | 2.45 | 5680 | 74 | 696 | 124 |
| 29-Aug-97 | 2.51 | 8330 | 98 | 1088 | 154 |
| 30-Oct-97 | 2.41 | 4704 | 52 | 655 | 107 |
| 24-Dec-97 | 2.31 | 11127 | 120 | 1480 | 178 |
| 27-Feb-98 | 2.43 | 14220 | 141 | 2080 | 256 |
| 23-Apr-98 | 2.41 | 9970 | 100 | 1560 | 168 |
| 04-Jun-98 | 2.45 | 6265 | 70 | 673 | 108 |

* As calcium carbonate CaCO₃.

Table 5.18 Surface water chemistry, *continued*.

| Surface water location | pH | Alkalinity * (mg/L) | Acidity * (mg/L) | Dissolved constituents | | | |
|---------------------------|------|------------------------|---------------------|---------------------------|--------------|--------------|--------------|
| | | | | SO ₄ (mg/L) | Cu (mg/L) | Fe (mg/L) | Zn (mg/L) |
| Waterline Zone Pit | | | | | | | |
| 19-Jun-97 | 6.62 | N/A | <10 | N/A | <0.03 | 0.33 | 0.55 |
| 29-Aug-97 | 6.82 | N/A | <10 | N/A | <0.03 | 0.01 | 0.47 |
| 30-Oct-97 | 6.55 | N/A | <10 | N/A | <0.01 | 0.10 | 0.58 |
| 24-Dec-97 | 6.55 | N/A | <10 | N/A | <0.01 | <0.03 | 0.26 |
| 27-Feb-98 | 7.20 | N/A | <10 | N/A | <0.03 | 0.03 | 0.50 |
| 21-May-98 | 6.67 | N/A | <10 | N/A | <0.01 | 0.40 | 0.33 |
| Tailings Pond | | | | | | | |
| 27-Jun-97 | 7.27 | 24 | N/A | 1400 | 0.012 | N/A | 0.056 |
| 25-Aug-97 | 7.46 | 23 | N/A | 1360 | 0.007 | N/A | 0.051 |
| 27-Oct-97 | 6.96 | 18 | N/A | 1560 | 0.023 | N/A | 0.090 |
| 29-Dec-97 | 7.08 | 23 | N/A | 1600 | 0.039 | N/A | 0.106 |
| 23-Feb-98 | 6.88 | 20 | N/A | 1430 | 0.026 | N/A | 0.110 |
| 27-Apr-98 | 7.18 | 20 | N/A | 1650 | 0.030 | N/A | 0.128 |
| Diversion Pond | | | | | | | |
| 27-Jun-97 | 7.45 | 56 | N/A | 2200 | 0.005 | N/A | 0.018 |
| 25-Aug-97 | 7.37 | 29 | N/A | 1800 | 0.002 | N/A | 0.016 |
| 27-Oct-97 | 7.25 | 33 | N/A | 1770 | 0.006 | N/A | 0.029 |
| 29-Dec-97 | 7.04 | 31 | N/A | 1980 | 0.006 | N/A | 0.062 |
| 23-Feb-98 | 6.94 | 46 | N/A | 1780 | 0.011 | N/A | 0.094 |
| 27-Apr-98 | 7.33 | 27 | N/A | 2610 | 0.004 | N/A | 0.020 |
| 04-May-98 | 7.31 | 16 | N/A | 2450 | 0.005 | N/A | 0.035 |
| Main Zone Pit | | | | | | | |
| 27-Jun-97 | 7.95 | 28 | N/A | 1660 | 0.003 | N/A | <0.005 |
| 25-Aug-97 | 8.37 | 34 | N/A | 1870 | 0.002 | N/A | <0.005 |
| 27-Oct-97 | 7.71 | 34 | N/A | 1730 | 0.004 | N/A | 0.022 |
| 29-Dec-97 | 7.16 | 69 | N/A | 1520 | 0.014 | N/A | 0.426 |
| 23-Feb-98 | 7.22 | 104 | N/A | 1220 | 0.026 | N/A | 1.07 |
| 30-Mar-98 | 6.75 | 90 | N/A | 1230 | 0.040 | N/A | 1.22 |

* As calcium carbonate CaCO₃.

5.6.2 Creeks and Diversion Channels

A diagram of the creeks and diversion channels can be seen in Figure 5.13 (or Figure 5.11 for conditions prior to any mining activity). Table 5.19 lists the water chemistry for the surrounding creeks and diversion channels for September 15, 1997 (see Table 5.7 for approximate locations).

Table 5.19 Creek and diversion channel water chemistry.

| River | pH | Temp. (°C) | Conductivity (mmhos/cm) | TDS (mg/L) | Major anions | | | Major cations | | |
|-----------------------|------|---------------|----------------------------|---------------|--------------|---------------------------|----------------------------|---------------|-------------|--------------|
| | | | | | Cl (mg/L) | SO ₄ (mg/L) | HCO ₃ (mg/L) | Na (mg/L) | K (mg/L) | Ca (mg/L) |
| East Bessemer | 6.85 | 9.4 | 82.7 | 64 | 0 | 9.5 | 32.5 | 28.8 | 23.0 | 36 |
| Bessemer Creek Bypass | 7.04 | 9.3 | 87.7 | 60 | 0 | 10.7 | 36.5 | 28.8 | 17.3 | 32 |
| Berzelius Creek | 6.83 | 11.0 | 186.8 | 124 | 0 | 46.1 | 44.7 | 36.0 | 9.4 | 84 |
| Lu Creek | 6.82 | 7.6 | 79.6 | 64 | 0 | 2.9 | 46.7 | 64.8 | 15.1 | 32 |
| Foxy Creek | 6.97 | 7.6 | 53.6 | 65 | 0 | 0.0 | 31.2 | 50.4 | 21.6 | 24 |
| Bessemer Creek | 7.23 | 9.6 | 719 | 551 | 0 | 317.2 | 41.6 | 237.6 | 63.4 | 332 |
| Buck Creek | 7.33 | 9.3 | 136.6 | 99 | 0 | 2.9 | 79.2 | 64.8 | 24.5 | 64 |
| Getty Creek | 7.31 | 9.4 | 276 | 216 | 0 | 116.2 | 4.3 | 72.0 | 45.4 | 108 |
| Bessemer Creek Bypass | 7.26 | 9.2 | 343 | 260 | 0 | 138.8 | 17.3 | 36.0 | 54.0 | 140 |

5.6.3 Seepage Water

Figure 5.20 is a drawing of the waste rock dump seepage while Table 5.20 lists the water chemistry for the seeps (see Table 5.7 for locations).

A detailed summary of the water quality is also included in Appendix A - Table A.2, Table A.3, Table A.4 and Table A.5.

Table 5.20 Water quality for seepage discharge.

| Seep | pH | Temp. (°C) | Conductivity (mmhos/cm) | Acidity * (mg/L) | Potential (mV) | Dissolved Constituents | | | |
|-------------------|------|---------------|----------------------------|---------------------|-------------------|------------------------|--------------|--------------|--------------|
| | | | | | | Cu (mg/L) | Fe (mg/L) | Zn (mg/L) | Mg (mg/L) |
| Seep 97-01 | | | | | | | | | |
| 25-Jun-97 | 5.45 | N/A | 2.85 | 66 | N/A | 0.14 | 40.4 | 0.541 | N/A |
| 16-Sep-97 | 6.33 | 11.0 | 3.11 | N/A | N/A | N/A | 3 | N/A | 20 |
| 19-Apr-98 | 6.20 | 4.5 | 2.84 | 35 | +120 | 0.05 | 24.6 | 0.757 | 154 |
| Seep 97-02 | | | | | | | | | |
| 25-Jun-97 | 2.88 | N/A | 3.67 | 638 | N/A | 1.49 | 160 | 1.97 | N/A |
| 16-Sep-97 | 2.70 | 10.5 | 3.7 | N/A | N/A | N/A | 50 | N/A | 25 |
| 19-Apr-98 | 2.70 | 3.4 | 5.14 | 3280 | +440 | 7.07 | 921 | 4.56 | 171 |
| Seep 97-03 | | | | | | | | | |
| 25-Jun-97 | 2.40 | N/A | 11.9 | 17500 | N/A | 94.6 | 3940 | 54.0 | N/A |
| 16-Sep-97 | 2.37 | 10.2 | 11.81 | N/A | N/A | N/A | 2480 | N/A | 80 |
| 19-Apr-98 | 2.90 | 2.4 | 10.84 | 14400 | +4120 | 78.7 | 2590 | 50.1 | 547 |
| Seep 97-04 | | | | | | | | | |
| 25-Jun-97 | 2.31 | N/A | 13.2 | 21300 | N/A | 153 | 5500 | 78.1 | N/A |
| 16-Sep-97 | 2.31 | 10.1 | 15.22 | N/A | N/A | N/A | 4670 | N/A | 130 |
| 19-Apr-98 | 2.50 | 6.4 | 14.14 | 21100 | +5320 | 269 | 6150 | 109 | 810 |
| Seep 97-05 | | | | | | | | | |
| 25-Jun-97 | 2.38 | N/A | 49.3 | 40200 | N/A | 403 | 6630 | 403 | N/A |
| 16-Sep-97 | 2.17 | 19.9 | 26.4 | N/A | N/A | N/A | 9860 | N/A | 600 |
| 19-Apr-98 | 2.30 | 16.7 | 27.8 | 50500 | +450 | 474 | 9680 | 345 | 2600 |
| Seep 97-06 | | | | | | | | | |
| 25-Jun-97 | 2.36 | N/A | 50.1 | 42800 | N/A | 419 | 6880 | 413 | N/A |
| 16-Sep-97 | - | - | - | - | N/A | - | - | - | - |
| 19-Apr-98 | 2.40 | 13.8 | 25.8 | 45400 | +430 | 431 | 9330 | 324 | 2340 |
| Seep 97-07 | | | | | | | | | |
| 25-Jun-97 | 2.25 | N/A | 58.1 | 56200 | N/A | 609 | 7780 | 492 | N/A |
| 16-Sep-97 | 2.07 | 13.3 | 32.1 | N/A | N/A | N/A | 10890 | N/A | 510 |
| 19-Apr-98 | 2.50 | 11.7 | 24.7 | 43800 | +480 | 422 | 6910 | 312 | 2510 |
| Seep 97-08 | | | | | | | | | |
| 25-Jun-97 | 2.26 | N/A | 54.6 | 42400 | N/A | 20.2 | 3790 | 537 | N/A |
| 16-Sep-97 | 2.11 | 18.2 | 31.9 | N/A | N/A | N/A | 3350 | N/A | 600 |
| 19-Apr-98 | 2.20 | 20.3 | 27.6 | 36300 | +4420 | 356 | 4810 | 459 | 3960 |
| Seep 97-09 | | | | | | | | | |
| 25-Jun-97 | 2.55 | N/A | 17.3 | 17900 | N/A | 8.75 | 1050 | 342 | N/A |
| 16-Sep-97 | 2.47 | 12.2 | 15.8 | N/A | N/A | N/A | 610 | N/A | 293 |
| 19-Apr-98 | 2.80 | 1.4 | 14.5 | 15100 | +410 | 133 | 1120 | 250 | 1820 |
| Seep 97-10 | | | | | | | | | |
| 25-Jun-97 | 2.08 | N/A | 49.6 | 62900 | N/A | 19.2 | 13600 | 237 | N/A |
| 16-Sep-97 | 2.12 | 11.4 | 22.5 | N/A | N/A | N/A | 10100 | N/A | 260 |
| 19-Apr-98 | 2.40 | 8.8 | 15.3 | 32100 | +450 | 355 | 7320 | 117 | 1110 |
| Seep 97-11 | | | | | | | | | |
| 25-Jun-97 | 2.08 | N/A | 67.9 | 83100 | N/A | 927 | 13200 | 478 | N/A |
| 16-Sep-97 | 2.04 | 30.4 | 12.5 | N/A | N/A | N/A | 10600 | N/A | 420 |
| 19-Apr-98 | 2.50 | 2.0 | 20.8 | 45900 | +460 | 335 | 9780 | 151 | 1430 |
| S - 1 | | | | | | | | | |
| 05-Mar-91 | N/A | N/A | N/A | 63700 | N/A | 1220 | 10800 | 774 | N/A |
| 14-Jul-94 | 1.46 | N/A | N/A | 78230 | N/A | 460 | 5940 | 384 | N/A |
| 27-Oct-95 | 2.53 | N/A | N/A | 30000 | N/A | 336 | 3430 | 445 | N/A |
| 14-Feb-97 | 2.05 | N/A | N/A | 47700 | N/A | 692 | 6450 | 534 | N/A |
| 25-Apr-97 | 2.15 | N/A | N/A | 52000 | N/A | 500 | 1538 | 555 | N/A |
| S - 2 | | | | | | | | | |
| 27-Oct-95 | 2.53 | N/A | N/A | 35700 | N/A | 576 | 7570 | 440 | N/A |
| 14-Feb-97 | 2.04 | N/A | N/A | 38900 | N/A | 460 | 4960 | 548 | N/A |
| 25-Apr-97 | 2.15 | N/A | N/A | 35300 | N/A | 604 | 10600 | 488 | N/A |
| S - 3 | | | | | | | | | |
| 05-Mar-91 | N/A | N/A | N/A | 101000 | N/A | 1910 | 16800 | 742 | N/A |
| 27-Oct-95 | 2.61 | N/A | N/A | 46200 | N/A | 336 | 4320 | 592 | N/A |
| 14-Feb-97 | 2.02 | N/A | N/A | 65500 | N/A | 682 | 10700 | 562 | N/A |
| 25-Apr-97 | 2.04 | N/A | N/A | 58600 | N/A | 115 | 1863 | 151 | N/A |

* As calcium carbonate CaCO₃.

- Indicates no data since there was no flow.

5.6.4 ARD Collection Water

Figure 5.22 shows the location of the ARD collection channels and Table 5.21 lists the water chemistry for the ARD collection channels. The water chemistry for C9 (Surge Pond) and C8 (Main ARD Pond) are given in Table 5.18 as they are essentially surface water data (see Table 5.12 for the weir coordinates).

Table 5.21 Water quality analysis for the ARD collection channels.

| Weir Location | pH | Acidity * (mg/L) | Dissolved Constituents | | |
|---------------|------|---------------------|------------------------|--------------|--------------|
| | | | Cu (mg/L) | Fe (mg/L) | Zn (mg/L) |
| C7 | | | | | |
| 27-Jun-97 | 2.34 | 10100 | 129.0 | 1370 | 136.0 |
| 29-Aug-97 | 2.38 | 15100 | 184.0 | 2224 | 177.0 |
| 30-Oct-97 | 2.35 | 5419 | 67.7 | 830 | 61.5 |
| 24-Dec-97 | 2.42 | 4574 | 50.4 | 595 | 51.2 |
| 27-Feb-98 | 2.25 | 27376 | 292.0 | 4700 | 268.0 |
| 23-Apr-98 | 2.33 | 13200 | 140.0 | 2430 | 106.0 |
| 04-Jun-97 | 2.39 | 8895 | 97.5 | 1055 | 103.0 |
| C11 | | | | | |
| 27-Jun-97 | 2.96 | 220 | 4.80 | 15.10 | 9.55 |
| 29-Aug-97 | 2.97 | 226 | 2.30 | 19.80 | 5.70 |
| 30-Oct-97 | 2.80 | 297 | 2.39 | 58.30 | 3.25 |
| 24-Dec-97 | 3.19 | 147 | 1.6 | 21.8 | 4.3 |
| 27-Feb-98 | 4.21 | 132 | 0.3 | 41.0 | 2.8 |
| 23-Apr-98 | 2.96 | 202 | 3.8 | 7.3 | 3.5 |
| 04-Jun-97 | 3.59 | 216 | 1.3 | 6.0 | 37.8 |
| ST | | | | | |
| 27-Jun-97 | 6.25 | <10 | 0.14 | 0.48 | 9.9 |
| 29-Aug-97 | 6.62 | <10 | 0.05 | 0.01 | 5.4 |
| 30-Oct-97 | 6.05 | 4 | 0.02 | 0.18 | 14.4 |
| 24-Dec-97 | 6.53 | <10 | 0.01 | 0.03 | 9.15 |
| 27-Feb-98 | 6.80 | <10 | 0.03 | 0.08 | 10.10 |
| 23-Apr-98 | 6.33 | <10 | 0.01 | 0.05 | 13.80 |
| 04-Jun-97 | 6.19 | <10 | 0.01 | 0.05 | 11.80 |

* As calcium carbonate CaCO₃.

A detailed summary of the water quality is also included in Appendix A, Table A.6.

5.6.5 ARD Sump Water

The location of the sumps can be seen in Figure 5.28. Table 5.22 lists the water quality for the sumps (see Table 5.9 for locations).

Table 5.22 Sump water quality.

| Sump | pH | Acidity * (mg/L) | Dissolved Constituents | | |
|----------------|------|---------------------|------------------------|--------------|--------------|
| | | | Cu (mg/L) | Fe (mg/L) | Zn (mg/L) |
| Sump #1 | | | | | |
| 24-Oct-96 | 2.85 | 344 | 8.80 | 32.00 | 5.2 |
| 26-Jun-97 | 2.94 | 334 | 5.83 | 9.20 | 4.7 |
| 21-Dec-97 | 2.98 | 492 | 8.69 | 10.90 | 8.1 |
| Sump #2 | | | | | |
| 24-Oct-96 | 4.11 | 222 | 4.40 | 2.86 | 8.8 |
| 29-Aug-97 | 3.23 | 215 | 3.93 | 2.08 | 5.3 |
| 19-Sep-97 | 3.09 | 243.3 | 3.73 | 2.48 | 5.15 |
| 21-Dec-97 | 3.54 | 1794 | 16.3 | 3.63 | 26.9 |
| Sump #3 | | | | | |
| 26-Jun-97 | 2.50 | 8000 | 146.00 | 996 | 78.5 |
| 21-Dec-97 | 2.35 | 25964 | 360 | 3620 | 244 |
| Sump #4 | | | | | |
| 24-Oct-96 | 2.47 | 9840 | 164 | 916 | 83 |
| 14-Feb-97 | 2.46 | 16300 | 269 | 1660 | 136 |
| 26-Jun-97 | 2.47 | 8070 | 142 | 370 | 78 |
| 19-Sep-97 | 2.41 | 10960 | 175 | 1020 | 103 |
| 21-Dec-97 | 2.28 | 32623 | 432 | 4560 | 280 |
| Sump #5 | | | | | |
| 24-Oct-96 | 4.66 | 36.0 | 1.34 | 0.14 | 1.46 |
| 14-Feb-97 | 5.50 | 15.0 | 1.40 | 24.60 | 1.56 |
| 19-Sep-97 | 4.45 | 32.1 | 2.00 | 0.08 | 2.32 |
| 21-Dec-97 | 5.43 | 22 | 1.40 | 0.31 | 2.73 |
| Sump #6 | | | | | |
| 04-Oct-95 | 7.29 | <10 | 0.02 | 0.02 | 0.02 |
| Sump #7 | | | | | |
| 24-Oct-96 | 4.06 | 77 | 0.60 | 0.56 | 0.64 |
| 19-Sep-97 | 3.96 | 28.1 | 0.40 | 0.28 | 0.58 |

* As calcium carbonate CaCO₃.

5.6.6 Piezometer Water

The following subsections provides the water quality analysis of groundwater from the regional and waste rock dump piezometers.

5.6.6.1 Regional Piezometers

The location of the regional piezometers can be seen in Figure 5.26. Table 5.23 lists the water chemistry for these piezometers (see Table 5.14 for locations).

Table 5.23 Regional piezometer water chemistry data.

| Piezometer | pH | Conductivity (μ mhos/cm) | Alkalinity * (mg/l) | Dissolved Constituents | | | |
|---------------------|------|----------------------------------|------------------------|---------------------------|--------------|--------------|--------------|
| | | | | SO ₄ (mg/L) | Cu (mg/L) | Al (mg/L) | Zn (mg/L) |
| RH 82-02-01 | | | | | | | |
| 28-Jun-96 | 7.66 | 529 | N/A | 92.1 | 0.001 | 0.007 | <0.005 |
| 23-Sep-96 | 7.62 | 508 | N/A | 91.3 | <0.001 | 0.007 | <0.005 |
| RH 82-03-01 | | | | | | | |
| 25-Mar-96 | 5.62 | 1000 | N/A | 518 | <0.001 | 0.075 | 0.172 |
| 28-Jun-96 | 5.80 | 984 | N/A | 482 | <0.001 | 0.062 | 0.170 |
| 23-Sep-96 | 6.03 | 1010 | N/A | 578 | 0.009 | 0.093 | 0.175 |
| 04-Nov-96 | 5.96 | 1060 | N/A | 456 | <0.005 | 0.078 | 0.165 |
| 31-Mar-97 | 5.84 | 1020 | N/A | 553 | 0.002 | 0.184 | 0.164 |
| 30-Jun-97 | 5.19 | 990 | N/A | 494 | 0.002 | 0.070 | 0.169 |
| 29-Sep-97 | 5.83 | 1010 | N/A | 550 | 0.004 | 0.061 | 0.184 |
| 22-Dec-97 | 5.65 | 945 | N/A | 478 | 0.001 | 0.060 | 0.167 |
| RH 82-05-03 | | | | | | | |
| 28-Jun-96 | 6.92 | 767 | N/A | 314 | 0.003 | 0.005 | 0.007 |
| 04-Nov-96 | 6.64 | 785 | N/A | 299 | <0.001 | 0.010 | <0.005 |
| 22-Dec-97 | 6.65 | 662 | N/A | 290 | <0.001 | 0.017 | <0.005 |
| RH 82-06-01 | | | | | | | |
| 28-Jun-96 | 7.58 | 1090 | N/A | 164 | 0.001 | <0.005 | <0.005 |
| 11-Apr-96 | N/A | N/A | N/A | N/A | <0.001 | 0.009 | <0.005 |
| 30-Jun-97 | 7.55 | 1060 | N/A | 166 | <0.001 | <0.02 | 0.073 |
| 22-Dec-97 | 7.31 | 988 | N/A | 176 | <0.001 | <0.02 | <0.005 |
| RH 82-06-02 | | | | | | | |
| 28-Jun-96 | 7.78 | 1150 | N/A | 164 | 0.001 | <0.005 | <0.005 |
| 11-Apr-96 | 7.59 | 1200 | N/A | N/A | <0.001 | 0.008 | <0.005 |
| 30-Jun-97 | 7.65 | 1150 | N/A | 249 | <0.001 | <0.02 | <0.005 |
| 22-Dec-97 | 7.44 | 1070 | N/A | 257 | <0.001 | <0.005 | <0.005 |
| RH 82-06A-01 | | | | | | | |
| 28-Jun-96 | 7.54 | 994 | N/A | 144 | <0.001 | 0.009 | <0.005 |
| 11-Apr-96 | 7.36 | 1040 | N/A | 155 | 0.003 | 0.012 | <0.005 |
| 30-Jun-97 | 7.39 | 978 | N/A | 156 | 0.002 | <0.02 | <0.005 |
| 22-Dec-97 | 7.29 | 909 | N/A | 164 | <0.001 | <0.005 | <0.005 |

* As calcium carbonate CaCO₃.

Table 5.23 Regional piezometer water chemistry data, *continued*.

| Piezometer | pH | Conductivity (μ mhos/cm) | Alkalinity * (mg/l) | Dissolved Constituents | | | |
|-----------------|-------|----------------------------------|------------------------|---------------------------|--------------|--------------|--------------|
| | | | | SO ₄ (mg/L) | Cu (mg/L) | Al (mg/L) | Zn (mg/L) |
| RH 90-10 | | | | | | | |
| 28-Jun-96 | 7.66 | 665 | N/A | 83.7 | 0.003 | 0.010 | 0.012 |
| 04-Nov-96 | 7.59 | 677 | N/A | 85.5 | 0.008 | 0.022 | 0.018 |
| 30-Jun-97 | 7.62 | 655 | N/A | 81 | <0.001 | <0.02 | 0.009 |
| RH 90-11 | | | | | | | |
| 28-Jun-96 | 7.63 | 1100 | N/A | 365 | 0.007 | 0.016 | 0.012 |
| 30-Jun-97 | 7.43 | 1090 | N/A | 410 | <0.001 | <0.01 | 0.005 |
| RH 90-12 | | | | | | | |
| 28-Jun-96 | 7.80 | 595 | N/A | 101 | 0.002 | 0.013 | 0.014 |
| 04-Nov-96 | 7.73 | 618 | N/A | 103 | 0.002 | 0.020 | <0.005 |
| 30-Jun-97 | 7.57 | 621 | N/A | 118 | 0.002 | 0.01 | 0.02 |
| RH 90-13 | | | | | | | |
| 05-Jun-91 | 7.50 | N/A | 274 | 215 | 0.038 | 0.049 | 0.008 |
| RH 90-14 | | | | | | | |
| 28-Jun-96 | 11.30 | 1860 | N/A | 555 | 0.008 | 0.096 | 0.009 |
| 04-Nov-96 | 11.40 | 1880 | N/A | 699 | 0.011 | 0.166 | 0.016 |
| 30-Jun-97 | 11.40 | 1840 | N/A | 720 | 0.018 | 0.15 | 0.02 |
| 29-Dec-97 | 11.0 | 1590 | N/A | 775 | 0.003 | 0.011 | <0.005 |
| RH 90-15 | | | | | | | |
| 21-Dec-95 | 11.80 | 3590 | N/A | 213 | 0.036 | 0.046 | <0.005 |
| 28-Jun-96 | 11.20 | 1510 | N/A | 7.1 | 0.046 | 0.065 | 0.069 |
| 30-Jun-97 | 11.80 | 2080 | N/A | 19 | 0.246 | 20.10 | 0.17 |
| 29-Dec-97 | 11.6 | 3970 | N/A | 33 | 0.308 | 1.25 | 0.160 |
| RH 90-16 | | | | | | | |
| 29-Jun-95 | N/A | N/A | N/A | N/A | 0.001 | 0.069 | <0.005 |
| 29-Dec-97 | 6.7 | 255 | N/A | 70 | 0.013 | 0.042 | 0.192 |
| RH 90-20 | | | | | | | |
| 04-Nov-96 | 7.40 | 1270 | N/A | 422 | <0.001 | 0.069 | 0.010 |
| 30-Jun-97 | 7.43 | 1080 | N/A | 489 | <0.001 | 0.023 | <0.005 |
| 29-Dec-97 | 6.94 | 1110 | N/A | 424 | N/A | N/A | N/A |

* As calcium carbonate CaCO₃.

5.6.6.2 Waste Rock Dump Piezometers

The locations of the waste rock dump piezometers are shown in Figure 5.28. Table 5.24 lists the water chemistry for water samples collected from these piezometers (see Table 5.16 for locations). Samples for P 97-02, P 97-04 and P 97-05 could not be obtained for analysis as the water levels were too low.

Table 5.24 Waste rock dump piezometer water chemistry.

| Piezometer | pH | Temp. (°C) | Conductivity (mmhos/cm) | Acidity * (mg/L) | Potential (mV) | Dissolved Constituents | | | |
|----------------|------|---------------|----------------------------|---------------------|-------------------|------------------------|--------------|--------------|--------------|
| | | | | | | Cu (mg/L) | Fe (mg/L) | Zn (mg/L) | Mg (mg/L) |
| P 97-01 | | | | | | | | | |
| 17-Sep-97 | 3.53 | 8.7 | 13.67 | N/A | N/A | N/A | 610 | N/A | 249 |
| 18-Apr-98 | 2.70 | 9.0 | 17.26 | 19700 | +400 | 203 | 2900 | 405 | 2000 |
| P 97-03 | | | | | | | | | |
| 17-Sep-97 | 3.21 | 17.1 | 25.5 | N/A | N/A | N/A | 2830 | N/A | 352 |
| 18-Apr-98 | 2.50 | 10.7 | 37.5 | 48700 | +400 | 549 | 10500 | 717 | 4820 |

* As calcium carbonate CaCO₃.

A detailed summary of the water quality is also included in Appendix A, Table A.7.

5.6.7 Runoff Water

The runoff was sampled for the 1998 freshet and the results are shown in Table 5.25. A detailed summary of the water quality is also included in Appendix A, Table A.8.

Table 5.25 Runoff water chemistry.

| Sample | pH | Temp. (°C) | Conductivity (µmhos/cm) | Acidity * (mg/L) | Potential (mV) | Dissolved Constituents | | | |
|---------------|------|---------------|----------------------------|---------------------|-------------------|------------------------|--------------|-------------|--------------|
| | | | | | | Ca (mg/L) | Mg (mg/L) | K (mg/L) | Na (mg/L) |
| Runoff | | | | | | | | | |
| 19-Apr-98 | 5.20 | 2.2 | 323 | 25 | +210 | 36.60 | 11.2 | 3 | <2 |

* As calcium carbonate CaCO₃.

Chapter 6 Modelling Program

6.1 Introduction

The groundwater flow regime system was modelled for the Equity Silver Mine site using GMS (Groundwater Modelling System) and FEMWATER. GMS is a graphical interface for performing groundwater simulations (ECGL, 1998) and was developed by the Department of Defense (USA). FEMWATER is an analysis code that is supported by GMS for performing groundwater flow and transport simulations (Lin *et al.*, 1997). The three dimensional finite element program models flow and transport in the saturated and the unsaturated zone. FEMWATER can do simulations of flow only, transport only, combined sequential flow and transport and coupled density-dependent flow and transport. The model is capable of handling heterogeneous and anisotropic media. Analysis modes include both steady state and transient conditions.

6.2 Three Dimensional Mesh Generation

The generation of the three dimensional finite element mesh required four steps. The first step involved the development of a conceptual model which was created to form a two dimensional mesh. Three dimensional iso-surfaces termed TIN's (Triangulated Irregular

Network) representing the hydrostratigraphy were developed into a three dimensional mesh by projection to the two dimensional mesh.

6.2.1 Conceptual Model

The conceptual model consisted of a series of nodes and arcs. The arcs are defined by a series of nodes and represent specific characteristics that are to be preserved in the mesh. The red arcs define the study area, waste rock dump and the open pits. The remaining arcs represent the geology, piezometers, sumps, creeks and ponds that are also conserved in the two dimensional mesh. The conceptual model used to represent the mine site is shown in Figure 6.1.

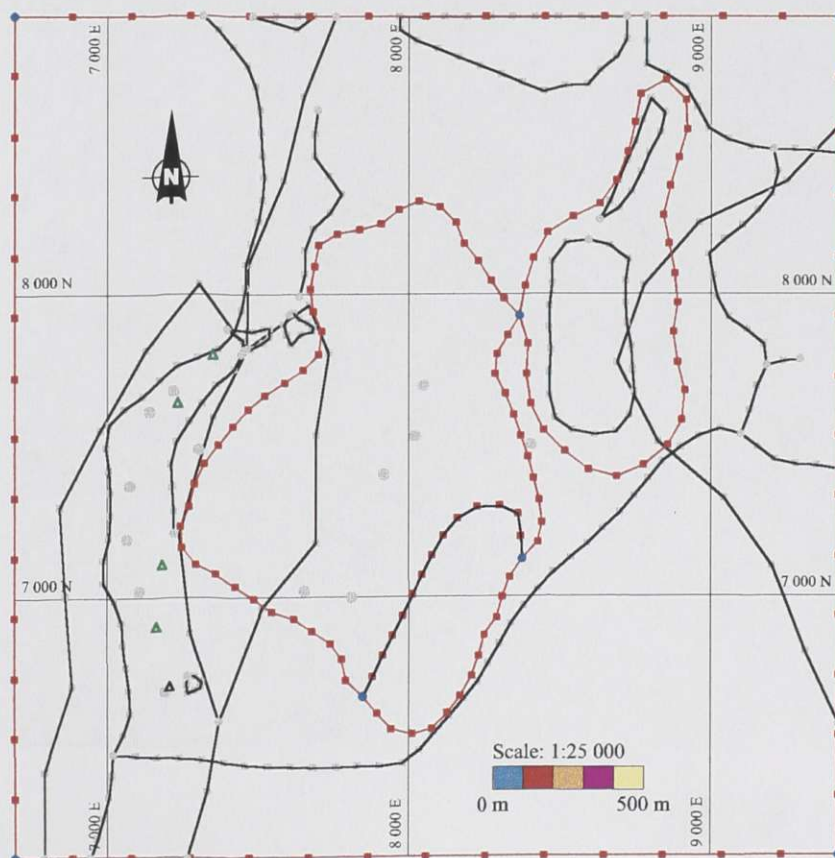


Figure 6.1 Conceptual model.

The five green triangles represent refine points for sump #1, #2, #4, #5 and #7. The mesh must be refined around a source or sink area due to the steep hydraulic gradients. The conceptual model consists of 440 nodes, 35 arcs and 5 refine points.

6.2.2 Two Dimensional Mesh

A two dimensional mesh was generated from the conceptual model. This algorithm honors the nodes and the refine points in the conceptual model. The two dimensional mesh is shown in Figure 6.2.

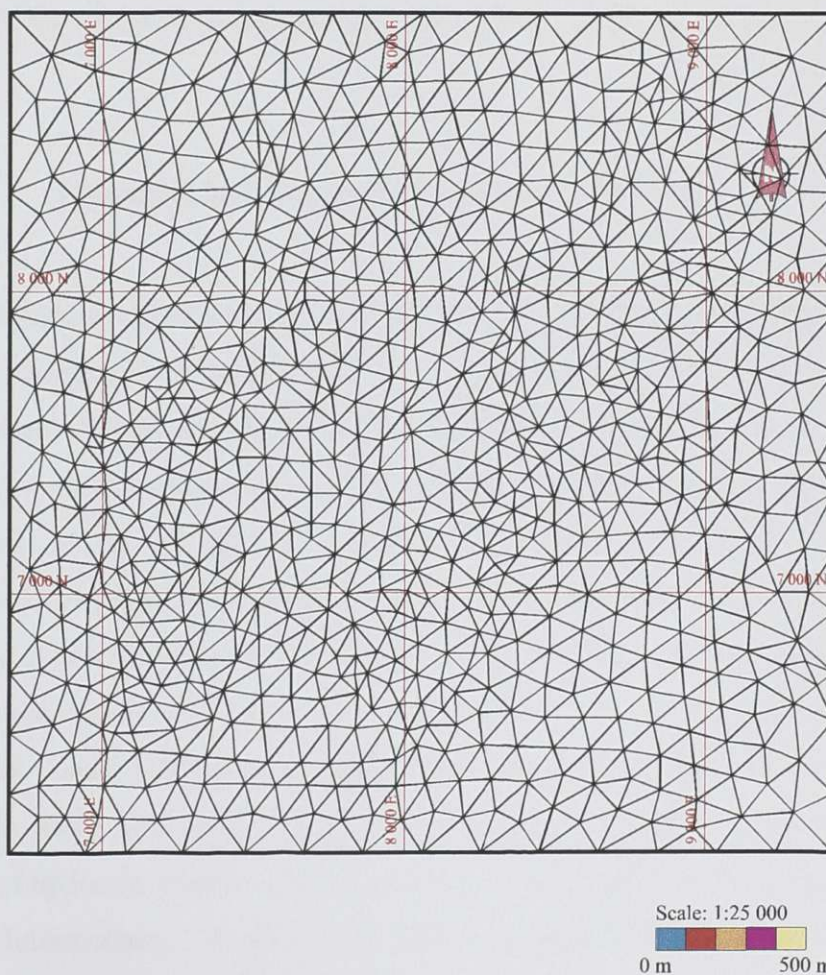


Figure 6.2 Two dimensional mesh.

Triangular elements are preferred over quadrilateral elements due to the planar surface of a triangular face in three dimensions, which may not be the case for quadrilateral elements. Element configuration is explained further in Section 6.2.4.

The mesh consists of 864 nodes, a maximum node half band width of 58 and 1,667 triangular elements.

A two dimensional mesh that covers only the waste rock dump was derived from the mesh in Figure 6.2 by removing all of the elements outside of the area in order to produce the waste rock three dimensional finite elements. The waste rock dump mesh consists of 201 nodes, a maximum node half band width of 23 and 336 triangular elements.

6.2.3 Triangulated Irregular Network (TIN)

The Triangulated Irregular Network's (TIN's) were derived from the isopachs in Section 5.2 and the topographical maps in Section 5.3. The lower boundary of the modelled area is located at an elevation of 800 m and is termed the Baseline TIN. The Bedrock TIN is located at the current topographical map (without the waste rock dump) minus the till isopach and 10 m of fractured bedrock. The fractured bedrock TIN (termed *Frac_Bedrock*) is simply the Bedrock TIN plus 10 m in elevation since the upper 10 m of the bedrock is believed to be fractured. The Till TIN is the topographical map (without the waste rock dump). The waste rock TIN (termed *Waste_Rock*) is the topographical map with the waste rock dump included. Three intermediate TIN's have been included between the waste rock TIN and the Till TIN due to the four orders of magnitude difference of hydraulic conductivity between the two materials. The intermediate TIN's are termed *Intermediate_1*, *Intermediate_2* and *Intermediate_3* and are located 1, 2 and 3 meters above the till TIN respectively. The intermediate TIN's reduce the maximum difference in hydraulic conductivity to one order of magnitude between materials. All of the intermediate and waste rock TIN's are projected over the waste rock dump area and

not the total area as described in Figure 6.2. The Cover TIN represents the soil cover that was placed on the waste rock dump and is 0.8 m above the Waste_Rock TIN.

6.2.4 Three Dimensional Mesh

The three dimensional mesh was developed from the projection of all of the TIN's onto the two dimensional mesh. The elements between the TIN's are subdivided into a prescribed amount that defines the number of internal layers of elements in a specific material. The horizontal layers of elements have vertical boundaries with different material properties where the geology changes. This is the case for the bedrock and the fractured bedrock which both contain five different geological units within the layers. The till layer is assumed to be homogenous throughout the mine area. The 1 m intermediate layers represent a gradual change of hydraulic conductivity of the waste rock to approach that of the glacial till in three steps and is also assumed to be homogeneous. This gives rise to 15 separate materials (the three intermediate layers are artificial and have properties that vary in succession between the till and the waste rock). The pits result in non-continuous hydrostratigraphy of the fractured bedrock and the till layers; thus, the number of two dimensional elements reduces to 1,478 from 1,667. A portion of the elements in these layers were eliminated in the Main Zone Pit area. The elements that extend over the Southern Tails area were simply renamed to the Intermediate_1 layer which represents the first waste rock layer. Table 6.1 describes the distribution of the three dimensional elements.

The mesh consists of 8,071 nodes, a maximum node half bandwidth of 996 and 13,202 wedge elements. Wedge elements are preferred over hexahedral elements due to the planer surfaces on all sides of the wedge, which may not be the case for hexahedral elements. The particle tracking algorithm may break down in FEMWATER if a particle crosses a non-planer face (ECGL, 1998). This is a particular concern when mass transport is modelled.

Table 6.1 Description of the three dimensional elements.

| Layer | 2D Mesh elements | TIN's | | Number of layers | Number of elements |
|----------------------------------|------------------|--------------|--------------|------------------|--------------------|
| | | Lower | Upper | | |
| Bedrock | 1667 | Baseline | Frac_Bedrock | 2 | 3334 |
| Fractured bedrock | 1478 | Frac_Bedrock | Bedrock | 2 | 2956 |
| Till | 1478 | Bedrock | Till | 2 | 2956 |
| Southern Tails fill | 65 | N/A | N/A | 4 | 260 |
| Intermediate 1 | 336 | Till | Till+1 | 1 | 336 |
| Intermediate 2 | 336 | Till+1 | Till+2 | 1 | 336 |
| Intermediate 3 | 336 | Till+2 | Till+3 | 1 | 336 |
| Waste rock | 336 | Till+3 | Waste_Rock | 6 | 2016 |
| Soil Cover | 336 | Waste_Rock | Cover | 2 | 672 |
| Total number of elements: | | | | | 13202 |

A three dimensional representation of the finite element mesh with a vertical exaggeration of 2.6 is shown in Figure 6.3.

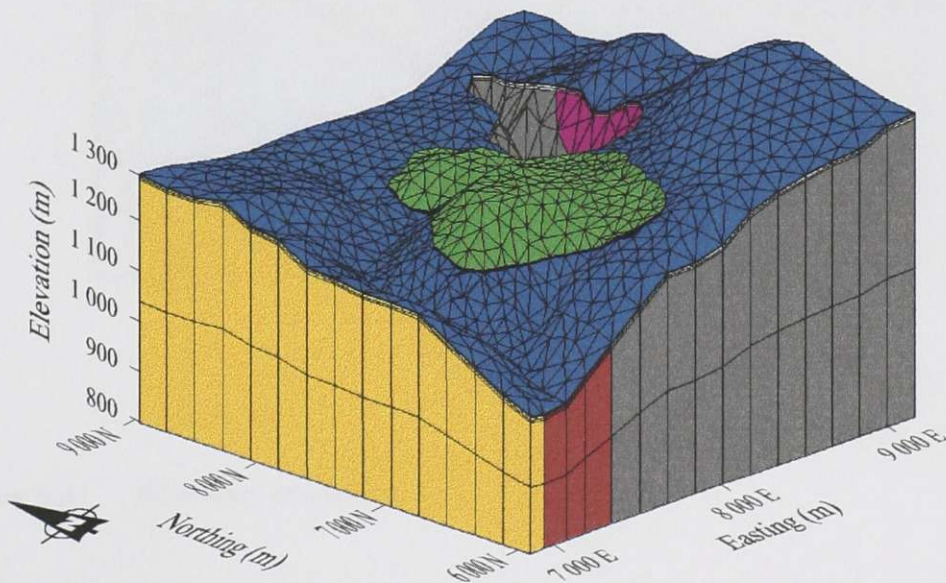


Figure 6.3 Three dimensional mesh.

6.3 Boundary Conditions

The boundary conditions at the mine site consist of constant head, infiltration rates and pumping rates which are shown in Figure 6.4.

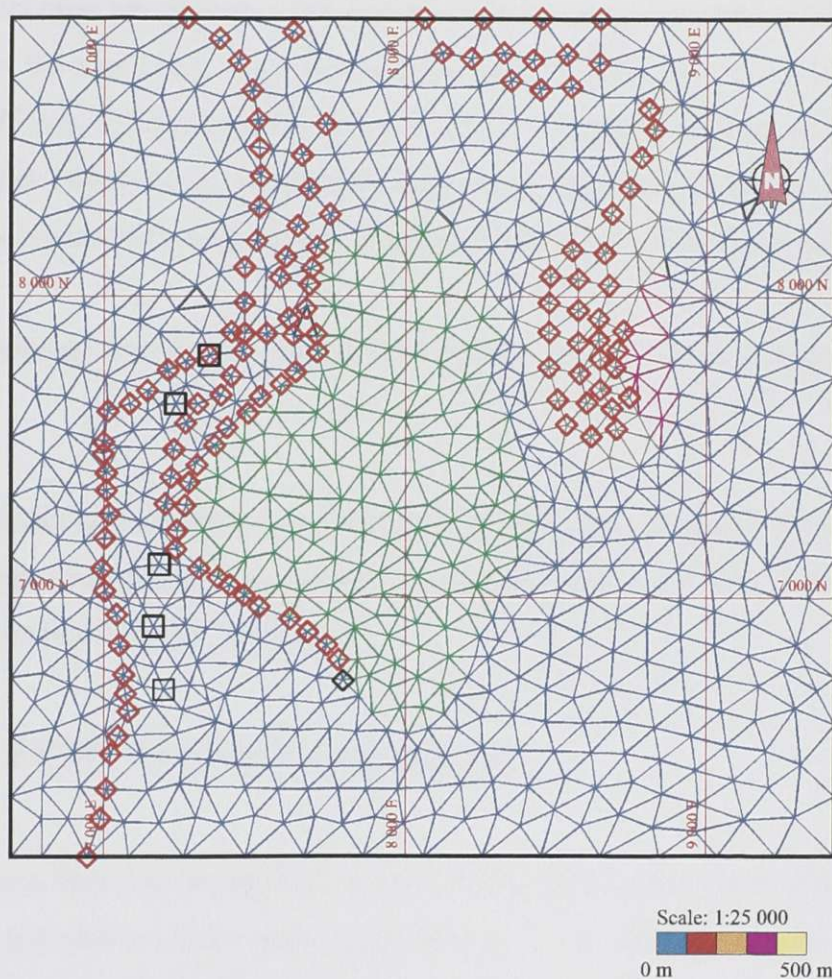


Figure 6.4 Boundary conditions.

The diamonds in Figure 6.4 represent constant head. The string of diamonds on the west side represent Bessemer Creek. The individual strings of diamonds in the center region represent the acid rock drainage collection ditches. The south and west end of the waste rock dump is also set to a constant head boundary. The Main Zone Pit and Waterline

Zone Pit are constant head locations and are seen in the northeastern area. The diamonds on the north side of the map area represent the Tailings Pond. The heads for the creek, seepage faces on the waste rock dump and the ARD ditches are set at the elevation head. The pit and pond water are set in accordance to the values presented in Chapter 5.

Variable flux rates are applied to the ground surface and are described in Chapter 3. The flux rate for the waste rock dump was found to be 6 % of the total precipitation or a rate of 1.1×10^{-9} m/s. A flux of 2×10^{-9} m/s or 10 % of the total precipitation was arbitrarily set to regions outside of the waste rock dump. Regional recharge rates of 10, 20 and 30 % were also simulated in order to gain a sense of sensitivity of infiltration rates.

The black squares represent the groundwater sumps. The sumps pump from the fractured bedrock.

The outer limits of the modelled area represent groundwater divides. The groundwater is divided along these lines due to topography and represent a zero flow boundary. These boundary conditions are set in the model.

6.4 FEMWATER Run Options

A steady state, flow only simulation was used for the model presented herein. A transient model was not used as steady state conditions exist in the field (see Section 5.4.1). Mass lumping was used which indicates if the mass matrix should be lumped. The solution is less accurate but potentially more stable (Lin *et al.*, 1997). The solving method was the pointwise iterative matrix solver which uses the basic successive iterative method. The quadrature defines the technique of numerical integration. The quadrature used was a gaussian / gaussian which is used for both element and surface integration. The weighting factor used was a backward difference one. The relaxation parameter for solving the non-linear flow equations was set to 0.050 and 1.00 for the linear equations. A transient simulation was performed in order to aid in the convergence of the model.

Iteration and convergence criterion were also specified. The number of iterations for non-linear flow was set to 100 and 500 for linear flow. Ten cycles for the rain / seepage boundary were set. The steady state convergence criteria was set to 0.020 m and 0.001 m for transient simulations.

Chapter 7 Data Analysis and Discussion

7.1 Introduction

The objective of this thesis was to determine the water balance for the waste rock dump. Hydrological characterization of the waste rock dump was performed in order to assess all of the hydrological parameters. This chapter analyzes the hydrological data collected during the thesis program.

7.2 Spring Freshet

Measurements from the 1998 freshet offer information on the flow patterns and drainage characteristics of the waste rock dump. The runoff was measured along with the waste rock dump piezometric water levels and seepage flow rate hydrographs.

7.2.1 Runoff

The runoff was measured at three of the five stations for the waste rock dump and is described in Section 4.3.1. Table 7.1 summarizes the results from the runoff flow measurements.

Table 7.1 Summary of the runoff flow measurements.

| Contributing area | Area (ha) | Cumulative flow (m ³) | Equivalent water depth (mm) | Portion of total area |
|-------------------|--------------|-----------------------------------|-----------------------------|-----------------------|
| R 98-01 | 94.2 | 72625 | 77 | 42.4% |
| R 98-02 | 9.1 | 3054 | 34 | 4.1% |
| R 98-03 | 8.2 | 3236 | 39 | 3.7% |
| R 98-04 | 4.9 | N/A | N/A | 2.2% |
| R 98-05 | 42.5 | N/A | N/A | 19.1% |
| Outside catchment | 63.1 | N/A | N/A | 28.4% |
| Total | 222.0 | 78,915 | 71 | 100.0% |

The total snowfall less sublimation and mass transfer was an equivalent of 84 mm of water for the start of the 1998 spring freshet (see Section 5.4.1.2). An additional 15 mm of rain fell during the freezing period and was added to the snow equivalent. Thus, the total input of water into the system is 99 mm of equivalent water. With the use of SoilCover, infiltration during the freshet period was calculated to be 55 mm of water and 53 mm of changes in storage. The change in storage term is high due to drying periods in the previous season and the thawing process of the soil. The net infiltration during the runoff period is 2 mm. The evaporation was not calculated by SoilCover but is assumed to be negligible during this period. Thus, the total equivalent water available for runoff calculated by SoilCover was 44 mm, or 15 % of the total snowfall. The amount of runoff is dependant on the amount of storage that must be displaced prior to runoff. This term is highly sensitive to porosity and hydraulic conductivity of the non-compacted till. The value calculated by SoilCover does however fall within the range measured in the field. The amount of water that is able to runoff from the total precipitation during the freezing period is illustrated in Figure 7.1.

The measured runoff at the R 98-01 station was 77 mm of equivalent water depth. The topography of the R 98-01 catchment area consists mainly of valleys, valley slopes and some portion of level plains. The snow accumulation rates in the valleys and valley slopes

are higher than that of level plains. This would explain the higher value of runoff measured at this particular station.

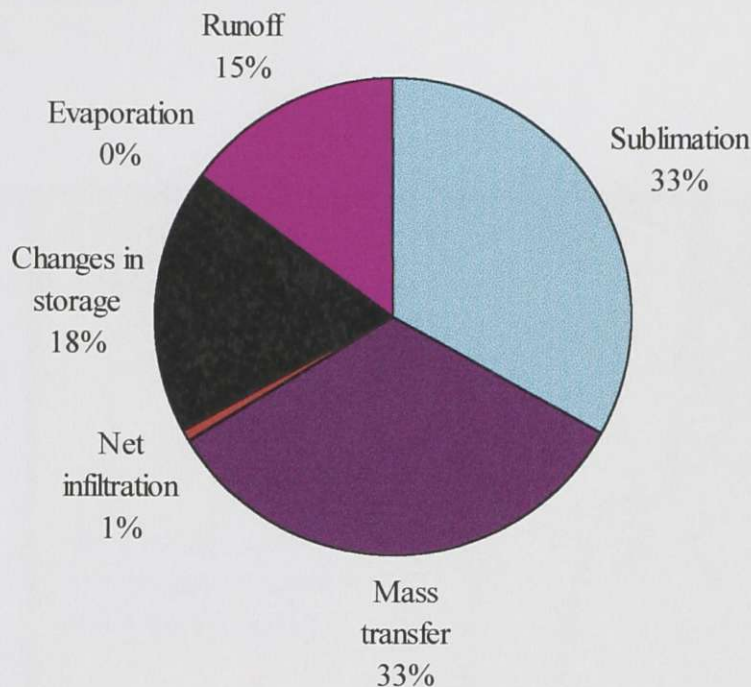


Figure 7.1 Available runoff from total precipitation during the freezing period.

The catchment areas for the R 98-02 and R 98-03 stations are similar in terms of topographical features. The equivalent water depths for these two stations were 34 mm and 39 mm respectively. These similarly low values are due to the mainly ridge and level plain topography of the catchment areas.

In summary, the total catchment area of the instrumented runoff is apparently an over estimate of the runoff of the total site due to the large area of valleys and valley slopes in the R 98-01 catchment area. The total runoff for the catchment area is likely between 34 mm and 71 mm. The estimate provided by the SoilCover model is considered reasonable.

The runoff flow rates exhibited a definite diurnal variation in response to incoming radiation and the associated air temperature. Figure 7.2 illustrates a typical plot of daily variations in incoming radiation, air temperature and the runoff flow rate at the R 98-02 station. The ordinate axis is normalized to compare the characteristics of the individual components.

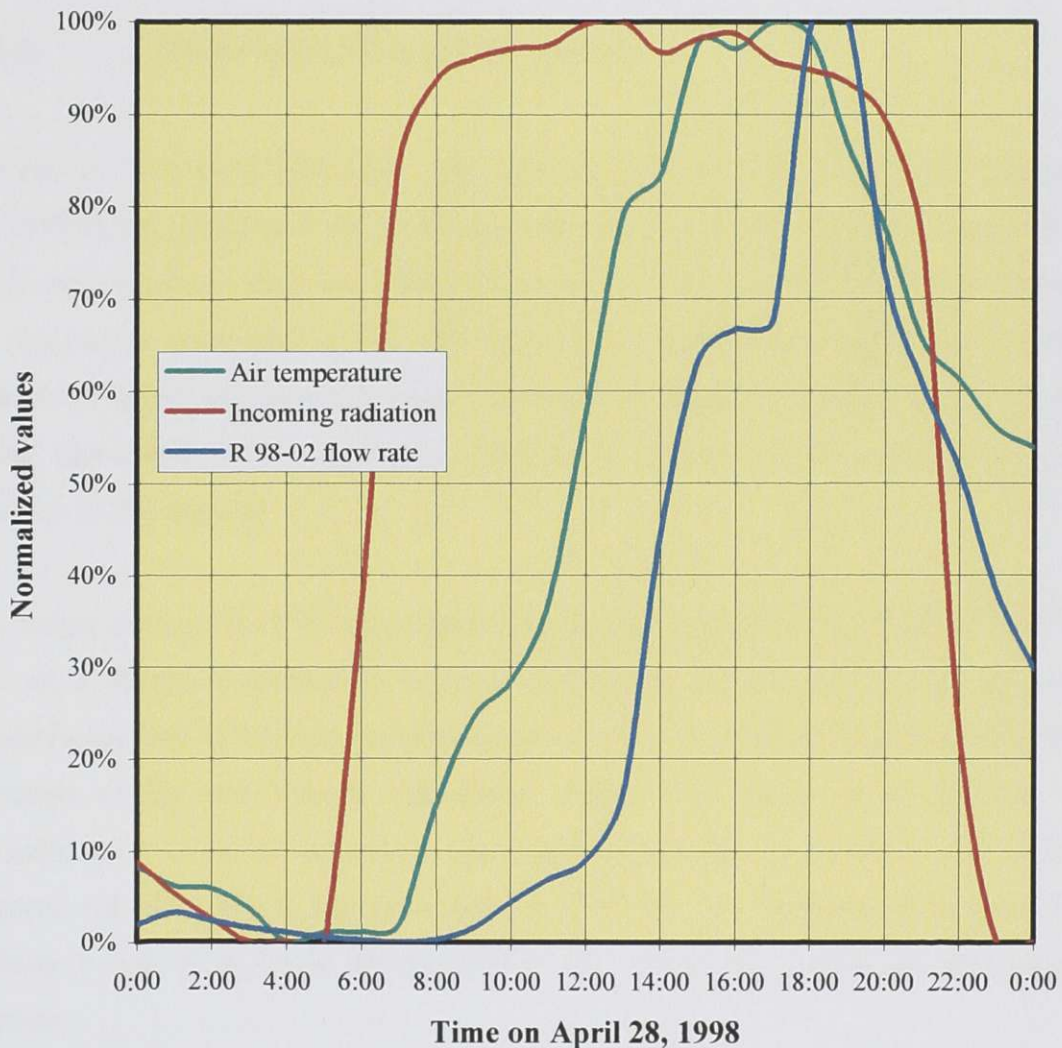


Figure 7.2 Comparison between daily air temperature, incoming radiation and R 98-02 flow rate.

The incoming radiation acts as an energy input into the system and peaks at about 1:00 p.m. The air temperature reacts to the increase in energy input and peaks four hours later, at 5:00 p.m. The delay is the result of heat storage components in the air, land, water and snow. The flow rate in the R 98-02 station is the result of the melting snow and peaks at 7:00 p.m. The delayed peak is due to storage components of heat in the snow pack and storage in the draining water within the catchment area.

7.2.2 Waste Rock Dump Piezometers

The rise of water level within the waste rock dump piezometers were observed during the 1998 freshet period and the results are explained in Section 4.3.2. The rise in water levels were extremely small and difficult to measure; thus, it is questionable to attribute the response to groundwater. The low heads in the piezometers suggest that a water table in the waste rock does not exist. The source of water is apparently ponded water within depressions in the underlying glacial till or perched water tables due to the presence of fine material.

The source of water for P 97-02 seems to be from the Southern Tails Zone Pit. This pit acts as a hydraulic connection between the fractured rock and the waste rock. Groundwater flow in the fractured rock enters the pit from exposed fractured rock in the highlands to the east (Golder Associates, 1983). The source of the increase in groundwater is from the snowmelt. The water level in the pit increases due to this response and thus affects the water level in P 97-02. The Southern Tails Zone Pit spillway is only 4 m below the tip of P 97-02, which may explain the more rapid response.

A similar process near P 97-02 is seemingly occurring near P 97-03. The southwest portion of the Main Dump is on a very thin or nonexistent layer of glacial till. A hydraulic connection between the fractured bedrock and the waste rock will result if the till is non-continuous in certain areas. The long delay time in P 97-03 may be a result of this area

being recharged from other areas other than the Southern Tails Dump and possibly regions north and east of the Southern Tails Zone Pit.

The rise in water levels for the remaining piezometers to the north of P 97-02 and P 97-03 are the result of groundwater also. The source for groundwater is apparently from the fault line beneath the Bessemer Dump (Klohn Leonoff, 1984). The water levels in P 97-01, P 97-04 and P 97-05 all peak around the same time period (see Table 4.8); which leads to the assumption that they are all related to the same process of groundwater discharge. The source of water in the fault zone is seemingly a part of a regional groundwater flow regime system that is recharged from areas north and east of the Bessemer Dump. These areas include the Tailings Pond and areas surrounding the Main Zone Pit.

7.2.3 Seepage Faces

The seepage face flow rates for the 1998 freshet are described in Section 4.3.3 and illustrated in Figure 4.17. The seeps all appear to peak around the same time period and do so before the waste rock dump piezometers since they are lower in elevation and will thus respond to the increases in the regional groundwater. All of the seeps on the south and southwest side of the Main Dump are apparently fed by regional groundwater in the exposed fractured rock in the southwest corner of the Main Dump and the Southern Tails Zone Pit.

The long duration peak in Seep 97-09 is the result of runoff water that is mixed with groundwater. The seepage collection consists of a long ditch in which runoff may easily enter. The runoff in this area may be prolonged due to trees lining the ditch which restrict the radiation necessary for snowmelt.

7.3 FEMWATER Results

The waste rock dump and surrounding area was modelled using FEMWATER and was described in Chapter 6. The system was initially modelled with a continuous glacial till layer beneath the waste rock and absence of any fault zones or groundwater discharge points. The model calculated a total of 46 mm/year of water over the area of the waste rock dump discharging from the seeps during the study period under a 10 % of total precipitation recharge rate to the regional system. This value is slightly above the infiltration rate of 36 mm/year which was applied to the surface of the waste rock dump.

The waste rock drainage flow discharged through the seeps can be calculated using the Getty Creek Pond water and the sump water (shown in Figure 5.24) subtracted from the weir flow (shown in Figure 5.25). This value is calculated at 318 mm/year of water over the study area. The results of the FEMWATER model suggests the waste rock dump behaves as a closed system that drains all of the water that has infiltrated. This does not appear correct since a low rate of groundwater discharge is computed from the waste rock dump if a continuous glacial till base is assumed to exist under the dump. The glacial till base acts as a liner which drains the water above it. The large discrepancy between the flow rates observed in the waste rock dump seepage faces and the infiltration through the soil cover and into the waste rock forms the key question for this study. The hypothesis which is proposed is that the large portion of seepage from the waste rock dump which can not be attributed to infiltration must be derived from regional groundwater discharge.

The magnitude of groundwater flow is contributed by geologic structure. The fault zone beneath Bessemer Dump described in Section 5.2.1 was identified as a source of groundwater discharge which may contribute to the water balance problem. Another source of groundwater discharge may be due to non-continuous glacial till beneath the Main Dump described in Section 5.2.6.

The waste rock dump was modelled with a discontinuous glacial till in the southwest portion of the Main Dump and a fault zone inserted beneath the Bessemer Dump. The model calculated 111 mm/year of water to drain from the waste rock dump with a 10 % of total precipitation recharge rate to the regional system. This value is still somewhat lower than the drainage measured from the dump. The model simulations were run for recharge rates of 20 and 30 % which generated seepage rates of 208 mm/year and 296 mm/year respectively. The 30 % regional recharge rate is a close match to the observed drainage and may represent actual field conditions.

Figure 7.3 illustrates the computed pressure heads in the waste rock dump for a regional recharge rate of 30 % of precipitation. The model shows that the highlands to the east and northwest are unsaturated while portions in the center of the map area are saturated. Bessemer Creek and the ARD collection ditches are in this area and represent constant head. High pressures were calculated south of the Main Dump near Getty Creek. These ambient factors match the field conditions as the Getty Creek area is known to be a groundwater discharge area. The existence of minor land slides in this area further reinforce that there is groundwater discharge.

Figure 7.4 shows the total head in the fractured rock which is the main flow avenue for the system. The open areas represent the open pits, where the media is non-continuous.

The flow in the fractured rock originates in the highlands to the east and near the Tailings Pond in the north. Groundwater passes through the waste rock dump area then into the lowland in the southwest valley. This plot shows that the waste rock dump may experience high amounts of groundwater discharge if there is a hydraulic link between the fractured rock and the waste rock. It should be recalled that a hydraulic link may exist between the Southern Tails Zone Pit, non-continuous glacial till areas and the fault zone in the Bessemer Dump area. Figure 7.5 shows the total head in the glacial till. The open areas represent the fault zone and the area of non-continuous glacial till.

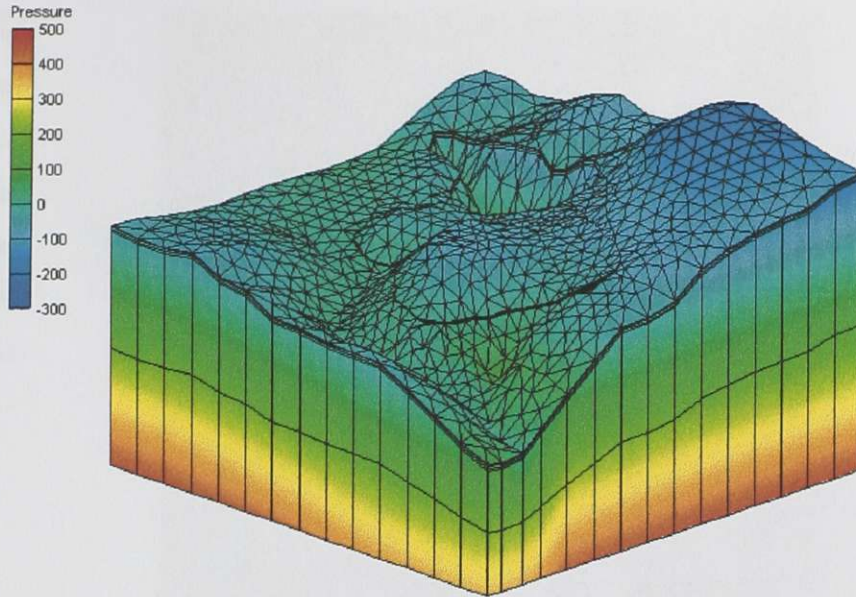


Figure 7.3 Computed pressure heads in the waste rock dump area for non-continuous till and 30 % of precipitation recharge rate.

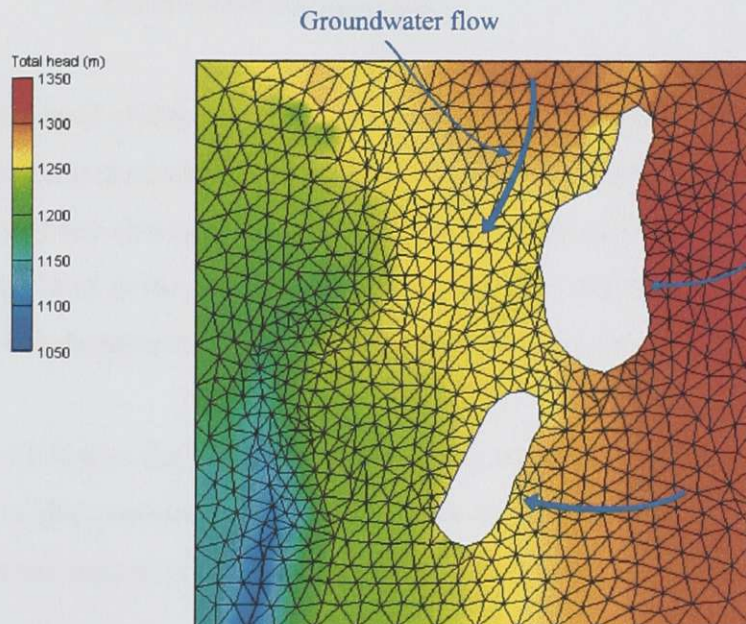


Figure 7.4 Total head in the fractured rock for non-continuous till and 30 % of precipitation recharge rate.

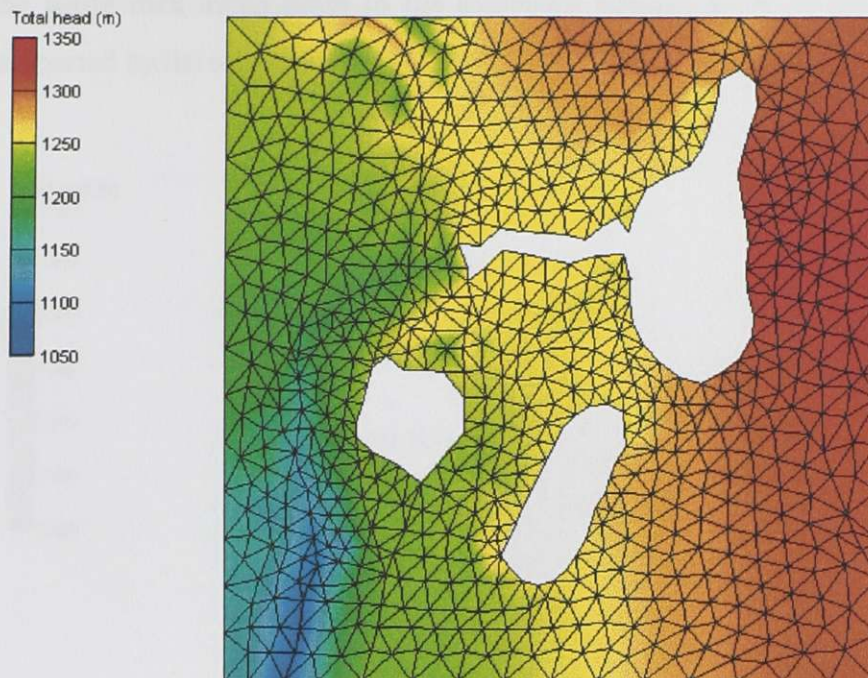


Figure 7.5 Total head in the glacial till for non-continuous till and 30 % of precipitation recharge rate.

The total head characteristics in the glacial till are similar to that in the fractured rock. The hydraulic conductivity in the glacial till is much lower than that of the fractured rock; thus, the fluxes through this media are small compared to the flow in the fractured rock. The total head in the glacial till is lower than the total head in the fractured rock in the waste rock dump area, which suggests an upward gradient and groundwater discharge.

Figure 7.6 shows the total head in the waste rock. Groundwater flow in the waste rock drains to the southwest. This corresponds to actual field conditions with the seepage faces in this region which is shown in Figure 7.6.

The fault line beneath the Bessemer Dump and the Southern Tails Zone Pit is partly responsible for the flow pattern predicted by FEMWATER. Groundwater discharge into

the waste rock dump flows to the southwest portion of the dump. This prediction is supported by the seepage faces that exist in the field.

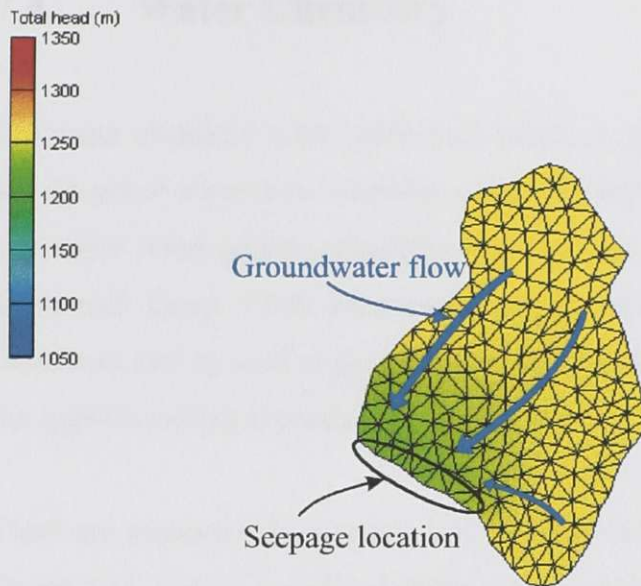


Figure 7.6 Total head in the waste rock for non-continuous till and 30 % of precipitation recharge rate.

Further evidence for verification includes the absence of a water table within the waste rock dump predicted by FEMWATER. Water contents in the waste rock were computed to be in the range of 2 % and 5 % which is close to the measured values seen in Figure 4.7.

The predicted flow characteristics for the mine site are in accordance to the hypothesis that significant amounts of groundwater discharge are discharging to the foundation of the waste rock dump. The flows in the fractured rock suggest that groundwater discharge occurs in the waste rock dump area. The flows within the waste rock shows

that the infiltrating water and groundwater discharge exits the waste rock dump in the southwest portion of the dump.

7.4 Water Chemistry

The water chemistry offers additional insight to groundwater flow paths. Sulfate, SO_4 , and the pH of water is an indication of the oxidation process of sulphide minerals. These two major water quality parameters may be used to track groundwater flow from the waste rock dump. Other parameters such as acidity, conductivity and total dissolved solids may also be used as an aid in describing groundwater flow and are also related to the sulphide oxidation process.

There are numerous components that facilitate the ARD collection system as shown in Figure 5.13. Getty Creek Pond drains the groundwater and surface water directly south of the Main Dump. The water quality typically exhibits a pH of about 3.1 suggesting that the water is a direct result of acid water in the waste rock dump. The FEMWATER modelling showed this area to be a groundwater discharge area which is recharged from areas in the waste rock dump. Acid water flow may be possible through the exposed fractured rock beneath the waste rock. The slightly higher pH values of 3.3 in the spring opposed to a pH of 3.0 in the winter suggests that the acid water is mixed with some amount of groundwater upon discharge in the Getty Creek area during the freshet. The sumps west of the Main Dump are similar in nature to the characteristics of Getty Creek Pond and are assumed to be part of the same hydrologic system.

The Surge Pond and ARD Pond contain typical acid water that is formed from a mixture of all of the drained water from the waste rock dump and the pumped water from the sumps and Getty Creek. The pH increases about 0.2 pH units during the spring freshet and during the fall rainy season. This contributes to the theory that fresh water enters the ARD collection system by means of runoff water and that groundwater enters the waste

rock dump. The peak in the spring is larger than that in the fall suggesting increased mixing effects of fresh water in the spring.

The Waterline Zone Pit is slightly acidic and has low heavy metal contents which is typical for a groundwater discharge. The slight acidity may be the result of minor sulphide oxidation on the pit walls conversely the Main Zone Pit is slightly basic with high sulfate concentrations which is due to water and sludge that is pumped from the water treatment process into the Main Zone Pit.

The creeks and diversion channels are typical in terms of pH and dissolved chemical constituents, which may be partly due to the high rates of precipitation and runoff. Major contamination to these water sources are not an issue.

The seepage discharge out of the waste rock is typical acid rock drainage, being low in pH and high in sulfate concentrations. Figure 7.7 illustrates the changes in conductivity with time. The three sample points indicate the summer of 1997, the fall of 1997 and the 1998 spring freshet.

Figure 7.7 shows that the conductivity, which is proportional to the total dissolved solids, decreases during the high infiltration periods, i.e. the fall rainy season and the spring freshet. This suggests that fresh groundwater enters into the dump during fall rains and spring freshet and feeds the seeps. This characteristic is in accordance to the proposed flow model in the southwest portion of the dump.

The water quality at the weir stations was also investigated. Weirs C7 and C11 contain typical acid water that is derived from a mixture of the water that exists in the collection ditch. They are similar to the collection ponds in that they exhibit slightly higher pH water in the fall rainy season and spring freshet. The water quality for the weir stations can be reviewed in Table 5.21.

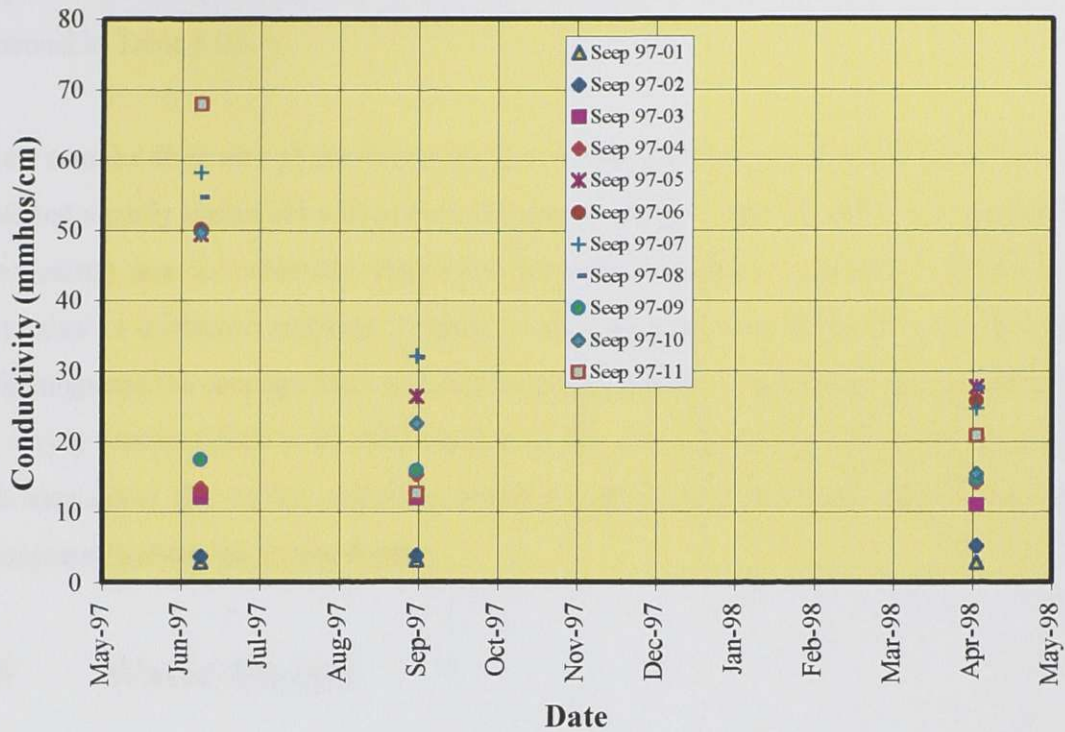


Figure 7.7 Conductivity of seepage discharge.

The Southern Tails (ST) weir exhibits pH values slightly acidic as well as high zinc levels. The pH is typically 6.3 and zinc concentrations of about 10 mg/L. The high concentrations of zinc exist due to the ability to be stable in near neutral pH waters. The Southern Tails weir is at the extreme southeast portion of the dump and drains directly out of the dump. The waste rock may be hydraulically connected to the fractured rock in the area of the Southern Tails Zone Pit. This flow is mostly groundwater that is derived from discharge out of the exposed fractured rock within the pit. The drainage that occurs out of this pit is caused by the spilling over of groundwater out of the pit.

The water quality in the regional piezometers is typical of groundwater, with slightly elevated levels of sulfate. The water in these piezometers originates in the local uplands to the west, thus having no acid water characteristics. The FEMWATER model also

supports this observation. The water quality for the regional piezometers may be reviewed in Table 5.23.

Water samples from two of the five waste rock dump piezometers (P 97-01 and P 97-03) exhibited slightly higher pH values than the seepage water. The pH of the seepage water was typically near 2.3 while the waste rock dump piezometers are closer to 2.9. This may occur due to additional sulphide oxidation occurring between the interior of the waste rock dump and the seepage face. The pH decreases and the conductivity increases during the spring freshet which is in contradiction to the characteristics of the seepage water. This may occur due to the oxidation which occurs directly above the piezometers and subsequent flushing the spring freshet.

7.5 Water Budget

The water balance approach described in Section 3.2.2 may be applied to the waste rock dump. The water balance equation is as follows:

$$\frac{Q_d t_d}{A_{wr}} = \gamma R + GD + B + \Delta S \quad [7.1]$$

- Where:
- Q_d = Flow in the collection ditch (L/s)
 - t_d = Time that the flow in the collection ditch occurs (s)
 - A_{wr} = Area of the waste rock dump (m^2)
 - γ = Runoff collection coefficient
 - R = Runoff (mm)
 - GD = Groundwater discharge component (mm)
 - B = Base flow (mm)
 - ΔS = Change in storage (mm)

The ARD flow on the left hand side of Equation [7.1] is calculated from the total weir flows minus the sump flow and the Getty Creek Pond flow. These components pump groundwater and surface water into the ARD collection facility. The waste rock dump flow rates for the study period are shown in Figure 7.8.

The average flow rate for the study period was 22.4 L/s and the total volume of acid rock drainage from the Waste rock dump was 705,960 m³/year. These figures translate into 318 mm of water per year over the area of the waste rock dump.

The runoff collection coefficient was determined using the runoff catchment areas shown in Figure 4.9. An area of 63.1 ha out of a total area of 222 ha (28.4 %) was not collected off the waste rock dump and was allowed to flow into the ARD collection system. Thus, the runoff collection coefficient is 0.284. The runoff for the study period was calculated, using SoilCover, at 94 mm (see Section 5.4.1.3). Hence, the runoff contribution to the ARD collection facility is computed to be 27 mm/year or 59,940 m³/year.

The net infiltration into the waste rock dump due to precipitation on the soil cover is the sum of groundwater seepage and the base flow. This was described in Section 3.2.2 and shown as Equation [7.2].

$$NI = B + GS \quad [7.2]$$

Where: NI = Net infiltration (mm)

GS = Groundwater seepage component (mm)

Groundwater seepage to the waste rock through the glacial till occurs as there is an upward gradient in the underlying fractured rock (i.e. as determined by the FEMWATER model). A net infiltration of 36 mm/year was calculated using SoilCover. Therefore, the base flow from precipitation on the soil cover that reports to the ARD collection ditches is equal to the net infiltration which was shown to be 36 mm/year or 79,920 m³ per year.

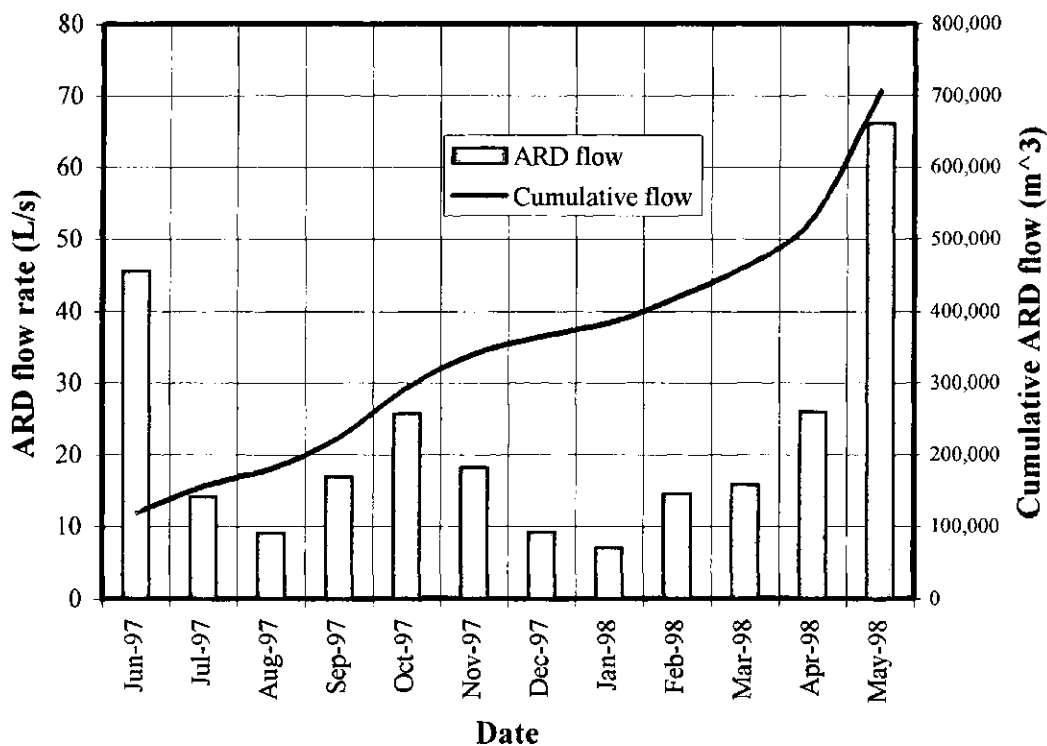


Figure 7.8 Acid rock drainage flow rates out of the waste rock dump.

The changes in storage for the dump based on a system that is slowly being drained was calculated as 3 mm or 6,660 m³ per year. The flow due to changes in storage can be reviewed in Figure 5.19.

The analysis and estimates provided above show that the runoff component, 27 mm/year (9 %), infiltration, 36 mm/year (11 %) and the changes in storage, 3 mm/year (1 %) account for approximately 21 % of the total 318 mm/year ARD flow. The remaining flow must be derived from groundwater discharge from the regional groundwater flow discharging to the foundation of the waste rock dump. This flow is computed to be 252 mm/year, which is a volume of 559,440 m³ or a flow rate of 17.7 L/s. The partitioning of the ARD flow is illustrated in Figure 7.9. The results of the FEMWATER modelling showed that for a regional recharge rate of 30 %, 193 mm/year, and a waste rock dump

infiltration rate of 5 %, 36 mm/year, of total precipitation, the discharge from the waste rock dump is equal to 296 mm/year which is similar to the value computed above.

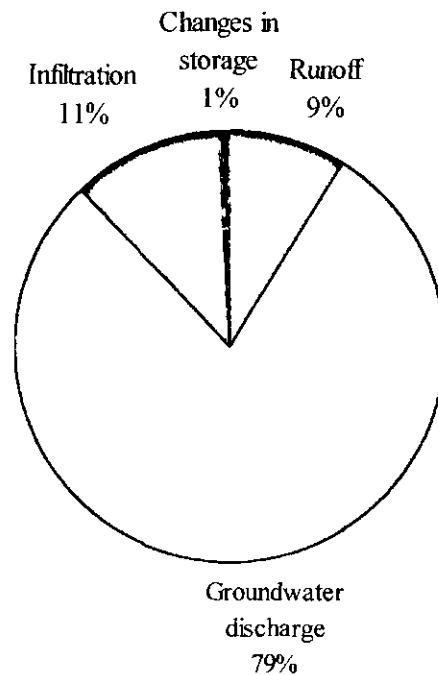


Figure 7.9 Water balance components of the acid rock drainage.

7.6 Summary

The proposed drainage quantities and characteristics are described in this chapter. The basis for this hypothesis is derived from the hydrological characterization. In other words the system may be explained based on the results from: geologic structure, topography, surface hydrology, groundwater and water chemistry. A flow model may be proposed with the comprehensive characterization of these elements.

Chapter 8 Summary and Conclusions

8.1 Summary of Thesis Objectives

The main objective of this thesis was to completely characterize the hydrologic system at Equity Silver Mine Ltd. The waste rock dump has experienced a water imbalance since the placement of the engineering soil cover system. The amount of acid rock drainage was approximately 50 % of total precipitation while only 6 % was infiltrating through the soil cover system. The water imbalance was evaluated by use of this hydrologic characterization technique proposed in this thesis.

This thesis included a general background and a brief description of the mine site. The history and general operation of the mine site is overviewed. A literature review provided an insight into some of the physical processes observed at the mine site. Previous studies pertaining to site characterization at the mine site were discussed. There have been numerous studies performed for Equity Silver Mine due to the high rate of sulphide oxidation and toe seepage flow rates. Literature pertaining to hydrogeologic and hydrologic characterization of waste rock dumps was also examined. The literature review showed that there is a lack of understanding regarding the quantity and characteristics of water flow through waste rock dumps. Some of the theoretical

processes that pertained to this study were examined. The hydrologic budget equation at the soil-atmosphere interface and for a regional system were considered. The formulation of three dimensional groundwater flow was used as an introduction to the formulae used by FEMWATER, the groundwater model used in this thesis. The method of solution used by FEMWATER was also considered. A two phase field program was initiated during this study. Piezometers were installed in the waste rock dump and the spring freshet was also characterized. The spring freshet characterization entailed the measurement of surface runoff, piezometer water level hydrograph and seepage flow rate hydrograph. The hydrologic characterization included the investigation of five main elements: geologic structure, topography, surface hydrology, groundwater and water chemistry. The computer modelling program is also investigated in terms of background, mesh generation, boundary conditions and run options. The spring freshet was analyzed on the basis of field observations and measurements. The groundwater flow model and the water chemistry was also analyzed. These observations reflect the use of the five elements of hydrological characterization.

The methodology used in this thesis follows the classic scientific method, which is observe, measure, explain and verify. The flows out of the waste rock were observed and a water balance problem seemed evident. The components of flow and other hydrological parameters were measured in this thesis study. With this information, an explanation of all of the hydrological components was proposed. The general hypothesis was that a significant portion of the acid rock drainage was due to groundwater discharge to the base of the waste rock dump. The hypothesis was verified by use of the hydrologic budget equation for a regional system and other water balance relationships. The water chemistry and spring freshet characteristics were also used to verify the hypothesis.

8.2 Conclusions

This section lists the conclusions that were drawn from this thesis study.

1. The waste rock dump produces a quantity of seepage equal to 50 % of the total precipitation (642 mm/year) which is approximately an order of magnitude greater than what was previously believed to infiltrate through the soil cover. Previous estimates of infiltration suggested a rate less than 5 % of total precipitation. This imbalance formed the main objective of this study.
2. A one year study period was investigated from June 1, 1997 until June 1, 1998. During this time 363 mm of water fell as rain and 279 mm of snow water equivalent; for a total of 642 mm of precipitation. The remaining hydrological components were calculated using SoilCover and are as follows: 15 % runoff, 51 % evapotranspiration and 4 % infiltration. Snow relocation was estimated at 15 % sublimation, 15 % mass transfer. The change in storage for this time period was -9 mm; thus the net infiltration was 6 % of total precipitation. This value agrees with lysimeters installed in the field.
3. The time for equilibrium with respect to change in storage due to drainage in the waste rock dump was determined to be 9 years. The waste rock experienced elevated rates of infiltration during uncovered conditions. The fluxes were rapidly decreased with the construction of the soil cover, hence the waste rock will continue to drain water for this period of time. However, the flow out of the waste rock at the current time was 3 mm/year (1 %) of the total acid rock drainage.

4. Sources of groundwater discharge were identified as: the exposed fractured rock within the Southern Tails Zone Pit, exposed fractured rock at the base of the southwest corner of the Main Dump and the fault zone beneath the Bessemer Dump. Regional groundwater recharge areas exist to the east and northeast of the waste rock dump and the Tailings Pond.
5. The hydrographs for the freshet seepage flow rates and waste rock dump piezometer levels are a response to increases in groundwater discharge from an area of exposed fractured rock in the recharge areas. The results from FEMWATER support the proposed hydrological flow system. Areas of groundwater recharge and discharge calculated by the model match field observations and the proposed hypothesis. The water chemistry also supports the proposed hydrological flow system. Characteristically, low values of conductivity and increases in pH during the fall rainy season and spring freshet indicate a process of dilution of the acid water. The dilution is the result of the mixing of fresh groundwater and acid water.
6. An analysis on the ARD collection ditch showed that a total of 705,960 m³ drained from the dump during the one year study period. This is an equivalent of 318 mm per year of water over the waste rock dump area. The runoff component was calculated from the hydrological characterization as 9 % of the total drainage from the waste rock dump. The infiltration contribution was analyzed in the same manner and accounts for 11 % of the total drainage. The change in storage in the waste rock was discussed previously and accounts for only 1 % of the drainage. The remaining 79 % is attributed to the groundwater discharge component.

8.3 Recommendations

The runoff and infiltration water entering the ARD collection system at the mine site is difficult to effectively reduce. This is partly due to the low contribution these components make. It would also be difficult to effectively reduce these components. The major problem regarding the acid rock drainage is the groundwater discharge into the waste rock. Unfortunately, changes to groundwater flow regime systems are extremely difficult to undertake; however, some recommendations are provided:

1. Conduct a more detailed study to ensure the infiltration rates through the soil cover are correct.
2. The groundwater in the fractured bedrock in the areas surrounding the Southern Tails Dump may be pumped with wells to lower the flux rate into the waste rock.
3. A form of cutoff wall or grouting of the fractured bedrock may also decrease discharge rates into the waste rock dump.
4. Pumping water from the Main Zone Pit may produce a groundwater sink and portions of the groundwater flow may be intercepted there.

8.4 Future Research

The objectives of this thesis project were met by characterizing the hydrological system of the waste rock dump at Equity Silver Mine. The methodology presented herein will act as an assessment tool to predict water movement through waste rock dumps. Even though objectives herein were met, some future research efforts may be made:

1. Continuous monitoring on toe seepage would be a useful tool in understanding the flow through the waste rock dump.
2. Monitoring of flow rates at the remaining runoff stations coupled with toe seepage flow rates may offer more insight to the surface hydrological components.
3. Measuring the water content profile throughout the waste rock would be beneficial and provide a more thorough understanding of the infiltration characteristics during rain events.
4. A regional groundwater investigation would be beneficial in terms of accurately describing the regional groundwater flow regime system. The FEMWATER model would then be able to expand to include this data.
5. The FEMWATER model could be used to predict the decrease in groundwater discharge through the waste rock dump for the following alternatives: pumping water out of the fractured bedrock, construction of a cutoff wall or lowering of the water table in the Main Zone Pit.

References

- Ayres, B.K., 1997. Field monitoring of soil-atmosphere fluxes through uranium mill tailings and natural surface soils at Cluff Lake, Saskatchewan. M.Sc. Thesis, Department of Civil Engineering, University of Saskatchewan, Saskatoon, Saskatchewan, Canada.
- Aziz, M., 1998. Personal communication with Mr. M. Aziz, Environmental Coordinator, Equity Silver Mines Limited
- Blyth, F.G.H. and de Freitas, M.H., 1984. A geology for engineers. Seventh edition. Edward Arnold (Publishers) Ltd., London, England.
- Church, B.N., 1971. Geology of the Owen Lake, Parrot Lakes and Goosly Lake area; BC Ministry of Energy, Mines and Petroleum Resources. Geology, exploration and mining in British Columbia 1970, pp. 119-128.
- Church, B.N. and Barakso, J.J., 1990. Geology, litho-geochemistry and mineralization in the Buck Creek area, British Columbia. Mineral Resources Division-Geological Survey Branch, Province of British Columbia, Ministry of Energy, Mines and Petroleum Resources, paper 1990-2.
- Cyr, J.B., Pease, R.B. and Schroeter, T.G., 1984. Geology and mineralization at the Equity Silver Mine. Economic geology. Volume 79. pp. 171-179.
- ECGL, 1998. Engineering Computer Graphics Laboratory. GMS 2.1 User manuals. Brigham Young University. Provo, Utah, USA.

- Equity Silver Mine Limited, 1997. Placer Dome Canada - Equity division environmental report - 1996. Aziz, M.
- Feasby, D.G., Tremblay, G.A., and Weatherell, C.J., 1997. A decade of technology improvement to the challenge of acid drainage – A Canadian perspective. Proceedings from the Fourth International Conference on Acid Rock Drainage. Vancouver, British Columbia, Canada.
- Fetter, C.W., 1993. Contaminant hydrogeology. Macmillan Publishing Company, New York, New York, USA.
- Frind, E.O., 1982. Simulation of long-term transient density-dependant transport in groundwater. Water Resources Research. Volume 5. pp. 73-78.
- Freeze, R.A. and Cherry, J.A., 1979. Groundwater. Prentice-Hall, Inc., New York, New York, USA.
- Germann, P. and Beven, K., 1985. Kinematic wave approximation to infiltration into soils with sorbing macro pores. Water Resources Research. Volume 21. Number 7. pp. 990-996.
- Ghomshei, M., Holmes, A., Denholm, E., Lawrence, R. and Carriou, T., 1997. Acid rock drainage from the Samatosum waste dump, British Columbia, Canada. Proceedings from the Fourth International Conference on Acid Rock Drainage. Vancouver, British Columbia, Canada.
- Golder Associates, 1983. Hydrogeological study. Hydrogeological investigation-Equity Silver Mines' property. Submitted to Equity Silver Mines Limited. Rawlings, G.E. and Guiton, R.

- Herasymuik, G.M., 1996. Hydrogeology of a sulphide waste rock dump. M.Sc. Thesis, Department of Civil Engineering, University of Saskatchewan, Saskatoon, Saskatchewan, Canada.
- Isabel, D., Gélines, P.J., Bourque, M., Nastev, M. and Précourt, S., 1997. Water budget for the waste rock dump at La Mine Doyon, Québec. Presented to CANMET. MEND Report # 1.14.2d. Report # GREGI-94-05.
- Istok, J. 1989. Groundwater modelling by the finite element method. American Geophysical Union. Washington, DC, USA.
- Jones, N.L., Richards, D.R. and Evans, R.A., 1995. A graphical environment for three dimensional finite element groundwater modelling. Proceedings of the International Symposium on Groundwater Management. pp. 373-378.
- López, D.L., Smith, L. and Beckie, R., 1997. Modelling water flow in waste rock piles using the kinematic wave theory. Proceedings from the Fourth International Conference on Acid Rock Drainage. Vancouver, British Columbia, Canada.
- Klohn Leonoff, 1984. Waste dump stability review. Submitted to Equity Silver Mines Limited. Bruce, I.G. and Olsen, M.T.
- Klohn Leonoff, 1990. Estimate of seepage from main zone pit. Submitted to Equity Silver Mines Limited. McCreadie, H. and Smith, H.R.
- Klohn Leonoff, 1991a. Acid mine drainage southwest waste dump area site investigation. Submitted to Equity Silver Mines Limited. Gill, R. and Smith, H.R.
- Klohn Leonoff, 1991b. Hydrogeological study. Submitted to Equity Silver Mines Limited. Emerson, D. and Smith, H.R.

- Klohn Leonoff, 1991c. Summary report, southern tails waste dump soil cover. Submitted to Equity Silver Mines Limited. Lam, David, J.S. and Rice, S.
- KPA Engineering Ltd., 1993. Hydrology study. Submitted to Equity Silver Mines Limited.
- Lin, Hsin-Chi, J. and Deliman, Patrick, N., 1995. Application of the GMS-FEMWATER model to two case studies involving flow and transport. Proceedings of the International Symposium on Groundwater Management. pp. 407-411.
- Lin, Hsin-Chi, J., Yeh, Gour-Tsyh, Cheng, Jing-Ru, Cheng, Hwai-Ping and Jones, Norman, L., 1997. FEMWATER: a three dimensional finite element computer model for simulating density-dependant flow and transport in variably saturated media. Users manual.
- Newman, L., 1994. Analysis performed by the University of Saskatchewan, Saskatoon, Saskatchewan, Canada.
- Newman, L.L., Herasymuik, G., Barbour, S.L., Fredlund, D.G. and Smith, T., 1997. The hydrogeology of waste rock dumps and a mechanism for unsaturated preferential flow. Proceedings from the Fourth International Conference on Acid Rock Drainage. Vancouver, British Columbia, Canada.
- O'Kane, M., 1995. Instrumentation and monitoring of an engineered soil cover system for acid generating mine waste. M.Sc. Thesis, Department of Civil Engineering, University of Saskatchewan, Saskatoon, Saskatchewan, Canada.
- Pomeroy, J.W. and Gray, D.M., 1995. Snowcover – accumulation, relocation and management. NHRI Science Report No. 7. Division of Hydrology, University of Saskatchewan, Saskatoon, Saskatchewan, Canada.

- SDS Drilling, 1997. Drilling contractors. Specialized Drilling Services, A division of Boart Longyear Inc., 1348 East Georgia Street, Vancouver, BC, V5L 2A8, Canada.
- Smith, L., Lopez, D.L., Beckie, R., Morin, K., Dawson, R. and Price, W., 1995. Hydrogeology of waste rock dumps. Final report to Department of Natural Resources Canada. Contract No.: 23440-4-1317/01-SQ.
- Stewart, J., 1991. Multivariable calculus. Second edition. Brooks/Cole Publishing Company. Pacific Grove, California, USA.
- SoilCover, 1997. SoilCover user's manual. Unsaturated Soils Group, Department of Civil Engineering, University of Saskatchewan, Canada.
- Swanson, D.A., 1995. Predictive modelling of moisture movement in engineered soil cover systems for acid generating mine waste. M.Sc. Thesis, Department of Civil Engineering, University of Saskatchewan, Saskatoon, Saskatchewan, Canada.
- Tipper, H.W. and Richards, T.A., 1976. Jurassic stratigraphy near Endako, British Columbia. Canadian Journal of Earth Sciences. Volume 7. pp. 1172-1178.
- Uwiera, M., 1998. Numerical simulation of brine migration in the vicinity of a potash mine. M.Sc. Thesis, Department of Geological Sciences, University of Saskatchewan, Saskatoon, Saskatchewan, Canada.
- Whiting, D.L., 1985. Surface and groundwater pollution and potential. In design of non-impounding mine waste dumps. Society of Mining Engineers of America Institute of Mining, Metallurgy and Petroleum Engineers Inc. New York, NY, USA. Page 91-97.

Wright Engineers Limited, 1976. Sam Goosly project. Houston, BC technical economic study. Volume II. Geology, ore reserves and mining.

Appendix A Detailed Water Quality Analysis

A.1 Introduction

The following detailed water quality analysis was performed by Analytical Service Laboratories Ltd. (ASL), located at 1988 Triumph Street, Vancouver, BC, V5L 1K5, phone: (604) 253-4188, fax: (604) 253-6700. ASL stated that the samples had to be diluted prior to being tested due to the complex nature of the samples (i.e. low pH and high solids content). Upon dilution a precipitate formed causing changes in the levels of some of the constituents, mainly sulfate. Thus the data had to be adjusted and the corrected form is included herein.

Table A.1 contains chemical data for the surface water. Table A.2, A.3 and A.4 contain chemical data of the waste rock dump seeps (Seep 97-01 to Seep 97-11). Table A.5 contains past chemical data of the waste rock dump seeps (S - 1, S - 2 and S - 3). Table A.6 contains chemical data for the ARD collection system.

Table A.1 Detailed chemical data for the surface water areas.

| | Surge | |
|--|--------------|---------------|
| | 05-Mar-91 | |
| | (mg/l) | (meq/l) |
| Physical tests | | |
| Conductivity (µmhos / cm) | N/A | N/A |
| pH | N/A | N/A |
| Total Dissolved Solids | N/A | N/A |
| Acidity and alkalinity | | |
| Acidity (as CaCO ₃) | 9920 | N/A |
| Alkalinity (as CaCO ₃) | <1.0 | N/A |
| Major anions | | |
| Bicarbonate, HCO ₃ ⁻ | N/A | N/A |
| Carbonate, CO ₃ ²⁻ | N/A | N/A |
| Bromide, Br ⁻ | N/A | N/A |
| Fluoride, F ⁻ | 0.13 | 0.01 |
| Chloride, Cl ⁻ | 900 | 25.39 |
| Sulfate, SO ₄ ²⁻ | 16200 | 337.28 |
| Nutrients | | |
| Ammonia Nitrogen, N | N/A | N/A |
| Nitrate Nitrogen, N | N/A | N/A |
| Nitrite Nitrogen, N | N/A | N/A |
| Total Dissolved Phosphate, P | 1.61 | N/A |
| Major cations | | |
| Aluminum, Al ³⁺ | 815 | 90.62 |
| Antimony, Sb ³⁺ | <0.20 | 0.00 |
| Arsenic, As ³⁺ | 6.94 | 0.28 |
| Barium, Ba ²⁺ | <0.010 | 0.00 |
| Beryllium, Be ²⁺ | 0.200 | 0.04 |
| Bismuth, Bi ³⁺ | <0.10 | 0.00 |
| Boron, B ³⁺ | <0.10 | 0.00 |
| Cadmium, Cd ²⁺ | 3.29 | 0.16 |
| Calcium, Ca ²⁺ | 319 | 15.92 |
| Chromium, Cr ³⁺ | <0.015 | 0.00 |
| Cobalt, Co ²⁺ | 5.27 | 0.18 |
| Copper, Cu ²⁺ | 119 | 3.75 |
| Iron, Fe ²⁺ | 1320 | 47.27 |
| Lead, Pb ²⁺ | <0.050 | 0.00 |
| Lithium, Li ⁺ | N/A | N/A |
| Magnesium, Mg ²⁺ | 1440 | 118.49 |
| Manganese, Mn ²⁺ | 345 | 12.56 |
| Molybdenum, Mo ⁶⁺ | 0.497 | 0.03 |
| Nickel, Ni ²⁺ | 9.03 | 0.31 |
| Phosphorous, P ⁵⁺ | 47.7 | 7.70 |
| Potassium, K ⁺ | N/A | N/A |
| Selenium, Se ⁴⁺ | <0.20 | 0.00 |
| Silicon, Si ⁴⁺ | 36.7 | 5.23 |
| Silver, Ag ⁺ | <0.015 | 0.00 |
| Sodium, Na ⁺ | N/A | N/A |
| Strontium, Sr ²⁺ | 3.47 | 0.08 |
| Thallium, Tl ⁺ | N/A | N/A |
| Tin, Sn ⁴⁺ | N/A | N/A |
| Titanium, Ti ⁴⁺ | N/A | N/A |
| Vanadium, V ³⁺ | <0.030 | 0.00 |
| Zinc, Zn ²⁺ | 301 | 9.21 |
| Major cations | 4772 | 311.82 |
| Major anions | 17100 | 362.67 |
| Total | 21872 | N/A |
| Ion balance difference | | -7.54% |
| TDS difference | | N/A |

Table A.3 Detailed chemical data for the waste rock dump seeps (Seep 97-05 to Seep 97-08).

| | Seep 97-05 | | | | Seep 97-06 | | | | Seep 97-07 | | | | Seep 97-08 | | | |
|--------------------------------------|---------------------|----------------------|---------------------|----------------------|---------------------|----------------------|---------------------|----------------------|---------------------|---------------------|----------------------|---------------------|----------------------|---------------------|---------------------|----------------------|
| | 25-Jun-97 (mg/l) | 16-Apr-98 (meq/l) | 16-Apr-98 (mg/l) | 25-Jun-97 (meq/l) | 25-Jun-97 (mg/l) | 16-Apr-98 (meq/l) | 16-Apr-98 (mg/l) | 25-Jun-97 (meq/l) | 16-Apr-98 (mg/l) | 25-Jun-97 (mg/l) | 16-Apr-98 (meq/l) | 16-Apr-98 (mg/l) | 25-Jun-97 (meq/l) | 16-Apr-98 (mg/l) | 25-Jun-97 (mg/l) | 16-Apr-98 (meq/l) |
| Physical tests | | | | | | | | | | | | | | | | |
| Conductivity ($\mu\text{mhos/cm}$) | 49300 | N/A | N/A | N/A | 50100 | N/A | N/A | N/A | 58100 | N/A | N/A | N/A | 54600 | N/A | N/A | N/A |
| pH | 2.38 | N/A | N/A | N/A | 2.36 | N/A | N/A | N/A | 2.25 | N/A | N/A | N/A | 2.26 | N/A | N/A | N/A |
| Total Dissolved Solids | 71800 | N/A | 112000 | N/A | 75100 | N/A | 97000 | N/A | 96300 | N/A | 80300 | N/A | 77100 | N/A | 86200 | N/A |
| Acidity and alkalinity | | | | | | | | | | | | | | | | |
| Acidity (as CaCO_3) | 40200 | N/A | 50500 | N/A | 42800 | N/A | 45400 | N/A | 56200 | N/A | 43800 | N/A | 42400 | N/A | 36300 | N/A |
| Alkalinity (as CaCO_3) | <1 | N/A | <1 | N/A | <1 | N/A | <1 | N/A | <1 | N/A | <1 | N/A | <1 | N/A | <1 | N/A |
| Major anions | | | | | | | | | | | | | | | | |
| Bicarbonate, HCO_3^- | <1 | 0.00 | - | 0.00 | <1 | 0.00 | - | 0.00 | <1 | 0.00 | - | 0.00 | <1 | 0.00 | - | 0.00 |
| Carbonate, CO_3^{2-} | <1 | 0.00 | - | 0.00 | <1 | 0.00 | - | 0.00 | <1 | 0.00 | - | 0.00 | <1 | 0.00 | - | 0.00 |
| Chloride, Cl^- | 6.2 | 0.17 | 12.5 | 0.35 | 7.3 | 0.21 | 11.5 | 0.32 | 14.7 | 0.41 | 13.7 | 0.39 | 9.3 | 0.26 | 16.4 | 0.46 |
| Sulfate, SO_4^{2-} | 55900 | 1163.81 | 47700 | 993.09 | 57500 | 1197.12 | 39700 | 826.54 | 68600 | 1428.22 | 39300 | 818.21 | 65000 | 1353.27 | 48300 | 1005.58 |
| Major cations | | | | | | | | | | | | | | | | |
| Aluminum, Al^{3+} | 4200 | 466.99 | 4710 | 523.69 | 4410 | 490.34 | 4420 | 491.45 | 5450 | 605.97 | 3890 | 432.52 | 4180 | 464.76 | 4100 | 455.87 |
| Antimony, Sb^{3+} | <2 | 0.00 | 2 | 0.05 | <2 | 0.00 | <2 | 0.00 | 0.783 | 0.02 | 1 | 0.02 | 0.184 | 0.00 | <2 | 0.00 |
| Arsenic, As^{3+} | 33 | 1.32 | 90 | 3.60 | 35 | 1.40 | 87 | 3.48 | 59 | 2.36 | 55 | 2.20 | 24 | 0.96 | 34 | 1.36 |
| Barium, Ba^{2+} | <0.1 | 0.00 | <0.05 | 0.00 | 0.1 | 0.00 | <0.1 | 0.00 | <0.1 | 0.00 | <0.05 | 0.00 | <0.1 | 0.00 | <0.1 | 0.00 |
| Beryllium, Be^{2+} | 0.53 | 0.12 | 0.55 | 0.12 | 0.55 | 0.12 | 0.5 | 0.11 | 0.71 | 0.16 | 0.48 | 0.11 | 0.64 | 0.14 | 0.57 | 0.13 |
| Bismuth, Bi^{3+} | 2 | 0.03 | <0.5 | 0.00 | 1 | 0.01 | 2 | 0.03 | 1 | 0.01 | <0.5 | 0.00 | 2 | 0.03 | 2 | 0.03 |
| Boron, B^{3+} | 0 | 0.00 | <0.5 | 0.00 | <1 | 0.00 | <1 | 0.00 | <1 | 0.00 | <0.5 | 0.00 | <1 | 0.00 | <1 | 0.00 |
| Cadmium, Cd^{2+} | 3.54 | 0.18 | 3.34 | 0.17 | 3.66 | 0.18 | 2.47 | 0.12 | 4.34 | 0.22 | 2.94 | 0.15 | 4.72 | 0.24 | 3.76 | 0.19 |
| Calcium, Ca^{2+} | 517 | 25.80 | 500 | 24.95 | 528 | 26.35 | 476 | 23.75 | 513 | 25.60 | 442 | 22.06 | 540 | 26.95 | 549 | 27.40 |
| Chromium, Cr^{3+} | 1.3 | 0.08 | 2.34 | 0.14 | 1.4 | 0.08 | 2.2 | 0.13 | 2.1 | 0.12 | 1.87 | 0.11 | 1.2 | 0.07 | 1.5 | 0.09 |
| Cobalt, Co^{2+} | 19.1 | 0.65 | 20.4 | 0.70 | 19.6 | 0.67 | 19.8 | 0.67 | 23.6 | 0.80 | 16.7 | 0.57 | 20.2 | 0.69 | 18.7 | 0.64 |
| Copper, Cu^{2+} | 403 | 12.68 | 474 | 14.92 | 419 | 13.19 | 431 | 13.56 | 609 | 19.17 | 422 | 13.28 | 406 | 12.78 | 356 | 11.20 |
| Iron, Fe^{2+} | 6630 | 237.43 | 9680 | 346.66 | 6880 | 246.39 | 9330 | 334.13 | 7780 | 278.62 | 691 | 2.47 | 3790 | 135.73 | 4810 | 172.26 |
| Lead, Pb^{2+} | <0.5 | 0.00 | <0.3 | 0.00 | <0.5 | 0.00 | <0.5 | 0.00 | <0.5 | 0.00 | <0.3 | 0.00 | <0.5 | 0.00 | <0.5 | 0.00 |
| Lithium, Li^+ | 4.2 | 0.61 | 4.27 | 0.62 | 4.4 | 0.63 | 3.9 | 0.56 | 5.8 | 0.84 | 4.06 | 0.58 | 5.8 | 0.84 | 5.5 | 0.79 |
| Magnesium, Mg^{2+} | 2700 | 222.18 | 2600 | 213.95 | 2790 | 229.58 | 2340 | 192.55 | 3760 | 309.40 | 2510 | 206.54 | 4730 | 389.22 | 3960 | 325.86 |
| Manganese, Mn^{2+} | 411 | 14.96 | 373 | 13.58 | 421 | 15.33 | 345 | 12.56 | 506 | 18.42 | 328 | 11.94 | 594 | 21.62 | 510 | 18.57 |
| Molybdenum, Mo^{6+} | <0.3 | 0.00 | <0.2 | 0.00 | <0.3 | 0.00 | <0.3 | 0.00 | <0.3 | 0.00 | <0.2 | 0.00 | <0.3 | 0.00 | <0.3 | 0.00 |
| Nickel, Ni^{2+} | 47.6 | 1.62 | 49 | 1.67 | 49.2 | 1.68 | 46.1 | 1.57 | 60.6 | 2.06 | 41.3 | 1.41 | 51.6 | 1.76 | 44.3 | 1.51 |
| Phosphorous, P^{5+} | 168 | 27.12 | 344 | 55.53 | 180 | 29.06 | 320 | 51.66 | 284 | 45.85 | 228 | 36.81 | 135 | 21.79 | 149 | 24.05 |
| Potassium, K^+ | <20 | 0.00 | <10 | 0.00 | <20 | 0.00 | <20 | 0.00 | <20 | 0.00 | <10 | 0.00 | <20 | 0.00 | <20 | 0.00 |
| Selenium, Se^{4+} | <2 | 0.00 | <1 | 0.00 | <2 | 0.00 | <2 | 0.00 | <2 | 0.00 | <1 | 0.00 | <2 | 0.00 | <2 | 0.00 |
| Silicon, Si^{4+} | 68.8 | 9.80 | 63.3 | 9.02 | 78.4 | 11.17 | 61.9 | 8.82 | 75.1 | 10.70 | <0.3 | 0.00 | 95.4 | 13.59 | 97.8 | 13.93 |
| Silver, Ag^+ | <0.1 | 0.00 | 0.1 | 0.00 | <0.1 | 0.00 | 0.1 | 0.00 | <0.1 | 0.00 | 0.08 | 0.00 | <0.1 | 0.00 | <0.1 | 0.00 |
| Sodium, Na^+ | <20 | 0.00 | <10 | 0.00 | <20 | 0.00 | <20 | 0.00 | <20 | 0.00 | <10 | 0.00 | <20 | 0.00 | <20 | 0.00 |
| Strontium, Sr^{2+} | 0.34 | 0.01 | 1.06 | 0.02 | 0.51 | 0.01 | 1.13 | 0.03 | 0.74 | 0.02 | 0.95 | 0.02 | 0.26 | 0.01 | 0.37 | 0.01 |
| Thallium, Tl^+ | 3 | 0.01 | 3 | 0.01 | 2 | 0.01 | <5 | 0.00 | 3 | 0.01 | 3 | 0.01 | 3 | 0.01 | <5 | 0.00 |
| Tin, Sn^{4+} | <0.3 | 0.00 | <0.2 | 0.00 | <0.3 | 0.00 | <0.3 | 0.00 | <0.3 | 0.00 | <0.2 | 0.00 | <0.3 | 0.00 | <0.3 | 0.00 |
| Titanium, Ti^{4+} | <0.1 | 0.00 | 0.08 | 0.01 | 0.2 | 0.02 | 0.1 | 0.00 | <0.1 | 0.00 | 0.1 | 0.00 | <0.1 | 0.00 | <0.1 | 0.00 |
| Vanadium, V^{5+} | 3.5 | 0.34 | 3.8 | 0.37 | 3.4 | 0.33 | 3.1 | 0.30 | 2.9 | 0.28 | 2.6 | 0.26 | 1.8 | 0.18 | 1.9 | 0.19 |
| Zinc, Zn^{2+} | 403 | 12.33 | 345 | 10.55 | 413 | 12.63 | 324 | 9.91 | 492 | 15.05 | 312 | 9.54 | 537 | 16.42 | 459 | 14.04 |
| Major cations | 15619 | 1034.25 | 19269 | 1220.32 | 16240 | 1079.17 | 18216 | 1145.40 | 19634 | 1335.68 | 8331 | 740.60 | 15123 | 1107.79 | 15103 | 1068.10 |
| Major anions | 55906 | 1163.99 | 47713 | 993.44 | 57507 | 1197.33 | 39712 | 826.86 | 68615 | 1428.64 | 39314 | 818.59 | 65009 | 1353.53 | 48316 | 1006.05 |
| Total | 71525 | N/A | 66982 | N/A | 71748 | N/A | 57928 | N/A | 88248 | N/A | 47645 | N/A | 80132 | N/A | 63420 | N/A |
| Ion balance difference | -5.90% | | 10.25% | | -5.19% | | 16.15% | | -3.36% | | -5.00% | | -9.98% | | 2.99% | |
| TDS difference | 0.38% | | 50.30% | | 1.82% | | 50.44% | | 8.73% | | 51.05% | | 3.86% | | 30.45% | |

Table A.4 Detailed chemical data for the waste rock dump seeps (Seep 97-09 to Seep 97-11).

| | Seep 97-09 | | | | Seep 97-10 | | | | Seep 97-11 | | | |
|--|------------|---------|-----------|---------|------------|---------|-----------|---------|------------|---------|-----------|---------|
| | 25-Jun-97 | | 16-Apr-98 | | 25-Jun-97 | | 16-Apr-98 | | 25-Jun-97 | | 16-Apr-98 | |
| | (mg/l) | (meq/l) | (mg/l) | (meq/l) | (mg/l) | (meq/l) | (mg/l) | (meq/l) | (mg/l) | (meq/l) | (mg/l) | (meq/l) |
| Physical tests | | | | | | | | | | | | |
| Conductivity (μ mhos/cm) | 17300 | N/A | N/A | N/A | 49600 | N/A | N/A | N/A | 67900 | N/A | N/A | N/A |
| pH | 2.55 | N/A | N/A | N/A | 2.08 | N/A | N/A | N/A | 2.08 | N/A | N/A | N/A |
| Total Dissolved Solids | 34400 | N/A | 27400 | N/A | 97500 | N/A | 58900 | N/A | 128000 | N/A | 68300 | N/A |
| Acidity and alkalinity | | | | | | | | | | | | |
| Acidity (as CaCO ₃) | 17900 | N/A | 15100 | N/A | 62900 | N/A | 32100 | N/A | 83100 | N/A | 45900 | N/A |
| Alkalinity (as CaCO ₃) | <1 | N/A | <1 | N/A | <1 | N/A | <1 | N/A | <1 | N/A | <1 | N/A |
| Major anions | | | | | | | | | | | | |
| Bicarbonate, HCO ₃ ⁻ | <1 | 0.00 | - | 0.00 | <1 | 0.00 | - | 0.00 | <1 | 0.00 | - | 0.00 |
| Carbonate, CO ₃ ²⁻ | <1 | 0.00 | - | 0.00 | <1 | 0.00 | - | 0.00 | <1 | 0.00 | - | 0.00 |
| Chloride, Cl ⁻ | 7.7 | 0.22 | 10 | 0.28 | 22.4 | 0.63 | 10.1 | 0.28 | 15.6 | 0.44 | 11.5 | 0.32 |
| Sulfate, SO ₄ ²⁻ | 24900 | 518.41 | 17200 | 358.10 | 71300 | 1484.43 | 35700 | 743.26 | 97800 | 2036.15 | 39800 | 828.62 |
| Major cations | | | | | | | | | | | | |
| Aluminum, Al ³⁺ | 1570 | 174.56 | 1360 | 151.21 | 3880 | 431.41 | 2120 | 235.72 | 7660 | 851.69 | 2850 | 316.88 |
| Antimony, Sb ³⁺ | <1 | 0.00 | <1 | 0.00 | 3 | 0.07 | <2 | 0.00 | 3 | 0.07 | <2 | 0.00 |
| Arsenic, As ³⁺ | 3 | 0.12 | 4 | 0.16 | 234 | 9.37 | 83 | 3.32 | 166 | 6.65 | 81 | 3.24 |
| Barium, Ba ²⁺ | <0.05 | 0.00 | 0.09 | 0.00 | <0.1 | 0.00 | 1.2 | 0.02 | <0.1 | 0.00 | <0.1 | 0.00 |
| Beryllium, Be ²⁺ | 0.27 | 0.06 | 0.2 | 0.04 | 0.45 | 0.10 | 0.24 | 0.05 | 0.83 | 0.18 | 0.29 | 0.06 |
| Bismuth, Bi ³⁺ | 0.6 | 0.01 | 0.8 | 0.01 | <1 | 0.00 | <1 | 0.00 | <1 | 0.00 | 2 | 0.03 |
| Boron, B ³⁺ | <0.5 | 0.00 | <0.5 | 0.00 | <1 | 0.00 | <1 | 0.00 | <1 | 0.00 | <1 | 0.00 |
| Cadmium, Cd ²⁺ | 3.5 | 0.17 | 2.43 | 0.12 | 2.3 | 0.11 | 0.96 | 0.05 | 4.4 | 0.22 | 1.2 | 0.06 |
| Calcium, Ca ²⁺ | 430 | 21.46 | 311 | 15.52 | 515 | 25.70 | 356 | 17.77 | 553 | 27.60 | 414 | 20.66 |
| Chromium, Cr ³⁺ | 0.32 | 0.02 | 0.35 | 0.02 | 3.3 | 0.19 | 1.7 | 0.10 | 3.8 | 0.22 | 2.1 | 0.12 |
| Cobalt, Co ²⁺ | 8.75 | 0.30 | 7.36 | 0.25 | 19.2 | 0.65 | 10.1 | 0.34 | 31.5 | 1.07 | 12.8 | 0.44 |
| Copper, Cu ²⁺ | 154 | 4.85 | 133 | 4.19 | 835 | 26.28 | 355 | 11.17 | 927 | 29.18 | 335 | 10.54 |
| Iron, Fe ²⁺ | 1050 | 37.60 | 1120 | 40.11 | 13600 | 487.04 | 7320 | 262.14 | 13200 | 472.72 | 9780 | 350.24 |
| Lead, Pb ²⁺ | <0.2 | 0.00 | <0.3 | 0.00 | <0.5 | 0.00 | <0.5 | 0.00 | <0.5 | 0.00 | <0.5 | 0.00 |
| Lithium, Li ⁺ | 2.29 | 0.33 | 1.72 | 0.25 | 4.5 | 0.65 | 2.7 | 0.39 | 8.7 | 1.25 | 3.5 | 0.50 |
| Magnesium, Mg ²⁺ | 2470 | 203.25 | 1820 | 149.76 | 2200 | 181.03 | 1110 | 91.34 | 4030 | 331.62 | 1430 | 117.67 |
| Manganese, Mn ²⁺ | 378 | 13.76 | 283 | 10.30 | 285 | 10.38 | 141 | 5.13 | 500 | 18.20 | 175 | 6.37 |
| Molybdenum, Mo ⁶⁺ | <0.1 | 0.00 | <0.2 | 0.00 | <0.3 | 0.00 | <0.3 | 0.00 | <0.3 | 0.00 | <0.3 | 0.00 |
| Nickel, Ni ²⁺ | 18.4 | 0.63 | 15.3 | 0.52 | 49.6 | 1.69 | 25.5 | 0.87 | 80.8 | 2.75 | 31.9 | 1.09 |
| Phosphorous, P ³⁺ | 27 | 4.36 | 31 | 5.00 | 389 | 62.80 | 165 | 26.64 | 482 | 77.81 | 504 | 81.36 |
| Potassium, K ⁺ | <10 | 0.00 | <10 | 0.00 | <20 | 0.00 | <20 | 0.00 | <20 | 0.00 | <40 | 0.00 |
| Selenium, Se ⁴⁺ | <1 | 0.00 | <1 | 0.00 | <2 | 0.00 | <2 | 0.00 | <2 | 0.00 | <4 | 0.00 |
| Silicon, Si ¹⁺ | 75.7 | 10.78 | 1 | 0.14 | 84.1 | 11.98 | <0.5 | 0.00 | 86.3 | 12.29 | <1 | 0.00 |
| Silver, Ag ⁺ | <0.05 | 0.00 | <0.05 | 0.00 | <0.1 | 0.00 | 0.2 | 0.00 | <0.1 | 0.00 | 0.3 | 0.00 |
| Sodium, Na ⁺ | <10 | 0.00 | <10 | 0.00 | <20 | 0.00 | <20 | 0.00 | <20 | 0.00 | <40 | 0.00 |
| Strontium, Sr ²⁺ | 1.09 | 0.02 | 0.98 | 0.02 | 3.05 | 0.07 | 2.5 | 0.06 | 1.78 | 0.04 | 0.6 | 0.01 |
| Thallium, Tl ⁺ | 0.7 | 0.00 | <1 | 0.00 | 3 | 0.01 | <2 | 0.00 | 5 | 0.02 | <4 | 0.00 |
| Tin, Sn ⁴⁺ | <0.1 | 0.00 | <0.2 | 0.00 | <0.3 | 0.00 | <0.3 | 0.00 | <0.3 | 0.00 | <0.6 | 0.00 |
| Titanium, Ti ⁴⁺ | <0.05 | 0.00 | 0.23 | 0.02 | 0.1 | 0.01 | 1.6 | 0.00 | 0.2 | 0.02 | <0.2 | 0.00 |
| Vanadium, V ⁵⁺ | <0.1 | 0.00 | <0.2 | 0.00 | 2.1 | 0.21 | 1 | 0.10 | 4.3 | 0.42 | 6.3 | 0.62 |
| Zinc, Zn ²⁺ | 342 | 10.46 | 250 | 7.65 | 237 | 7.25 | 117 | 3.58 | 478 | 14.62 | 717 | 21.93 |
| Major cations | 6536 | 482.75 | 5342 | 385.31 | 22350 | 1257.00 | 11815 | 658.79 | 28227 | 1848.65 | 16347 | 931.84 |
| Major anions | 24908 | 518.62 | 17210 | 358.38 | 71322 | 1485.07 | 35710 | 743.54 | 97816 | 2036.59 | 39812 | 828.94 |
| Total | 31443 | N/A | 22552 | N/A | 93672 | N/A | 47525 | N/A | 126042 | N/A | 56158 | N/A |
| Ion balance difference | | -3.58% | | 3.62% | | -8.32% | | -6.04% | | -4.84% | | 5.84% |
| TDS difference | | 8.98% | | 19.41% | | 4.00% | | 21.38% | | 1.54% | | 19.51% |

Table A.5 Detailed chemical data for the waste rock dump seeps (S - 1, S - 2 and S - 3).

| | S - 1 | | | | S - 2 | | | | S - 3 | |
|--------------------------------------|---------------|----------------|---------------|---------------|---------------|----------------|---------------|----------------|---------------|----------------|
| | 05-Mar-91 | | 27-Oct-95 | | 05-Mar-91 | | 27-Oct-95 | | 27-Oct-95 | |
| | (mg/l) | (meq/l) | (mg/l) | (meq/l) | (mg/l) | (meq/l) | (mg/l) | (meq/l) | (mg/l) | (meq/l) |
| Physical tests | | | | | | | | | | |
| Conductivity ($\mu\text{mhos/cm}$) | N/A | N/A | 26000 | N/A | N/A | N/A | 34300 | N/A | 28300 | N/A |
| pH | N/A | N/A | 2.53 | N/A | N/A | N/A | 2.53 | N/A | 2.61 | N/A |
| Total Dissolved Solids | N/A | N/A | 67000 | N/A | N/A | N/A | 76400 | N/A | 85400 | N/A |
| Acidity and alkalinity | | | | | | | | | | |
| Acidity (as CaCO_3) | 63700 | N/A | 30000 | N/A | 63700 | N/A | 35700 | N/A | 46200 | N/A |
| Alkalinity (as CaCO_3) | <1.0 | N/A | N/A | N/A | <1.0 | N/A | N/A | N/A | N/A | N/A |
| Major anions | | | | | | | | | | |
| Bicarbonate, HCO_3^- | N/A | N/A | N/A | N/A | N/A | N/A | N/A | N/A | N/A | N/A |
| Carbonate, CO_3^{2-} | N/A | N/A | N/A | N/A | N/A | N/A | N/A | N/A | N/A | N/A |
| Bromide, Br^- | N/A | N/A | <10 | 0.00 | N/A | N/A | <10 | 0.00 | <10 | 0.00 |
| Fluoride, F^- | <0.02 | 0.00 | 90 | 4.74 | <0.02 | 0.00 | 112 | 5.90 | 127 | 6.68 |
| Chloride, Cl^- | 1900 | 53.59 | 60 | 1.69 | 2500 | 70.52 | 100 | 2.82 | 50 | 1.41 |
| Sulfate, SO_4^{2-} | 87500 | 1821.71 | 39700 | 826.54 | 121000 | 2519.16 | 46600 | 970.19 | 48400 | 1007.67 |
| Nutrients | | | | | | | | | | |
| Ammonia Nitrogen, N | N/A | N/A | 0.301 | N/A | N/A | N/A | 0.618 | N/A | 0.173 | N/A |
| Nitrate Nitrogen, N | N/A | N/A | 0.040 | N/A | N/A | N/A | <1 | N/A | <1 | N/A |
| Nitrite Nitrogen, N | N/A | N/A | 0.008 | N/A | N/A | N/A | 0.007 | N/A | 0.031 | N/A |
| Total Dissolved Phosphate, P | 418 | N/A | 102 | N/A | 0.160 | N/A | 89.0 | N/A | 270 | N/A |
| Major cations | | | | | | | | | | |
| Aluminum, Al^{3+} | 5280 | 587.07 | 3130 | 348.02 | 8060 | 896.17 | 4720 | 524.80 | 3500 | 389.15 |
| Antimony, Sb^{3+} | 3.1 | 0.08 | <4.0 | 0.00 | 10.2 | 0.25 | <4.0 | 0.00 | <4.0 | 0.00 |
| Arsenic, As^{3+} | 190 | 7.61 | 34.2 | 1.37 | 424 | 16.98 | 58.6 | 2.35 | 25.5 | 1.02 |
| Barium, Ba^{2+} | <0.10 | 0.00 | <0.20 | 0.00 | <0.10 | 0.00 | <0.20 | 0.00 | <0.20 | 0.00 |
| Beryllium, Be^{2+} | 0.82 | 0.18 | 0.47 | 0.10 | 1.03 | 0.23 | 0.6 | 0.13 | 0.60 | 0.13 |
| Bismuth, Bi^{3+} | <1.0 | 0.00 | 4.7 | 0.07 | <1.0 | 0.00 | 3.8 | 0.05 | 5.5 | 0.08 |
| Boron, B^{3+} | <1.0 | 0.00 | <2.0 | 0.00 | <1.0 | 0.00 | <2.0 | 0.00 | <2.0 | 0.00 |
| Cadmium, Cd^{2+} | 10.1 | 0.50 | 3.96 | 0.20 | 12.8 | 0.64 | 3.61 | 0.18 | 5.81 | 0.29 |
| Calcium, Ca^{2+} | 429 | 21.41 | 482 | 24.05 | 382 | 19.06 | 541 | 27.00 | 555 | 27.70 |
| Chromium, Cr^{3+} | 0.22 | 0.01 | 1.01 | 0.06 | 1.05 | 0.06 | 1.78 | 0.10 | 0.99 | 0.06 |
| Cobalt, Co^{2+} | 26.7 | 0.91 | 16.6 | 0.57 | 39.8 | 1.36 | 23.3 | 0.79 | 20.1 | 0.68 |
| Copper, Cu^{2+} | 1220 | 38.40 | 336 | 10.58 | 1910 | 60.11 | 576 | 18.13 | 336 | 10.58 |
| Iron, Fe^{2+} | 10800 | 386.77 | 3430 | 122.84 | 16800 | 601.64 | 7570 | 271.10 | 4320 | 154.71 |
| Lead, Pb^{2+} | <0.50 | 0.00 | <1.00 | 0.00 | <0.50 | 0.00 | <1.00 | 0.00 | <1.00 | 0.00 |
| Lithium, Li^+ | N/A | N/A | 4.10 | 0.59 | N/A | N/A | 4.07 | 0.59 | 4.78 | 0.69 |
| Magnesium, Mg^{2+} | 5680 | 467.39 | 3740 | 307.76 | 5600 | 460.81 | 2980 | 245.22 | 4930 | 405.68 |
| Manganese, Mn^{2+} | 691 | 25.16 | 519 | 18.89 | 688 | 25.05 | 471 | 17.15 | 708 | 25.77 |
| Molybdenum, Mo^{6+} | <0.30 | 0.00 | <0.60 | 0.00 | <0.30 | 0.00 | <0.60 | 0.00 | <0.60 | 0.00 |
| Nickel, Ni^{2+} | 66.9 | 2.28 | 40.2 | 1.37 | 103 | 3.51 | 55.9 | 1.90 | 47.4 | 1.62 |
| Phosphorous, P^{4+} | 389 | 62.80 | 86.9 | 14.03 | 854 | 137.86 | 254 | 41.00 | 81.6 | 13.17 |
| Potassium, K^+ | N/A | N/A | <4.0 | 0.00 | N/A | N/A | <4.0 | 0.00 | <4.0 | 0.00 |
| Selenium, Se^{4+} | <2.0 | 0.00 | <4.0 | 0.00 | <2.0 | 0.00 | <4.0 | 0.00 | <4.0 | 0.00 |
| Silicon, Si^{4+} | 80.9 | 11.52 | 65.0 | 9.26 | 56.8 | 8.09 | 61.2 | 8.72 | 84.1 | 11.98 |
| Silver, Ag^+ | <0.15 | 0.00 | <0.30 | 0.00 | <0.15 | 0.00 | <0.30 | 0.00 | <0.30 | 0.00 |
| Sodium, Na^+ | N/A | N/A | <4.0 | 0.00 | N/A | N/A | <4.0 | 0.00 | <4.0 | 0.00 |
| Strontium, Sr^{2+} | 0.73 | 0.02 | 0.75 | 0.02 | 1.34 | 0.03 | 0.32 | 0.01 | 0.43 | 0.01 |
| Thallium, Tl^+ | N/A | N/A | <2.0 | 0.00 | N/A | N/A | 2.0 | 0.01 | 3.3 | 0.02 |
| Tin, Sn^{4+} | N/A | N/A | <6.0 | 0.00 | N/A | N/A | <6.0 | 0.00 | <6.0 | 0.00 |
| Titanium, Ti^{4+} | N/A | N/A | <0.20 | 0.00 | N/A | N/A | <0.20 | 0.00 | <0.20 | 0.00 |
| Vanadium, V^{5+} | 2.57 | 0.25 | 0.82 | 0.08 | 2.93 | 0.29 | 3.3 | 0.32 | 1.52 | 0.15 |
| Zinc, Zn^{2+} | 774 | 23.67 | 445 | 13.61 | 742 | 22.69 | 440 | 13.46 | 592 | 18.11 |
| Major cations | 25645 | 1636.03 | 12341 | 873.45 | 35689 | 2254.83 | 17770 | 1173.01 | 15223 | 1061.59 |
| Major anions | 89400 | 1875.30 | 39850 | 832.97 | 123500 | 2589.68 | 46812 | 978.91 | 48577 | 1015.76 |
| Total | 115045 | N/A | 52191 | N/A | 159189 | N/A | 64582 | N/A | 63800 | N/A |
| Ion balance difference | -6.81% | | 2.37% | | -6.91% | | 9.02% | | 2.21% | |
| TDS difference | N/A | | 24.85% | | N/A | | 16.76% | | 28.95% | |

Table A.6 Detailed chemical data for the ARD collection system.

| | C 3 | | C 5 | | C 6 | | C 7 | |
|--------------------------------------|-----------|---------|-----------|---------|-----------|---------|-----------|---------|
| | 05-Mar-91 | | 05-Mar-91 | | 05-Mar-91 | | 05-Mar-91 | |
| | (mg/l) | (meq/l) | (mg/l) | (meq/l) | (mg/l) | (meq/l) | (mg/l) | (meq/l) |
| Physical tests | | | | | | | | |
| Conductivity ($\mu\text{mhos/cm}$) | N/A | N/A | N/A | N/A | N/A | N/A | N/A | N/A |
| pH | N/A | N/A | N/A | N/A | N/A | N/A | N/A | N/A |
| Total Dissolved Solids | N/A | N/A | N/A | N/A | N/A | N/A | N/A | N/A |
| Acidity and alkalinity | | | | | | | | |
| Acidity (as CaCO_3) | 39000 | N/A | 51100 | N/A | 51600 | N/A | 49000 | N/A |
| Alkalinity (as CaCO_3) | <1.0 | N/A | <1.0 | N/A | <1.0 | N/A | <1.0 | N/A |
| Major anions | | | | | | | | |
| Bicarbonate, HCO_3^- | N/A | N/A | N/A | N/A | N/A | N/A | N/A | N/A |
| Carbonate, CO_3^{2-} | N/A | N/A | N/A | N/A | N/A | N/A | N/A | N/A |
| Bromide, Br^- | N/A | N/A | N/A | N/A | N/A | N/A | N/A | N/A |
| Fluoride, F^- | 0.03 | 0.00 | <0.02 | 0.00 | <0.02 | 0.00 | <0.02 | 0.00 |
| Chloride, Cl^- | 1100 | 31.03 | 1300 | 36.67 | 1200 | 33.85 | 1200 | 33.85 |
| Sulfate, SO_4^{2-} | 45100 | 938.96 | 66200 | 1378.25 | 65900 | 1372.01 | 63200 | 1315.79 |
| Nutrients | | | | | | | | |
| Ammonia Nitrogen, N | N/A | N/A | N/A | N/A | N/A | N/A | N/A | N/A |
| Nitrate Nitrogen, N | N/A | N/A | N/A | N/A | N/A | N/A | N/A | N/A |
| Nitrite Nitrogen, N | N/A | N/A | N/A | N/A | N/A | N/A | N/A | N/A |
| Total Dissolved Phosphate, P | 239 | N/A | 135 | N/A | 165 | N/A | 280 | N/A |
| Major cations | | | | | | | | |
| Aluminum, Al^{3+} | 2490 | 276.86 | 3870 | 430.29 | 3870 | 430.29 | 3720 | 413.62 |
| Antimony, Sb^{3+} | 4.6 | 0.11 | 4.8 | 0.12 | 4.8 | 0.12 | 5.6 | 0.14 |
| Arsenic, As^{3+} | 163 | 6.53 | 194 | 7.77 | 195 | 7.81 | 186 | 7.45 |
| Barium, Ba^{2+} | <0.10 | 0.00 | <0.10 | 0.00 | <0.10 | 0.00 | <0.10 | 0.00 |
| Beryllium, Be^{2+} | 0.32 | 0.07 | 0.54 | 0.12 | 0.56 | 0.12 | 0.54 | 0.12 |
| Bismuth, Bi^{3+} | <1.0 | 0.00 | <1.0 | 0.00 | <1.0 | 0.00 | <1.0 | 0.00 |
| Boron, B^{3+} | <1.0 | 0.00 | <1.0 | 0.00 | <1.0 | 0.00 | <1.0 | 0.00 |
| Cadmium, Cd^{2+} | 4.56 | 0.23 | 12.8 | 0.64 | 7.21 | 0.36 | 7.09 | 0.35 |
| Calcium, Ca^{2+} | 416 | 20.76 | 413 | 20.61 | 408 | 20.36 | 407 | 20.31 |
| Chromium, Cr^{3+} | <0.15 | 0.00 | <0.15 | 0.00 | <0.15 | 0.00 | <0.15 | 0.00 |
| Cobalt, Co^{2+} | 13.7 | 0.47 | 20.3 | 0.69 | 20.6 | 0.70 | 19.9 | 0.68 |
| Copper, Cu^{2+} | 498 | 15.67 | 785 | 24.71 | 788 | 24.80 | 751 | 23.64 |
| Iron, Fe^{2+} | 9230 | 330.55 | 10700 | 383.19 | 10700 | 383.19 | 10200 | 365.28 |
| Lead, Pb^{2+} | <0.50 | 0.00 | <0.50 | 0.00 | <0.50 | 0.00 | <0.50 | 0.00 |
| Lithium, Li^+ | N/A | N/A | N/A | N/A | N/A | N/A | N/A | N/A |
| Magnesium, Mg^{2+} | 1550 | 127.55 | 3310 | 272.37 | 3410 | 280.60 | 3290 | 270.73 |
| Manganese, Mn^{2+} | 235 | 8.56 | 421 | 15.33 | 446 | 16.24 | 434 | 15.80 |
| Molybdenum, Mo^{6+} | <0.30 | 0.00 | <0.30 | 0.00 | <0.30 | 0.00 | <0.30 | 0.00 |
| Nickel, Ni^{2+} | 32.7 | 1.11 | 50.2 | 1.71 | 50.6 | 1.72 | 48.7 | 1.66 |
| Phosphorous, P^{5+} | 360 | 58.11 | 386 | 62.31 | 380 | 61.34 | 361 | 58.28 |
| Potassium, K^+ | N/A | N/A | N/A | N/A | N/A | N/A | N/A | N/A |
| Selenium, Se^{4+} | <2.0 | 0.00 | <2.0 | 0.00 | <2.0 | 0.00 | <2.0 | 0.00 |
| Silicon, Si^{4+} | 41.0 | 5.84 | 56.5 | 8.05 | 57.5 | 8.19 | 56.3 | 8.02 |
| Silver, Ag^+ | <0.15 | 0.00 | <0.15 | 0.00 | <0.15 | 0.00 | <0.15 | 0.00 |
| Sodium, Na^+ | N/A | N/A | N/A | N/A | N/A | N/A | N/A | N/A |
| Strontium, Sr^{2+} | 5.93 | 0.14 | 3.63 | 0.08 | 3.43 | 0.08 | 3.46 | 0.08 |
| Thallium, Tl^+ | N/A | N/A | N/A | N/A | N/A | N/A | N/A | N/A |
| Tin, Sn^{4+} | N/A | N/A | N/A | N/A | N/A | N/A | N/A | N/A |
| Titanium, Ti^{4+} | N/A | N/A | N/A | N/A | N/A | N/A | N/A | N/A |
| Vanadium, V^{5+} | 1.79 | 0.18 | 2.14 | 0.21 | 2.05 | 0.20 | 1.9 | 0.19 |
| Zinc, Zn^{2+} | 236 | 7.22 | 435 | 13.30 | 458 | 14.01 | 443 | 13.55 |
| Major cations | 15283 | 859.94 | 20665 | 1241.50 | 20802 | 1250.14 | 19935 | 1199.88 |
| Major anions | 46200 | 969.99 | 67500 | 1414.92 | 67100 | 1405.86 | 64400 | 1349.64 |
| Total | 61483 | N/A | 88165 | N/A | 87902 | N/A | 84335 | N/A |
| Ion balance difference | | -6.01% | | -6.53% | | -5.86% | | -5.87% |
| TDS difference | | N/A | | N/A | | N/A | | N/A |

Table A.7 Detailed chemical data for the waste rock dump piezometers.

| | P 97-01 | | P 97-03 | |
|--------------------------------------|--------------|---------------|---------------|----------------|
| | 18-Apr-98 | | 18-Apr-98 | |
| | (mg/l) | (meq/l) | (mg/l) | (meq/l) |
| Physical tests | | | | |
| Conductivity ($\mu\text{mhos/cm}$) | N/A | N/A | N/A | N/A |
| pH | N/A | N/A | N/A | N/A |
| Total Dissolved Solids | 36000 | N/A | 159000 | N/A |
| Acidity and alkalinity | | | | |
| Acidity (as CaCO_3) | 19700 | N/A | 48700 | N/A |
| Alkalinity (as CaCO_3) | <1 | N/A | <1 | N/A |
| Major anions | | | | |
| Bicarbonate, HCO_3^- | <1 | 0.00 | <1 | 0.00 |
| Carbonate, CO_3^{2-} | <1 | 0.00 | <1 | 0.00 |
| Chloride, Cl^- | 5.2 | 0.15 | 12.6 | 0.36 |
| Sulfate, SO_4^{2-} | 24100 | 501.75 | 77500 | 1613.51 |
| Major cations | | | | |
| Aluminum, Al^{3+} | 1310 | 145.66 | 6970 | 774.97 |
| Antimony, Sb^{3+} | 1 | 0.02 | <4 | 0.00 |
| Arsenic, As^{3+} | 14 | 0.56 | 85 | 3.40 |
| Barium, Ba^{2+} | 0.34 | 0.00 | <0.2 | 0.00 |
| Beryllium, Be^{2+} | 0.2 | 0.04 | 1 | 0.22 |
| Bismuth, Bi^{3+} | 0.6 | 0.01 | 3 | 0.04 |
| Boron, B^{3+} | <0.5 | 0.00 | <2 | 0.00 |
| Cadmium, Cd^{2+} | 3.96 | 0.20 | 5.5 | 0.27 |
| Calcium, Ca^{2+} | 299 | 14.92 | 437 | 21.81 |
| Chromium, Cr^{3+} | 0.51 | 0.03 | 2.3 | 0.13 |
| Cobalt, Co^{2+} | 8.36 | 0.28 | 34.3 | 1.17 |
| Copper, Cu^{2+} | 203 | 6.39 | 549 | 17.28 |
| Iron, Fe^{2+} | 2900 | 103.86 | 10500 | 376.03 |
| Lead, Pb^{2+} | 1.1 | 0.01 | <1 | 0.00 |
| Lithium, Li^+ | 1.65 | 0.24 | 5.9 | 0.85 |
| Magnesium, Mg^{2+} | 2000 | 164.58 | 4820 | 396.63 |
| Manganese, Mn^{2+} | 373 | 13.58 | 719 | 26.17 |
| Molybdenum, Mo^{6+} | <0.2 | 0.00 | <0.6 | 0.00 |
| Nickel, Ni^{2+} | 18.7 | 0.64 | 86 | 2.93 |
| Phosphorous, P^{3+} | 42 | 6.78 | 504 | 81.36 |
| Potassium, K^+ | <10 | 0.00 | <40 | 0.00 |
| Selenium, Se^{4+} | <1 | 0.00 | <4 | 0.00 |
| Silicon, Si^{4+} | 55.3 | 7.88 | <1 | 0.00 |
| Silver, Ag^+ | <0.05 | 0.00 | 0.3 | 0.00 |
| Sodium, Na^+ | <10 | 0.00 | <40 | 0.00 |
| Strontium, Sr^{2+} | 1.4 | 0.03 | 0.6 | 0.01 |
| Thallium, Tl^+ | 1 | 0.00 | <4 | 0.00 |
| Tin, Sn^{4+} | <0.2 | 0.00 | <0.6 | 0.00 |
| Titanium, Ti^{4+} | 0.4 | 0.03 | <0.2 | 0.00 |
| Vanadium, V^{3+} | 0.5 | 0.05 | 0.5 | 0.05 |
| Zinc, Zn^{2+} | 405 | 12.39 | 405 | 12.39 |
| Major cations | 7641 | 478.18 | 25128 | 1715.73 |
| Major anions | 24105 | 501.90 | 77513 | 1613.87 |
| Total | 31746 | N/A | 102641 | N/A |
| Ion balance difference | | -2.42% | | 3.06% |
| TDS difference | | 12.56% | | 43.08% |

Table A.8 Detailed chemical data for runoff water.

| | Runoff | |
|--------------------------------------|-----------|---------|
| | 18-Apr-98 | |
| | (mg/l) | (meq/l) |
| Physical tests | | |
| Conductivity ($\mu\text{mhos/cm}$) | N/A | N/A |
| pH | N/A | N/A |
| Total Dissolved Solids | 284 | N/A |
| Acidity and alkalinity | | |
| Acidity (as CaCO_3) | 25 | N/A |
| Alkalinity (as CaCO_3) | 13 | N/A |
| Major anions | | |
| Bicarbonate, HCO_3^- | 13 | 0.00 |
| Carbonate, CO_3^{2-} | <1 | 0.00 |
| Chloride, Cl^- | 0.5 | 0.01 |
| Sulfate, SO_4^{2-} | 131 | 2.73 |
| Major cations | | |
| Aluminum, Al^{3+} | 1.1 | 0.12 |
| Antimony, Sb^{3+} | <0.2 | 0.00 |
| Arsenic, As^{3+} | <0.3 | 0.00 |
| Barium, Ba^{2+} | 0.05 | 0.00 |
| Beryllium, Be^{2+} | <0.005 | 0.00 |
| Bismuth, Bi^{3+} | <L0.1 | 0.00 |
| Boron, B^{3+} | <0.1 | 0.00 |
| Cadmium, Cd^{2+} | <0.01 | 0.00 |
| Calcium, Ca^{2+} | 36.6 | 1.83 |
| Chromium, Cr^{3+} | <0.01 | 0.00 |
| Cobalt, Co^{2+} | 0.02 | 0.00 |
| Copper, Cu^{2+} | 0.11 | 0.00 |
| Iron, Fe^{2+} | 1.43 | 0.05 |
| Lead, Pb^{2+} | <0.05 | 0.00 |
| Lithium, Li^+ | <0.01 | 0.00 |
| Magnesium, Mg^{2+} | 11.2 | 0.92 |
| Manganese, Mn^{2+} | 0.355 | 0.01 |
| Molybdenum, Mo^{6+} | <0.03 | 0.00 |
| Nickel, Ni^{2+} | <0.05 | 0.00 |
| Phosphorous, P^{5+} | <0.3 | 0.00 |
| Potassium, K^+ | 3 | 0.08 |
| Selenium, Se^{4+} | <0.2 | 0.00 |
| Silicon, Si^{4+} | 3.67 | 0.52 |
| Silver, Ag^+ | <0.01 | 0.00 |
| Sodium, Na^+ | <2 | 0.00 |
| Strontium, Sr^{2+} | 0.356 | 0.01 |
| Thallium, Tl^+ | <0.2 | 0.00 |
| Tin, Sn^{4+} | <0.03 | 0.00 |
| Titanium, Ti^{4+} | <0.01 | 0.00 |
| Vanadium, V^{5+} | <0.03 | 0.00 |
| Zinc, Zn^{2+} | 0.075 | 0.00 |
| Major cations | 58 | 3.55 |
| Major anions | 145 | 2.74 |
| Total | 202 | N/A |
| Ion balance difference | | 12.84% |
| TDS difference | | 33.52% |

The samples were analyzed in accordance to "Methods for Chemical Analysis of Water and Wastes (USEPA)", "Manual for Chemical Analysis of Water, Wastewaters, Sediments and Biological Tissues (BCMOE)" and / or "Standard Methods for the Examination of Water and Wastewater (APHA)".

Appendix B Detailed Climatological and Hydrological Data

B.1 Introduction

Table B.1 includes a complete set of climatological data for the study period of June, 1997 to June, 1998 that was obtained from the on site weather station. The freezing period started approximately November 1, 1997 and lasted until the 1998 freshet period. The freshet period started on April 15, 1998 and lasted for 27 days until May, 11, 1998. The total snowfall and rainfall is inputted as an equal amount of precipitation that is applied evenly throughout the runoff period. The data was used in the SoilCover analysis.

Table B.2 and B.3 lists the hydrological data used to calculate the individual components of the water budget for the regional and waste rock dump area respectively.

Table B.1 Climatological data, continued.

Table with 14 columns: Julian Day, Date, Max. temp. (°C), Max. hum., Max. wind (km/hr), Min. temp. (°C), Min. hum., Min. wind (km/hr), Precip. (mm), Net rad. (MJ/m²/day). It contains two sets of data spanning from 274 to 334, representing months from October 1997 to November 1997 and December 1997 to January 1998.

